CRANFIELD UNIVERSITY

RUKSHAN NAVARATNE

INVESTIGATION OF IMPACT OF ENGINE DEGRADATION ON OPTIMUM AIRCRAFT TRAJECTORIES

SCHOOL OF AEROSPACE, TRANSPORT AND MANUFACTURING
CENTRE FOR PROPULSION

PhD Thesis
Academic Year: 2015 / 2016

Supervisor: Dr Vishal Sethi & Prof. Pericles Pilidis
April 2016

CRANFIELD UNIVERSITY

SCHOOL OF AEROSPACE, TRANSPORT AND MANUFACTURING
PhD Thesis

PhD

Academic Year 2015 / 2016

RUKSHAN NAVARATNE

INVESTIGATING THE IMPACT OF ENGINE DEGRADATION ON OPTIMUM AIRCRAFT TRAJECTORIES

Supervisor: Dr. Vishal Sethi & Prof. Pericles Pilidis
April 2016

This thesis is submitted in partial fulfilment of the requirements for the degree of Doctor of Philosophy
(NB. This section can be removed if the award of the degree is based solely on examination of the thesis)

© Cranfield University 2016. All rights reserved. No part of this publication may be reproduced without the written permission of the copyright owner.

ABSTRACT

The continuous growth in flight operations has led to public concern regarding the impact of aviation on the environment with its anthropogenic contribution to global warming. Several solutions have been proposed in order to reduce the environmental impact of aviation. However most of them are long term solutions such as new environmental friendly aircraft and engine designs. In this respect, management of aircraft trajectory and mission is a potential short term solution that can readily be implemented. Therefore, in order to truly understand the optimised environment friendly trajectories that can be actually deployed by airlines, it is important to investigate the impact of degraded engine performance on real aircraft trajectories at multi-disciplinary level. Several trajectory optimisation studies have been conducted in this direction in the recent past, but engines considered for the studies were clean and trajectories were ideal and simple.

This research aims to provide a methodology to enhance the conventional approach of the aircraft trajectory optimisation problem by including engine degradation and real aircraft flight paths within the optimisation loop (framework); thereby the impact of engine degradation on optimum aircraft trajectories were assessed by quantifying the difference in fuel burn and emissions, when flying a trajectory which has been specifically optimised for an aircraft with degraded engines and flying a trajectory which has been optimised for clean engines.

For the purpose of this study models of a clean and two levels of degraded engines have been developed that are similar to engines used in short range and long range aircraft currently in service. Degradation levels have been assumed based on the deterioration levels of Exhaust Gas Temperature (EGT) margin. Aircraft performance models have been developed for short range and long range aircraft with the capability of simulating (generating) vertical and horizontal flight profiles provides by the airlines. An emission prediction model was developed to assess NOx emissions of the mission. The contrail prediction model was adopted from previous studies to predict contrail formation. In addition, a multidisciplinary aircraft trajectory optimisation framework was developed and employed to analyse short range flight trajectories between London and Amsterdam and long range flight trajectories between London and Colombo under three cases. Case_1: Aircraft with clean engines, Case_2 and Case_3 were Aircraft with two different levels of degraded engines having a 5% and 10% Exhaust Gas Temperature (EGT) increase respectively. Three different multi objective optimisation studies were performed; (1) Fuel burn vs Flight time, (2) Fuel burn vs NOx emission, and (3) Fuel burn

vs Contrails. Finally optimised trajectories generated with degraded engines were compared with the optimised trajectories generated with clean engines.

The most significant results obtained relate to the fuel burn which indicates that; For the long range aircraft the fuel burn would be reduced by 0.4% (i.e. 252 kg) with engines having 5% EGT increase and 0.6% (i.e. 384kg) with highly degraded engines having 10% EGT increase. Whereas for short range aircraft the effect of the approach is greater and the aircraft would achieve 0.9% (i.e. 14kg) and 1.1% (i.e. 17kg), reductions in the fuel burn with the optimised trajectories when the engines are degraded by 5% and 10% EGT increases. These savings over a year with highly degraded engines would equate to more than 140 tons per aircraft over a long haul flight such as London to Colombo and 6.2 tons on a short haul flight such as London to Amsterdam. Less significant were the optimisation of the trajectories to achieve a minimum flight time. For a long haul flight, the flight time was reduced by 0.23% (i.e. 1.4min) and 0.43% (i.e. 2.5min) and for short haul flight a reduction of 0.41% and 0.6% when the engines are degraded by the same 5 and 10% levels. NOx and contrails are a global concern so it is interesting to observe that for the long range aircraft a significant reduction in the NOx formation by 0.7% and 1.2% was observed, whereas the short range aircraft achieved even greater reductions of 1.2% and 1.9% for the same EGT levels of degradation. In all cases and based on the atmospheric profiles chosen, contrails were completely avoided by the both aircraft with a fuel penalty of 0.35% (233kg) and 0.8% (543kg) for long range and 0.6% (9kg) and 1% (16kg) for short range aircraft when engines were degraded by 5% and 10% EGT increase.

The results have shown impact of engine degradation on optimum aircraft trajectories are significant and in order to reduce fuel burn and emissions aircraft need to fly on an optimised trajectory customised for the degraded engine performance. Finally to increase the simulation quality and to provide more comprehensive results, a refinement and extension of the framework with additional models have recommended.

Keywords:

Engine Performance Degradation, Aircraft Emissions, Trajectory Optimisation

Acknowledgements

I thank Almighty God, Jesus Christ and the Holy Spirit, for the infinite grace given to fulfil my desires.

I would like to thank my supervisors Dr Vishal Sethi and Professor Pericles Pilidis for their technical support and continual guidance given throughout my research.

My sincere gratitude goes to Professor Pericles Pilidis for not only funding my PhD and for his invaluable advice, guidance and encouragement but also for helping me through difficult times during my research.

I am extremely grateful to my parents Victor and Evangeline for their love, caring, prayers and sacrifices for educating and preparing me for my future. I am very much thankful to my wife Nishani, and my two children Dilesh and Tashiya for their patience, understanding and continuing support to complete this research work.

Special thanks go to my best friend William Camillary for his valuable advice and technical guidance imparted during our discussions. My sincere thanks go to Dr Tony Jackson, Professor Vessilios Pachidis, and the late Dr Kenneth Ramsden.

I also extend my heartfelt thanks to my learned friends and research colleagues Devaiah Nalianda, Hugo Pervier, Uyioghosa Igie, Atma Prakash, Nqubile Khani, Weiquen Gu, Benjamin Venediger, Christos Tsoskas, Joao Ramos

I am very grateful to Professor Herb Saravanamuttoo at Carliton University, Dr Erwin Stenzel at Airbus Group, Matthew Xuereb and Matthew Samuut at the University of Malta, Mr Tyrone Navaratne and to those members of engineering staff at Sri Lankan Airlines for their valuable support and technical advice.

I also extend my thanks to the administration staff of the Department of Power and Propulsion at Cranfield University, Mrs Gillian Hargreaves, Mrs Nicola Datt, Mrs Claire Bellis and Mr Josh Redmond for their unstinting support throughout the course of my PhD

Lastly, but not least, I thank Ms Joan Parr for helping me in many ways, always having words of encouragement and for her gratefully received prayers and blessings.

TABLE OF CONTENTS

LIST OF FIGURES

LIST OF TABLES

LIST OF ABBREVIATIONS

ACARE	Advisory Council for Aeronautical Research in Europe
ACC	Active Clearance Control
ADM	Aircraft Dynamic Model
AGL	Above Ground Level
APM	Aircraft Performance Model
ATC	Air Traffic Control
ATM	Air Traffic Management
BADA	Base of Aircraft Data
BPR	Bypass Pressure Ratio
CAEP	Committee on Aviation Environmental Protection
CPM	Contrail Prediction Model
CPT	Corner Point Temperature
DOC	Direct Operating Cost
DOT	Department of Transport
EEM	Engine Emission Model
EGT	Exhaust Gas Temperature
EI	Emission Index
EPM	Engine Performance Model
EPN	Effective Perceived Noise
EPR	Engine Pressure Ratio
FADEC	Full Authority Digital Engine Control
FAR	Fuel Air Ratio
FCM	Fuel Composition Method
FPR	Fan Pressure Ratio
FF	Fuel Flow
FPR	Fan Pressure ratio
FOD	Foreign Object Damage
FW	Fuel Weight
GA	Genetic Algorithms
GATAC	Green Aircraft Trajectories under ATM Constrains
GUI	Graphical User Interface
HPC	High Pressure Compressor
HPT	High Pressure Turbine
HSCT	High Speed Civil Transport

ICAO	International Civil Aviation Organisation
ISA	International Standard Atmosphere
ITD	Integrated Technology Demonstrator
JTI	Joint Technology Initiative
LAN	Local Area Network
LAQ	Local Air Quality
LCF	Low Cycle Fatigue
LPC	Low Pressure Compressor
LPT	Low Pressure Turbine
LTO	Landing and Take Off
MADS	Mesh Adoptive Direct Search
MLW	Maximum Landing Weight
MMR	Molar Mass ratio
MPW	Maximum Pay Load
MTM	Management of Trajectory and Mission
MTOW	Maximum Take Off Weight
MZFW	Maximum Zero Fuel Weight
NCP	Noise Calculation Programmes
NLC	Noise Level Calculations
NOAA	National Oceanic Atmospheric Administration
NSGA	Non-dominated Sorting Genetic Algorithm
NLC	Noise Level Calculation
N1	Low Pressure Spool Speed
N2	High Pressure Spool Speed
OAT	Outside Air Temperature
OEW	Operating Empty Weight
OPP	Optimised Procedure Profile
OPR	Overall Pressure Ratio
PCN	Spool Speed
QC	Quota Count
RH	Relative Humidity
RPK	Revenue Passenger Kilometres
UHC	Un-burn Hydro Carbon
SEL	Sound Exposure Level
SESAR	Single European Sky ATM Research
SFC	Specific Fuel Consumption

SGO	Systems for Green Operations
SID	Standard Instrument Departure
SLS	Standard Level Static
TBC	Thermal Barrier Coating
TERA	Techno-Economic Environmental Risk Assessment
TET	Turbine Entry Temperature
TO	Take Off
TOC	Top Of Climb
TOD	Top of Descent
TRL	Technology Readiness Level
ZDT1	Zitzler, Deb and Thiele Function 1
ZDT3	Zitzler, Deb and Thiele Function 3
ZDT4	Zitzler, Deb and Thiele Function 4
ZDT6	Zitzler, Deb and Thiele Function 6

1 Introduction

This chapter introduces the research topic and outlines the general context for the study. The objectives of the research project are summarised together with the main contributions to knowledge. The project scope and the methodology followed during the research in order to achieve the objectives are also included in this chapter. In addition, a description of the structure of the thesis is also provided.

1.1 Aviation impacts on the environment

Aviation has become an essential element of today's global society, bringing people and cultures together and creating economic growth. It is estimated that, globally, 2.97 billion passengers travel by air each year and account for 28.5 million aircraft movements, in 34,765 city pair routes which is equivalent to 5.4 trillion passenger kilometres per year. The demand for air travel expected to grow at the rate of 5% next 20 years and number of aircraft will double by 2033 (Epstein 2013). The market projection associated with the growth of revenue passenger kilometres (RPK) and expected number of aircraft is shown in Figure 1.1.

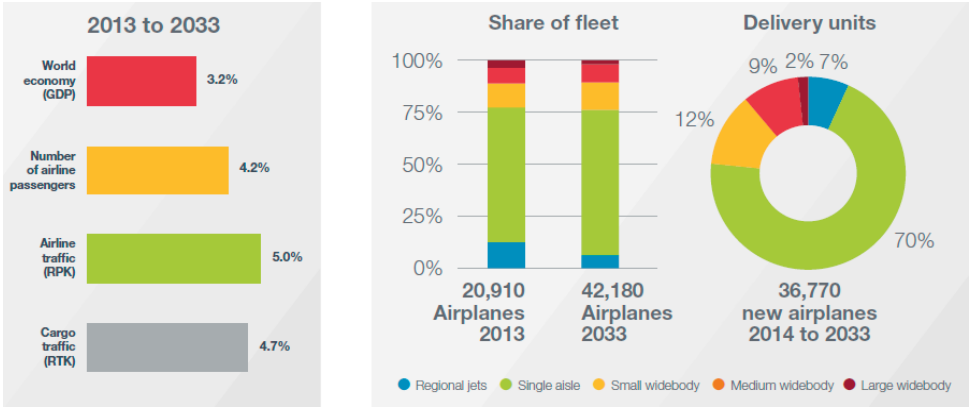

Figure 1-1 Aviation market outlook (Epstein 2013)

However, the continuous increase in aircraft operation will severely affected the climate, environment, human health and comfort, especially in the vicinity of the airports. Aircraft emissions are of particular concern to the global environment due to the altitude at which they are emitted. Numerous studies confirm that the biggest environmental impacts are caused by the consumption of fuel and the emission of gases; global warming results from: CO_2, H_2O and contrails, acid rains and health risks from: NO_x, CO, and unburnt hydrocarbons (UHCs). Although today air transport only produces 2 % of man-made CO_2 emissions, this is expected to increase to 3 % by 2050 with the continuous and steady growth of traffic (if appropriate measures are not taken, refer Figure 1.2). The other emission source of particular concern is noise which is a nuisance near airports during the aircraft landing and take-off (LTO) cycles.

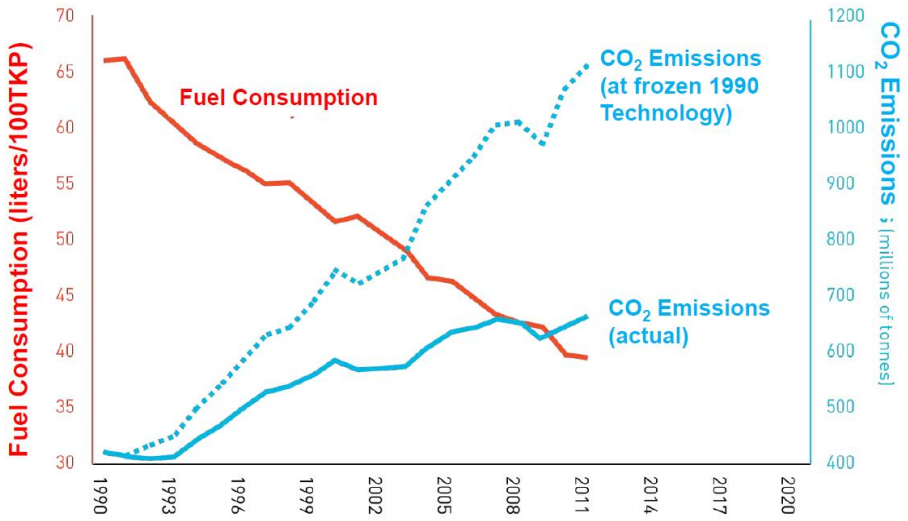

Figure 1-2 Fuel consumption and CO_2 emission trends (Epstein 2013)

1.2 Project background and research motivation

Considering the critical and complex nature of the problem regarding the environmental footprint of aviation, several organisations worldwide have focused their efforts through large collaborative projects such as Clean Sky Joint Technology Initiative (JTI). Clean Sky is a European public-private partnership between the aeronautical industry and the European Commission operates under six ITDs with a budget of 1.6 billion Euros. The main objective of the research programme is to achieve the environmental goals set by ACARE Vision 2020 and associated Strategic Research Agenda to reduce CO_2 by 50%, NO_x by 80% and Noise by 50% compared to the year 2000. The ability to meet these targets will only be possible with a strong commitment to vigorously improve existing technologies and achieve new breakthroughs. Over the last few years several alternatives have been proposed but most of them are long term solutions such as changing aircraft and engine configurations. Hence, researchers have started focusing and developing strategies that can be implemented in the short term. The management of trajectory and mission is one of the key solutions identified that can contribute to achieving the above objectives and is a measure that can be readily implemented.

In order to truly understand the optimised environmentally friendly trajectories that can be actually deployed by air lines, it is important to investigate the impact of degraded engine performance on these trajectories at a multi-disciplinary level assessing the trade-offs between, fuel burn, mission time, emissions and direct operating cost. This will bring environmentally sustainable and economically feasible solutions to the operator. In this context, this research project has motivated the continued development of a multi-disciplinary aircraft trajectory optimisation framework (GATAC) comprising performance simulation and emission prediction models for use in Techno-economic and Environmental Risk (TERA) assessments.

Figure 1-3 Clean Sky research programme structure (Clean Sky 2010)

1.3 Research objectives

The main objectives of the research project are defined below and contribute to the development of a multi-disciplinary aircraft trajectory optimisation tool GATAC (Green Aircraft Trajectories under ATM Constrains), which has been collaboratively developed by Cranfield University and other partners as a part of the Clean Sky SGO ITD. The key research objectives are as follows;

- The investigation of the effects of engine degradation on the overall engine performance of short range and long range flight missions
- The development of a trajectory optimisation framework to generate more realistic trajectories with engine degradation and real flight paths
- The evaluation of the trade-off between fuel burn, flight time and NO_x emissions and contrail formation of short range and long range aircraft through multi-objective trajectory optimisation

1.4 Methodology

In this work, optimised trajectories generated with clean engines will be compared with the optimum trajectories generated with degraded engines under the same conditions. For this purpose commercially available short range and long range aircraft will be considered with conventional high bypass ratio turbofan engines. To perform the comparisons and assessments, several appropriate numerical engineering models have been considered and coupled with a GA based optimiser as a part of GATAC trajectory optimisation framework. The detail sequence of the procedures followed in the methodology is given below.

First step was to identify a suite of models required to achieve the objectives set for this work. Firstly, a clean engine and two degraded engine models have been developed similar to engines used in short range and long range aircraft currently in service. The degradation levels have been achieved based on the deterioration levels of EGT margins. Then, aircraft dynamic models have been developed for short range and long range aircraft with the capability of generating vertical and horizontal flight profiles provided by the airline. Other necessary models such as emission prediction model, and direct operating cost model also developed. However, an existing contrail model has been used to predict contrail generation. Once the models were developed to suit the needs, they have been integrated within the framework in order to create architecture capable of handling data interaction between models. The extensive work on optimisation strategy has been carried out in order to ensure that a capable and well suited

optimiser would be available to perform multi-objective optimisation with a large number of variables and constraints. The optimiser was subsequently integrated within the developed framework to perform bi-objective optimisation and generate Pareto-fronts based on various sets of objectives and constraints.

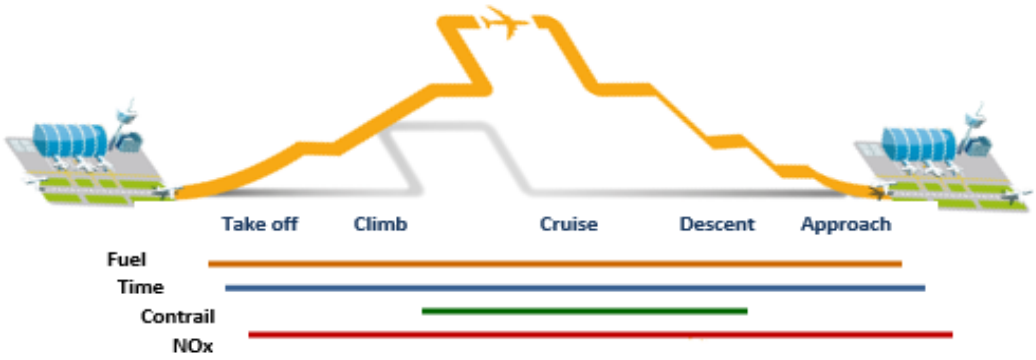

Figure 1-4 Objectives considered for the optimisation in the methodology

1.5 Contribution to knowledge

The contribution to knowledge in this research aims to provide a methodology to enhance the conventional approach of the aircraft trajectory optimisation problem by including engine degradation and real aircraft flight paths within the optimisation loop (framework); thereby the impact of engine degradation on optimum aircraft trajectories were assessed by quantifying the difference in fuel burn and emissions, when flying a trajectory which has been specifically optimised for an aircraft with degraded engines and flying a trajectory which has been optimised for clean engines.

1.6 Thesis structure

The works of the present research project which are summarised in this thesis are presented in seven chapters. Chapter 1 provides a general introduction to the problem addressed in this project in an attempt to provide an idea of the general context in which the research project was developed. It also consists of the general and specific objectives of the research project. The methodology followed during the research in order to achieve the research objectives as well as main contributions to knowledge is also included in this Chapter.

Chapter 2 is a review of the literature available on the trajectory optimisation studies conducted to minimise the environmental impact of aviation. The initial part of the chapter covers the aviation pollutants under focus and in-depth review on aircraft trajectory optimisation studies conducted for various environmental objectives. The various techniques used to solve trajectory optimisation problems, including the advantages and disadvantages of each technique are also reviewed. The chapter also provide the main limitations of the aircraft trajectory optimisation problems studied in the past. The final part of the chapter covers the multi-objective, multi-disciplinary aircraft trajectory optimisation studies done at Cranfield University and summarises how further contribution can be made in the field, by identifying the gaps in the literature and justify the claims to contribution to knowledge.

Chapter 3 focuses on engine degradation and the impact of degradation on the performance deterioration of the engine. Short range and long range aircraft engines are studied. The initial part of the chapter discusses the various degradation mechanisms and their influence on the main engine components. The various levels of degradation mechanisms are simulated to analyse the sensitivity of engine performance to component degradation. The impact of degradation on engine performance parameters of net thrust, sfc and key monitoring parameters such as fuel flow, spool speeds, engine pressure ratio and exhaust gas temperature were assessed at different engine operating points. Finally one clean and two degraded engine models for short range and long range aircraft were created based on the EGT margin deterioration data provided from the Srilankan Airline. These models were integrated with the aircraft dynamic models which have been used in the optimisation frame work.

Chapter 4 describes the framework which has been developed to conduct trajectory optimisation studies. The initial part of this chapter explains the details of the models used in the framework including development, testing, validation and the main limitations of each model. Then next section focuses on the optimisation strategy which has been used for this work. It discusses its unique capabilities of handling multi-objective aircraft trajectory optimisation problem with large number of variables and constraints in detail. Benchmarking and testing of

this optimiser against other optimisers is also presented. The final part of the chapter discusses the system level integration and model interaction with the optimiser within the framework to generate aircraft trajectories.

Chapter 5 focuses on the trajectory optimisation studies conducted using the developed optimisation framework discussed in Chapter 4 for a long range aircraft with the different level of degraded engines. Initial part of the Chapter discusses the simulation of trajectories and multidisciplinary trajectory optimisation process within the framework. The problem definition, mission route, and optimisation set up also discussed. Trajectory optimisation studies were performed for minimum fuel burn, minimum NOx, and minimum contrails under three case studies. Finally optimised trajectories generated with degraded engines were compared with the optimised trajectories generated with clean engines as potential environmentally friendly trajectories for airline operations.

Chapter 6 used to describes the similar studies performed for a short range aircraft with degraded engines. The main intention of the Chapter 6 is to understand the aircraft trajectory optimisation of a short range aircraft with degraded engines under the same objectives as discussed in Chapter 5. The initial part of the chapter discusses the details of the integrated framework, problem definition, optimisation objectives and the optimisation set-up. The latter part of the chapter provides the optimisation results achieved for the different test cases. Optimised trajectories generated with degraded engines are compared with the trajectories generated with the clean engines as described in Chapter 5.

Finally Chapter 7 summaries the overall conclusions of the work presented in each of the individual chapters. The author's main contributions to knowledge in the area of environment friendly aircraft operational procedures and trajectory optimisation are also presented. The main limitations are highlighted and recommendations for further work are appropriately made. The thesis also includes some appendices which provide supporting information for the analysis and discussions carried out in the chapters of the main body.

2 Literature Review

2.1 Introduction

An initial literature review has been carried in order to have a better understanding of the key aircraft pollutants and their operational impact on the environment. The latter part of the review is performed to understand the various proposed methods and ways of reducing the aircraft emissions in future. More emphasis is given towards the aircraft trajectory optimisation studies conducted to reduce the impact of main aviation emissions as one of the identified solutions. In order to facilitate its understanding, this part of the review is presented in two parts: the first part discusses the various types of optimisation techniques used to solve aircraft trajectory optimisation problem. The advantages and disadvantages of each method also reviewed; and the second part discusses the trajectory optimisation studies performed with different optimisation techniques to reduce the impact of aircraft pollutants identified in the first part of the review. Finally the summary of the review is presented with the identification of areas which has not been addressed by the previous research in the context of contribution to knowledge.

2.2 Key environmental pollutants under focus

Aviation has become an essential element of today's global society, bringing people and cultures together and creating economic growth. The growth in air transport has been estimated at an annual average rate of about 5 % over the past twenty years (Green 2003). Pollution emissions from aircrafts have become of great public concern due to their impact on health and environment. The past decade has witnessed rapid changes both in the regulations for controlling emissions and in the technologies used to meet these challenges. In this context, the organisation such as ICAO and ACARE has identified several pollutants as aviation emissions (ICAO 2010, European 2010).

2.2.1 Carbon dioxide emissions

Carbon Dioxide (CO_2) is categorising as a dominant anthropogenic greenhouse emissions, as it is retained in the atmosphere for over a hundred years (Green 2003). Globally civil aviation is estimated to account for approximately 2% of anthropogenic CO_2 emissions, compared with 16% from other modes of transport and over 30% from electricity generation and heat supply. In Europe ACARE (Advisory Council for Aeronautical Research in Europe) has set very stringent goals for aviation industry to be achieved by 2020. One of the set goals is a reduction of 50% CO_2 as based on the year 2000 (Pervier 2013). Currently there is no definitive standard or global regulation framework actually exists to manage CO_2 emissions and aviation emissions in general. However, in 2009, under the leadership of ICAO, a "globally-harmonised agreement to address climate change from a specific sector" was agreed upon and consequently the ICAO has now completed their "global carbon dioxide standards" in 2013 (Khun 2010). For CO_2 emission, ICAO targets a 1.5 to 2.0% annual improvement in fuel efficiency globally until year 2050 with 2005 as the base year. It has planned to achieve this by first attaining "Carbon Neutral Growth" by 2020 through medium term goals and an absolute reduction of net CO_2 emissions by 50% in 2050, compared to 2005 levels as long term goals (ICAO 2010). The below Figure 2.1 shows, the proposed CO_2 reduction measures overtime.

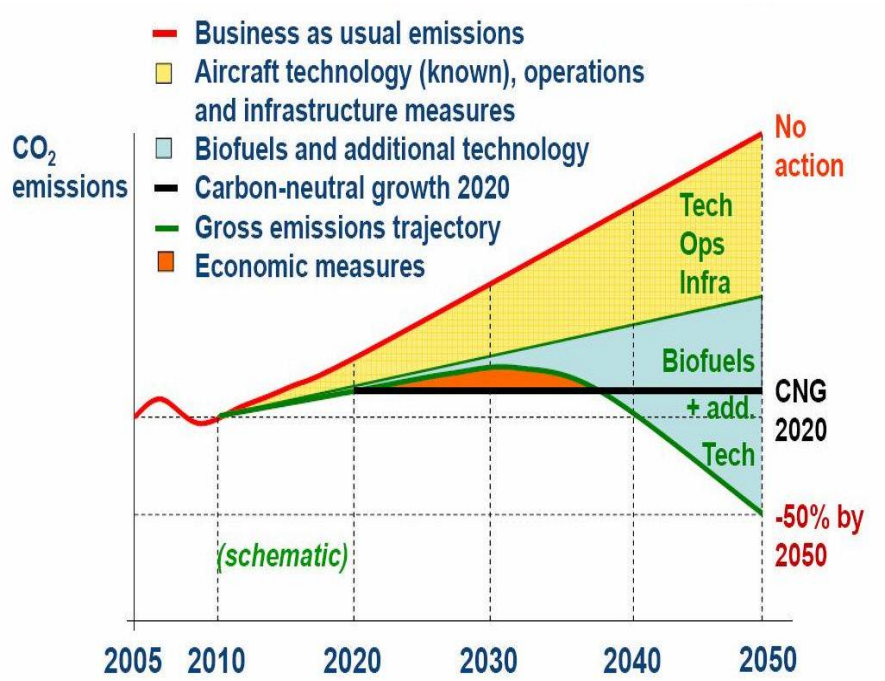

Figure 2-1 Future Carbon reduction goals as proposed by (ICAO 2010)

2.2.2 Aviation noise

Literature (Torres 2011) indicates that aircraft noise is acknowledged to be "one of the most objectionable impact of aircraft operations." Aircraft noise has been known to affect sleep patterns of population around the vicinity of airports, in turn affecting human concentration and resulting in "fatigue, stress, feeling of anger, frustration and powerlessness to control the noise". These factors affect people's quality of life and therefore have resulted in the fact that all current international standards, with respect to aviation noise, are concerns with communities around the airports.

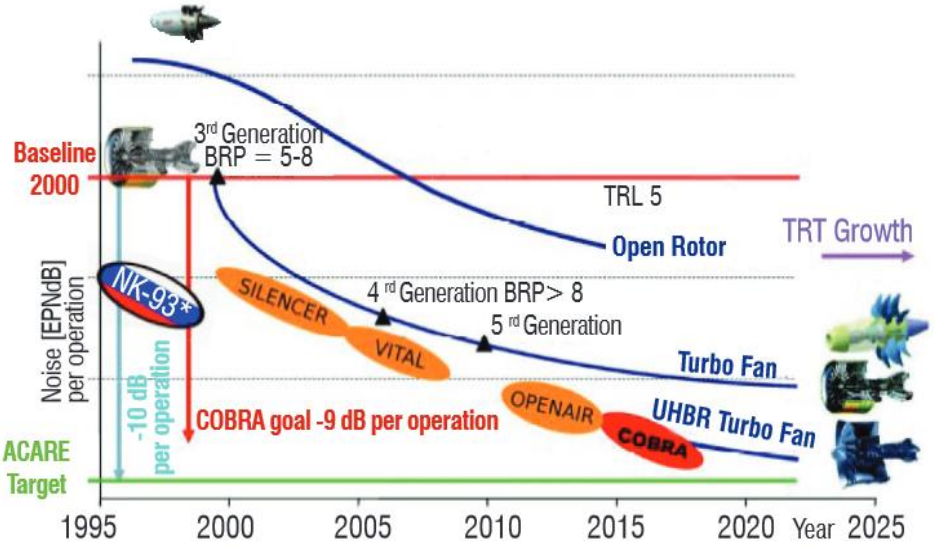

Figure 2-2 Aircraft noise reduction trends (Leylekian 2014)

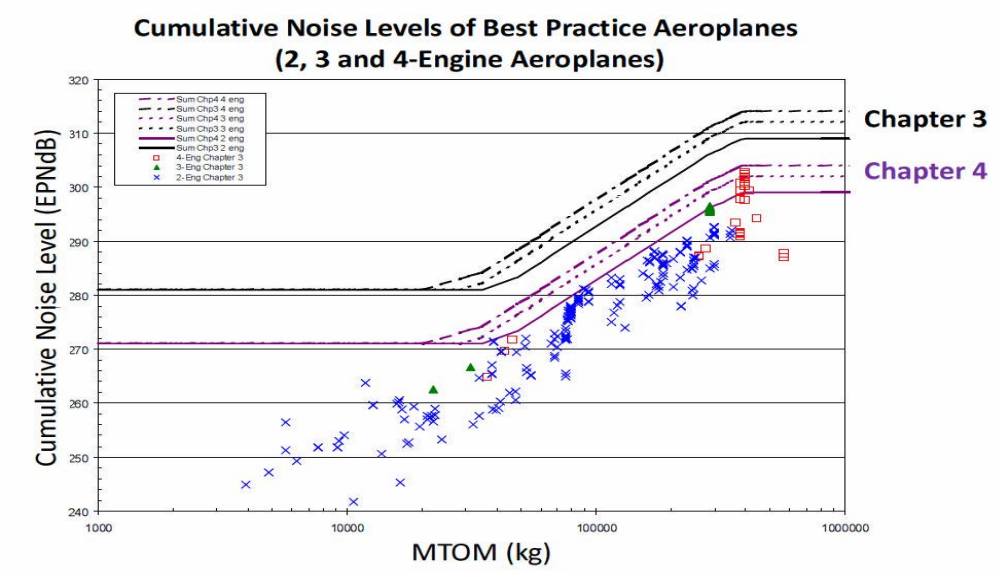

Figure 2-3 Noise standards for civil aviation by ICAO (ICAO 2010)

Through the technological advancement, current aircraft are 75% quieter than they were 50 years ago (Leylekian 2014). This has been primarily possible due to the progressive increase in engine bypass ratio driven by the demand from the airlines for better fuel economy. The other reason was due to the continuously imposed stringent noise regulations stipulated for civil aircraft by ICAO. The current regulations are covered under Chapter 4 of Annex 16 to the Convention on Civil Aviation. It is applicable for all aircraft which entered into service after 2006 and is based on stipulated noise levels for a particular Maximum Take-off Weight (MTOW). The Figure 2.3 shows the cumulative noise levels (EPNdB - Effective Perceived Noise Level) against the MTOW of various aircraft having different number of engines (ICAO 2010). The specific maximum noise levels have calculated from the readings taken from three defined measuring points, which are to the side-line of the runway at Take-off, under the flight path at Take-off and under the flight path on final approach. Also it is important to note that apart from the ICAO noise regulations, Department of Transport (DOT) also has introduced a Quota Count System to administrate the night noise quotas in some airports such as London Heathrow, Gatwick and Stansted. The main feature of the system is that each aircraft given a quota count (QC) rating (e.g. QC/0.5, QC/1, QC/2, etc.) according to how much noise it makes. Aircraft are classified separately for landing and take-off. The information used are based on the noise certification data recorded when aircraft are required to possess a noise certificate after demonstrating their compliance with the ICAO noise certification standards.

2.2.3 Oxides of nitrogen (NOx)

The formation of oxides of nitrogen is results from the oxidation of atmospheric nitrogen in high temperature regions of the flame in the combustor (Singh, 2009). NO_x is mainly made of NO and NO_2. There are three types of NO_x formed during the combustion process: (1) fuel NO_x – comes from nitrogen being oxidised by combustion air, (2) thermal NO_x – generated by nitrogen reacting with a surplus of oxygen at high temperatures, and (3) prompt NO_x – results from the formation of hydrogen cyanide (HCN) and then oxidising to form nitric oxide (NO). Also there are two important factors which influence the formation of NO_x during the combustion process. The first factor is the combustion flame temperature. An increased in combustion flame temperatures will cause an exponential rise in the NO_x formation rate (above 1600K), conversely flame with lower temperatures significantly reduce the NO_x formation rate. The second factor is the residence time of the combustion process. Therefore to reduce NO_x formation, it is necessary to cool the flame as quickly as possible and to reduce the time available for combustion (Singh 2009).

Research over the years has been found in providing scientific evidence to establish the effects of NO_x emissions on the environment and global warming. According to the literature (Lee et al., 2009) NO_x can have different undesirable effects on the environment depending on in which atmospheric layer they are generating and released. Scientific research indicates that in upper atmosphere layers of the stratosphere, NO_x will cause the stratospheric ozone (O_3) to decrease. A reduction of ozone layer cause an increase in ultra-violate radiation at ground level, since there is less ozone available to absorb the radiation from the sun at the upper atmosphere. An increased risk for skin cancer can be one consequence of the ozone layer depletion (Penner, 1999). In the low atmospheric layers of the troposphere specially close to ground level, NO_x emissions will cause the formation of ozone, and contribute to various health / environmental problems. A detail elaboration of atmospheric effects due to NO_x and their formation mechanisms can be found in (Brasseur, 1998) while (Penner, 1999) provides the future growth of NO_x.

The effects of NO_x emission on ground level (specially near airports) is well established. Thus, ICAO regulations to improve Local Air Quality (LAQ) due to NO_x emissions during LTO cycle are currently prioritised. Figure 2.4 shows the transition of the LTO NOx standards over the years. The current standards for NO_x are specified under CAEP/6 which stipulated the NO_x emissions in g/kN based on the overall pressure ratio (ICAO, 2010). The first regulation imposed for NOx emissions by ICAO was in 1981 (CAEE standards as indicated in Figure 2.4), and from then it has been reduced to 50%. The CAEP/6 standard which is currently in force will be further improve upon, to more stringent levels (up to 15%) over the current limit for all engines certified from 2014, to form CAEP/8 (Thrasher, 2010). However, still ICAO stand on the effects of cruise NO_x may be considered currently noncommittal. Literature indicates that there is broad correlation between the amounts of NO_x produced in the LTO cycle, with the amounts produced at cruise. However, there is current standard or database exists and ICAO is seeking further scientific evidence on the relative importance of cruise NO_x before formulating any standards or regulations (European 2010).

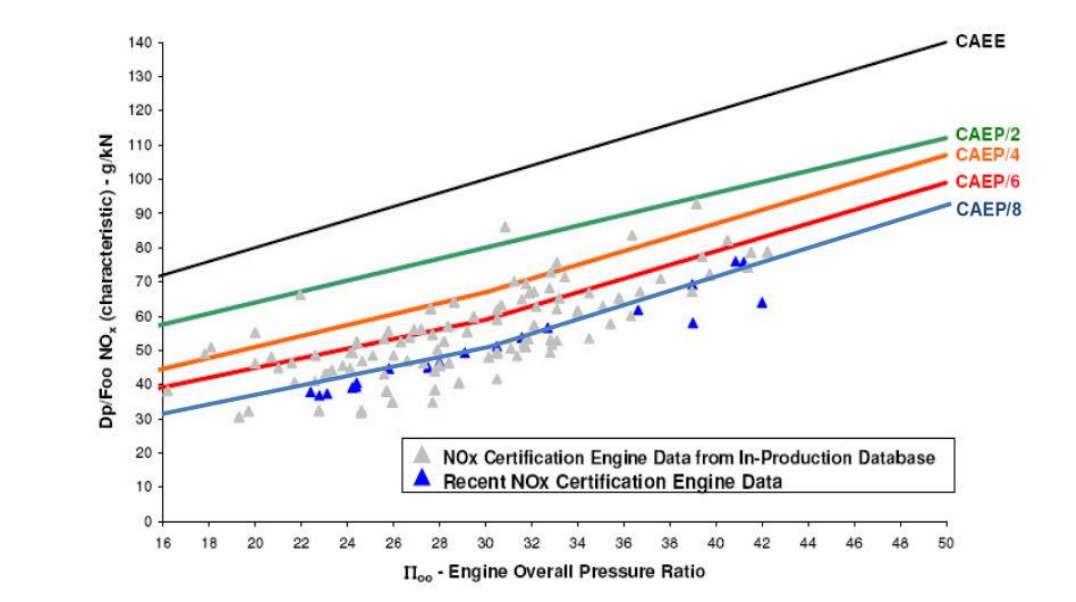

Figure 2-4 NOx Emission standards for Civil Aviation by ICAO (ICAO 2010)

2.2.4 Contrails and cirrus could formation

Aircraft engines emit 1.23 tons of water vapour for every single ton of kerosene burned as a complete combustion by-product. At the cruise altitude, under conditions of low ambient temperatures and high relative humidity, exhaust stream is cooled by mixing with the outside air and the water vapour condenses to form line shaped visible trails. These trails are also known as condensation trails or contrails. Small particles in the exhaust stream mostly soot and aerosol particles produced during the combustion provide the nuclei for condensation. Depending on the atmospheric conditions, the trails may evaporate again within a short period of time or it may persist as a visible trail for several hours or more and form cirrus clouds. Research in this area is continuously ongoing and current literature suggests that contrails and induced cirrus clouds may results in climate change as they tend to absorb and emit infrared terrestrial radiation and reflect visible radiation from sun. A recent (Sridhar, 2011) reports that persistent contrails may have a three to four times greater effect on climate than carbon dioxide emissions.

Lee et al (2009), investigated that there is no method that will prevent the formation and persistence of these contrails. If an aircraft flies through an ice-saturated air mass, contrails will form and persist. Also literature says ice-saturation tends to occur in defined volumes of cold relatively humid air which have been characterized as “moist lenses” (Lee 2009). These have maximum vertical extent of a few kilometers and a maximum horizontal length of about

thousand kilometers. As Lee et al., (2009) noticed, these lenses could, in principle be avoided by flying over it or under it or around it. There are several reasons why this method would be premature to recommended and standardized as an operational procedure to avoid contrails: the fundamental scientific understanding is not yet sufficiently robust, neither air traffic management nor weather predicting are currently well placed to support such a procedure; and finally the impact of fuel burn, CO_2 emissions and DOC for the airline not yet well understood. Therefore this is one of the important areas to be investigated under trajectory optimization for minimum aviation emissions.

2.3 Aircraft trajectory optimization for minimum emissions

As discussed above environmental issues associated with aircraft operations are currently one of the most critical aspects of commercial aviation (Green 2003). This is a result of both the continuing growth in air traffic, and increase public concern in the anthropogenic contribution to climate change. According to Clark (2003), there are three possible options in order to reduce environmental pollutions from an aircraft; (a) the number of operations must be reduced, (b) the type of aircraft must be changed or (c) the way aircraft fly must be changed with new rules and procedures. However, due to the fact that passenger traffic is expected to increase over the next years (Epstein 2013); it seems unlikely that the number of operations can be reduced. Therefore a combination of the last two options (b) and (c) seems to be a viable approach to the problem. However, changing the type of the aircraft is a difficult task which takes a long time. So this turns out to be an alternative solution in the long-term. It is therefore realised that emphasis needs to be placed towards assessing the feasibility of fly the aircraft differently and setting new or modifying the operational rules and procedures that decrease the impact of aircraft operations to the environment and climate change (Clark 2003). Therefore, the optimisation of trajectories could be a solution that can readily be implemented.

2.3.1 Numerical methods use in trajectory optimisation

In this section a particular emphasis is placed on some of the main mathematical optimisation techniques and their suitability to aircraft trajectory optimisation problems. The optimisation can be seen as the process of obtaining the best result or the best possible solution under any given set of circumstances. Thus, optimisation can be defined as the science of determining the best solutions to certain mathematically defined problems, which are often representation of

physical reality (Fletcher 1987). Invariably, it involves selecting the best decision from a number of options or a set of candidate decisions. When it requires simultaneous optimisation of more than one objective function, a multi objective problem arises. Multi-objective optimisation also referred to as vector optimisation problem and consists of optimising a number of objective functions. In such problems, no single optimal solution exists, rather a set of equally valid solutions, known as the Pareto optimal set (Deb, 2010) and it can be stated in general form of;

$$\min \boldsymbol{f_m}(\boldsymbol{X}),\ \boldsymbol{m} = \mathbf{1}, \mathbf{2}, \ldots\ldots, \boldsymbol{M}$$

$$subject\ to \quad g_j(X) \geq 0 \qquad j = 1, 2, \ldots\ldots, J$$

$$h_k(X) = 0, \quad k = 1, 2, \ldots\ldots\ldots, K$$

When x is the vector of n decision variables, $X = (x_1, x_2, x_3 \ldots\ldots, x_n)^T$, and decision space. Each decision variable is bound as follows; $x_i^{(l)} \leq x_i \leq x_i^{(u)}$, $i=1, 2, 3, \ldots\ldots, n$

There is no single optimisation method available for efficiently solve all the optimisation problems. Thus a number of optimisation techniques have been developed in the past and most of them are tailor made for a specific problem. One such group of developed methods is the optimum seeking methods which also known as mathematical programming techniques. These techniques are particularly important because they determine the minimum of a function of several variables under prescribed set of constraints. There are several ways of classifying an optimisation problem in order to describe the available methods for solving the relevant optimisation problem (Walsh, 1975; Schwefel, 1981; Bunday, 1984; and Rao 1996). A complete summary of the classification can be found in Rao (1996).

Accordance with the above classification of optimisation problems, the aircraft trajectory optimisation problem can be classified as constrained, dynamic, optimal control, nonlinear, real valued, deterministic and non-separable problem. Since a number of parameters will be involved during the optimisation process and it is assumed there are number of local minima or maxima, therefore the problem can also be classified as multi-dimensional and multi model (Celis 2010).

There are number of mathematical programming techniques that can be used to find the minima or maxima of a function within a given set of constraints. However, it is not within the intentions of this work to detail every technique available for solving optimisation problems, thus only those that have been widely used in aircraft trajectory optimisation are presented here. Most important optimisation methods can be grouped under three broad categories (Schwefel 1981). They are: (i) classical methods, (ii) random search method, and (iii) evolutionary methods.

(i) Classical Methods

Classical methods are generally classified into Direct Search Methods and Gradient Search Methods. In direct search methods only the values of the objective function and constraints are used in the search process (Schwefel 1981). They are usually fast and are known to require a less number of iterations to achieve the convergence. One of the main advantages of direct search method is that, it is easy to apply for different problems with little modifications to the algorithm. Because of its simplicity, the algorithm has been used for many successful practical applications (Norvig and Rassell 2003). Gradient based methods use not only the objective functions and constraints, also first and/or second order derivatives of objective functions and/or constraints to guide the search process, assuming that the objective functions are differentiable (Norvig and Rassell 2003). These methods have the advantage of converging with lesser evaluations, and hence much faster. They however have been found disadvantageous when used in discontinuous and non-differentiable problems.

Classical methods are therefore considered fast and can be used to tackle variety of problems. But some tines get stuck at local optima (or at a sub optimal solution) and may have problems in discrete search spaces. Trajectory optimisation problems may contain non-linearity, some variables used could contain complex interactions and with a design space that may have numerous undesirable local optima. Classical methods have, therefore not been found entirely suitable for this kind of applications (Hartjes at. el., 2011).

(ii) Random Search Methods

According to Schwefel (1981), random search methods are all those ones in which the parameters vary according to probabilistic, instead of deterministic rules. This means the parameters are subjected to randomness which however does not necessarily imply arbitrariness. The randomness of the optimisation parameters allows the searching process to explore

solutions in many different directions independent of the structure of the objective function. On the other hand, due to the randomness the optimisation process sometimes does not take optimal steps towards the solution and hence may require a significant amount of computational cost. However, relative simplicity of the random search method and its independence from the information about the objective functions make them applicable to many cases. In particular, when deterministic optimisation algorithms do not have desired success due to situations such as, (i) partial derivatives of the objective functions are discontinuous, (ii) the finite steps considered are large, (iii) calculated values are subjected to stochastic perturbation. Further information about random search methods and its applications can be found in Schwefel (1981).

(iii) Evolutionary Methods

Evolutionary methods are based on the principles of natural evolution and reproduction. The basic idea of using evolutionary concepts in creating a problem solving algorithm was first conceptualised by John Holland and his colleagues of University of Michigan (Holland 1975, Deb 2002 and Quagliarella 1998). It basically uses the principle of 'survival of the fittest and extinction of the weaker species through natural selection. The salient points of the theory suggest that strong individuals in a population have a greater chance of passing their genes to future generations via reproduction (cross-over) and therefore over a period of time (after many generations species carrying the correct combination of genes become the dominant population. During the lengthy process of evolution random changes may occur in genes (mutation), thus changing characteristic of an individual chromosome and its future generations. However, if these processes provides an additional benefit / advantage in terms of survival or fitness, new species evolve or they are duly eliminated through the process of natural selection. The most important evolutionary methods are; (1) Evolutionary Programming, Evolutionary Strategies, (3) Genetic Programming and (4) Genetic Algorithms (GAs). Among all evolutionary techniques GAs are most widely used, and they have had a significant impact on optimisation (Norvig and Russell 2003).

Like other evolutionary techniques, GA also follows the same basic process in finding solutions. However it is important to note that the study undertaken uses a real parameter genetic algorithm and not the binary coded genetic algorithm, the essential difference being the variables are all treated as real numbers and not binary bits. The difference is very significant and hence the reader is referred to literature for more detail explanations (Fonseca 1993 and Deb 2002). In GA, the variables used are termed as genes. A set of genes used at any instance form a chromosome. The set of chromosomes defines the population. The solutions thus

calculated using the variables or genes form the raw fitness of each chromosome in the population. The genetic algorithm sorts the chromosomes out based on their fitness and based on a pre-set population count, the algorithm eliminates the least fit individuals. Finally the fit individuals selected form a new generation. Amongst the fit individuals (or chromosomes) selected, a further set is randomly selected to form a mating pool and genetic operators are utilised to cross-over (essentially reproduction where two chromosomes are used to create offspring) and mutate (wherein the operator introduces a random 'genetic change') the selected chromosome. The crossed over and mutated offspring are again merged into the population and fitness value of each chromosome is calculated. The process then continues iteratively to form new generations till prefixed criteria, such as maximum fitness possible or maximum generations are reached.

Generally evolutionary methods, in particular GAs are considered to be well suited to solve problems in which functions relating inputs to outputs are unknown and many have an unexpected behaviour. They also have been found to be effective where standard nonlinear programming techniques would be inefficient, computationally expensive, and in most cases find a relative optimum that is the closest to the starting point (Rao 1996)

It has been argued (Betts, 1998) that evolutionary methods are not adequate enough to solve trajectory optimisation problems as they involving some sort of stochasticity during the searching process and computationally inferior when compared to gradient based techniques in classical methods. This inadequacy argument originated from considering that trajectory optimisation problems are not characterised by discrete variables. However, work conducted by Navaratne 2012, Gu 2012, Nalianda 2012, Yokoyama 2001, Miki 2002, Celis 2010, Pervier 2011 and Celis 2014, justify the fact that GA is indeed suitable for this class of optimisation problems. Even more, for aircraft trajectory optimisation involving multi model integration, where the characteristics of the functions relating inputs to outputs are unknown Thus algorithms of this type appear to be the only practical alternative solution. A number of reasons that GA is effective for solving aircraft trajectory optimisation problem comparing to other methods are given below:

- Genetic Algorithms are robust, they use probabilistic rules and an initial random population to guide their search in comparison to classical methods (which are fixed transition rules), and hence can recover from early mistakes and enable them to handle a wide class of problems.
- GAs make use of a parallel processing to search for the optimum, which means that they are explore the solution space in multiple directions at once. If one

path turns out to be a dead end, they can easily eliminate it and progress in more promising directions, thereby increasing the chances of finding the optimal solution.

- GAs required minimum problem information, hence can be made problem independent with a limited increase in complexity
- GAs flexible in exploration and exploitation of the decision variable space. Genetic algorithms allow better control of exploration and exploitation of the decision variable space by varying the parameters involved in genetic operators (mutation and crossover), unlike classical methods which have fixed degrees of transition rules and hence have fixed degrees of exploration and exploitation. Therefore, this allows the algorithm to recover quickly out of a local optimum region, if encountered.
- GAs can implement and execute parallel. They can be easily and conveniently used in parallel systems with multiple processers to evaluate solutions in a distributed manner and hence enable reduction of computational time substantially.

From the all the above stated optimisation methods, GAs have been chosen for trajectory optimisation, because of their large number of successful applications worldwide. However, it is important to highlight that the combination (hybridisation) of GA with other optimisation techniques has also been considered for aircraft trajectory optimisation (Patra 2013). This is due to the fact that although GAs are extremely efficient optimisation techniques, they are not the most efficient for the entire search phase (Patra 2013). Thus hybrid optimisation methods have been developed as they have the potential to improve the performance in a given search phase. For an example GA techniques use for the random search phase during the beginning of the optimisation process to increase the quality of the initial population and gradient based technique at the later part of the optimisation process to refine the quality of the optimum point once the global optimum region has been found (Yokoyama 2001 and Patra 2013). The next part of this Chapter reviews the applications of each optimisation technique used in aircraft trajectory optimisation problems for minimum emissions.

2.3.2 Trajectory Optimisation work done in the past

A large amount of work has been done in the area of trajectory optimisation to reduce environmental emissions. Torrens (2011) studied and investigated how aircraft can take off and climb with a minimum environmental impact. Multi objective optimisation of a short range commercial aircraft with turbofan engine was considered. Trajectories were optimised for CO_2, NO_x, Noise and DOC for the take off and climb phase. The approach and landing phases were not considered as engines are operated at low power settings for which emissions of NO_x are low, and the concentration of NO_x is thus mainly affected by departure. The noise propagation was calculated through the Airbus Noise Level Calculation (NLC) programme. The gaseous emissions NO_x and CO_2 were computed using a fuel flow correlations DuBois (2006). DOC was calculated using the concept of airline cost index. The optimisation was performed using the mult-MADS (Mesh Adoptive Direct Search) algorithm Audet et al, (2006). The complexity of the problem was increased by including large number of constraints use in the departure procedures. Aircraft performance limitations (e.g. maximum altitude, maximum load factor, maximum allowed speeds for each configuration etc), specific safety conditions to NADPs (e.g. initialisation conditions of the procedures, minimum engine rating, etc) or en-route constraints concerning obstacles clearance were some of these constraints. The upper and lower bounds of the optimisation variables were based on the ICAO recommendations for NADPs and ATM constraints. It was found that trajectories with NO_x and noise reduction for the departure can be achieved lot at the expense of fuel burn which finally associated with CO_2 and DOC. It was concluded that operating cost cannot be neglected, but are smaller as compared to the potential gains due to the optimisation of low NO_x and noise. The main limitations of Torrens (2011), is that only the departure was optimised. No real engine performance and degradation were taken into account.

Visser and Winjen (2001) at TU Delft carried out a lot of research for optimisation of noise reduction trajectories. The methodology used by them laid the foundation and footsteps to develop a more generic tool for aircraft noise optimisation in future work. This is because the optimisation process used specific information such as the population distribution in the areas surrounding the airport. The noise model was incorporated with geographic information and was integrated with optimisation algorithm to analyse and design noise abatement procedures for a given airport. Fuel consumption and noise produced were the objectives used to minimise. A composite performance measure, consisting of the performance index using the weighing combination method was applied on the conflicting objectives. The awakening parameter was

used to see the impact of the noise produced by the optimisation process by taking population density distribution into account.

The awakening parameter is used as a function of sound exposure level (SEL). It is used as a parameter to see impact of true noise produced which calculates the number of people expected to get awake in one single event. Results were found that modification in flight paths would reduce the impact of noise on the surrounding communities while taking the constraints into account. The aircraft used for the analysis was Boeing 737-300 type at Amsterdam Airport Schiphol (AAS). It was found by applying the optimisation process the noise impact was reduced from 5042 to 3312 (about 35%) when compared to the baseline with an only 1% increase in the consumption of fuel during departure. It was also seen that for noise optimal trajectory was shifted from a densely populated communities to rural regions. The author did conclude that the tool developed is fairly flexible and generic and further optimisation algorithms and more robust models should be used to reduce the noise impact further. The above case was used during the departure at the airport. During the arrival, it was found that for a noise optimised trajectory using the same airport and the aircraft, the awakenings were reduced from 3166 to 1495 which is almost half when compared to the baseline trajectory. This noise optimal trajectory would only accounts to 30 kg more fuel burnt (15% more) and an additional time of 50s (about 10%). The main limitations of their work are, the trajectories they have used for the study were simple and engine degradation was not considered.

Reiko (2013) at DLR performed a trajectory optimisation study to assess the environmental and operational impact of a short range aircraft. The Airbus A320 type narrow aisle aircraft was selected. The flight path from Munich's Josef Strauss Airport (EDDM) to Amsterdam's Schiphol Airport (EHAM) has been designed and considered as the main scenario for the study. The design trajectory had a baseline distance of 761kn and flight time of approximately one hour and 16 minutes. The study was performed under two case studies. The cruise phase was optimised for the operation objectives of fuel and time, whereas arrival and departure phase was optimised for the environmental objectives of Time and NOx. In these phases different criteria may be important and meaningful to the assessment. The Noise and NOx emissions are normally most relevant in flight phases when the aircraft is close to the ground and populated areas. Amsterdam arrival was selected due to dense population and governmental regulations, and high restrictions exist with respect to noise emissions.

The general approach to simulate and optimise a trajectory from city to city is to use simplified two degree of freedom aircraft models along with standard gradient based optimisers. In order to more efficiently deal with the aforementioned objectives, Raiko (2013), introduced a modular wrapper model which consisted of trajectory parameterisation module, path controller and more detailed inverse aircraft model. Multi-criterial optimisation approach was used with genetic algorithm for the optimisation process (NSGA2 and GA2 algorithm). The results of the Raiko (2013) indicates, during the cruise a maximum saving of 9% in fuel mass and 6.4% in flight time could be achieved with the chosen parameter bounds. During the arrival phase the time reduction of 18% or 4 minutes was achieved.

Weiqun Gu (2013), looked into multi-disciplinary optimisation of short and medium range aircraft trajectories with turbofan, turboprop and propfan engines. Trajectories were optimised for different objectives for different flight phases of the trajectory. During the climb phase, noise and fuel burnt were optimised. The cruise phase was optimised for fuel burnt and time, while descent phase was optimised for noise and NOx. It was the first time that multi objective optimisation study was conducted for complete mission under different flight phases with different objectives and constraints. Gu's framework consisted of engine performance model, aircraft performance model, noise prediction model and emission model with a GA based NSGAMO optimiser. The optimisation carried out was bi-objective and the results obtained were thoroughly optimised compared to the initial set of reference results. The open rotor which is planned to come into service in 2030 was also assessed within the optimisation framework to achieve more economical and greener commercial aircraft. The research also included the implementation of neural networks to obtain the engine performance results with improved computational time. The main limitation of Gu (2013) work is that, it was restricted to basic aircraft trajectories, thus the author recommend more realistic aircraft trajectories need to be considered. The effects of engine degradation were not considered.

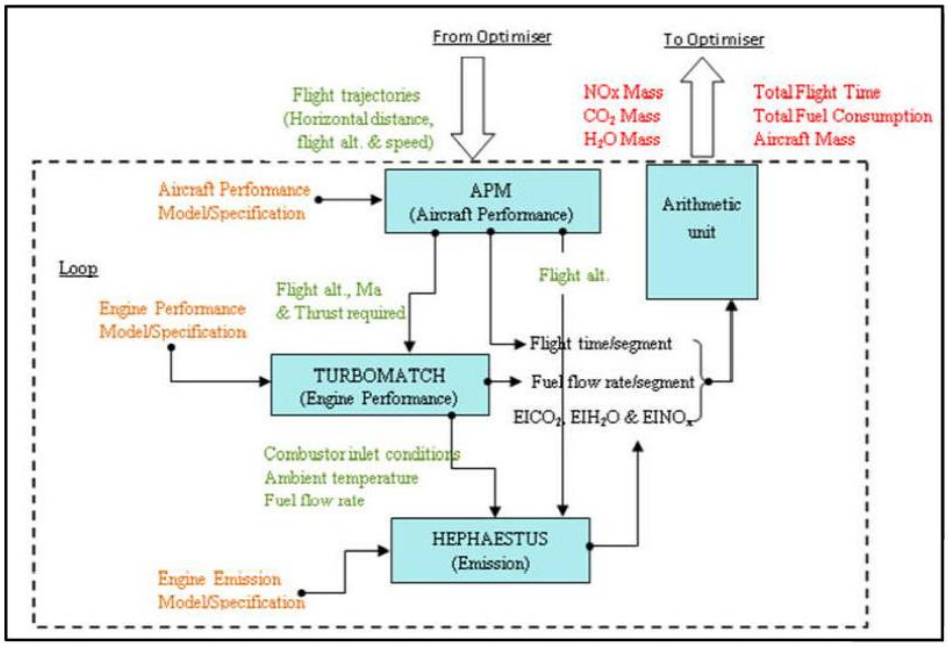

Figure 2-5 MDO framework used for trajectory optimisation (Gu 2013)

The effect of aircraft condensation trails or contrails on the climate change is another pollutant interested in recent years. Contrails form in the wake of aircraft for various reasons, but most important are the emission of water vapour and it may have a three to four times greater effect on climate than CO_2 emissions. According to Sridhar al et, (2010) the effect of persistent contrails on climate forcing requires a flight trajectory optimisation with fuel and contrails models that can develop alternative flight paths to enable trade-off between persistent contrails mitigation and fuel consumption to make acceptable aviation operational decisions. Sridhar al et (2010), developed an algorithm to calculate optimal trajectories for aircraft while avoiding the region of airspace that facilitate persistent contrail formation, focusing the subsonic aviation emissions at cruise altitude in the upper and lower stratosphere. Their strategy was to adjust cruise altitude in real time and re-route the aircraft around regions of airspace that facilitate persistent contrail formation. In their study they have used an aircraft model, aircraft fuel consumption model, developed based on Eurocontrol's Base of Aircraft Data Revision 3.6 (BADA – $f_{c=}t.SFC.Th$) and contrail formation model (CFM). The contrail formation model was developed using National Oceanic & Atmospheric Administration (NOAA) which frequently update with short range weather forecasts. The trajectory optimisation was performed considering the optimisation problem as a non-linear optimal control problem with ATM constraints, which was computationally efficient.

In first part of the study, the trade-off between persistent contrails formation and additional travel times at 10 different cruising altitudes for Chicago to New York were investigated. Additional travel times required for completely avoid persistent contrail formation was 4.3%, compared to time optimised trajectory. In the second part of their study, the trade-off between persistent contrails formation and additional fuel consumption was investigated. They have found when altitude was optimised to avoid contrails completely, total fuel consumption will be increased by 2%, compared to fuel optimised trajectory. Also found allowing a further increase in fuel consumption does not resulted in a proportionate decrease in travel times. The results in this work were based on traffic for a day and used the same type of aircraft on all routes. The limitation of Sridhar et al., (2010) work is that not using an engine performance model with the aircraft model to represent the real aircraft operation. Also the complete traffic and weather data was not used for extended periods of time to get a better understanding of the complex relation between fuel efficiency and the impact on environment.

Celis et al. (2009) investigated and demonstrated the capabilities of different optimisation methods for aircraft trajectory optimisation problem. The main aim of the study was to established preliminary requirements for effective optimisation methods for multivariable problems applied to aircraft trajectories. Commercially available GA based optimiser and Polyphemus optimiser were selected to analyse one or more phases of flight profile and results obtained correspond to a single objective optimisation process only.

The optimisation process involved three computational models; aircraft performance model, engine performance model and emission prediction model. The aircraft performance model was developed using a generic aircraft performance tool AMP corresponding to a typical medium size single aisle, twin engine (turbofan) aircraft with a maximum take-off weight (MTOW) of about 72000kg and a seating capacity of about 150 passengers. The engine performance was modelled using CU in-house gas turbine simulation code Turbomatch and to calculate gaseous emissions, Hephaestus emission prediction software was used. Additional details of these computational models can be found in Celis et al. (2010). The flight time, fuel burn and NOx emissions were selected as optimisation objectives. The results obtained during the optimisation process are presented in Figure 2-6 and Figure 2-7. The results obtained from Polyphemus optimiser agreed with the results from other commercially available optimisers with an average variation of 2%. Also it is worth to notice that, although GA based optimisers' extremely efficient optimisation techniques, they are not the most efficient for the entire search spaces. Thus author suggest to develop hybrid optimisation methods as they have the potential

to improve the performance in a given wider search space. For an example, GA techniques can be used in the random search space during the beginning of the optimisation process (to increase the quality of the initial population) and hill climbing phase at the end of the process (to refine the quality of the optimisation point, once the global optimisation region has been found).

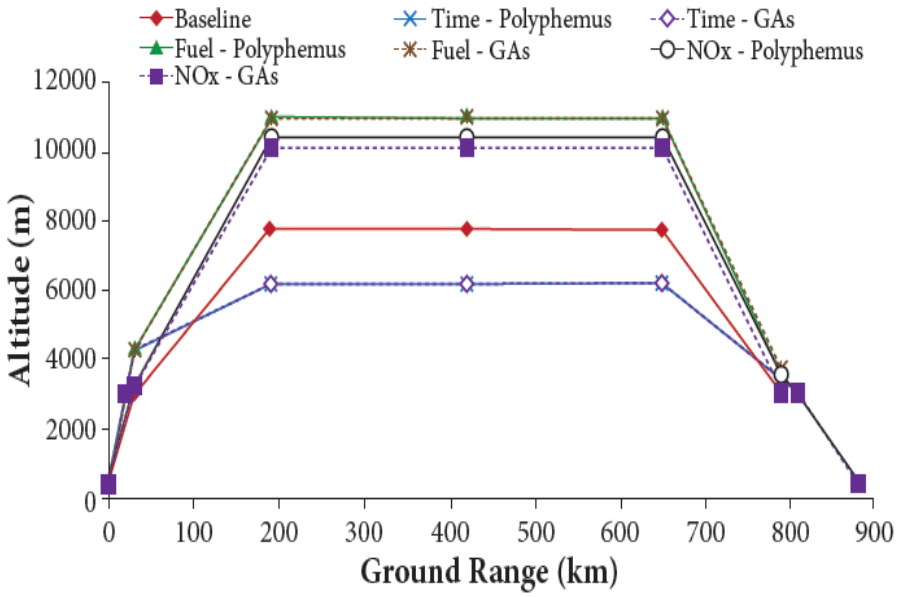

Figure 2-6 Optimum trajectories from different optimisers (Celis 2010)

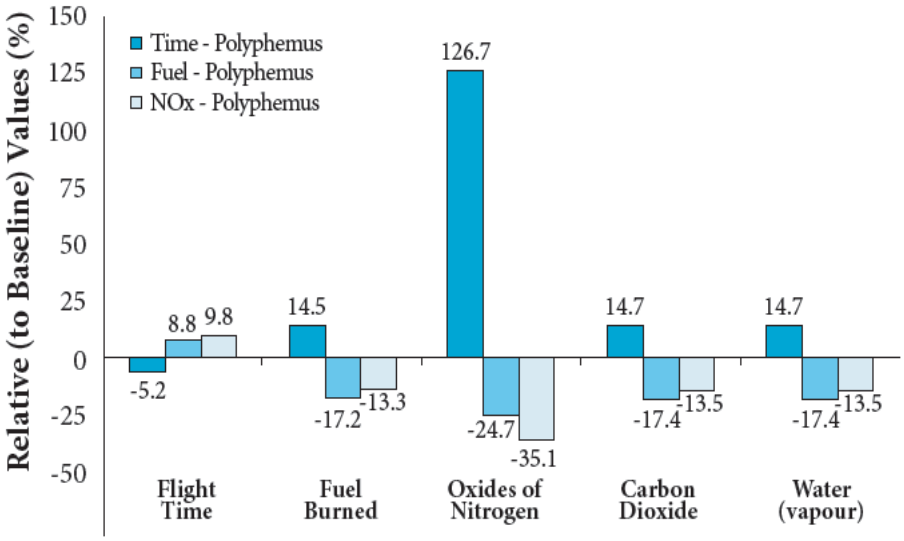

Figure 2-7 Environmental gains achieved from Polyphemus (Celis 2010)

Patra (2014) developed a Hybrid optimiser for the application of aircraft trajectory optimisation. The Hybrid optimiser combines the features of a Global Search method and a Local Search Method and applied it to multi objective – multi disciplinary aircraft trajectory optimisation problem. The Global Search method used in this case was Genetic Algorithm (GA) based on Non-dominated Sorting Genetic Algorithm – NSGA11 (Deb et al., 2002) which effective for global searching and solving non-liner, non-differential and multi Modal problems. The local search method used was Nelda Mead which is based on simplex method which is more effective in exploring attractive solutions locally. The Hybridise optimiser was given potentially better solutions in terms of convergence of solutions towards the optimal solutions and diversity of solutions. Patra used his initial development of Hybrid Optimiser jointly with the current author to test and benchmark on ZDT functions (ZDT1, ZDT 3 & ZDT 6) against the optimiser NSGAMO2 (Non-dominated Genetic Algorithm Multi Objective 2- the optimiser developed based on Genetic Algorithm only), which was one of the well-established and widely used optimiser for trajectory optimisation (Hugo SAE). The better results, of both in terms of 15% average improvements towards the optimal solutions and 20% average improvement of diversity of solution were found (Patra & Navaratne, 2012). Further, hybrid optimiser was used in a multi objective optimisation framework to perform two and three objectives optimisation problem in three case studies. In the first case study the hybrid optimiser was applied on a simple departure setup and was found to be producing better solutions in terms of convergence against the NSGAMO2 optimiser. In the second case study the aircraft trajectory optimisation framework was extended to optimised three objectives and the last case study simulated the flight from London Heathrow Airport in United Kingdom to Amsterdam Schiphol Airport in Netherlands.

In each case the hybrid optimiser solutions outperformed better solutions in terms of convergence. During the complex and constrained descent phase, the hybrid optimiser had 3.5 times more feasible solutions in respect to the global search method of NSGAMO2, which showed that the solutions obtained were much better in terms of diversity as well. The conclusion of the Patra's (2014) work was that Hybrid (i.e. combination of global and local search method) can provide better solutions than both traditional global search and local search methods on its own in terms of convergence speed towards the optimal solutions and divergence of the optimal solutions. The main limitation of Patra (2014) is that trajectories considered for the assessments was restricted to basic aircraft trajectories and improved engine performance and aircraft performance models with operational constraints to generate more realistic aircraft trajectories need to be considered.

As seen in literature, aircraft can be flying differently to minimise the emissions, but proposed modified or new trajectories should be able to accommodate all the ATM controls required. Therefore, it is important to review the current and future aircraft operational policies and procedures. In this part of the section a brief review of the operational aspects will be provided. Aircraft operation and operational procedures are continuously revised in the recent past in order to accommodate various changes. Among them, introduction of new aviation policies being an important factor when environmental effects such as gaseous or noise emissions in aircraft operation are concerned. The International Civil Aviation Organisation (ICAO) and Committee on Aviation Environmental Protection (CAPE) regulatory update policies and standards on aircraft engine emissions which for example, address the engine certification requirements in terms of pollutants emitted at Landing and Take-off (LTO) cycle as shown in Figure 2.8, which accounts for emissions at typical operational modes. It provides an operational allowance for the engine power settings at idle, take-off, departure, and approach conditions. However, still there are specific regulatory requirements enforced for emissions released beyond LTO cycle such as cruise conditions (ICAO 2006).

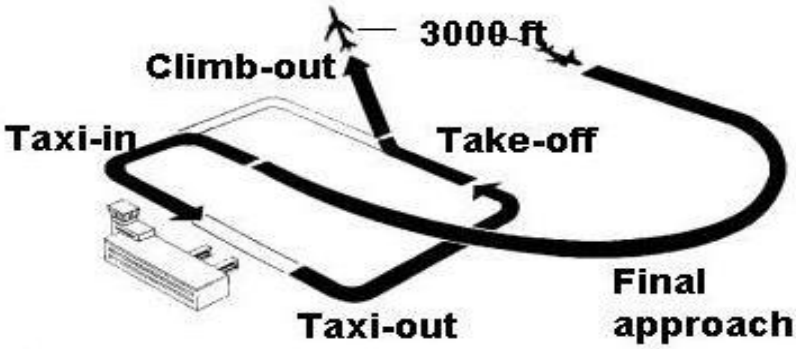

Operating mode	Power setting	Time in mode
1. Taxi / idle	7% take-off thrust	26.0 minutes
2. Take-off	100% std day take-off thrust	0.7 minutes
3. Climb	85% take-off thrust	2.2 minutes
4. Approach	30% take-off thrust	4.0 minutes

Figure 2-8 Landing and Take-Off (LTO) cycle (ICAO, 2010)

Several countries such as Switzerland and Sweden have introduced local legislations which allow airports to introduce emission based landing charges depending on the amount of NOx emitted during the landing and take-off, to reduce environmental pollutions. However, all the airports are operating their airspace based on, one or more strategic objectives: (a) safety, (b)

capacity, (c) efficiency, (d) accessibility and (e) environment (ICAO 2006). The ICAO has published comprehensive description of guidelines to construct visual and instrumental flight procedures while maintaining acceptable levels of safety (ICAO 2006). These guidelines cover standard operating procedures such as regular departure, en-route and approach profiles as well as more specific procedures such as noise abatement flight profiles for take-off approach and landing.

Torres (2011) investigated a methodology for reducing the environmental footprint of aircraft based on the optimisation of departure procedure. The feasibility of this study was illustrated with a current in-production Airbus single aisle aircraft departing from an ideal airport. For the purpose of the study three environmental criteria (noise, NO_x and CO_2 emissions) have been optimised in pairs. The noise perceived on ground is estimated through the Airbus Noise Level Calculation Program (NLC), the Airbus software delivered to airlines to predict operational noise. The NLC uses a database dedicated to each aircraft and engine combined model to compute the overall generated noise. This databased, derived from the static engine noise tests and Airbus airframe noise models, and contains total aircraft noise spectra depending on speed, aerodynamic configuration, and engine thrust rating. NOx emission was computed using the fuel flow correlations method given in DuBois (2006) and emission index of EI_{NOx}. The typical threshold altitude was selected at 3000ft above ground level (AGL) based on the airport location and atmospheric conditions, as NOx are harmful for air quality in the lower troposphere. The amount of CO_2 emissions was also calculated based on the fuel burn correlations given in the DuBois (2006).

$$NO_x = \int_{h=0}^{h\ threshold} (EINOx.FF)dt$$

The take-off flight path was modelled through an enhanced NADP (E-NADP) pattern, which is an extended version of NADP1 and NADP2 patterns. While the standard NADP1 and NADP2 patterns start at the altitude of 800 ft, whereas the E-NADPs proposed in this study start at 35 ft. The problem was formulated through a multi objective non linear, constrained optimisation problem and to solve the problem more efficiently, the multi-MADA method was proposed. This free derivative algorithm approximates the Pareto optimal fronts by solving a series of single objective optimisation using the MADS optimisation method. The results of the problem were in the optimal of the considered environmental criteria and their associated optimal flight path. Also it is important to note that, the study was performed in a research perspective using

Airbus-designed software and keeping in mind that operational feasibility has not been confirmed. Further related work suggested assessing the validity of optimal departure results in more advanced scenarios.

Another factor which influences aircraft operation is air traffic management (ATM) or air traffic control (ATC). As outlined in the introduction Chapter of this work air traffic has significantly grown in the recent past and is expected to grow by two to three times in next 25 years (NextGen, 2007 and Jensen, 2007). The management of trajectories and missions is one of the identified solutions found to reduce the fuel burn and environmental emissions due to aircraft operations. Therefore the current ATM system should able to cope up not only with the increase in air traffic with the current routes, also accommodate various proposed economical and environmentally friendly trajectories by relaxing the current controls.

With this aim, Soler and Zapata (2012), developed a framework for aircraft trajectory planning and optimisation. The main objective of their work was to implement green aircraft trajectories under more efficient ATM procedures under SESAR project, as current air traffic management is a complex, highly regulated and inefficient system (SESAR, 2008). SESAR (Single European Sky ATM Research) is a technology initiative established to reduce aircraft emissions and fuel consumption in flight profiles. In particular, 8-14 min gain per flight on average, 300-500 kg reduction in fuel per flight on average and 945-1575 kg reduction of CO_2 emissions per flight on average by 2020 (SESAR, 2008). The authors developed their methodology on "Optimised Procedured Profiles (OPPs)", which are based on a relaxation of current procedures by setting, in general, just one procedure per phase and relaxing some trigger conditions of switching between phases. To evaluate the methodology, A320 type aircraft short and medium range vertical optimised procedure profiles were compared with fully procedure profiles, those used in the current paradigm and free-flight profiles, considered as optimal performance benchmarks. Authors considered this problem as a conventional optimal control problem (Soler, et al., 2010). Trajectories were optimised for the fuel burn and flight time. Aircraft performance, flight procedures, and the resulting consumptions were analysed and discussed. The short range aircraft flight profiles for the fully procedure, optimised procedure and free-flight are shown in Table 2-1, to Table 2-3. The fuel saving achieved coincided with the ones expected by SESAR (300-500 kg per flight on average).

Table 2-1 Short range fully procedured flight profile

Phase	Name	AC	ET	OP	OC[a]
0	TO	TO	$V = 1.3V_{S_{IC}}$	T_{max}	$V_{CAS} < 250$ kt
1	IC	IC	$V = 1.3V_{S_{CR}}$	T_{max}	$V_{CAS} < 250$ kt
2	Res. free climb	CR	$h = 10,000$ ft	T_{max}	$V_{CAS} < 250$ kt
3	Climb accel	CR	$V_{CAS} = 300$ kt	$h = 10,000$ ft, T_{max}	——
4	Climb CAS	CR	Mach $= 0.78$	CAS $= 300$ kt, T_{max}	——
5	Climb Mach	CR	$h = FL320$	$M = 0.78$, T_{max}	——
6	Cruise	CR	——	$h = FL320$, $M = 0.78$	——
7	Descent Mach	CR	$V_{CAS} = 300$ kt	$M = 0.78$, T_{min}	——
8	Descent CAS	CR	$h = 10,000$ ft	CAS $= 300$ kt, T_{min}	——
9	Descent decel	CR	$V_{CAS} = 250$ kt	$h = 10,000$ ft, T_{min}	——
10	Res. free descent	CR	$h = 6000$ ft	T_{min}	$V_{CAS} < 250$ kt
11	Approach	AP	$h = 2000$ ft.	PATH $= -3$ deg	$V_{CAS} < 250$ kt
12	Landing	LD	Final cond.	PATH $= -3$ deg	$V_{CAS} < 250$ kt

[a]OC refers to operational constraints due to operations near airports.

Table 2-2 Short-range optimised procedured flight profile (Soler, 2012)

Phase	Name	AC	ET	OP	OC
0	TO	TO	$V = 1.3V_{S_{IC}}$	——	$V_{CAS} < 250$ kt
1	IC	IC	$V = 1.3V_{S_{CR}}$	——	$V_{CAS} < 250$ kt
2	Res. free climb	CR	$h = 10,000$ ft	——	$V_{CAS} < 250$ kt
3	Climb accel	CR	——	$h = 10,000$ ft	——
4	Climb CAS	CR	——	CAS, T_{max}	——
5	Climb Mach	CR	——	M, T_{max}	——
6	Cruise	CR	——	HO	——
7	Descent Mach	CR	——	M	——
8	Descent CAS	CR	$h = 10,000$ ft	CAS	——
9	Descent decel	CR	——	$h = 10,000$ ft	——
10	Res. free descent	CR	$h = 6000$ ft	T_{min}	$V_{CAS} < 250$ kt
11	Approach	AP	$h = 2000$ ft	PATH	$V_{CAS} < 250$ kt
12	Landing	LD	Final cond.	PATH	$V_{CAS} < 250$ kt

Table 2-3 Short-range free flight profile (Soler, 2012)

Phase	Name	AC	ET	OP	OC
0	TO	TO	$V = 1.3V_{S_{IC}}$	——	$V_{CAS} < 250$ kt
1	IC	IC	$V = 1.3V_{S_{CR}}$	——	$V_{CAS} < 250$ kt
2	Res. free climb	CR	$h = 10,000$ ft	——	$V_{CAS} < 250$ kt
3	Free CL/CR/DS	CR	$h = 10,000$ ft	——	——
4	Res. free descent	CR	$h = 6000$ ft	——	$V_{CAS} < 250$ kt
5	Approach	AP	$h = 2000$ ft	——	$V_{CAS} < 250$ kt
6	Landing	LD	Final cond.	——	$V_{CAS} < 250$ kt

One important aspects of aircraft trajectory optimisation is engine performance. It is important to understand the impact of engine performance and performance deterioration over the time on the aircraft mission and also when trajectories are optimised for minimum environmental emissions. Lukachko and Waitz (1997) at MIT investigated the impact of representative paths of engine degradation on NOx emissions at cruise phase. The methodology for the study was based on analytically oriented technique similar to the approach used by Aker and Saravanamuttoo (1989). Three engine cycles were developed, using CF6-50C2 high bypass and GE90-85B ultra high bypass subsonic engines and supersonic turbo jet engine Olympus 593 Mk 610, which was proposed to power the proposed medium range 275 seat passenger European High Speed Civil Transporter (HSCT) with the Mach number of 2.0. Engine cycles were developed using the commercially available cycle deck GASTURB. Cycles were specified as completely as possible; employing data available in the open literature for primary (e.g. bypass ratio, pressure ratio, total mass flow and turbine entry temperature) and secondary (e.g. bleeds, cooling air etc.,) cycle parameters. Cycles were matched to performance data primarily through iterative on values for TETs and component efficiencies, pressure ratios and some secondary parameters. Cycle results were compared to typical published performance data for both design and off-design conditions resulting in thrust and SFC. The effect of engine degradation was introduced by changing the mass flow capacity and efficiencies of the components such as fan, LPC, HPC, HPT and LPT. Typical limits on changes in engine parameters for a turbo fan engine are given in Table 2-4. The emission prediction was achieved from correlating engine operating parameters with NOx emissions levels obtained from engine performance and data obtained via full scale engine tests at ground level and at altitude. The analysis and methodology was validated comparisons to test data available.

The results of the study indicates that for subsonic turbofans, HPC, LPC, fan and LPT degradation increases NOx emissions whereas deterioration of the HPT decreases NOx emissions. Degradation of the HPT and HPC had the largest effect on cycle parameters and NOx emissions. Increased sensitivity of NOx with increasing OPR or turbine entry temperature (TET) also observed. For the supersonic case, all degradation scenarios led to increased emissions, however, the sensitivity to changes in cycle parameters was smaller than for subsonic cases. In all cases, both turbine and compressor faults (degradation) an increase in EINOx was exacerbated by the changes in fuel flow and a decrease in EINOx was attenuated. In addition, scenario analysis of the Lukachiko (1997), confirmed the usefulness of the influence coefficients indicating fairly linear changes in cycle parameters with increasing degradation levels for HPT-only, HPC-only and HPT+HPC degradation cases. For a 3% SFC rise over all limit, decreases in NOx for turbofans with HTP-only degradation for all simulations fell

between -8% and -14% and increase in NOx for HPC only deterioration were between +10% and +25%. Combining these degradation effects resulted in a -1% to +4% changes in the NOx emissions. For the supersonic case changes were much smaller with 3% SFC limitation was resulted in +1% changes for both HPT-only and HPC-only scenarios, and +3% for the combines case. Finally several sources of uncertainties associated with the lack of performance data, and lack of detail information regarding the NOx correlations used were identified. The work of Lukachko and Waitz (1997) was limited only to investigate the effects of engine degradation on aircraft NO_x emissions of the cruise phase. The NO_x emission of complete mission was not considered. More realistic trajectories need to be considered.

Table 2-4 Typical degradation limits for a turbo fan engine (Waitz, 1997)

Parameter	Limit	Reason
Fan Mass Flow	-5.0%	LPC Surge
LPC Mass Flow	-8.0%	High turbine temperature
Fan Efficiency	-5.0%	High turbine temperature
HPC Mass Flow	-8.0%	High RPM
HPC Efficiency	-4.5%	High turbine temperature
HPT Nozzle Effective Area	+6.0%	LPC Surge
HPT Nozzle Effective Area	-6.0%	HPC Surge
HPT Efficiency	-5.0%	High turbine temperature
LPT Nozzle Effective Area	+8.0%	Low thrust
LPT Nozzle Effective Area	-6.0%	LPC surge
Combustor Exit Temperature	+2.5%	Turbine life
Specific Fuel Consumption	+4.0%	Economy

Segovia (2012) used Techno Economic Environmental Risk Assessment type approach to make preliminary analysis on clean and degraded engine performance for short range missions. The work presented by Segovia (2012), was based on the collaborative effort with the present author who provided technical leadership and direction has contributed to the preliminary requirements of this research. Segovia (2012) used a multidisciplinary multi objective optimisation framework developed in MATLAB to identify the optimum trajectories for the clean and degraded cases. The effects of engine degradation on the high pressure turbine (HPT)'s creep life, low cycle fatigue life and oxidation life were assessed. The engine model used for these assessments was a typical twin spool high bypass turbofan engine with separate exhaust similar to CFM56-5B2/3 engine used to power an Airbus A320 type civil aircraft. The design point for

the engine model was set at Take-off (TO) Sea Level Static (SLS) and International Standard Atmosphere (ISA) conditions. For the engine degradation, aircraft performance and life assessments, Segovia (2012), introduced 2% degradation in isentropic efficiency and flow capacity across the compressors and the turbines. The analysis were for single component degradation. The clean engine trajectory assessed at 10,668m cruise altitude and 0.8Mach number was set as the baseline (reference) trajectory against which the degraded and optimised trajectories were compared. For the optimisation assessments, full flight trajectories were assessed but the optimisation was only for cruise segment. The bounds for the variables (cruise altitude and cruise speed i.e. Mach number) ranged from 10,000m to 12,000m and 0.75 to 0.85 respectively. The climb and descent profiles were assumed to follow the same altitude and speed profiles as for the baseline trajectory.

The results of the study clearly indicate that degradation causes a drop in overall pressure ratio (OPR), mass flow and net thrust. The results showed an increase in SFC and fuel burn for the same thrust requirements and trajectory flown due to engine operating at high spool speeds and high turbine entry temperatures (TETs). Also results shows the effects of individual component degradation on mission fuel burn, HPT's life and impact of component degradation on the fuel burn optimised trajectories are presented in the below Table 2-5. As shown in the table the fuel burn optimised trajectories for the degraded engines differ from that of the clean engine. HPT blade and disc life reduction due to individual component degradation when the trajectories were optimised are also presented. The trajectory optimisation results compare well with the results of Gu (2013) and Venediger (2013) which showed that optimised trajectory for minimum fuel burn is achieved at lower optimal speeds and higher flight altitudes (where the aircraft drag is less).

Segovia (2012) concludes that optimising for fuel burn give more saving for the degraded engine than for the clean engine, savings which are likely to benefit the engine operating costs. The results demonstrate the importance of flying the optimised fuel burn trajectories since the economic impact will increase with the number of flights. The results of lifing assessments show that engine component degradation will shorten the HPT useful creep life, LCF life and oxidation life. The limitations of Segovia (2012) is that the degradation levels have been arbitrary introduced, and individual components have been degraded independent of each other, which is not in practice. The optimisation has been limited to only the cruise phase. The trajectories generated for the optimisations are simple 2D trajectories and any ATM constrains have not been considered.

Table 2-5 Trajectory variation for the clean and degraded cases (Sogovia, 2012)

Engine Configuration	Baseline Fuel Burn Delta [%]	Optimum Fuel Burn Delta [%]	Optimum Cruise Altitude [m]	Optimum Cruise Mach Number [-]
Clean	00.00	-4.80	12000	0.77
2% Fan*	11.90	5.30	11400	0.75
2% LPC*	24.80	7.70	11900	0.75
2% HPC*	13.30	4.70	11600	0.75
2% HPT*	09.90	3.40	11600	0.75
2% LPT*	09.90	4.90	11900	0.76
* Percentage represent level of degradation in efficiency and flow capacity				

Venediger (2013) analysed the commercial aircraft trajectories with the impact of engine performance degradation on fuel burn and NO_x emissions. The author uses the generic multi-disciplinary trajectory optimisation framework to identify the potential for optimised aircraft flight trajectories for short range and medium range missions. The engine model used in this work was typical twin spool high bypass turbofan engine with separate exhaust similar to the CFM56-5B3 engine used to power A320 type narrow body twin engine aircraft. The design point for the engine model was set at top of climb (TOC). To model the effects of engine degradation, 2% level of deterioration were made to the efficiencies and pressure ratios of main engine components such fan LPC, HPC and HPT. Analysis was done for single component degradation. The clean engine trajectory assessed at 10668m standard cruise altitude and 0.8 Mach number was set as the baseline trajectory against which the degraded and optimised trajectories were compared. Aircraft trajectory optimisation studies were conducted to minimise mission fuel burn, mission time and NOx emissions. For the optimisation assessments full flight trajectories were analysed but only the climb and cruise segments were optimised. Seventeen climb altitudes, cruise altitude and cruise Mach number with upper and lower bounds were selected as optimisation variables. The take-off, descent, approach and landing segments were kept the same for all trajectories.

The results found by the Venediger (2013) from the short range mission suggested a trade-off between fuel burn versus flight time and showed a fuel burn reduction of 3.0% or a reduction in flight time by 6.7% when compared to non-optimised base line trajectory. Whereas optimisation of fuel burn versus NOx emissions revealed the objectives to be non-conflicting. The medium range mission showed similar results with fuel burn reduction of 1.8% or flight time reduction of 7.7% when compared to base line degraded trajectory. Accordingly, non-

conflicting solutions for fuel burn versus NOx emissions have been achieved. Further, these results are well with the results shown by Segovia (2012), Chandran (2013) and Kelaidis et al (2009). The optimised trajectories identified by Venediger (2013), demonstrate possible potential solutions to reduce environmental impact. The main limitations of this work is that degradation levels have been arbitrarily introduced, and individual components have been degraded independent of each other, which is not the case in practice. The optimisation has been limited to only the climb and cruise phases. The engines considered for the optimisation was degraded but the aircraft performance model limited to generate only simple basic 2-D trajectories, which is not the case in real life representation. No aircraft traffic management constraints and procedures taken into account.

Nqobile (2014) also used Techno-economic Environmental Rick Assessment (TERA) type approach to investigate the change in engine life usage when optimising for flight mission fuel burn and the change in flight mission fuel burn when optimising for engine life usage; in both cases the effects of engine component degradation were considered and assessed. The author used the generic multi-disciplinary optimisation framework with several models as shown in Figure 2-9. The engine model used in this work was a typical twin spool high bypass turbofan engine similar to CFM56-7B27 engine which use to power Boeing 737-800 type twin engine narrow body single aisle aircraft. The design point for the engine model was set at TOC. Engine degradation was introduced by deteriorating flow capacity and efficiencies of the booster, HPC, HPT and LPT. The engine life calculated was based on HPT blade life and HPT disc life due to creep, fatigue and oxidation failure modes independent of each other. Mission fuel burn and engine life trajectory optimisation assessments were conducted to incorporate the effects of degradation after 3000, 4500 and 5250 cycles of operation. Further assessments were made linking aircraft performance to airport severity factors for the clean engine, after 3000cycles and 5250 cycles The trade-off between mission fuel burn and engine life optimised trajectories were presented in this work for three routes; London – Madrid, London – Ankora, and London – Abu Dhabi.

The results of the Nqobile (2014) study, indicates that airports at higher altitudes e.g. Cairo, suffer more severity due to high operating temperatures, but benefit from less climb fuel burn and lower operating costs. The severity and fuel burn for take-off at airports with higher ambient temperatures (OATs) was found to be more due to higher operating temperatures required. The operating costs at these airports were thus higher. The fuel burn optimised trajectories were found to be achieved at higher operating temperatures with reduced blade life (due to creep, fatigue and oxidation). In particular, for London – Madrid, the blade creep and

blade oxidation lives were found reduced by -3.4% and -2.1% respectively. These blade oxidation life optimised trajectories showed increase in fuel burn of +3.6% and +4.9% for London – Madrid and London – Ankara respectively. The blade creep life optimised trajectories for London – Abu Dhabi were found to benefit from less fuel burn during climb. The disc creep life optimised trajectories showed benefit in fuel burn for London – Ankara and London – Abu Dhabi.

Nqobile (2014), concluded his work with the following findings: (a) High OAT and high altitude airports such as Abu Dhabi require higher operating temperatures which have severe consequences on the component life, fuel burn and emissions. (b) Fuel burn optimised trajectories have a negative effect on the blade life (creep, fatigue and oxidation) due to higher maximum operating temperatures. However the reduction in fuel burn was more predominant than the reduction in life, thus benefitting to the operating costs. (c) Optimising for blade creep life benefits the fuel burn for London – Abu Dhabi due to less fuel burn at climb. (d) The blade oxidation life optimised trajectories were detrimental to the fuel burn due to slower cruise speeds and more time spent at cruise and descent. (e) The disc creep life optimised trajectories benefit the fuel burn for London – Ankara and London – Abu Dhabi due to flying at higher cruise attitudes and burning less fuel. As with the other studies that have been reviewed, the main limitations of Nqobile (2014) work was, degradation levels have been arbitrarily assigned and individual components have been degraded independent of each other. Also the study was limited to basic aircraft trajectories, which is not the case in practice, thus the author recommended, that more realistic aircraft trajectories need to be considered.

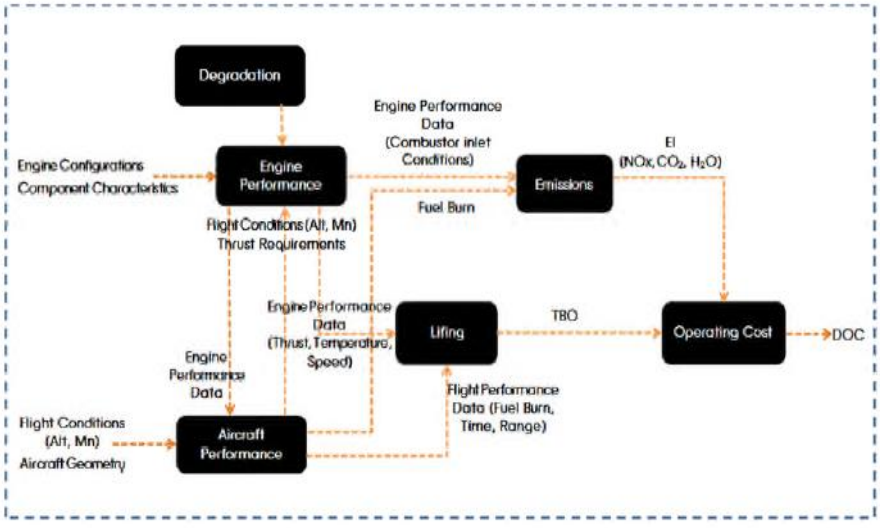

Figure 2-9 Flow Diagram of Multi-Disciplinary Framework (Nqobile 2014)

2.4 Summary

It can be seen from the literature a lot of research has been carried out in order to address the growing public concern about aircraft emissions. Aircraft noise, carbon dioxide, NOx and contrails are some of the main concerned emissions. Several solutions have been proposed to reduce aircraft emissions but most of them are long term solutions. Optimising the trajectories and missions is one of the key identified solutions found to minimise the aircraft emissions and is a measure that can be readily implemented. The approaches taken to identify these green trajectories are by simulating the aircraft, and engine in a multidisciplinary optimisation framework. Also it has been observed that, fairly high fidelity models have been developed to simulate, aircraft and, engine performance, and also to predict gaseous emissions and contrail formation. GA has been considered as one of the suitable optimisation technique to solve this kind of multi objective optimisation problems. In order to make the trajectories more realistic, several researchers have incorporated degraded engine performance into trajectory optimisation process. However, it was also found from the reviewed literature, degradation levels of components have been arbitrarily assigned independent of each other without taking the combine effects of components and variations of engine performance and monitoring parameters (such as EGT, EPR, N1, N2) into consideration. Also the studies were limited to basic aircraft trajectories, which are not the case in practice. Finally author found that more realistic aircraft trajectories need to be considered with degraded engines in order to truly understand the optimised environmental friendly trajectories that can actually be deployed by airlines.

3 Engine degradation and impact on performance

3.1 Introduction

This chapter focuses on engine degradation and the impact of degradation on the performance deterioration of the engines. Short range and long range aircraft engines are studied. The initial part of the chapter discusses the various degradation mechanisms and their influence on the main engine components. The various levels of degradation mechanisms are simulated to analyse the sensitivity of engine performance to component degradation. The impact of degradation on engine performance parameters of net thrust, sfc and key monitoring parameters such as fuel flow, engine pressure ratio and exhaust gas temperature were assessed at different engine operating points. Finally three short range and long range degraded engine models were created based on the engine performance data available in the public domain and EGT margin deterioration data provided by the Srilankan Airline. These models were integrated with the aircraft dynamic models which have been used in the optimisation frame work.

3.2 Degradation of aircraft engines

Engine degradation can be characterised as the combination of short term and long-term effects, both of which result in performance losses. These trends are shown schematically in Figure 3.1. As shown in the figure a rapid loss occurs during the engine's initial service flight followed by gradual performance deterioration until the engine is reconditioned. For both economical and mechanical reasons, only part of this total degradation is restored in the maintenance process resulting the engine returned to service with a reduced level of performance. As the engine continues operation, these unrecoverable losses increase with additional maintenance cycles. A portion of long term losses are cyclically restored with each shop visit. Generally initial (or short term) degradation is more closely associated with the engine design itself rather than the operational use of the engine. Long term (or time developing) losses are more related to the characteristics of the aircraft employing the engine and the flight path it operates. Also it is important to notice that degradation of some engine components are correlated with number of cycles rather than hours in operation.

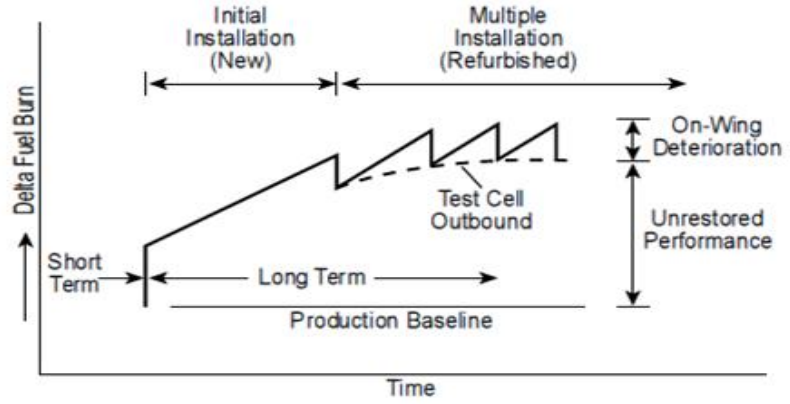

Figure 3-1 A model of engine performance deterioration (Waitz 2000)

3.3 Degradation mechanisms

As described above, engine degradation is associated with several aging and operating conditions that are of a time developing nature. These include physical distortion of engine parts due to various degradation mechanisms which will adversely affect the engine performance. Some of these effects can be reversed by cleaning or washing the engine which are called

recoverable degradation; others require the adjustments, repair, or replacement of components which are known as non-recoverable degradation. The degradation mechanisms of aircraft engines are different to industrial gas turbine engines, as aircraft are exposed to much wider operating conditions and various harsh environments. The main degradation mechanisms can be classified as follows;

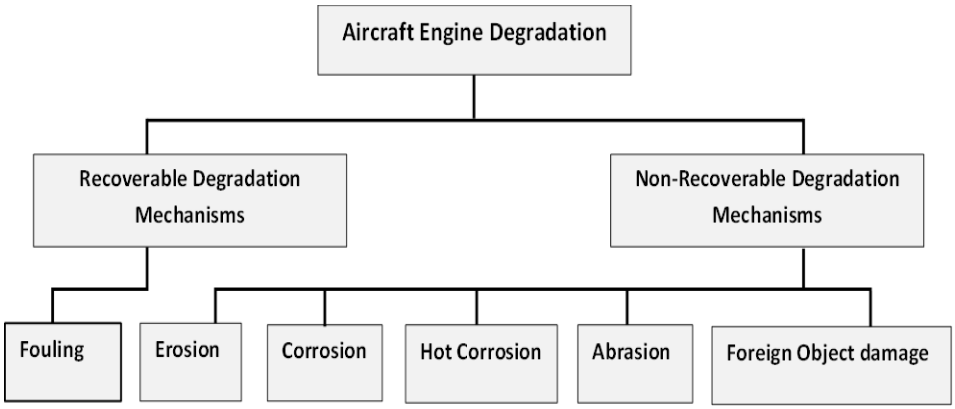

Figure 3-2 Classification of engine degradation and mechanisms

3.3.1 Fouling

The deterioration of flow capacity and efficiency caused by the contamination or adherence of particles to the aerofoils and annulus surfaces due to the presence of water mist and/or vapour is known as fouling. The particles go through the gas path of the engine and adhere to the blades and annulus surfaces. These deposits reduce the throat area, create surface roughness, and to some extend change the shape of the aerofoil, which change the aerodynamic behaviour. The result is reduction in thrust, drop of efficiency and increase fuel consumption. Sand, smoke, oil mist, sea salt, carbon and abradable wear are some common examples for particle deposits. The typical fouling particles are in the range of 2 to 10μm (Mound and Pilidis 2006). An example of a fouled compressor is shown in Figure 3.3. The most of the fouling effects can be removed from engine washing (online or off-line).

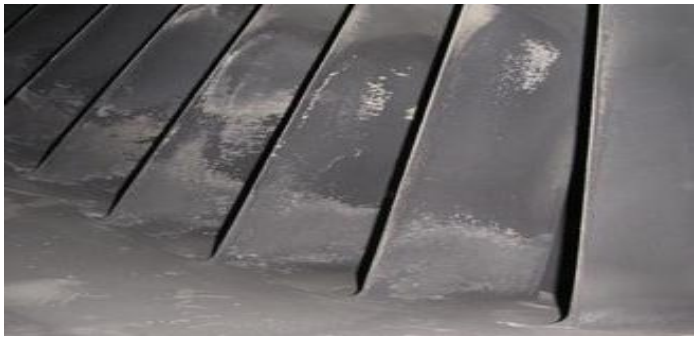

Figure 3-3 Fouling of compressor blades (Kurz 2007)

3.3.2 Erosion

Erosion is the abrasive removal of material from the flow path by hard particles impinging on flow surfaces. Aircraft engine erosion is affected by many factors such as the ingested particle shape and the size, blade geometry, blade material and operating conditions. Erosion is one of the main problems face by aircraft engines both at ground level and high altitudes. When the aircraft standing or moving on the runway with a high power settings as in the case of take off the engine suck solid particles such as sand, ice, hail, soot and dust. This is more critical in the case of wide body or four engine powered aircraft operate in narrow runways. Aircraft fly at high altitudes may suffer from sand storms and volcanic ashes. Erosion primarily attacks the rotor blades, stator vanes and outer shrouds. This result in increasing tip clearance, shortening blade chords, increasing pressure surface roughness, blunt the leading edge and sharpens the training edge of rotor blades. Detail review of erosion and particle deposition of aircraft engines can be found in Hamed (2006), and Burn (2011). Also it is worth to notice, that effects of erosion on commercial aircraft engines highly depend on number of flight cycles, irrespective of flying hours (Hamed 2006). An example of turbine blade erosion under different flight cycles is shown in Figure 3.3.

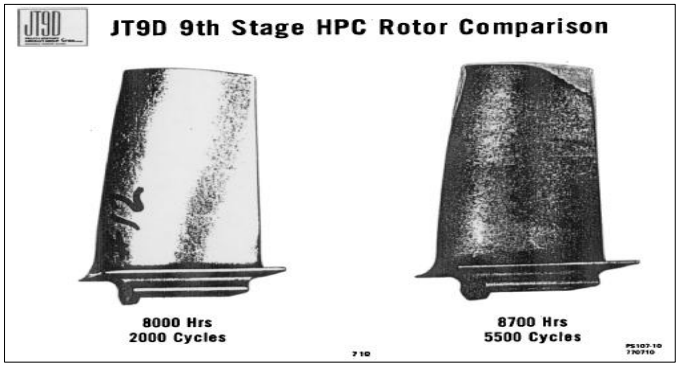

Figure 3-4 Effect of flight cycles on compressor blade erosion (Hamed 2006)

3.3.3 Corrosion

Corrosion is caused by contaminants in the inlet air, as well as by contaminants derived from the fuel and combustion. It is also accelerated by the impurities contained in the air due to the combustion of fuel in the engine. Corrosion is often produced by salt, such as sodium and potassium, but lead and vanadium are also common contributors. It is important to know that the corrosion process is self-propagating and will continue even if the source is removed. Corrosion tends to alter the flow path in two ways. It increases the surface roughness which causes thicker boundary layers on the blade sidewalls, but it may also remove materials, in particular, at the leading edge and trailing edges of the aerofoils in both cold and hot sections. Typically compressor corrosion results in a reduction in compressor flow capacity and isentropic efficiency. Furthermore changes in the flow capacity will subsequently alter the operating points of the compressor. In turbines it increases the effective area with the flow capacity and reduces the isentropic efficiency. Besides, corrosion diminishes the in-service life of the affected components. Coatings are usually applied on turbine and compressor aerofoils to protect from the corrosion.

3.3.4 Hot corrosion

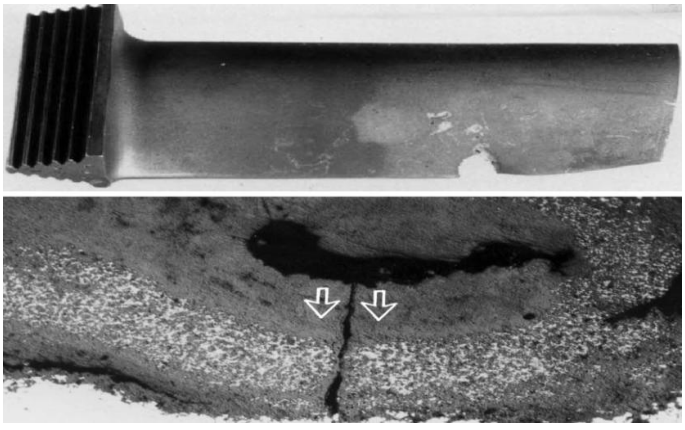

Figure 3-5 Hot corrosion attach observed in a HP turbine blade (Eliaz 2002)

Hot corrosion can be defined as “accelerated corrosion, resulting from the presence of salt contaminants such as Na_2SO_4, NaCl and V_2O_5 that combine to form molten deposits, which damage the protective surface oxides” at high temperatures (Eliaz al et. 2002). During

combustion in gas turbine engines, sulphur from the fuel reacts with sodium chloride from ingested air at elevated temperatures to form sodium sulphate. This sodium sulphate then deposits on the hot section components, such as nozzle guide vanes, and turbine rotor blades, resulting in accelerated oxidation and /or sulphidation attacks. For the oxidation and sulphidation reactions, oxygen and sulphur comes from the combustion process [sulphur in jet fuel is normally limited to 0.3%] (Eliaz al et. 2002), and sodium chloride from the sea water. Sometimes, runway dust may be a source of salt. This form of corrosion, unlike oxidation, can deplete the material at an unpredictable high rate. Consequently, the component load bearing capacity is reduced, eventually leading to a catastrophic failure. Similar in corrosion, primary effects of the hot corrosion cause reduction in mass flow and isentropic efficiency loss before reaching the final component failure. However, the ultimate failure of components may result from a combination of hot corrosion and another failure mechanism (for an example fatigue). An example of a component failure due to hot corrosion is shown in the Figure 3.5. Several approaches have been employed to control hot corrosion of gas turbines components. These approaches include advanced material selection, application of coatings, frequent washing of hot section components and control of fuel quality (Eliaz 2002)

3.3.5 Abrasion

Abrasion is caused when a rotating surface rubs on a stationary surface and it happens in both compressor and turbines. Many engines use abradable surfaces, where a certain amount of rubbing is allowed during operation of the engine, in order to establish required clearances. It is because the clearance between the blade tips and surrounding casing (shroud) tends to vary due to changes in thermal and mechanical loads on the rotating and stationary structures. Therefore tip sealing is more difficult and challenging task due to the frequency of changes in operating points as well as inertial (manoeuvre) and aerodynamic loads taking place during the flight. Basically, the main causes for abrasion is gyroscope effects (flight loads) of the aircraft, axisymmetric and asymmetric alignments, and temperature difference between the casing and rotors at different operating conditions. In the case of gyroscope effects, rubbing may be critical and flight loads are highest during manoeuvring at high flight speeds.

3.3.6 Foreign Object Damage (FOD)

FOD are commonly occurs when hard particles such as stones, sand, debris, mandrels, bits of tyres etc, are ingested into the engine. The high airflow required for operation of the engine creates a powerful suction effect, which tends to draw in small objects from the surroundings of the aircraft. These hard objects can impact the leading edge, trailing edge or somewhere on the body of the fan, compressor and turbine blades. They can also dent, crater, nick or even tear the blades. These effects can result in a reduction in both flow capacity and efficiency of the compressor and turbine. Foreign object damage by hard particles mostly occurs during the aircraft taxiing, on the runway, take-off and landing. The worst case condition is experienced during the take-off with maximum thrust which leads to maximum impact velocity. Typical impact velocities are in the region of 100 – 350 m/s, depending on the type of engine and impact location on the blades (Chen 2002). The typical FOD of first stage fan blades is shown in Figure 3.6.

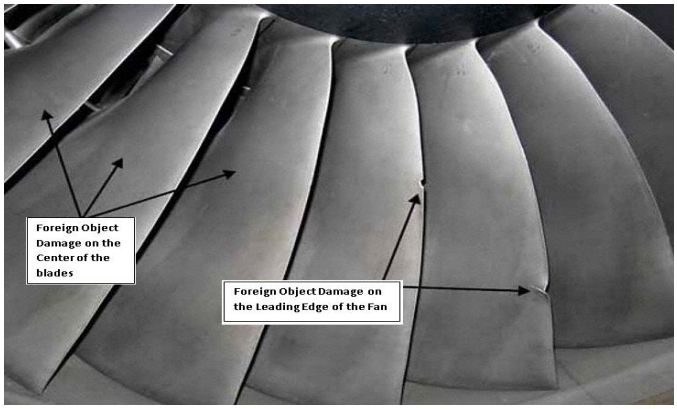

Figure 3-6 FOD of a fan blade (Yupu 2008)

The FOD can also be caused by soft body impacts. The classical example is the bird strike. Based on the experience of the MTU maintenance, 4% of their shop visits are FOD related and 50% of them are due to bird strike (Mao 2009). Bird strikes always occur on the pressure side and mainly on the leading edges of the blades. Depending on the incident angle of bird strikes, the fan blades slice the bird into pieces, which is known as slicing effect. The majority of bird strikes occur at very low altitudes, below 500 feet above ground level during the take-off and approach (Airbus Report 2004). The consequences of bird impact can be severe and thus it is necessary to ensure that the rotor blades should have adequate resistance against the bird impact, to reduce the flying accidents. FODs does not always lead to efficiency drop and sudden

catastrophic failure of components; yet such damage can dramatically reduce high cycle fatigue life of the components (Peters 2000). This has become a critical issue in the performance deterioration and life prediction of engine components.

3.4 Component degradation

The function of a gas turbine is a result of the fine tuned combination of many different components. Any of these components can show wear and tear over the life time, thus can adversely affect the operation of the overall engine system. In particular, the aerodynamic components such as the engine compressor, the combustor and the turbines have to operate in an environment that will invariably degrade their performance. Understanding of these, component degradation under various degradation mechanisms are the matter of interest of this section. Figure 3-7 shows the typical degraded components of an aero engine.

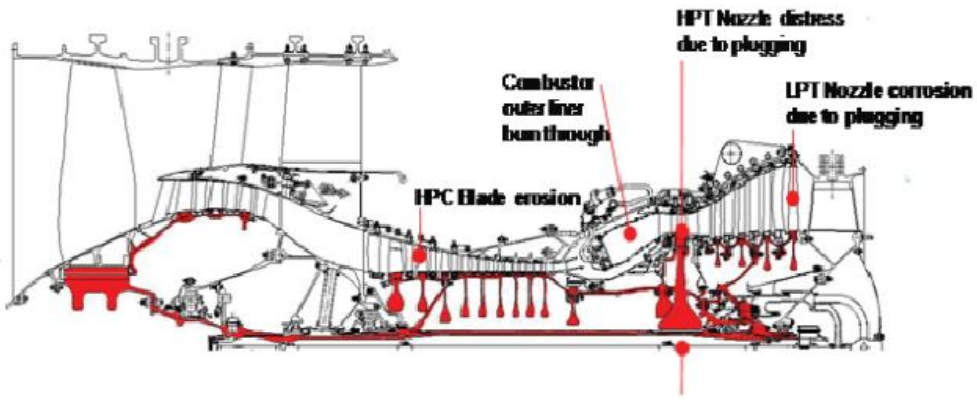

Figure 3-7 Components susceptible for degradation in a gas turbine

3.4.1 Compressor degradation

Three major effects determine the performance deterioration of a compressor: Changes in airfoil surface quality, changes in airfoil geometry and increased tip clearances. In order to judge the degradation of aerodynamic components of the compressor, we will first evaluate the effect of fouling, erosion, corrosion and other damage on the individual aerofoils. Fouling, corrosion and to some extent erosion generate a blade surface with increased roughness. Any increased roughness can increase the friction losses. It also may cause early transition from laminar to

turbulent boundary layers which increase loss of the pressure head. It became clear that the main influence of degradation appears around optimum incidence angles, while the far off-optimum performance hardly was influenced. It also becomes clear, that added roughness on the pressure side of the blades has a very small effect compared to added roughness on the suction side. If the blades operate at transonic velocities, deposits, or added roughness with the associated growth in boundary layer thickness will also reduce the possible flow through the blade rows. Thicker boundary layers on the blades and sidewalls reduce the flow capacity.

It has been recognised that compressor fouling is more common cause of performance deterioration. Typically 70 to 85 percent of all gas turbine engine performance losses are due to compressor fouling (Mund and Pilidis, 2006). It has been observed that compressor fouling could increase turbine entry temperature by 15^0C, flow reductions up to 8% and efficiency drop of 1%, (Acker, 1997). In addition, compressor fouling reduces the compressor surge margin and may increase the chances of compressor surge and stall occurring. Also fouling affect compressors LPC and HPC in different ways, as axial compressor is a machine where the aerodynamic performance of each stage depends on the earlier stages. Thus fouling occurs in the first few stages, there may be significant drop in compressor performance. From the experience and the literature, front compressor stages (LPC) are usually fouled worst. If the rear stages fouled, impact may not so high, but due to high temperatures deposits can become baked and difficult to remove. The baking effect is more severe on high pressure ratio engines ranging from 18:1 to 35:1 (Naeem 2008). Also deposits can have different characteristics depending on the nature of the fouling. Dry particles in dry atmospheres are likely to deposit in different areas, compared to sticky matters and oily compounds.

Erosion changes the blade profile and end wall loss which increase pressure losses, decrease flow capacity and component efficiency. The 1% loss in tip clearance reduces 2% compressor efficiency and 7.5% reduction in surge margin (Dunn al et. 1987). In turbine, inertial impact at high velocities of particles larger than few microns in diameter on aerofoil leading edges and pressure surfaces can cause erosion, again depending on the characteristics of the particles. Many particles bounce back and forth between the blunt leading edges of the rotor blades and nozzle vane training edges, which causes increasing nozzle area and lowering the turbine efficiency. Typically flow capacity for turbine may increase by 2% and efficiency decreased by 1%. In addition, erosion is one of the main causes for thermal barrier coating (TBC) damage (Naeem 2008). Furthermore clearance between the stationary and rotating parts (i.e. between stationary blades and the rotating hub or between rotating blades and the stationary casing) of the compressor have a tendency to open up due to abrasion. This results in unexpected leakage flows. These leakage flows reduce the possible head capability and

isentropic efficiency of the compressor. An increase of the rotor tip clearance from 1% of blade chord to 3.5% of blade chord reduces the pressure ratio of the stage by up to 15%. Carefully adjusting variable geometry, where available, could be used to counteract some of these mismatching effects of degradation.

Typically, a degraded compressor also will have a reduced surge or stall margin. Figure 3.8 shows the typical map of a compressor with the operating running line and the stall margin. Spakovszky (1999) and Graf et al., showed how compressor blade clearances reduce surge margin and efficiency of a compressor. If clearance increased from 2.9% (design value) to 4.3% the increase in surge flow coefficient of about 20% and reduction in design pressure coefficient of 12%. Similar study has been done by Frith (1992) with the 3% crop of compressor stages reduced airflow by 4.6% and pressure ratio by 3%. The compressor efficiency was reduced by 2.5%. The compressor pressure ratio and the compressor flow rate are not independent, and the compressor efficiency is determined by the resulting compressor operating point. Increase in tip clearance well as deteriorated airfoils will shift the pressure ratio and flow relationship for a given operating speed to lower rates, as well as to lower efficiencies. In general, for large civil aero gas turbine engine tip clearance reductions on the order of 0.010- in can increase SFC by 1% and EGT of 10^0C (Lattime 2002).

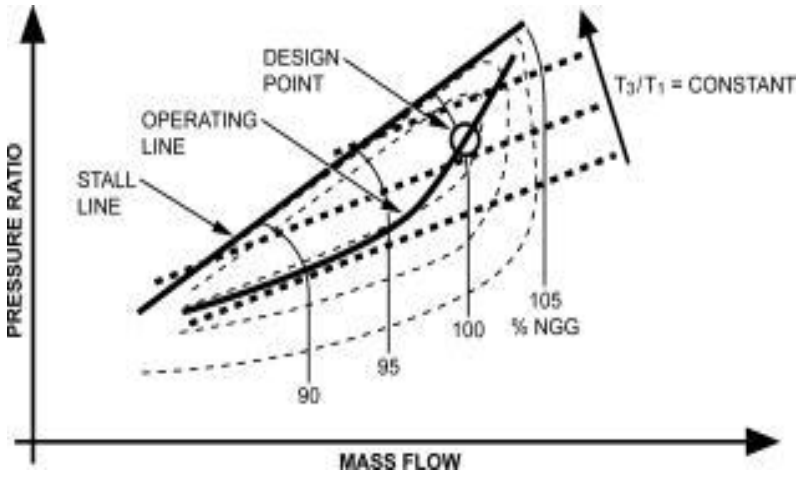

Figure 3-8 Typical compressor maps with operating running line (Nqobile 2012)

3.4.2 Combustor degradation

The combustion system is not likely to be the direct cause for engine degradation. The combustion efficiency will usually not decrease. However, mechanisms like erosion and hot corrosion may still affect the wall coatings, cooling holes and the exit geometry of the combustor. The potential changes in the cooling holes dimensions and exit geometry profile could influence the conditions inside the combustion chamber and as a result temperature distribution at the exit is become non-uniform. The problems with a distorted exit temperature distribution are threefold; (a) local temperature peaks can damage the nozzle guide vanes and turbine section, (b) the altered temperature profile will increase secondary flow activity, thus reducing the turbine efficiency, finally (c) the altered temperature profile also leads to give inaccurate control temperature measurements in different probe points with respect to temperature correlations derived from the true temperatures measured at the factory. Therefore original correlation is no longer valid for engine control. The engine could therefore be over fired (thus producing more power, but shortening the life) or under fired, thus losing the thrust and increase SFC.

3.4.3 Turbine degradation

Just as the compressor section, the turbine section also experiences the following effects that result in degradation: changes in airfoil surface quality, changes in airfoil geometry, and increased tip clearances. The corrosion and hot corrosion are the two main mechanisms largely influence these changes for turbine degradation. They tend to alter the flow path in two ways; increase the surface roughness, but they may also remove material, in particular, at the leading edges and trailing edges of the aerofoils of the turbine component. Especially, the turbine nozzles and turbine blades operating at or near chocked conditions, which are very sensitive to changes in the flow area. Increase surface roughness causes thicker boundary layers on the blades, nozzles and side walls and, thus may reduce the flow capacity essentially near choking conditions. Boyle (1994) found for a two stage axial turbine, the efficiency loss of 2.5% can cause for a 10.2μm surface roughness when compared with smooth blade surfaces. The studies also found that the most pronounced differences appear at the optimum operating point at the turbine, whereas the far off-optimum efficiency was almost the same for rough and smooth blades. It should also be noted that the losses due to clearances were in the same order of magnitude as the profile losses.

However, if the degradation of the turbine section leads to material removal, especially in the nozzle area, we will see the opposite effect of increasing the flow capacity for any given pressure ratio rather reducing the flow. Because the flow capacity of any nozzle is limited by the effective throat area, erosion of the trailing edge causes the throat area to increase and the exit flow angle to become more axial. This means a reduction of turning in the stator and the rotor, which will lead to reduced work extraction for this stage and to an increase flow capacity. Since turbine nozzle constitute a flow restriction, any change in the flow capacity of the turbine section will also impact the operating points of the engine compressor. Erosion of the blades also can lead to excessive blade metal temperatures and premature failures due to changes in the profile of the cooling holes which affects the effectiveness of blade cooling. Considerable research has been done in the past to predict cooling path profile changes and blockages in turbine blades.

Another situation is increasing the clearances between turbine rotor and the casing due to abrasion. When the engine accelerates at high temperature with a cold casing, the rotor expands to the highest and reduces the clearance between turbine blades and the casings i.e. take off in low outside temperatures; abrasion is the result. Increase in turbine clearance of 0.25mm can results in reduction of 0.5% in isentropic efficiency and 0.83% in flow capacity (Naeem 1999). This is the case when the casing is hot while the rotor decelerates, i.e. during the descent phase. To counteract this, modern commercial aircraft engines equipped with an active clearance control (ACC) system, which control clearances at different operating conditions. The cooler air from the fan and the HPC is fed into case mounted manifold and is controlled by the N2 shaft speed and flight altitude. This allows the engine to run at highest TET and shaft speeds, with minimum reduction of blade tip clearances and stage efficiencies (Kern 2010). The tip clearances can produce fuel and maintenance savings over hundreds of millions of dollars per year. Average maintenance cost to overhaul large civil aero engine can easily exceed one million dollars (Lattime 2002). Presently, these savings are unrealized due to the slow response of current clearance management systems and the lack of direct tip clearance measurements. Improved ACC systems will seek further reductions in cruise clearances (normally 0.015 – 0.020-in) while eliminating blade rubs to make significant impact on SFC and take off EGT margins.

The turbine also suffers from similar effects of fouling and it largely depends on the fuel used. Fuels with high ash content can result in severe fouling to the turbine. The particles also may plug the turbine blade cooling holes and promote damage due to overheating. Turbine cleaning is more difficult than compressor because it often requires some parts of the engine to be dismantled. In the case of turbine nozzle guide vane fouling, typically the

efficiency may be reduced by 1%. These efficiency reductions can be covered by higher turbine entry temperatures and spool speeds, but with the compromise of fuel consumption and engine life (Kurz 2007).

3.5 Degradation effects on engine performance

Engine component degradation leads to component mismatch and cause changes in the performance characteristics, which gives a compound effect on the overall engine performance. A degraded engine will seek for different steady state operating points in relation to that of a clean engine. The variation of these operating points causes reduction in thrust and increase in SFC. The thrust drop is compensated by increasing the spool speed or adjusting the firing temperature (TET) by engine control system FADEC (Full Authority Digital Engine Control). However in both cases will bring significant changes to engine performance parameters; engine pressure ratio (EPR), spool speeds (N1 and N2), fuel flow (FF), and exhaust gas temperature (EGT). Therefore EGT is considered as the key engine monitoring parameter for engine performance deterioration.

3.5.1 Key engine operating performance parameters

Several key engine operating parameters use for engine monitoring, this includes fan speed (N1-Speed) engine pressure ratio (EPR) and exhaust gas temperature (EGT). The fan speed always used as a thrust indicator, whereas EGT is used as engine degradation monitoring parameter or health monitoring parameter. Sometimes EPR and N2/N3-Speeds are also used for thrust monitoring. The following is a brief discussion of each of the performance parameters.

Engine Pressure ratio (EPR): is the total pressure ratio across the engine, taking the ratio of the total pressure at the exhaust (or turbine exit) to total pressure at the front of the fan/compressor. Some engine manufacturers use EPR to measure engine thrust. Low EPR can be a result of flameout and rapid fluctuation may be due to engine stall.

N1-Speed: is the rotational speed of the fan (or Booster compressor depending on the engine type) and is typically represent as a percentage of design rpm (revelutions per minintes). It is mainly use to indicate engine thrust. Again low N1-spool speeds can be a sign of engine flameout. Where as, rapid fluctuation of N1-speed can be a sign of an engine stall. N2-speed (or N3-speed if the engine is a three spool configuration) is the rotation of the high or intermediate

pressure compressor and is also presented as percentage of its design rpm. Rapid fluctuation of N2/N3-speed can be a sign of an engine stall.

Exhaust Gas Temperature (EGT): indicated in degrees "Celsius". It is the temperature at the engine exhaust and a measure of an engine's efficiency in producing its design level thrust; the higher the EGT the more wear and deterioration affects an engine. High EGT can be an indication of degraded engine performance. An excess EGT limits can lead to immediate damages of engine parts and/or a life reduction of engine parts. With this in mind it then becomes absolutely important to continuously monitor EGT and to keep the EGT as low as possible for as long as possible.

3.5.2 EGT Margin

Normally EGT reaches its peak during take-off, or just after lift-off. The difference between the maximum permissible EGT (red-line) and the peak EGT during take-off is called the EGT margin. The graphical representation of EGT margin and EGT Redline as a function of OAT (outside air temperature) is shown in Figure 3-9.

EGT Margin = EGT Redline – EGT Gauge Reading

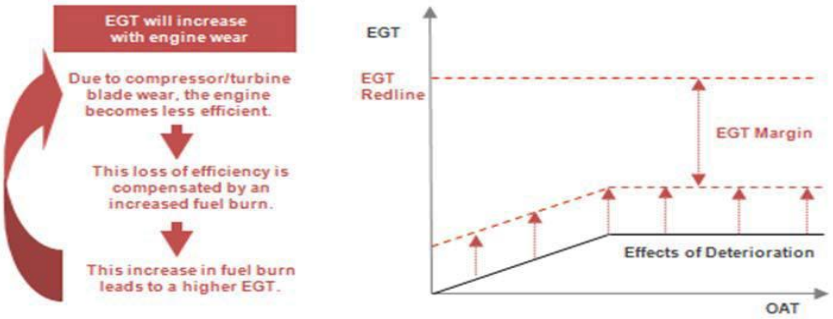

Figure 3-9 EGT margin deterioration cycle

In general, EGT margins are at their highest levels when the engines are new or just following refurbishment. Theoretically an engine can remain in operation until its EGT margin has reduced to zero. EGT margin is also sensitive to changes in Outside Air Temperatures (OAT). As the OAT increases so does EGT for a given thrust setting. This is because most engine power management systems are designed to maintain constant take-off thrust with rising OAT. The rise in EGT is traditionally linear up to the design corner point temperature (CPT) at which

point the EGT becomes controlling. The corner point temperature is where the EGT is highest when operating at maximum thrust conditions. Operating at a higher OAT beyond the corner point temperature is possible, however the thrust must be reduced (de-rated) to avoid an EGT redline exceedance.

3.6 Simulation of engine performance and degradation

Engine performance studies are often carried out assuming new engine characteristics. However, any engine shows performance deterioration from the time it commences operation due to various degradation mechanisms which have been discussed in the previous section. These mechanisms affect the component characteristics and eventually deteriorate the overall performance of the engine. Therefore it is important to investigate the effects of individual component degradation and their combined effects by simulating the overall performance at various operating points. For the purpose of this study, a short range and a long range two spool high bypass turbo fan engines were modelled.

Gas turbine performance code TURBOMATCH has been used to develop these engine models. The TURBOMATCH is a FORTRAN based; zero dimensional, gas turbine software developed at Cranfield University, (MachMillan, 1974) and Palma and Pachidis, 2005). The engine models are assembles from a collection of existing interconnected elements called "Bricks". Individual bricks are controlled by a numerical solver and represent the thermodynamic equivalent of gas turbine components including: intake, fan, compressors, turbines, and nozzles. A selection of appropriate, scalable 0D component characteristics – is also called maps are provided for each of the component that are used to describe their performance. Bricks are called up to assemble the architecture of the engine and a numerical solver (a modified version of Newton-Rapson method) is used to solve the mass and energy balance between the interconnected bricks or in other words components.

The initial Design Point calculations are carried out with the user defined specification of ambient condition, pressure ratio, and component efficiencies etc., as discussed subsequently in the next section. Convergence is achieved in the component matching after satisfying compatibility of non-dimensional rotational speed and flow between compressor and turbine components. The off-design operating points on the compressor and turbine maps are determined based on the calculated scaling factors given in equation 3.1 to 3.10. An iterative process is employed and it involves several trials to ensure that the variables are consistent with the matching constraints such as thrust setting, rotating speed, fuel flow and TET.

The equations used to calculate the scaling factors for the fan and compressors are given below;

$$PRSF = \frac{PR_{DP}-1}{PR_{Map.DP}-1} \quad (3.1)$$

$$MFSF = \frac{MF_{DP}}{MF_{Map.DP}} \quad (3.2)$$

$$CESF = \frac{\eta_{C,DP}}{\eta_{C,Map.DP}} \quad (3.3)$$

Also for the fan and compressor, the distance measured from the operating point to the surge line known as surge margin is also specified and it is defined by the following equation;

$$SM = \frac{PR_{DP}-PR_{High}}{PR_{High}-PR_{Low}} \ X\ 100 \quad (3.4)$$

The turbines drive the compressors and fan, thus scaling factor for turbine flow function is given by the equation below;

$$TFSF = \frac{TF_{DP}}{TF_{Actual}} \quad (3.5)$$

That of the shaft speed scaling factor is,

$$CNSF = \frac{CN_{DP}}{PCN} \quad (3.6)$$

PCN is the spools speed in percentage CN is the non-dimensional speed

$$CN = \frac{PCN}{\sqrt{TA}} \quad (3.7)$$

The scaling factor for the work function is

$$DHSF = \frac{DH_{DP}}{DH_{Map}} \quad (3.8)$$

The turbine efficiency scaling factor is the same formula as used for the compressor,

$$TESF = \frac{\eta_{T,DP}}{\eta_{T,Map.DP}} \quad (3.9)$$

The combustor efficiency is plot of combustor efficiency against temperature rise for different constant inlet pressures.

$$\eta_{Comb} = \frac{Ideal\ amount\ of\ fuel\ burn}{Actual\ amount\ of\ fuel\ burn} \ X\ 100 \quad (3.10)$$

The subscript DP is the specified new design point value and Map. DP, is the design point value on the standard maps.

After developing the engine model, engine degradation has been introduced by altering the performance parameters of the compressor and turbine components such as mass flow, and isentropic efficiencies by altering the above scaling factors as off-design operating points. The output of the code provide the calculation of the performance of the engine in terms of gross thrust, net thrust, fuel flow and specific fuel consumption. The detailed thermodynamic parameters of the components at inlet and outlet are also provided. Among them, exit temperature of the propelling nozzle EGT has been used as the key performance monitoring parameter to determine the overall level of engine performance deterioration. This is the standard practice in monitoring the engine performance by operators.

3.6.1 Typical degradation limits in engine parameters for turbofan engines

Despite a lack of data, representative limits of the extent to which engine may degrade can be established. For example Lukachko and Waitz (1997), suggested typical limits on changes in engine parameters due to various degradation mechanisms and reasons for the existence for a twin spool high bypass turbofan engine as shown in Table 3-1

Table 3-1 Typical limits of component degradation of a turbofan engine (Lukachko 1997)

Parameter	Limit	Reason
Fan Mass Flow	-5.0 %	LPC Surge
Fan Efficiency	-5.0 %	High Turbine Temperature
LPC Mass Flow	-8.0 %	High Turbine Temperature
HPC Mass Flow	-8.0 %	High RPM
HPC Efficiency	-4.5 %	High Turbine Temperature
HPT Nozzle Effective Area	-6.0 %	HPC Surge
HPT Nozzle Effective Area	+6.0 %	LPC Surge
HPT efficiency	-5.0 %	High Turbine Temperature
LPT Nozzle Effective Area	+8.0 %	Low Thrust
LPT Nozzle Effective Area	-6.0 %	LPC Surge

3.6.2 Degradation limits used for the simulation

Table 3-2 Degradation limits considered for simulations

Component	Mechanism	Degradation represented parameter			
		Parameter	Range	Parameter	Range
Compressor	Fouling	drop in η	0.0 to (-) 3.0 %	drop in Γ	0.0 to (-) 3.0 %
	Erosion	drop in η	0.0 to (-) 3.0 %	drop in Γ	0.0 to (-) 3.0 %
	Damage	drop in η	0.0 to (-) 3.0 %	drop in Γ	0.0 to (-) 3.0 %
Combustor	not considered				
Turbine	Erosion	drop in η	0.0 to (-) 3.0 %	rise in Γ	0.0 to (+) 3.0 %
	Corrosion	drop in η	0.0 to (-) 3.0 %	rise in Γ	0.0 to (+) 3.0 %
	Abrasion	drop in η	0.0 to (-) 3.0 %	rise in Γ	0.0 to (+) 3.0 %

3.7 Short range engine model

3.7.1 Short range engine model development

The short range engine model is developed based upon the CFM56-5B7 engine which is currently used to power the A320 type twin engine single isle aircraft. The configuration of the model is two spool high bypass ratio turbofan engine with a booster stage, separate exhausts, custom bleeds and cooling bleed off-takes. The schematic of the engine is given in Figure 3.10 and designated as CUSE (Cranfield University Short range Engine).

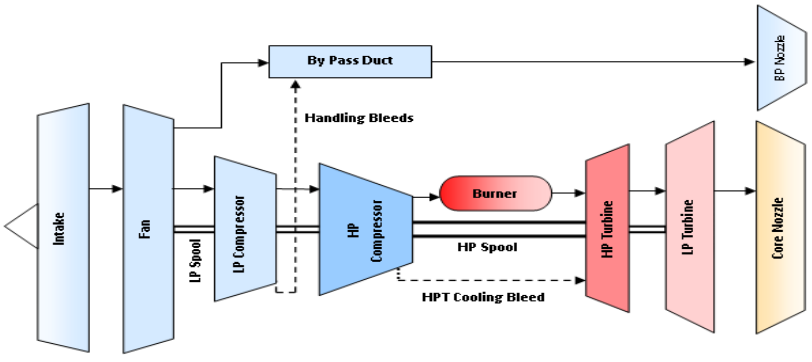

Figure 3-10 Schematic of the short range aircraft engine model (CUSE_0DL)

The design point of the engine model was selected at top of climb (TOC) i.e. Alt: 10668 m, Mach number 0.8, and the pressure recovery of 0.99 under International Standard Atmospheric

(ISA) conditions. Several iterations were performed using the model at design and off-design conditions to match the performance of the model with the data obtained from the public domain for the engine on which the design was based (CFM 2011, ICAO 2013)

The mass flow rate of the engine intake was estimated based on the measured nacelle area and assuming an average inlet Mach number of 0.55 – 0.65. The design point (at the top of climb) bypass ratio (BPR) and the turbine entry temperature (TET) were determined based on the overall pressure ratio (OPR) and the net thrust at top of climb. The optimum fan pressure ratio (FPR) corresponding to the calculated TET, overall pressure ratio (OPR) and bypass pressure ratio (BPR) were also determined. In addition to the above, compressor pressure ratios, component efficiencies, and compressor bleeds for turbine cooling, custom bleeds, and other parameters, were guessed and iterated to match the required engine performance at design point and off-design (maximum take-off and cruise) conditions (CFM 2011, ICAO 2013). Finally, the model has been tested and validated against different off-design conditions such as several thrust ratings and corresponding fuel flow rates available in the public domain. The Table 3-3 shows the comparison of the design and performance data of the simulated engine against the public domain literature.

In addition several off design performance simulations were carried out in order to evaluate the simulation capability of the developed model as a clean engine. The simulation results comprise of performance charts assessing the effect of flight altitude, speed (Mach number), ambient temperature and turbine entry temperature on the net thrust and specific fuel consumption (SFC). The Figure 3.11 indicates the variation of net thrust (F_n) as a function of flight altitude (Alt) and flight Mach number (Mach) for a fixed value of turbine entry temperature (TET). The value of TET chosen was the take-off point (TET =1650K). The Figure 3.12 indicates the variation of specific fuel consumption (SFC) as a result of changing flight altitude, and Mach number for the same fixed value of TET. The Figure 3.13 highlights in turn the variation of net thrust as a function of ambient temperature (T_{amb}) and turbine entry temperature (TET) at sea level static (SLS) condition (i.e. Alt=0m, and Mac =0). Finally, Figure 3.14 highlights the variation of SFC as a function of ambient temperature ((T_{amb}) and TET at sea level static (SLS). It may be noted that for these analysis the maximum TET considered was the TET corresponding to Take-off conditions. The charts broadly follow the expected trends and descriptions of the effects of altitude, flight Mach number and ambient conditions and TET on engine performance, provided in Saravanamuttoo (2013) and Mattingly (1996). The validated engine model has been used to simulate the various degradation scenarios, as described in Section 3.6.

Table 3-3 Short Range Aircraft engine model verification

ENGINE DP PARAMETERS OF CUSE_0DL				
Fan Pressure Ratio [-]		1.7		
By Pass Ratio [-]		5.7		
Overall Pressure Ratio [-]		32.6		
Mass Flow kg/s		165		
Fan Pressure Ratio [-]		1.70		
Booster Pressure ratio [-]		1.97		
HPC Pressure Ratio [-]		9.74		
Compressor Efficiencies		0.89		
Turbine Efficiencies		0.92		
Combustor Efficiency		0.99		
DP SIMULATION - CONDITIONS AND RESULTS				
DP Conditions				
Altitude [m]	10668.0			
Mach number [-]	0.8			
ISA [^{0}C]	0.0			
Parameter	**From Simulations**	**From Public domain**	**Variation**	**Reference**
Mass Flow	165.0			
Pressure Ratio	32.7	32.6	0.30 %	CFM (2013)
Thrust [N] TET – 1515 K	25054.0	25042.0	0.04 %	CFM (2013)
OD SIMULATION - CONDITIONS AND RESULTS				
OD Conditions				
Altitude [m]	0.00			
Mach number [-]	0.00			
ISA [^{0}C]	0.00			
Parameter	**From Simulations**	**From Public domain**	**Variation**	**Reference**
Mass Flow [kg/s]	403.8	406.0	1.1 %	CFM (2013)
BPR [-]	5.8	5.7	1.7 %	CFM (2013)
Pressure Ratio [-]	28.8	28.8	0.0 %	ICAO(2002)
Take-off Thrust [N] TET – 1655 K	120798.0	120000.0	0.7 %	CFM (2013)
Parameter	**From Simulations**	**From Public domain**	**Variation**	**Reference**
FF @ 100% PS [Kg/S] TET-1655 K	1.24	1.26	1.70 %	ICAO EDB [4]
FF @ 85% PS [Kg/s] TET 1560 K	0.99	1.03	2.70 %	ICAO EDB [4]
FF @ 30% PS [Kg/s] TET 1190 K	0.36	0.37	3.80 %	ICAO EDB [4]

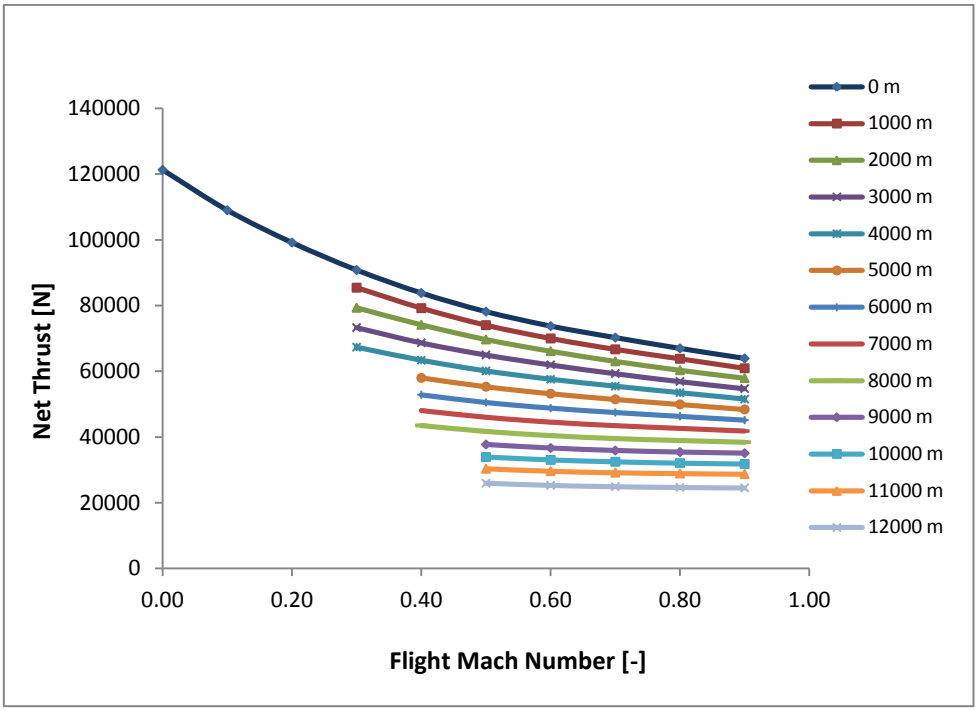

Figure 3-11 Variation of net thrust against flight Mach number and altitude for constant TET

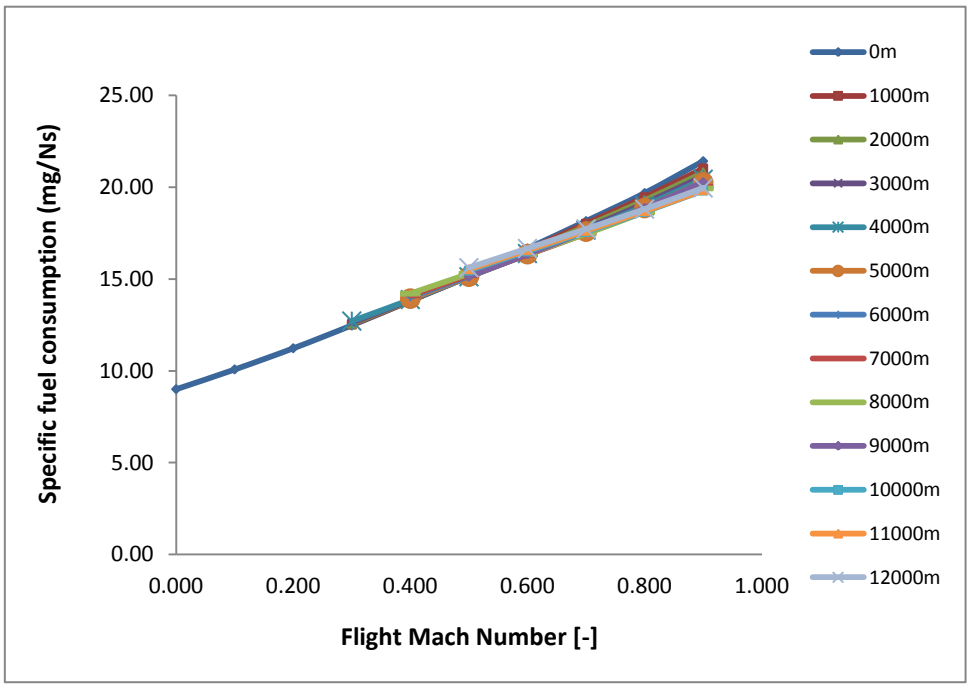

Figure 3-12 Variation of SFC as a function of altitude and Mach number for constant TET

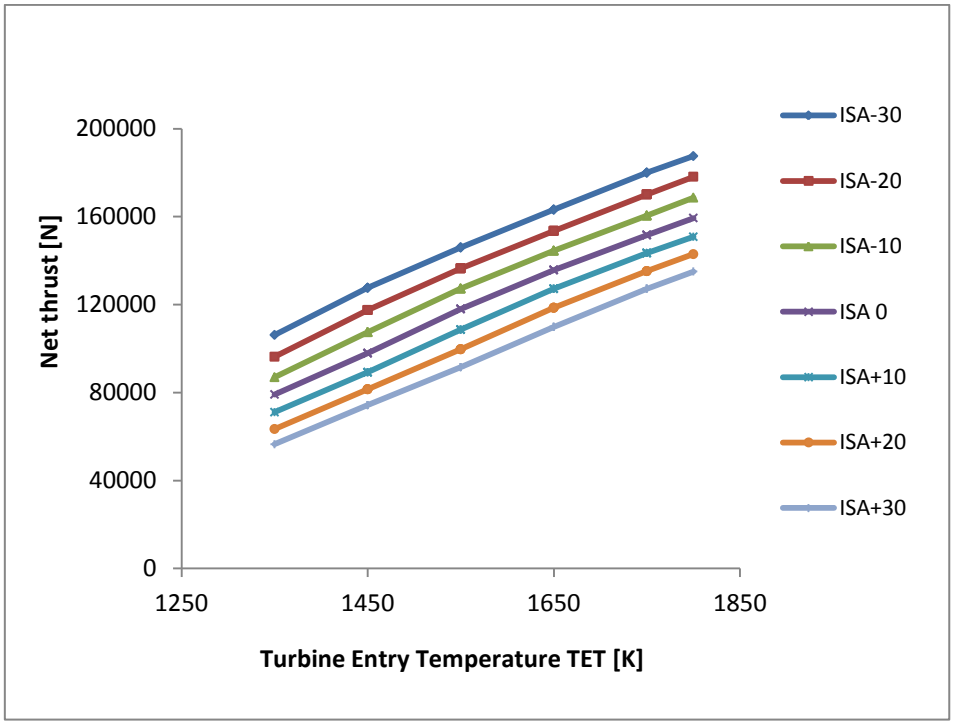

Figure 3-13 Variation of net thrust as a function of TET and ambient temperature

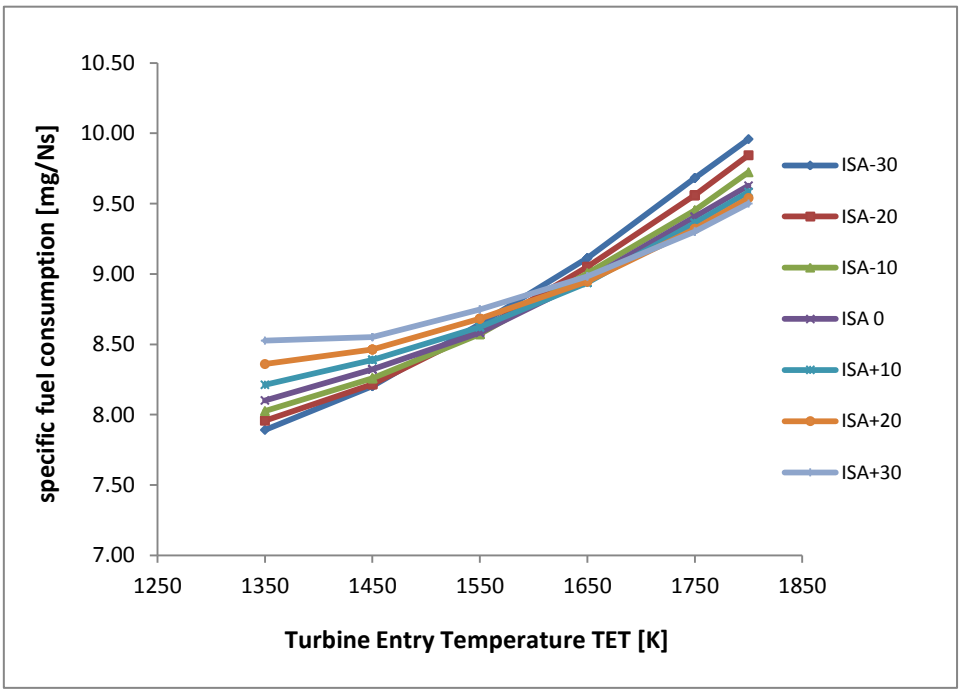

Figure 3-14 Variation of SFC as a function of TET and ambient temperature

3.7.2 Impact of degradation on engine performance at TOC

TOC is one of the main important points in an aircraft mission as most of the engines are designed for TOC. Figure 3-15 and Figure 3-16 shows the PR and net thrust drop due to individual and combined effects of compressor and turbine for constant TET. It can be observed that reduction in compressor and turbine mass flow show similar effects and gave the lowest effect on PR. Turbine efficiency and compressor efficiency are concern, turbine efficiency drop is more sensitive to PR than the compressor efficiency drop. As expected combined compressor and turbine degradation gave the most severe effects on PR drop of 4.5% and 6.2% drop for the maximum degradation limit 3%. Thus these effects significantly influence the thermal efficiency of the engine. Compressor mass flow and efficiency drop shows similar effects on net thrust drop. Deterioration of the turbine efficiency has a significant effect, and also similar to the combined effect of compressor mass flow and efficiency drop which is approximately -4.8% for the degradation limit of 3%. As expected combined effect of compressor and turbine mass flow and efficiency has the highest impact on the net thrust. However in practice net thrust needs to be kept constant.

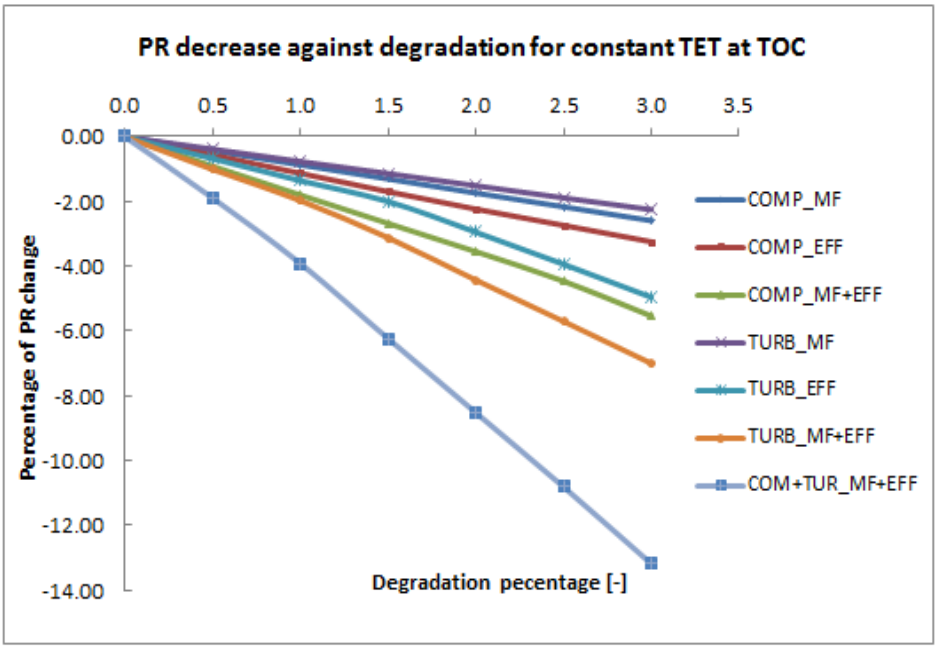

Figure 3-15 PR drop against degradation for constant TET at TOC

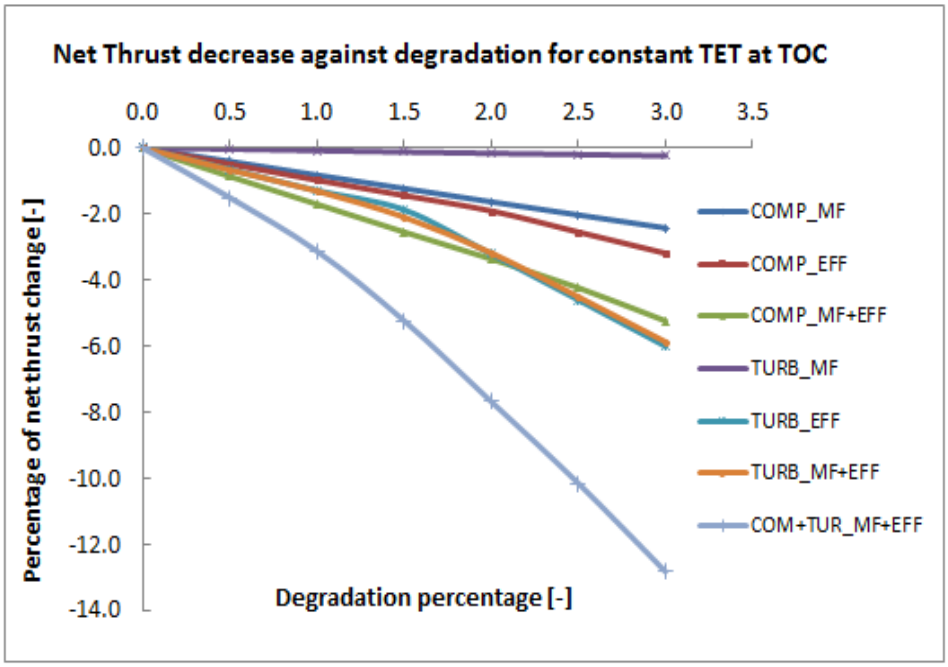

Figure 3-16 Net thrust drop against degradation for constant TET at TOC

Engines need to keep the required thrust levels constant, even if the engine components are degraded. The constant net thrust has been achieved by increasing the spool speed and fuel flow. As a result SFC and TET have increased however pressure ratio has come down. Figure 3-17 shows the increase of SFC for different levels of component degradations at constant thrust. Compressor mass flow and efficiency has the lowest impact on the SFC increase. However combined effect of mass flow and efficiency drop of compressor has the similar effect compared to mass flow drop of turbine. Turbine efficiency drop shows a significant increase in SFC and as a result combined effect of turbine has the highest component effect. Combined effect of compressor and turbine has increased the SFC by 5.8% for 3% limit of degradation. Increase in SFC reduces the thermal efficiency of the engine and as a result it reduces the overall efficiency. Figure 3-18 shows the PR drop for different degradation levels, whereas Figure 3-19 shows the corresponding increase in TET. As shown in the Figure 3-19, reduction in turbine mass flow has the lowest effect of 0.2% on TET for 3% degradation. Turbine efficiency drop has a significant effect on TET increase, which is similar to combined effect of compressor mass flow and efficiency drop. The corresponding increase of TET was 2%, whereas the total combined effect of compressor and turbine degradation has increased the TET by 5% at the same limit of 3%. Figure 3-20 shows the increase of EGT as a result of different component degradation and for their combined effects.

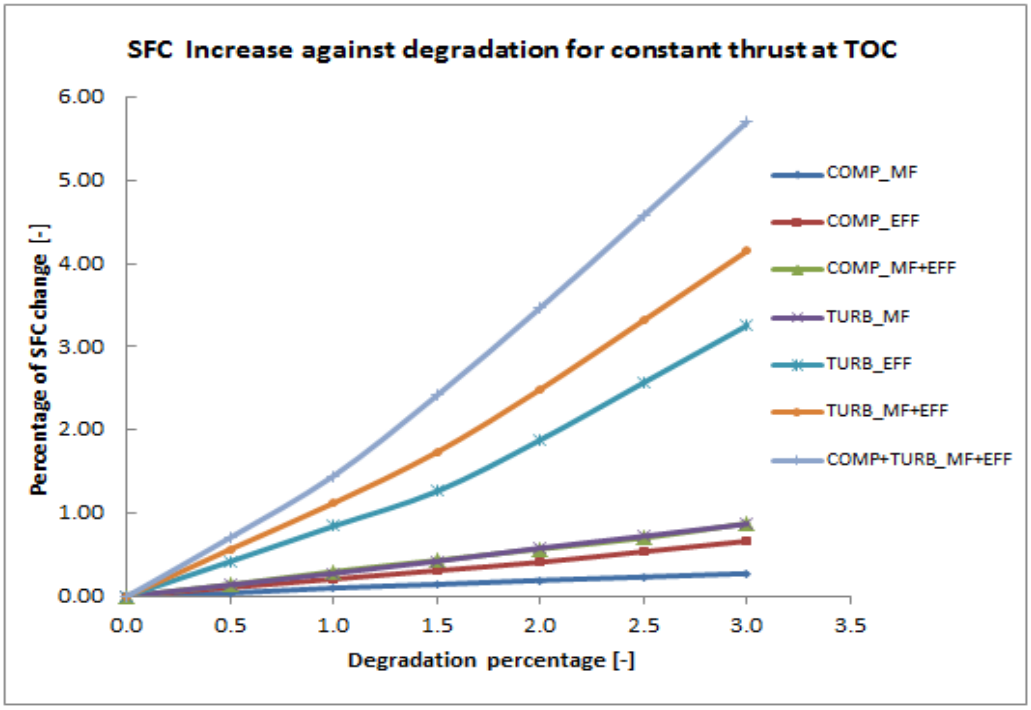

Figure 3-17 SFC increase against degradation for constant thrust at TOC

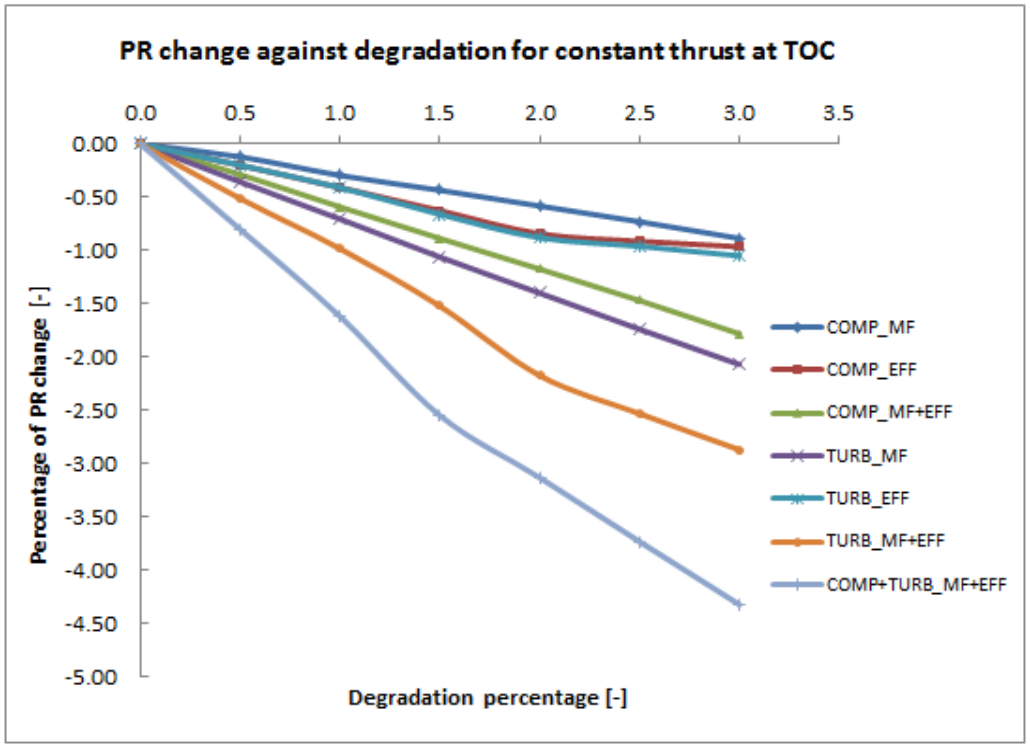

Figure 3-18 PR change against degradation for constant thrust at TOC

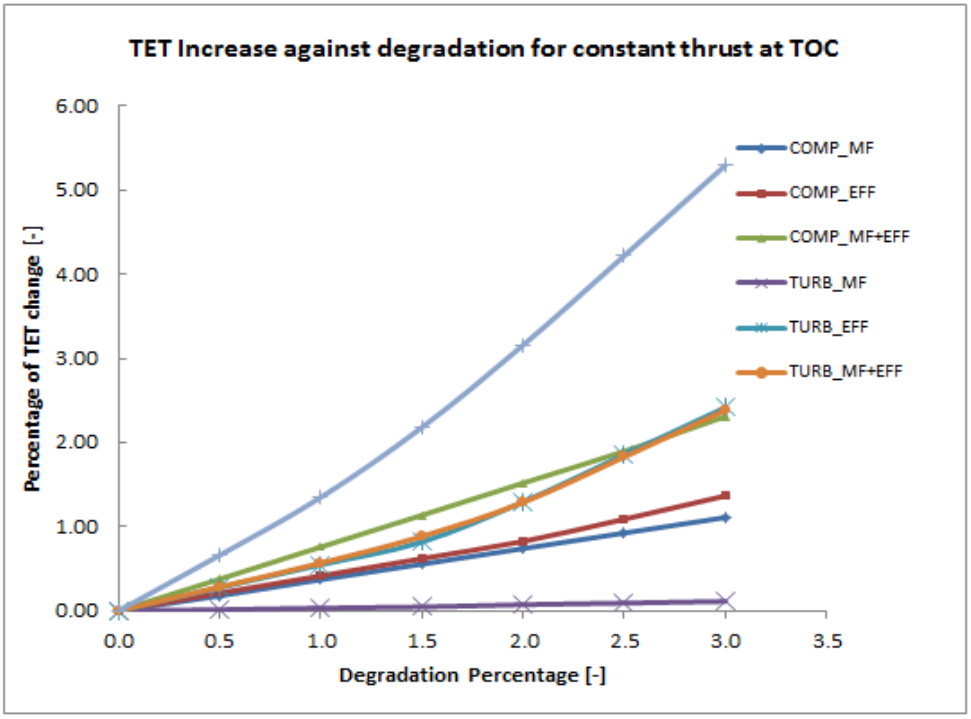

Figure 3-19 TET increase against degradation for constant thrust at TOC

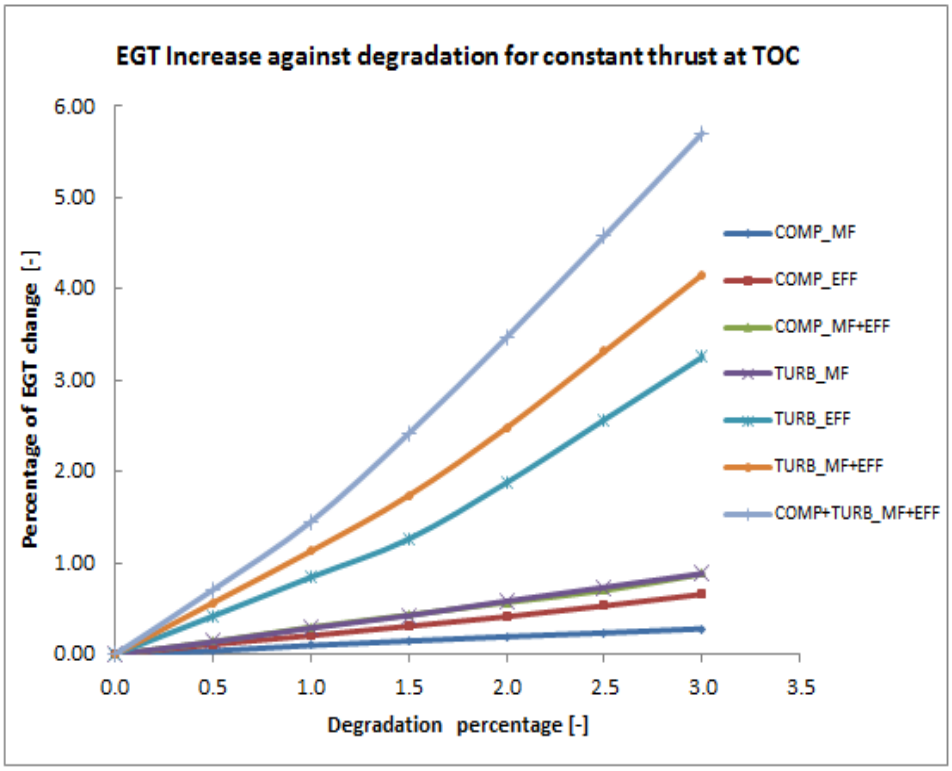

Figure 3-20 EGT increase against degradation for constant thrust at TOC

3.7.3 Impact of engine degradation on engine performance at TO

In this section, impact of component degradation on engine performance at take-off was investigated. Figure 3-21 shows the effect of different levels of component degradation on SFC at constant thrust. It can be observed that, drop of compressor mass flow has the lowest effect on SFC increase of 0.6% for the degradation limit of 3%. Compressor efficiency and turbine mass flow drop shows the similar effects, relatively closer to combined effect of compressor mass flow and efficiency drop. Turbine efficiency drop has shown a significant impact on the SFC, which is 5% increase of SFC for 3% degradation, whereas combined effect of turbine shows an increase of SFC by 6.0%. As expected, highest effect of 8.5% increase of SFC was shown due total combined effects of compressor and turbine. Even though component degradation has the highest impact on SFC at TO, it is important to notice that the engine operates at this condition only for a short period of time. Figure 3-22 shows the increase of specific thrust for same levels of component degradation.

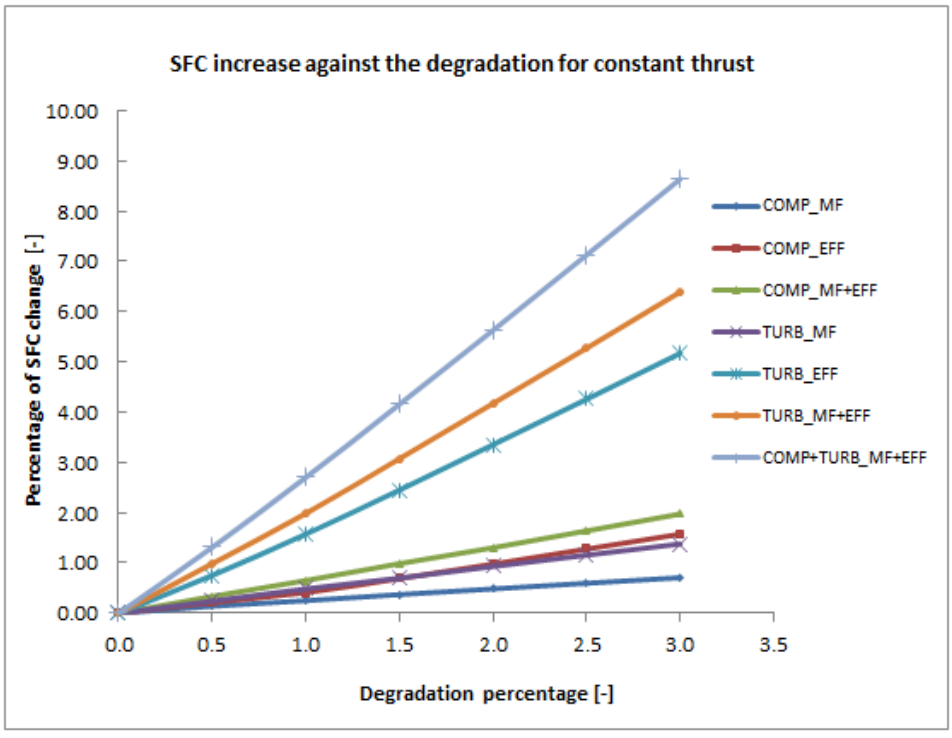

Figure 3-21 SFC increase against degradation for constant thrust at TO

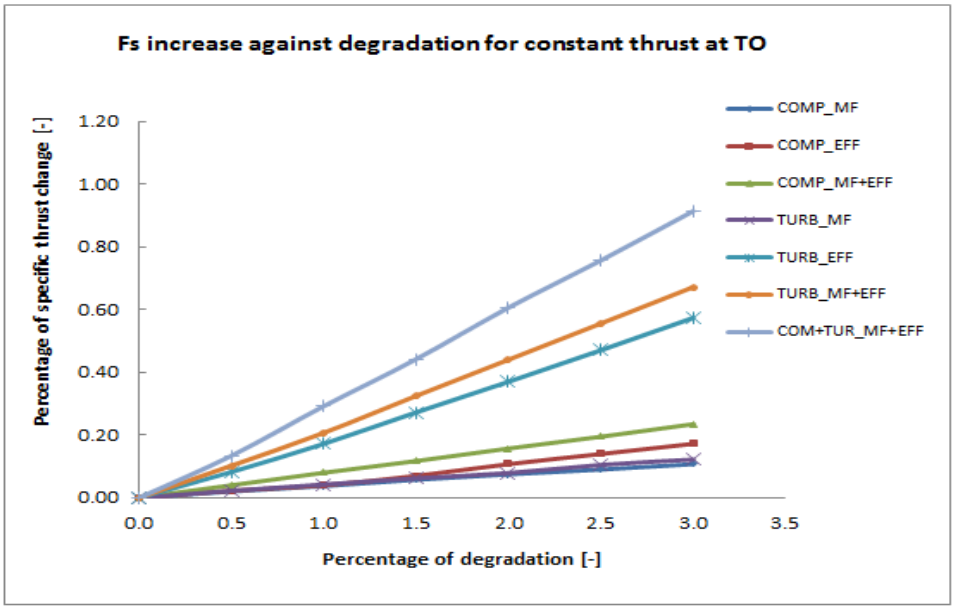

Figure 3-22 Specific thrust against degradation for constant thrust at TO

Figure 3-23 shows the increase of TET due to component degradation. This is the time engine operate at its maximum TET, thus it is important to investigate the impact of different degradation levels on the maximum TET. Compressor mass flow, and efficiency drop shows similar effects of 0.5% on TET up to degradation of 1.0% and increased the level of effect to 2.0% and 1.0% respectively when degradation reach to level of 3.%. Combined effects of mass flow and efficiency drop of compressor and turbine increase the TET by 2.8% and 3.5% respectively at the limit of 3% degradation. Also combined effect of compressor and turbine mass flow and efficiency drop has shown the highest effect of 6.5% on TET. However, it is important to state that, in practice such levels of degradation would not usually be reached. In general engines are operated at de-rated thrust and corresponding TET levels.

EGT reaches its peak during the take-off or just lift-off. It was expected maximum EGT to increase, when engine get degraded. As discussed in Section 3.5.2, increments in EGT have been used as a parameter for engine performance monitoring in practice. Figure 3-24 shows the increase of EGT with respect to different levels of component degradation. Latter part of the chapter, these EGT variations have been used to select the required levels of degraded engines for mission level assessments.

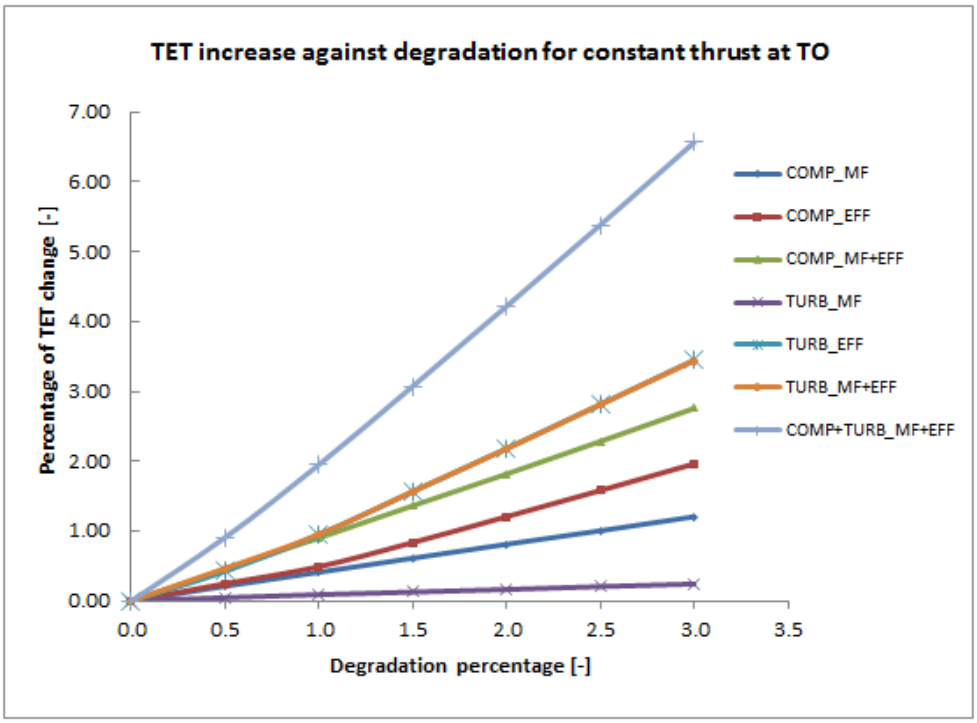

Figure 3-23 TET increase against degradation for constant thrust at TO

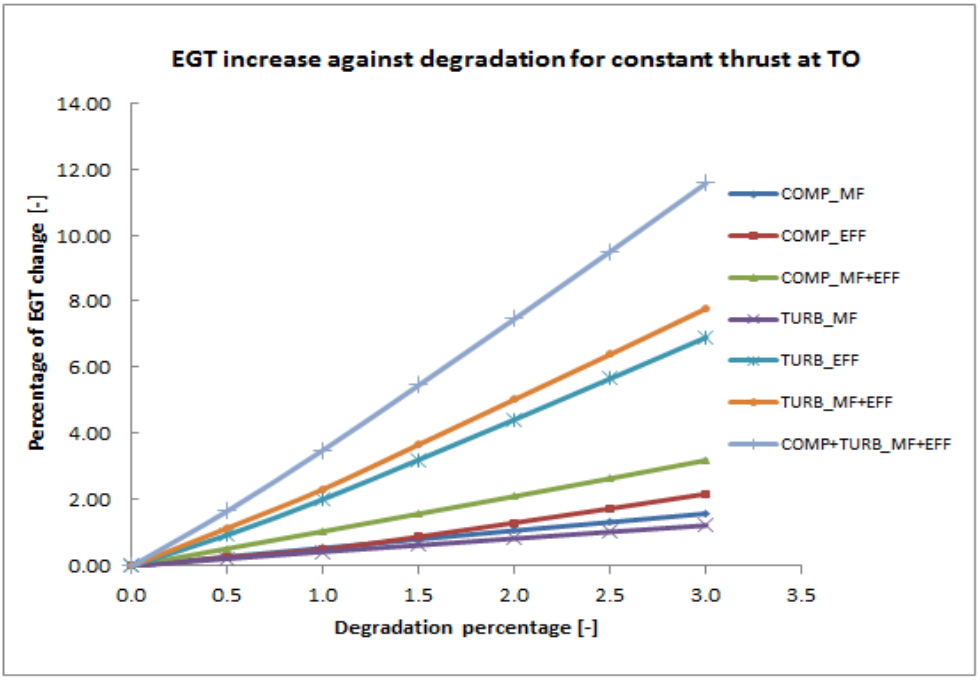

Figure 3-24 EGT increase against degradation for constant thrust at TOC

3.8 Long Range Engine Model

3.8.1 Long range engine model development

The long range engine model is developed based upon the CFM56-5C4 engine which is currently used to power the A340-200 type four engine wide body aircraft. The configuration of the model is two spool high bypass ratio turbofan engine with a booster stage, separate exhausts, custom bleeds and cooling bleed off-takes. The schematic of the engine is given in Figure 3.25.

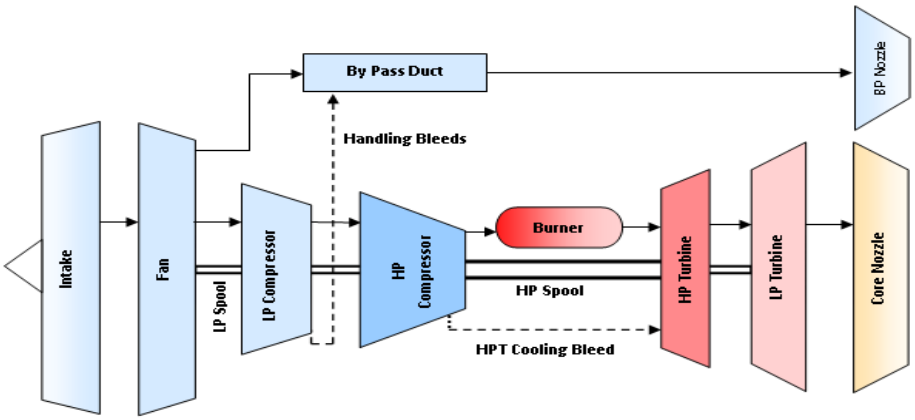

Figure 3-25 Schematic of the long range two spool high bypass turbofan engine model

The design point of the engine model was selected at top of climb (TOC) i.e. Alt: 10668 m, Mach number 0.8, and the pressure recovery of 0.99 under International Standard Atmospheric (ISA) conditions. Several iterations were performed using the model at design and off-design conditions to match the performance of the model with the data obtained from the public domain for the engine on which the design was based (CFM, 2011). The mass flow rate of the engine intake was estimated based on the measured nacelle area and assuming an average inlet Mach number of 0.55 – 0.65. The design point which is at the top of climb bypass ratio (BPR) and the turbine entry temperature (TET) were determined based on the overall pressure ratio (OPR) and the net trust at top of climb. The optimum fan pressure ratio (FPR) corresponding to the calculated TET, overall pressure ratio (OPR) and bypass ratio (BPR) were also determined. In addition to the above, compressor pressure ratios, component efficiencies, and compressor bleeds for turbine cooling, custom bleeds, and other parameters, were guessed and iterated to match the required engine performance at design point and off-design (maximum take-off and cruise) conditions (CFM, 2011, ICAO 2013). Finally, the model also has been tested and validated against different off-design conditions such as several thrust ratings and corresponding

fuel flow rates available in the public domain. The Table 3-4 shows the comparison of the design and performance data of the simulated engine against the public domain literature. In addition several off design performance simulations were also carried out in order to evaluate the simulation capability of the developed model as a clean engine.

The simulation results comprise of performance charts assessing the effect of flight altitude, speed (Mach number), ambient temperature and turbine entry temperature on the net thrust and specific fuel consumption (SFC). Figure 3.26 indicates the variation of net thrust (F_n) as a function of flight altitude (Alt) and flight Mach number (Mach) for a fixed value of turbine entry temperature (TET). The value of TET chosen for the take-off point was; TET =1745K. The Figure 3.27 indicates the variation of specific fuel consumption (SFC) as a result of changing flight altitude, and Mach number for the same fixed value of TET. The Figure 3.28 highlights in turn the variation of net thrust as a function of ambient temperature (T_{amb}) and turbine entry temperature (TET) at sea level static (SLS) condition (i.e. Alt=0m, and Mac =0). Finally, Figure 3.29 highlights the variation of SFC as a function of ambient temperature ((T_{amb}) and TET at sea level static (SLS). It may be noted that for these analysis the maximum TET considered was the TET corresponding to Take-off conditions. Also it can be observed that, the performance charts corresponding to the long rang engine model also broadly follow the expected trends of similar engines. The validated engine model has been used to simulate the various degradation scenarios, as described in Section 3.6.

Table 3-4 Long Range Aircraft engine model verification

ENGINE DP PARAMETERS OF CULE_0DL				
Fan Pressure Ratio [-]		1.6		
By Pass Ratio [-]		6.3		
Overall Pressure Ratio [-]		38.3		
Mass Flow kg/s		488		
Fan Pressure Ratio [-]		1.60		
Booster Pressure ratio [-]		1.8		
HPC Pressure Ratio [-]		13.3		
Compressor Efficiencies		0.89		
Turbine Efficiencies		0.92		
Combustor Efficiency		0.99		
DP SIMULATION - CONDITIONS AND RESULTS				
DP Conditions				
Altitude [m]	10668.0			
Mach number [-]	0.8			
ISA [^{0}C]	0.0			
Parameter	**From Simulations**	**From Public domain**	**Variation**	**Reference**
Mass Flow	488.9	483.0	1.22%	CFM (2013)
Pressure Ratio	38.4	38.3	0.30 %	CFM (2013)
Thrust [N] TET – 1660K	33785.0	33716.0	0.20 %	CFM (2013)
OD SIMULATION - CONDITIONS AND RESULTS				
OD Conditions				
Altitude [m]	0.00			
Mach number [-]	0.00			
ISA [^{0}C]	0.00			
Parameter	**From Simulations**	**From Public domain**	**Variation**	**Reference**
Mass Flow [kg/s]	488.9	483.0	1.2 %	CFM (2013)
BPR [-]	6.3	6.4	1.6 %	CFM (2013)
Pressure Ratio [-]	32.1			ICAO(2002)
Take-off Thrust [N] TET – 1745 K	150920.0	151232.0	0.2 %	CFM (2013)
Parameter	**From Simulations**	**From Public domain**	**Variation**	**Reference**
FF @ 100% PS [Kg/S] TET-1745 K	1.43	1.45	1.4 %	ICAO EDB [4]
FF @ 85% PS [Kg/s] TET 1610 K	1.16	1.19	2.5 %	ICAO EDB [4]
FF @ 30% PS [Kg/s] TET 1180 K	0.38	0.37	2.6 %	ICAO EDB [4]

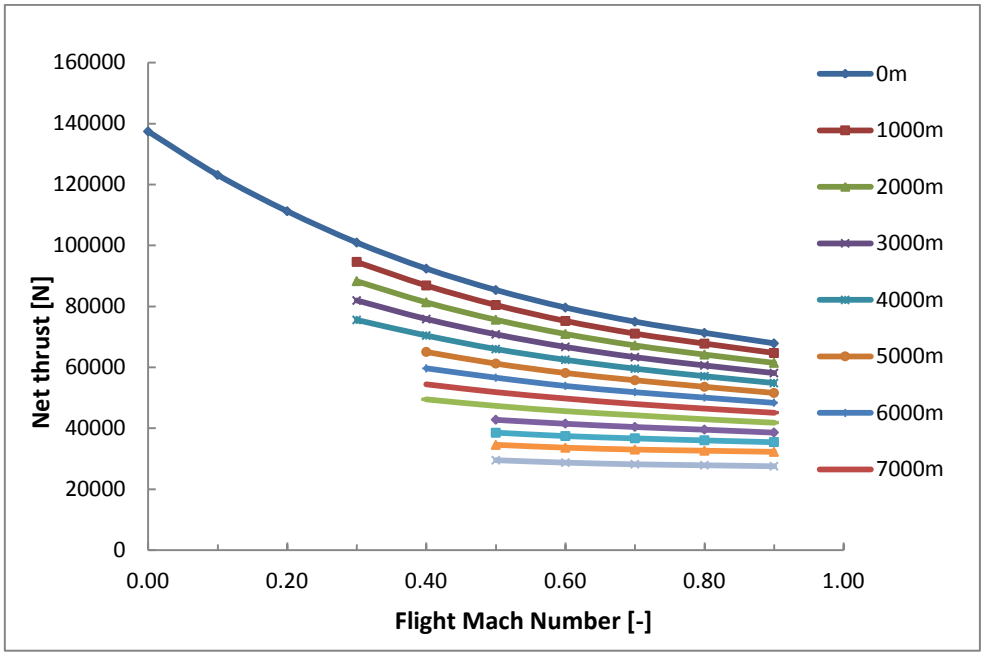

Figure 3-26 Variation of net thrust as a function of altitude and Mach number for the fixed TET

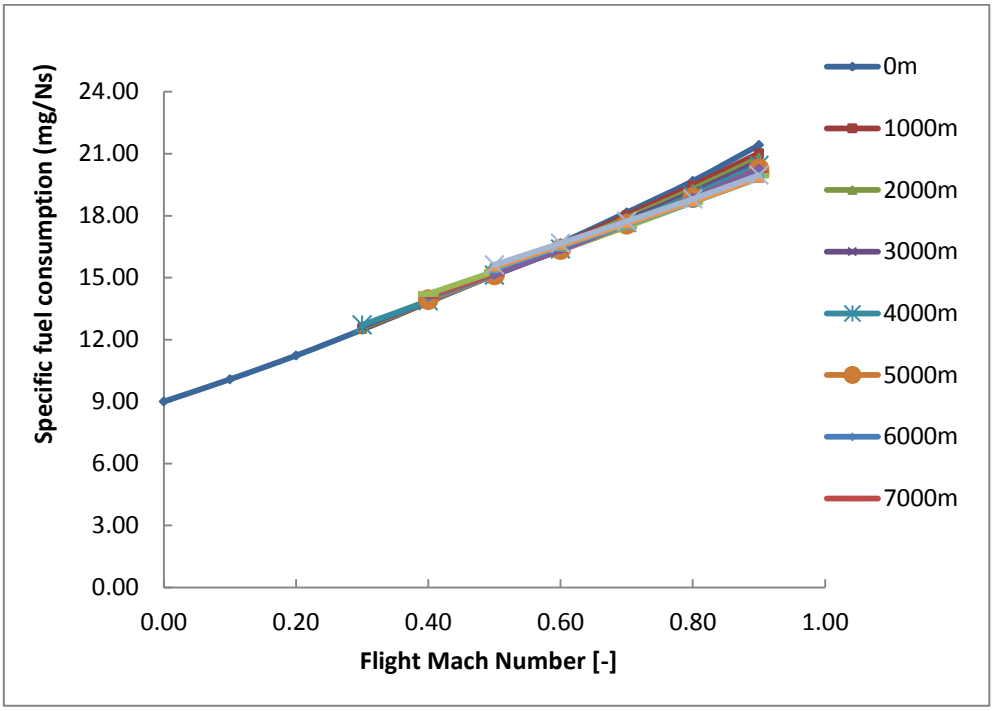

Figure 3-27 Variation of SFC as a function of altitude and Mach number for the fixed TET

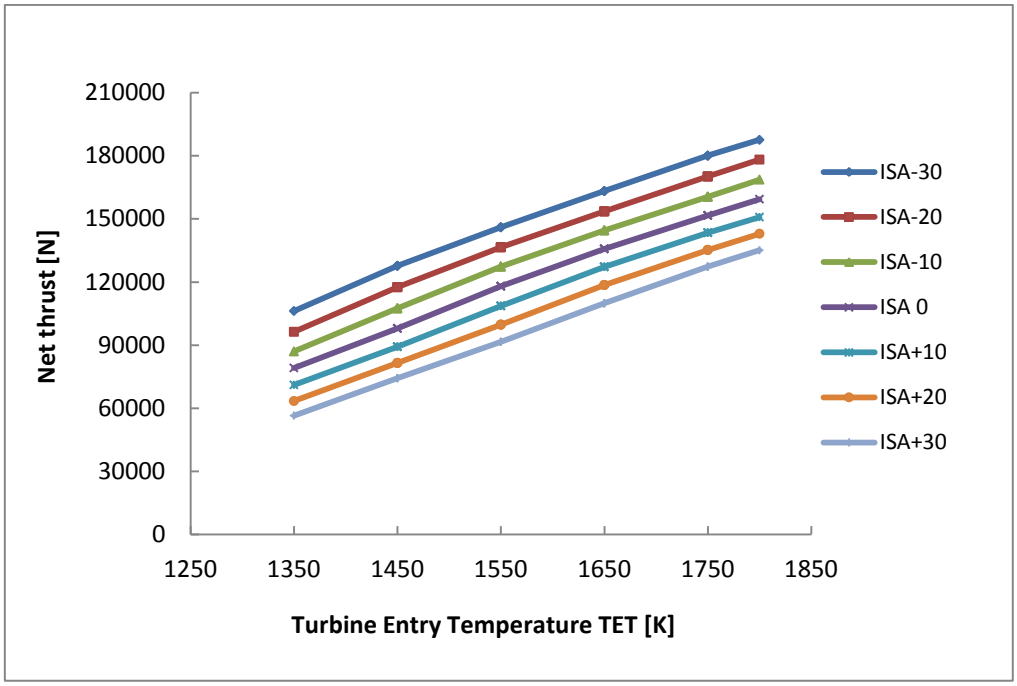

Figure 3-28 Variation of net thrust as a function of TET and ambient temperature

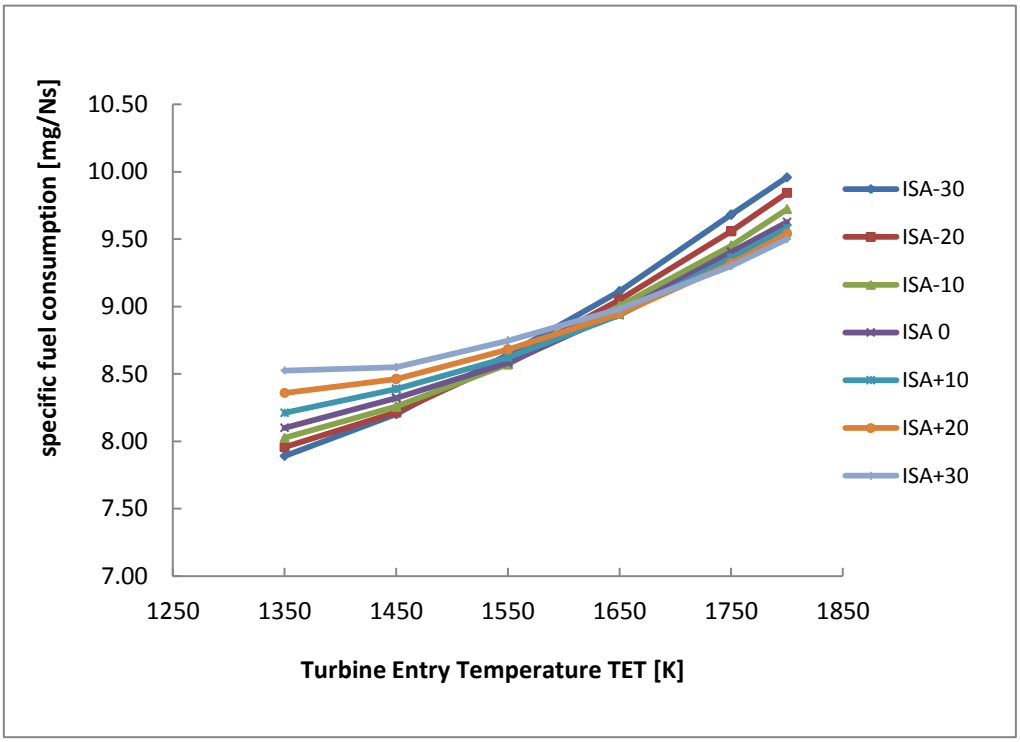

Figure 3-29 Variation of SFC as a function of TET and ambient temperature

3.8.2 Impact of degradation on engine performance at TOC

This part of the section is used present the results of various component degradation effects on engine performance at TOC. Simulations are performed similar to the short range aircraft engine. PR decrease against degradation for constant TET at TOC is presented in Figure 3-30. It can be observed that effect of compressor and turbine mass flow shows similar effects, with a reduction of 2% on PR at 3% degradation. Other component's mass flow and efficiency drops shows similar effects as discussed in previous section of the short range engine (CUSE_0DL) engine degradation.

Figure 3-31 shows the net thrust drop at constant TET for different levels of component degradation. Turbine mass flow deterioration shows the least effect of 0.5% on net thrust drop, whereas the effects due to other component deteriorations shows behaviour similar to Figure 3-16 of the short range engine model. As discussed in the previous section Figure 3-32 shows the effects of component deterioration on SFC increase at constant thrust. Compressor mass flow drop has the least effect on SFC increase, whereas effect of compressor efficiency, turbine mass flow and compound effect of compressor shows similar effects, which is approximately 0.5% for 3.0% degradation. Effect of turbine efficiency and combined effect of turbine mass flow and efficiency have a significant effect of 3% and 4% respectively for 3% limit of degradation. Figure 3-33 shows the variation of PR against degradation of compressor and turbine. Compressor mass flow shows the lowest effect on PR, up to 2.2% of degradation. It is important to notice that turbine efficiency drop has an effect of -0.5% up to 2% degradation and stays constant up to 3% maximum degradation. Other component effects show behaviour similar to short range engine. Figure 3-34 shows the effect of component degradation on TET. Turbine mass flow drop shows the least effect of 0.3% on TET. Compressor mass flow and compressor efficiency drop shows an effect of 1.1% and 1.5% increase of TET respectively for the maximum degradation limit of 3.0%. However, turbine efficiency, and combined effect of compressor and turbine shows similar effects on TET of 2.5% for the maximum degradation limit. It is important investigate the effect of TET as engine is spend most of its operating time on this condition (cruise). Variation of EGT against degradation for constant thrust is shown in Figure 3-35.

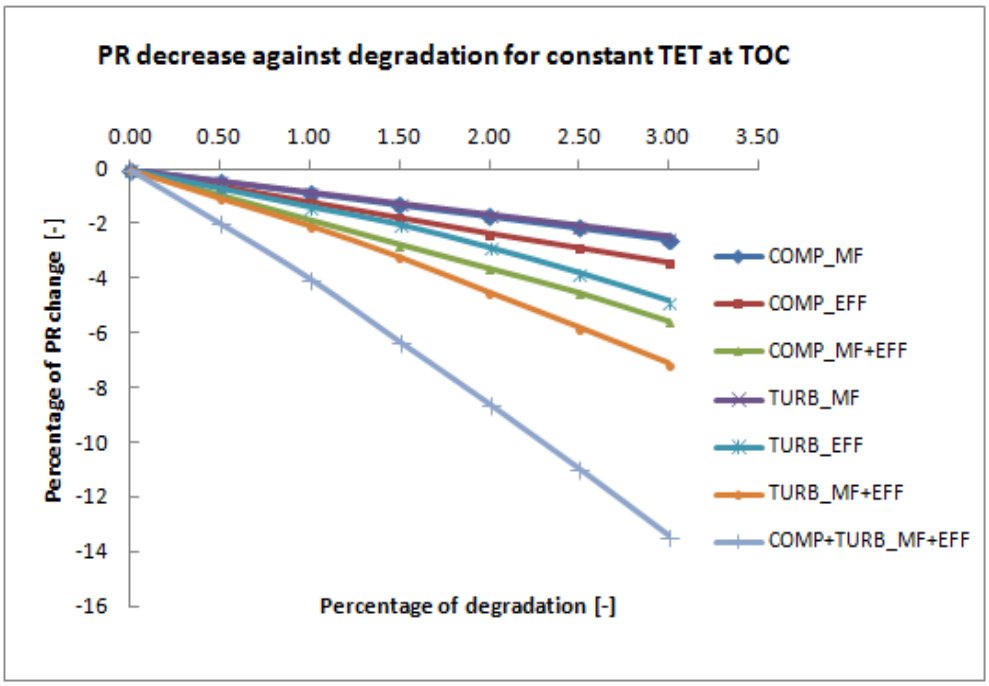

Figure 3-30 PR decrease against degradation for constant TET at TOC

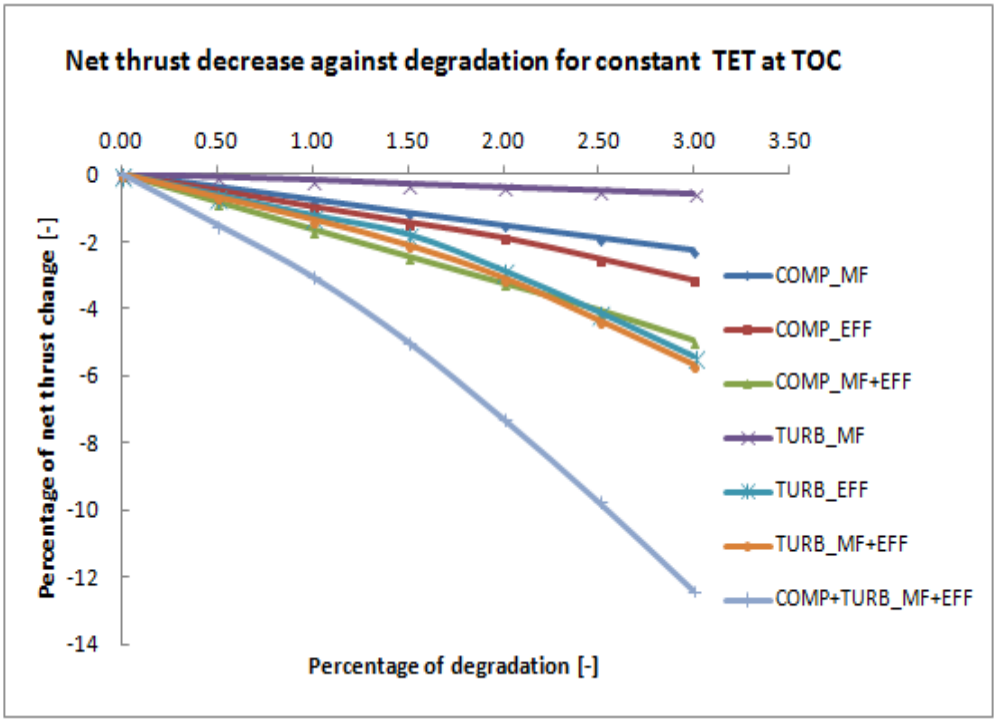

Figure 3-31 Net thrust decrease against degradation for constant TET at TOC

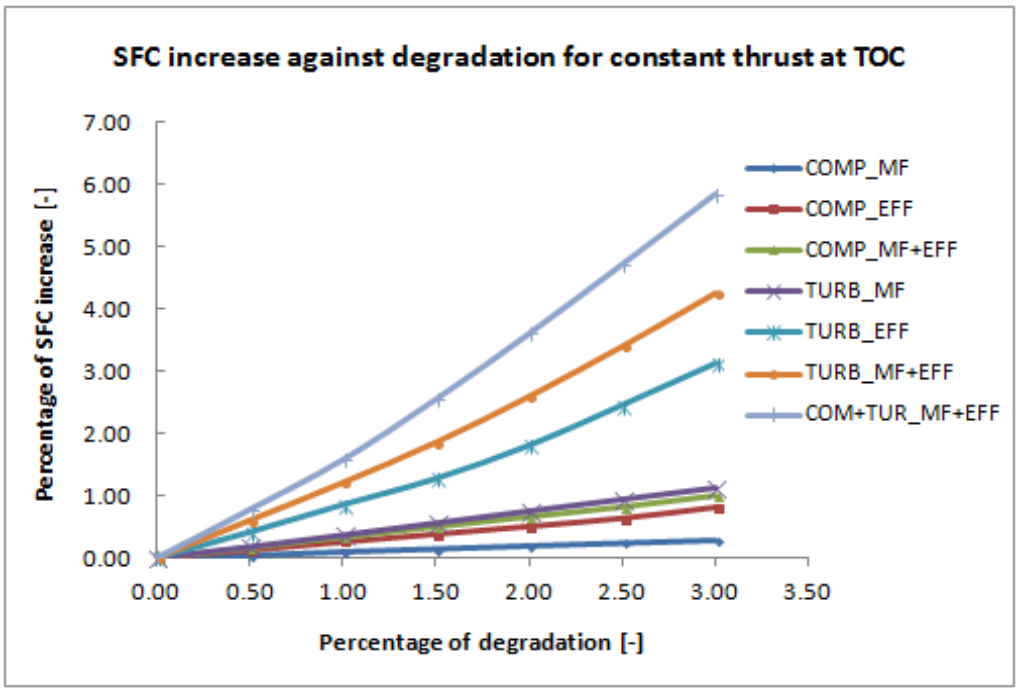

Figure 3-32 SFC increase against degradation for constant thrust at TOC

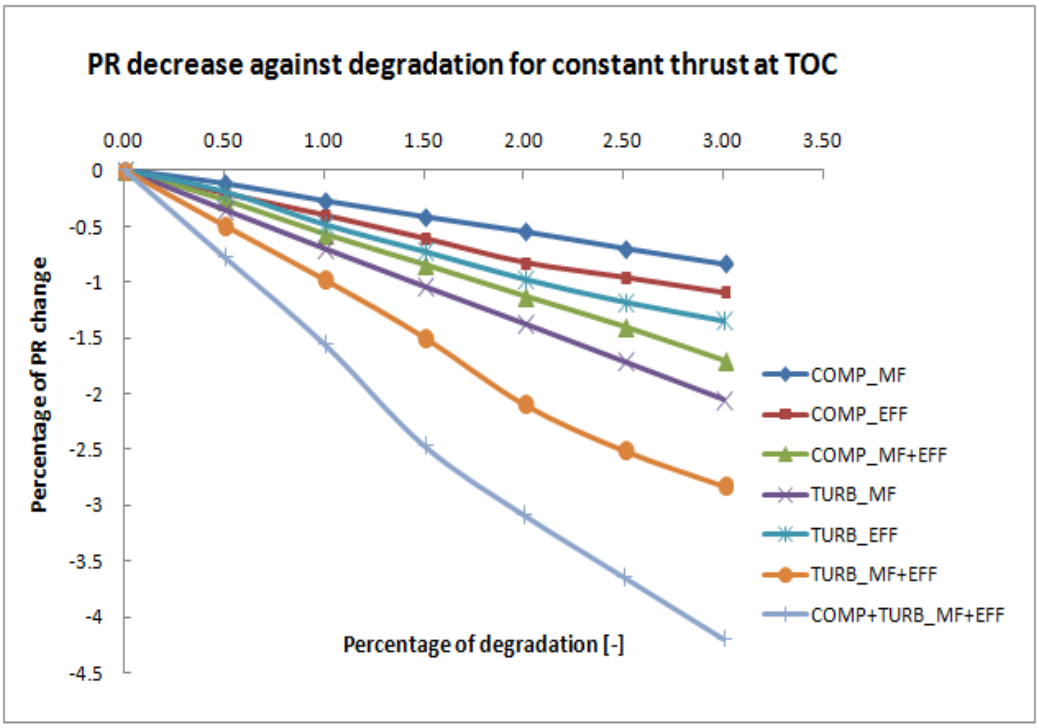

Figure 3-33 PR decrease against degradation for constant thrust at TOC

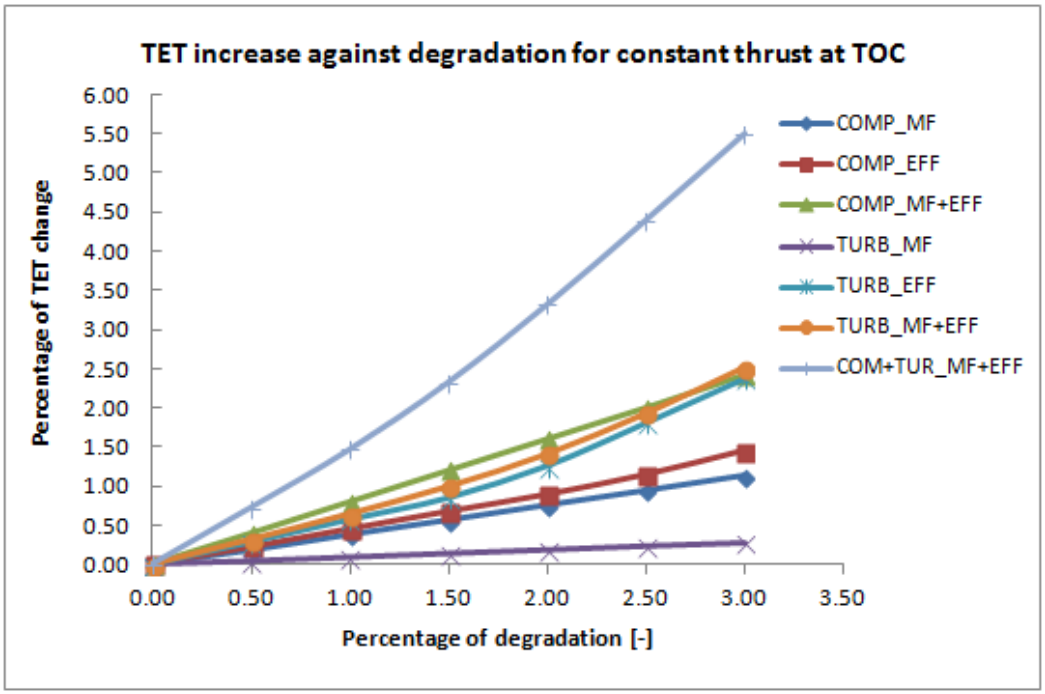

Figure 3-34 TET increase against degradation for constant thrust at TOC

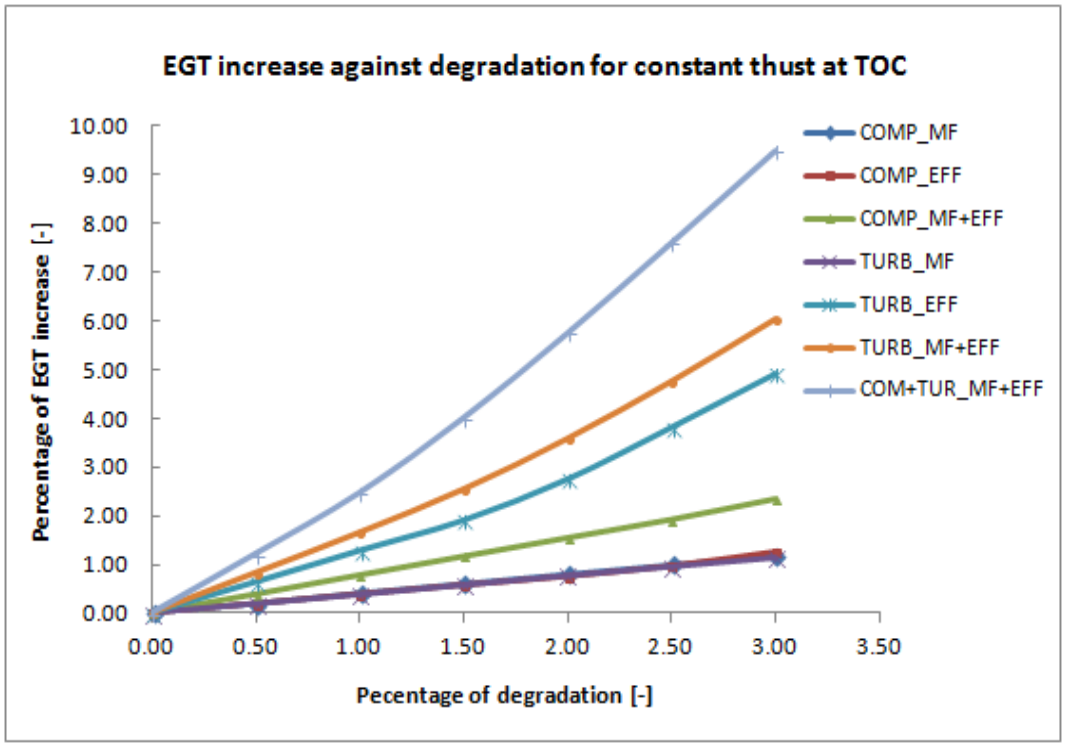

Figure 3-35 EGT increase against degradation for constant thrust at TOC

3.8.3 Impact of degradation on engine performance at TO

Figure 3-37 shows the impact of compressor mass flow and turbine mass flow drop increase the specific thrust, in order to keep the net thrust constant. Also it is important to notice that impact of the turbine mass flow drop is higher than the combined effect of compressor mass flow and efficiency drop. But impact of the turbine efficiency drop is much significant than the compressor efficiency drop as expected.

Figure 3-36 shows the degradation effects on SFC at constant thrust. It can be observed that the compressor mass flow has the lowest effect on SFC increase of 0.5% for the maximum degradation limit of 3%. It is also interested to notice that, drop in compressor efficiency, turbine mass flow and combined effect of mass flow and efficiency show similar effects on SFC increase which is 1.3% for the maximum degradation limit of 3%.

However, turbine efficiency, and combined effect of mass flow and efficiency drop have significant effect of 5% and 6.8% respectively for maximum level of 3%. As expected, combined effects of mass flow and efficiency drop of compressor and turbine has the highest impact of 9% increase on SFC for the same limit of 3% degradation. This is 0.5% higher than the short range engine. However, engine experience this high SFC only for a short period of time during its take-off.

Figure 3-37 shows the increase of specific thrust for various levels of component degradation, and Figure 3-38 shows the effects of component degradation on TET. Turbine mass flow drop shows the lowest effect of 0.4%, whereas combined effect of mass flow and efficiency of compressor and turbine shows the highest effect of 7%. Figure 3-39 shows the effect of various levels of component degradation on EGT increase. As described in the previous section EGT increase has been used to monitor the engine degradation and to define the required engines for the mission level assessments

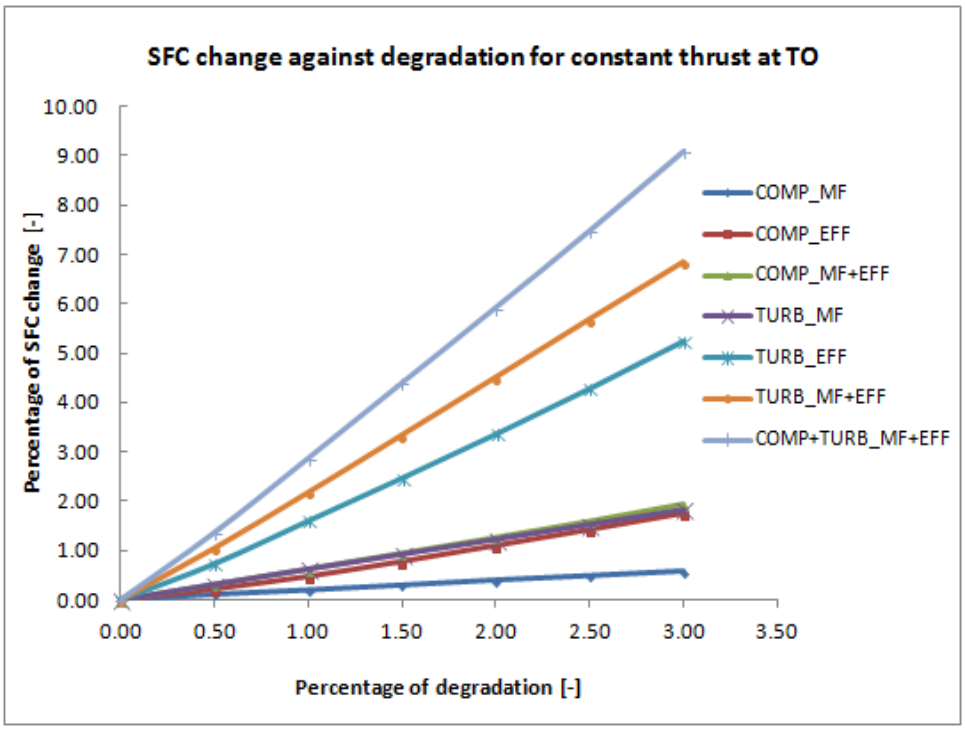

Figure 3-36 SFC increase against degradation for constant thrust at TO

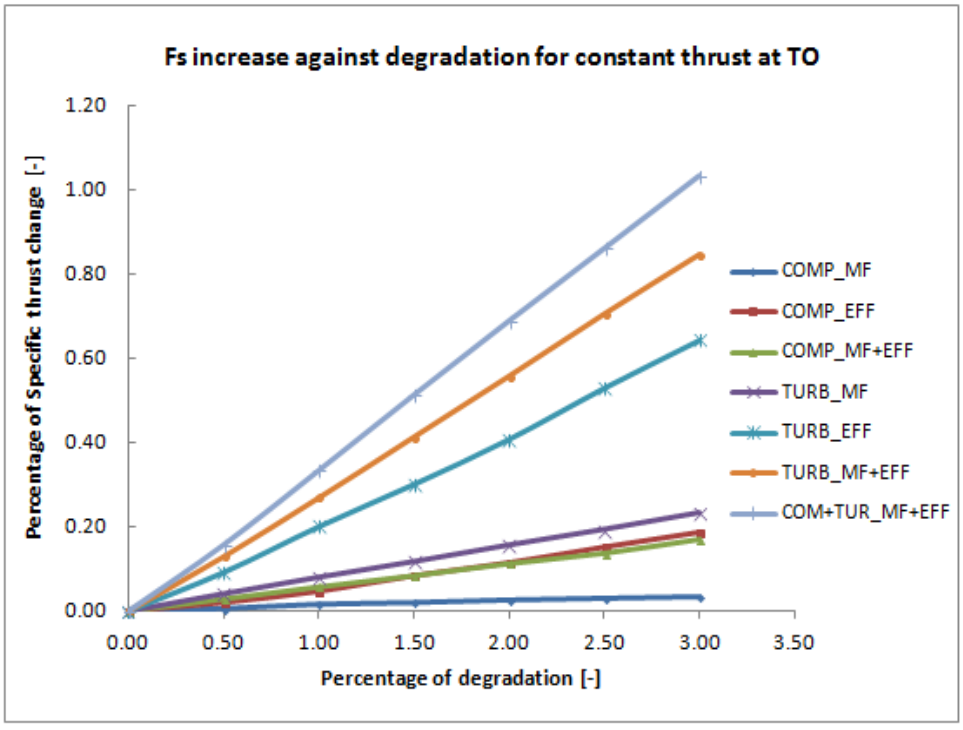

Figure 3-37 Specific thrust increase against degradation for constant thrust at TO

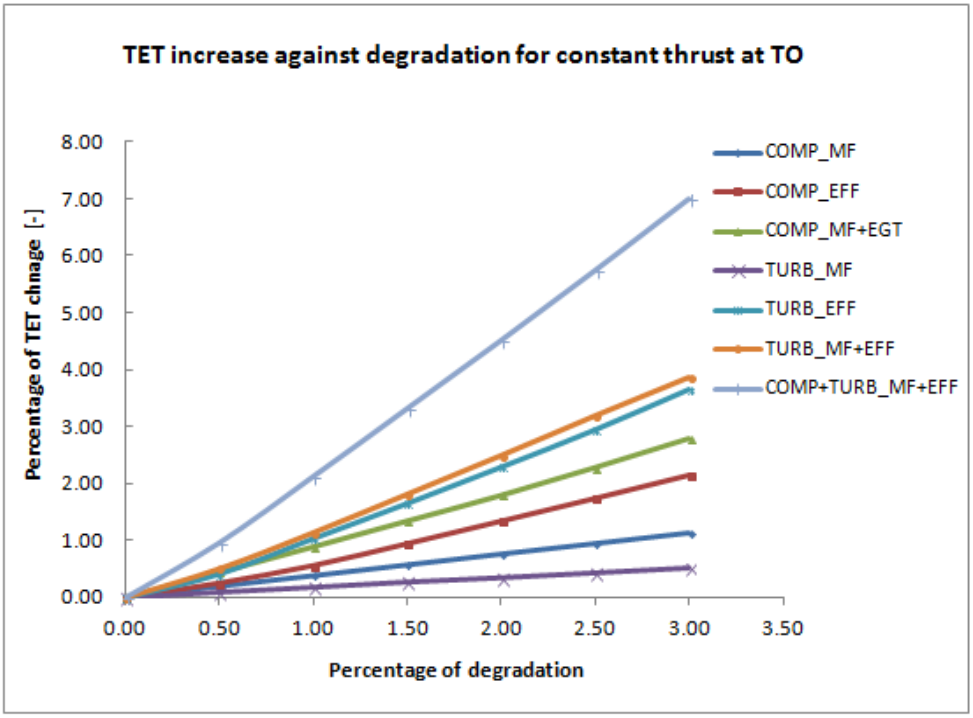

Figure 3-38 TET increase against degradation for constant thrust at TO

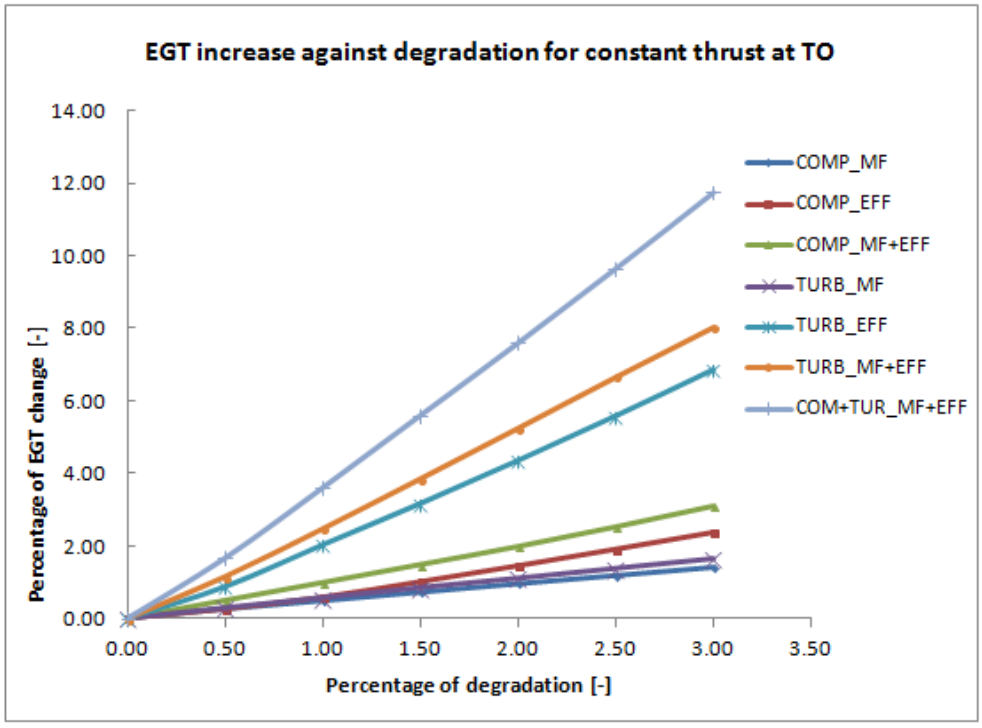

Figure 3-39 EGT increase against degradation for constant thrust at TO

3.9 Selection of degraded engines for trajectory optimisation

Engine component degradation leads to changes in the performance characteristics, which gives a compound effect on the overall engine performance. The variation of these operating characteristics causes reduction in thrust and increase in SFC. The thrust drop is compensated by increasing the spool speed or TET. However in both cases will bring significant changes to engine performance and monitoring parameters; such as SFC, engine pressure ratio (EPR), fuel flow (FF), and exhaust gas temperature (EGT). As described before, in this work EGT increase has been used as the key engine monitoring parameter for engine performance deterioration.

However, considering the engine performance data given in Lukachko, 1997 and CFM (2014) suggested maximum rise in EGT of 90 – 100 K may increase the SFC by 2 – 4%. Considering the given data and the above analysis author has chosen to use, 100K increase of EGT which is 10% increase of the TO EGT and corresponding SFC increase of 3% taken as reasonable values for the maximum degradation limit to investigate the effect of engine degradation on mission level performance. Therefore author has considered two degradation scenarios of 5% and 10% increase of EGT with respect to the EGT of base line clean engine at TO condition.

Two engine models have been selected from the parametric analysis conducted in the previous section. Combined effect of both compressor and turbine degradation has taken to simulate the 5% and 10% EGT increase for the both engines. Figure 3-40 shows the corresponding short range degraded engines which has been selected based on the EGT levels indicated in Table 3-5. Figure 3-41 show the similar criteria considered for selecting the long range degraded engine models. Table 3-6 shows the corresponding EGT values considered for the selection of models.

Table 3-5 Degradation limits considered for short range engine

CASE	Engine	Level of Degradation	Maximum Delta EGT
CASE_1	CUSE_0DL	0 % EGT Increase	50-100K
CASE_2	CUSE_1DL	5 % EGT Increase	
CASE_3	CUSE_2DL	10 % EGT Increase	

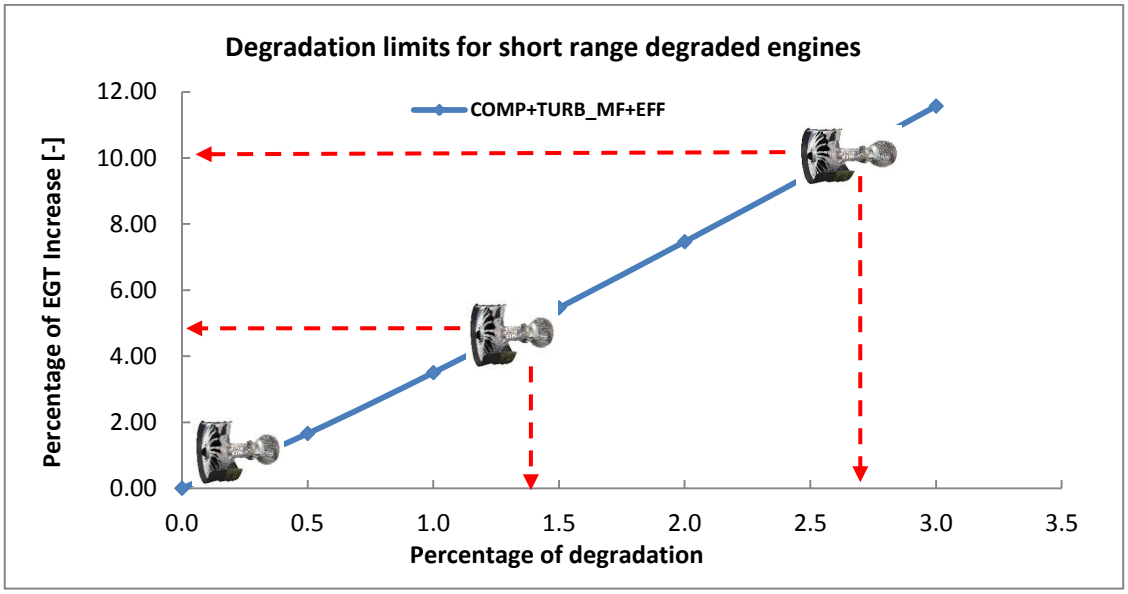

Figure 3-40 Degradation limits considered for short range engine

Table 3-6 Degradation limits considered for long range engine

CASE	Engine	Level of Degradation	Maximum Delta EGT
CASE_1	CULE_0DL	0 % EGT Increase	50-100K
CASE_2	CULE_1DL	5 % EGT Increase	
CASE_3	CULE_2DL	10 % EGT Increase	

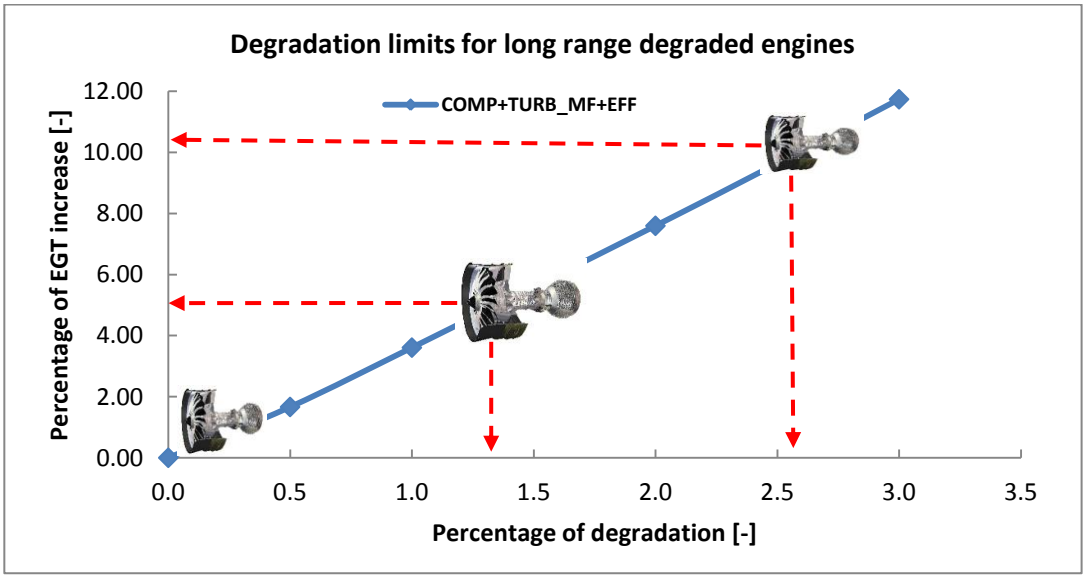

Figure 3-41 Degradation limits considered for long range engine

3.10 Summary

This chapter was focused on the key degradation mechanisms of aircraft engines. In order to understand the impact of engine degradation on engine performance a short range and a long range engine model have developed. The various levels of degradation mechanisms are simulated to analyse the sensitivity of engine performance to component degradation. The impact of degradation on engine performance parameters of net thrust, sfc and key engine monitoring parameters such as fuel flow, engine pressure ratio and exhaust gas temperature were assessed at TOC and TO conditions. Finally a clean and two degraded engine models were created for short range and long range aircraft based on the maximum EGT deterioration levels which CFM56-5B4 and CFM56-5C4 could achieve during their service. (i.e. maximum EGT increase of 10%, and 5% of the maximum EGT increase). The created models will be integrated with the aircraft dynamic models to develop the optimisation frame work in the next Chapter.

4 Generic Framework for Multi-Disciplinary Aircraft Trajectory Optimisation and Power Plant Integration

4.1 Introduction

In order to study the effects of engine degradation on optimum aircraft trajectories that can be implemented to reduce emissions, a multidisciplinary optimisation framework has been developed based on the aircraft trajectory optimisation tool GATAC. This chapter aims to provide the reader an understanding of this framework, and associated models utilised for the work. The chapter begins with a description of the optimisation framework which use to integrate the various models into a network and then goes on to describe each model in detail and their main limitations. In order to improve the confidence of the results produced by each model, several validation and verification tests were conducted. The next section of the chapter focuses on the optimisation strategy and the specific optimiser used for the trajectory optimisation. The capabilities of handling multi-objective aircraft trajectory optimisation problem with large no of variables and large no of constraints are discussed. Benchmarking and testing of the optimiser against other optimisers is also presented. Finally chapter concludes with a discussion of the system level model integration and model interaction in the framework which have been developed to conduct aircraft trajectory optimisation of short range and long range aircraft.

4.2 GATAC Environment

This section presents an overview of the main features and capabilities of the GATAC multi-disciplinary optimisation framework, which has been developed within Cranfield University as a part of current PhD work under SGO ITD (Integrated Technical Demonstrator) of the Clean Sky. This framework has been used throughout this PhD work, as author has contributed to the development of the framework by testing, validating and used for two Clean Sky project deliverables and test cases including several publications (Gu, and Navaratne 2012, and Navaratne 2013). The framework can be considered as a state-of the-art optimisation tool with the aircraft performance model (APM), engine performance models (EPM), engine emission model (EEM), contrail simulation model (CPM) and optimiser to perform multi-objective trajectory optimisation studies under Air Traffic Management (ATM) constraints. The top level structure of the framework is shown in Figure 4-1.

The architecture consists of, the GATAC Core, Model Suite, Post-Processing Suite, and Graphical User Interface (GUI). The GATAC core is the heart of the interaction framework and provides the connectivity between the various models. It also provides for the organisation of an evaluation process (within the Evaluation Handler) and includes functionalities such as parameter stores, data parsing, translation function and interfacing with models. It also supports the repeated calling of sets of models to enable trajectories to be evaluated step by step with number of steps being defined by the user at the set-up time. The core, therefore, is programmable as the user sets-up the problem at hand within the Evaluation Handler by defining connectivity between models and any data translation and other functions. This can be done either directly using a purposely defined domain specific language or graphically via GUI. In this way, the user effectively defines (formulates) the optimisation problem. The optimisation process takes place in the GATAC Core, using the optimisation algorithm chosen from a suite by the user.

A key feature of GATAC is that, the user can select any algorithm from the optimisation suite without the need to modify the problem formulation because; the framework caters for normalisation of data. Indeed, the algorithms in the optimisation suite are designed to handle normalised variable parameters. The normalised parameters are then de-normalised by the integration framework as specified by the user before being input to the evaluation handler. Similarly the data that are output from the evaluation handler are again normalised before being input to the optimiser to close the optimisation loop. As the data exchanged between the optimisation core and the models need to be defined according to the input and output data of each model and module. GATAC caters for the automatic definition of data structures by means

of a dictionary the automatic definition is carried out by GATAC at set-up time according to the output and input variables of the specific models and modules invoked in the problem definition. These data structures then enable the correct data transfer between the models and modules.

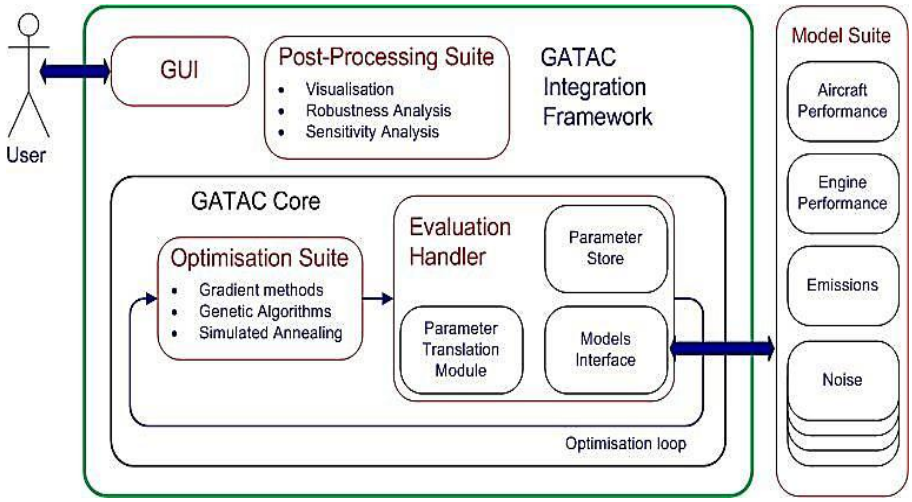

Figure 4-1 GATAC Framework

GATAC can be run either on a single stand-alone machine or a distributed system with multiple computers. In this case the model suite is replicated on a number of five different machines, on which a daemon will be running in the background. The daemon is even-triggered and instructed to run particular models by the Framework Manager, where the GATAC core resides. When its particular job is complete, the relevant daemon will return the results to the GATAC core. In this way, the core maintains full control of the optimisation process. Data exchange between the GATAC core and the daemons is achieved through Ethernet LAN connectivity between the respective computers. The model suite is distributed on a single machine or different machines acting as hosts. The data exchange between components carried out through Ethernet LAN. Figure 4.2 illustrates the architecture and operating network of the GATAC distributed system (Chircop 2010). Also at present, performance of the framework is able to demonstrate the Technology Readiness Level (TRL) level 5 platform, which is a measure that uses to access the maturity of evolving technologies prior to incorporating that technology into system or subsystem. The detail structure of the framework created for the specific application of assessing the impact of engine degradation of short range and long range aircraft are illustrated in following two chapters.

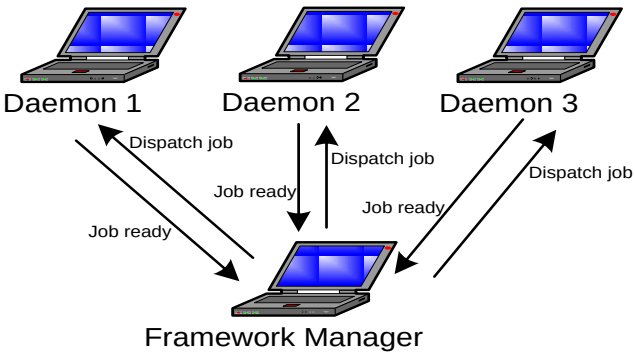

Figure 4-2 Distributed Operation of Optimization Framework

4.3 Engine performance models

4.3.1 Short Range Engine Models

For the purpose of this study three short range engine models have been developed to be used in conjunction with the aircraft performance model; one clean engine model and two degraded engine models. The configurations of the engines are typical twin spool high bypass turbofan engines similar in design characteristics to CFM56 5B4 engine which is currently used by the airlines to power the Airbus A320-200 aircraft. The complete details of the model development, model specifications, including testing and validation are given in Chapter 3. The developed engine model was considered as the baseline clean engine and was designated as CUSE_0DL (Cranfield University Short-range aircraft Engine with 0 Degradation Level).

Based on the developed clean engine model CUSE_0DL, two levels of degraded engine models have been created. As discussed in the previous Chapter, to simulate engine degradation in a simplified manner, specific engine component data have been changed in such a way that the engine performance parameters to reflect the corresponding levels of degradation. Therefore flow capacity and isentropic efficiency of the compressor and turbine components have been changed based on the limitations given in Lukachko and Waitze (1997). Then the degraded engines seek different steady

state operating points in relation to that of the clean engine. The variation of these operating points cause reduction in net thrust and increases SFC. The thrust drop is compensated by increasing the spool speed and adjusting the engine firing temperature (TET), which in turn increases the EGT of the engine. Therefore, EGT increase of 5% and 10% have been considered as the basis for create the two levels of degraded engines. Also data provided by Sri Lankan Airline was used to verify the EGT margins and levels of degradation. The two levels of degraded engines are designated as CUSE_1DL and CUSE_2DL respectively.

It must be noted that high detail of modelling and computational accuracy has a significant computational penalties. Therefore, in order to have the optimum balance of accuracy and computational speed, the engine performance of the all three engines have simulated over a wide range of operating envelop and resulting data-base was incorporated in Matlab/Simulink environment. The simulated data base was integrated with the aircraft performance model. The depicted simulated results of the clean and two degraded engines at zero altitude are shown in Figure 4.3, 4.4 and 4.5 respectively.

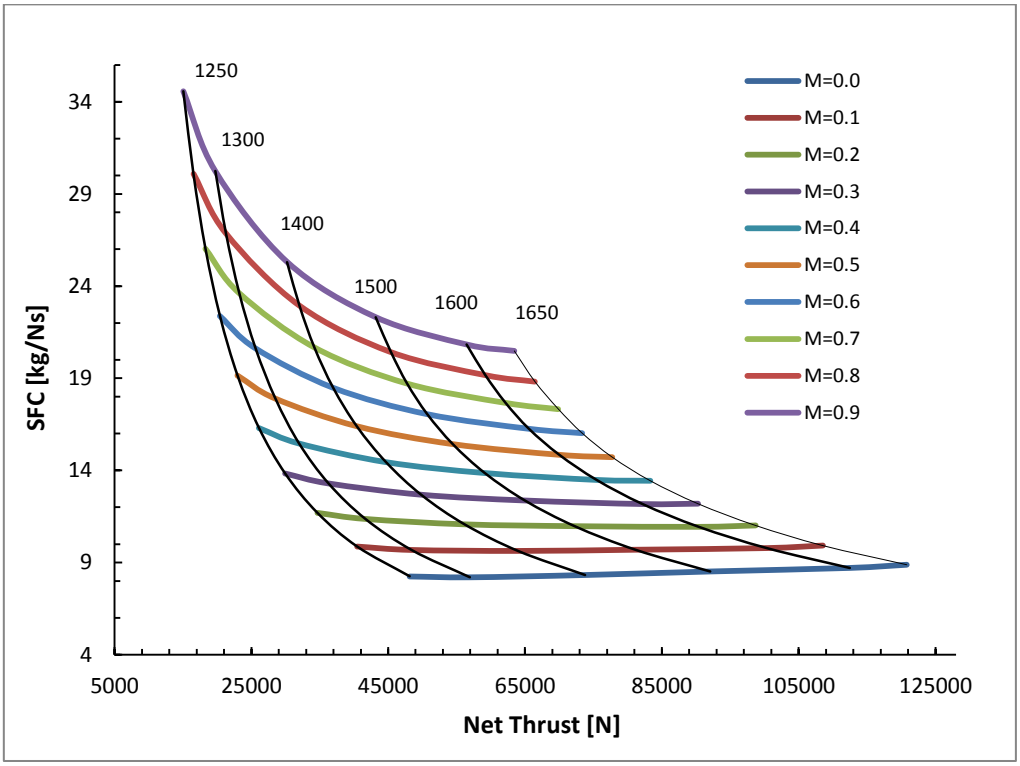

Figure 4-3 Net thrust and SFC variation as a function of TET and Mach number of CUSE_0DL

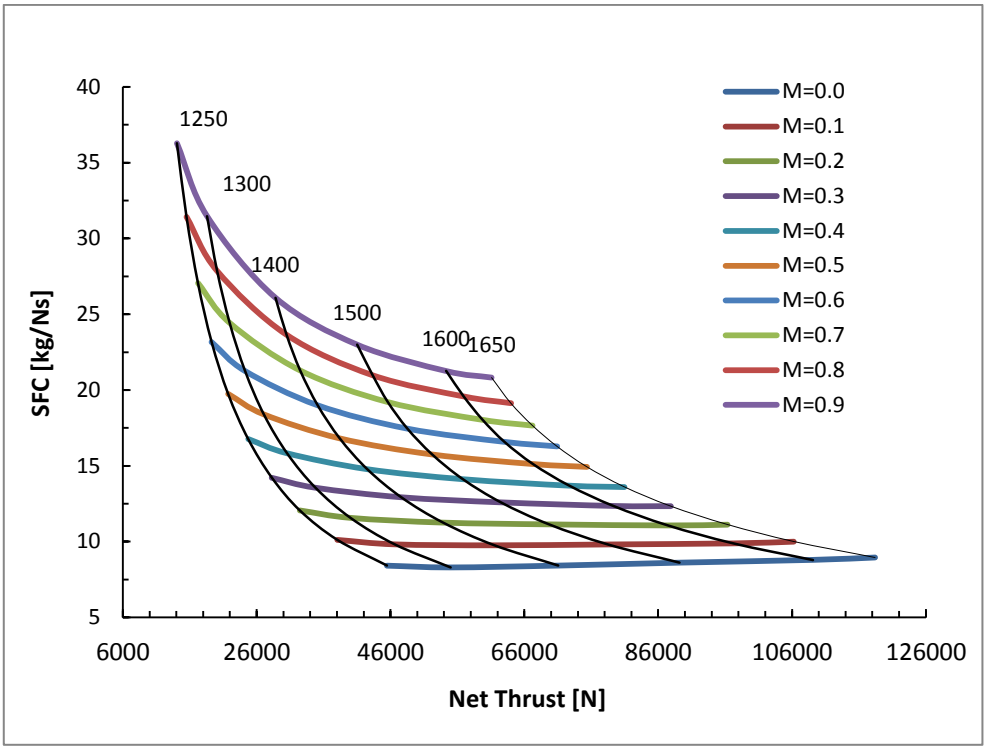

Figure 4-4 Net thrust and SFC variation as a function of TET and Mach number of CUSE_1DL

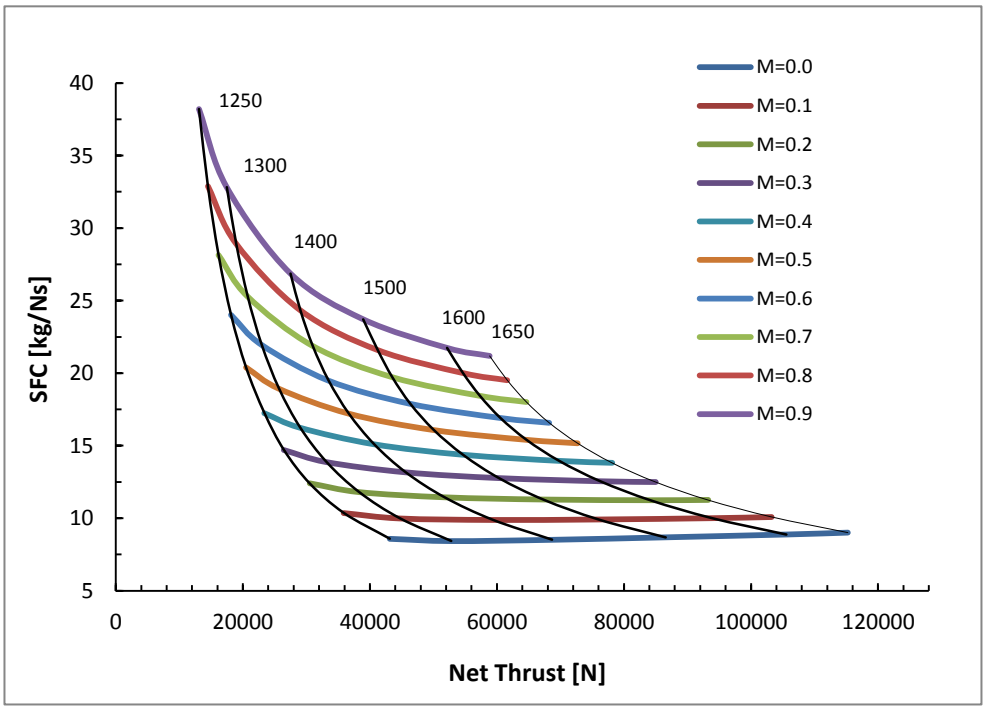

Figure 4-5 Net thrust and SFC variation as a function of TET and Mach number of CUSE_2DL

4.3.2 Long range engine models

The long range clean and two degraded engine models have developed based upon the CFM56-5C4 engine which is currently used to power the A340-200 type twin aisle wide body aircraft with four engines. The configuration of the model is two spool high bypass ratio turbofan engine with a booster stage, separate exhausts, custom bleeds and cooling bleed off-takes. The clean engine model was designated as CULE_0DL and complete model development including testing, validation and limitations are given in Chapter 3.

Based on the developed clean engine model, two long rang degraded engine models have been created in two degradation levels. To introduce engine degradation in a simplified manner isentropic efficiency and the mass flow rate of the compressor and turbine components was changed as per the limitations given in Lukachko and Waitze (1997). With these changes engine operates in a different steady state operating point compared to the clean engine, which cause reduction in net thrust and increase in SFC. The thrust drop is compensated by increasing the spool speed and adjusting the engine firing temperature (TET), which in turn increases the EGT of the engine. Therefore two levels of long range degraded engines models have been derived based on the EGT increase of 5% and 10%. In addition engine performance data provided by the Srilankan airline on CFM56-5C4 engine also considered. Degraded engines are designated as CULE_1DL and CULE_2DL respectively.

Similar to the short range engine models, simulated long range engine models have been used to performed a large amount of off-design calculations in a wider cross section of a flight envelop to build an engine performance database. As described before, this has been made to maintain a good balance of high degree of accuracy in detail modelling and computational speed by incorporating the database (engine deck) in a Matlab/Simulink computational environment while integrating models in the optimisation framework. The depicted simulated results of the clean and two degraded engines at zero altitude are shown in Figure 4.6, 4.7 and 4.8 respectively.

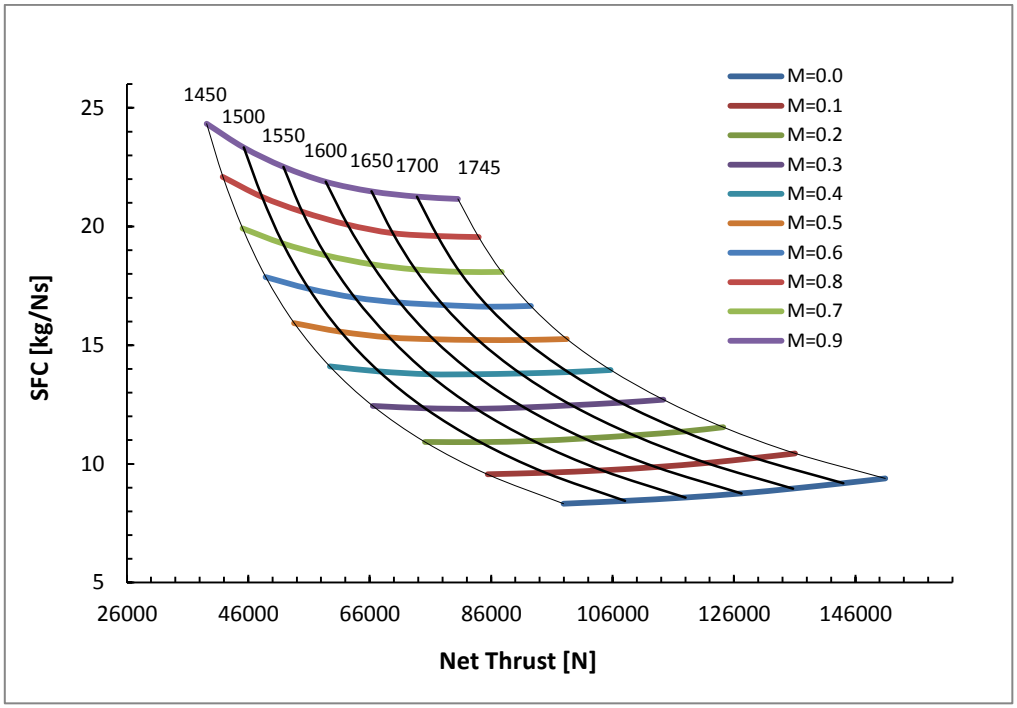

Figure 4-6 Net thrust and SFC variation as a function of TET and Mach number of CULE_0DL

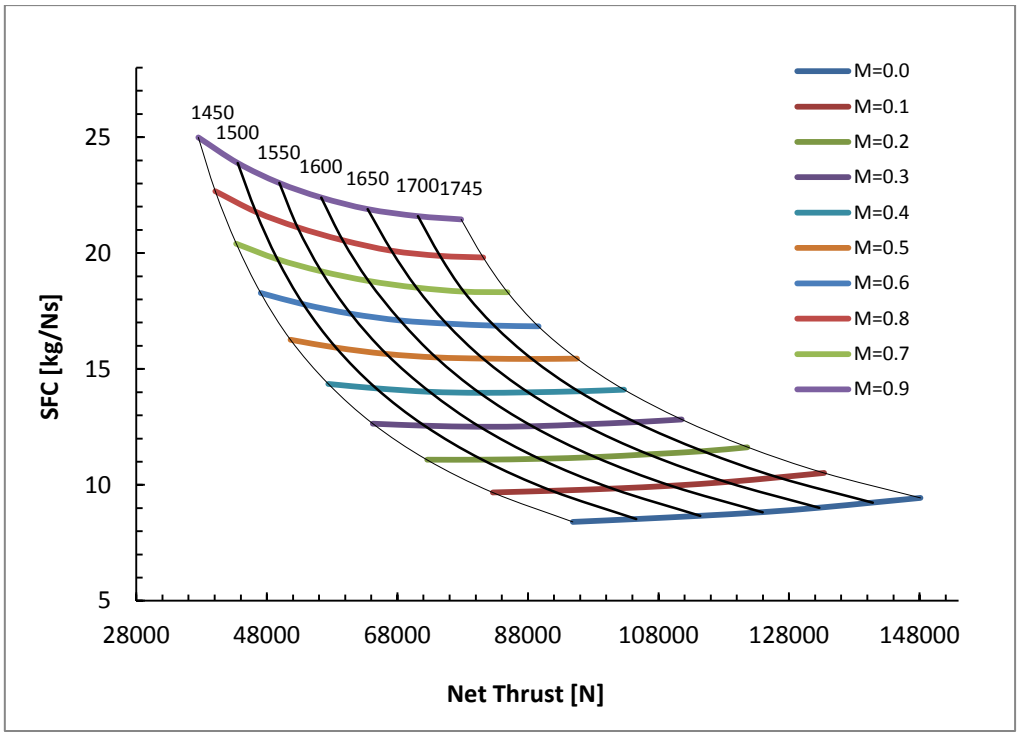

Figure 4-7 Net thrust and SFC variation as a function of TET and Mach number of CULE_1DL

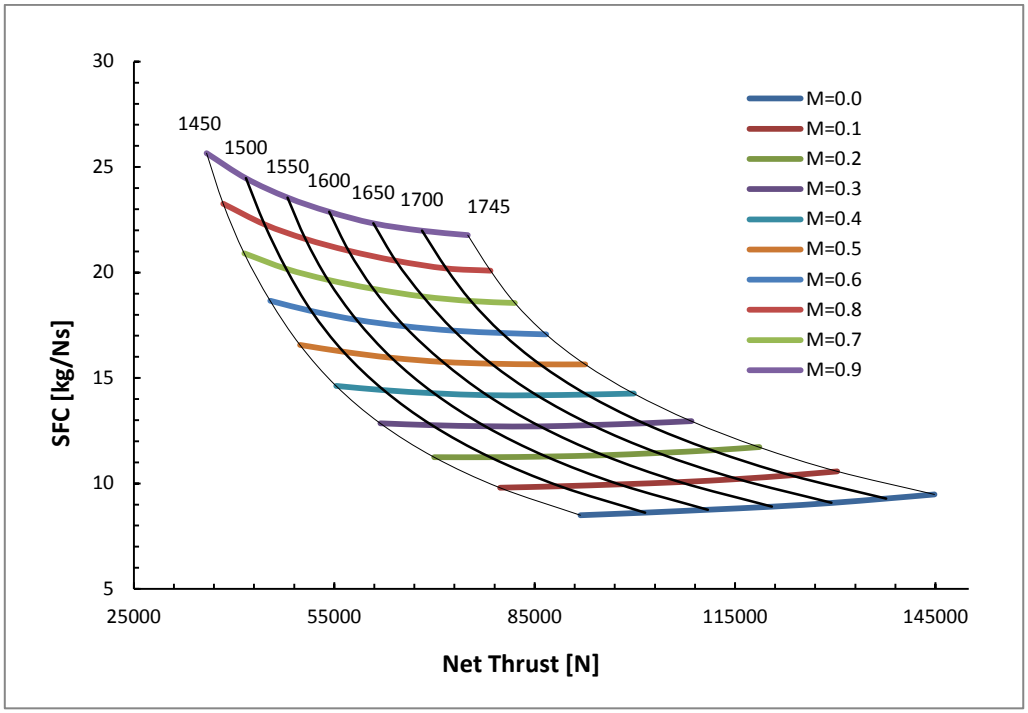

Figure 4-8 Net thrust and SFC variation as a function of TET and Mach number of CULE_2DL

4.4 Aircraft Performance Models

The aircraft performance model is an essential part of the model setup. During the initial part of the research, various aircraft performance models were considered for the use. Cranfield University's in-house integrated engine and aircraft performance tools, HERMES, and APM were initially used for the preliminary analysis (Navaratne 2013, Gu and Navaratne 2012). Based on the experience with the tools and in order to overcome the main limitation of representing 3D trajectories, and easily interchange different aircraft configurations within the framework, author has decided to use the ADM (Aircraft Dynamic Model) for the final part of the research.

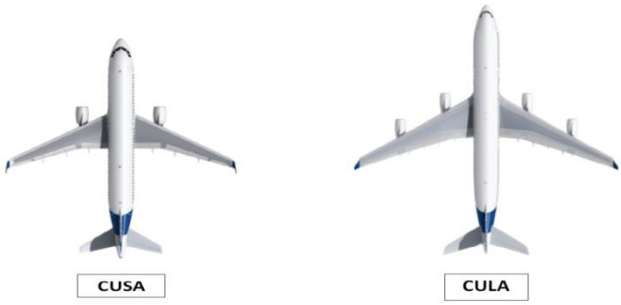

Figure 4-9 Configuration of short range aircraft (CUSA) and long range aircraft (CULA)

The ADM was adopted to create a short range and a long range aircraft model based on the Airbus A320-200 and A340-300 aircraft (Airplane Characteristics A320-200 and A340-300 (Airplane 2005). The aircraft models are designated as CUSA (Cranfield University Short-range Aircraft) for short range and CULA (Cranfield University Long range Aircraft) for long range aircraft. They were modelled using Aircraft Dynamic Model (ADM) which has been developed under SGO ITD of Clean Sky project. ADM is capable of aircraft trajectory generation for generic aircraft between two pre-defined positions in a 3D space. The ADM design architecture is based on a representation of Three Degree-of-Freedom (3-DOF) point mass model with a varying mass under aerodynamic, propulsive and gravitational forces with assumptions of symmetrical aircraft with thrust force parallel to the aircraft motion. In addition the assumption of spherical non rotating earth and no wind effects are also introduced to simplify the modelling problems. The 3-DOF equations of motion describing the aircraft states and governing translational movements along the longitudinal, lateral and vertical axes are listed in below Equations.

$$\frac{d\varphi}{dt} = \frac{V\cos\gamma\ \sin X + W_{\varphi}}{R_M + h}$$

$$\frac{d\lambda}{dt} = \frac{V\cos\gamma\cos X + W_{\lambda}}{\cos\varphi\ (R_T + h)}$$

$$\frac{dh}{dt} = V\sin\gamma + W_h$$

$$\frac{dV}{dt} = \frac{T\ (P,V,h) - D(L,V,h)}{m}\ .g\ sing\ \gamma$$

$$\frac{d\gamma}{dt} = \frac{g(n\cos ø - \cos\gamma)}{V}$$

$$\frac{dX}{dt} = \left(\frac{g}{V}\ .n\right)\left(\frac{\sin ø}{\cos\gamma}\right)$$

$$\frac{dm}{dt} = c\ (P,V,h)\ T(P,V,h)$$

Where P is the engine power setting, n is the load factor, ø is the bank angle, m is the aircraft mass, φ is the geodetic latitude, λ is the geodetic longitude, h is the altitude, V is the true air speed, γ is the flight path angle and χ is the heading. In the equations, R_M is the meridional radius of curvature, R_T is the transverse radius of curvature, W is the wind velocity and g is the earth gravity. Three control variables u = (P, n, ø) are used as inputs of the dynamic system and the seven state variables are described as x = (m, φ, λ, h, V, Y, X).

Aerodynamic forces are modelled by drag polar characteristics provided by the BADA dataset (Nuice 2012) and gravitational forces are modelled by using the International Standard Atmosphere (ISA) with constant gravity acceleration. The ADM generate 3D trajectories based on the given input variables. The lateral profile or ground track is generate based on the given latitude and longitudinal values of each waypoint. Based on the user defined number of segments (N_s), the trajectory is segmented. The ADM receives the normalized aircraft controls (Climb Rate and TET) provided from the engine deck which has been created from the engine simulation data. The determined aircraft equations of motion are integrated using Runge-Kutta 4^{th} degree integrator. Altitude and aircraft speed are used as variables to generate the vertical profile of the trajectory. Several other parameters such as initial and final position, speeds and aircraft initial mass are also required as inputs. The complete model development can be found in Clean Sky -SGO-ITD (2013).

4.4.1 Key assumptions and limitations

(1) All segments (climb, cruise and descent) are considered to be continuous and no step segments

(2) Changes of speeds between sub-segments are instantaneous as the implementation on overall fuel consumption due to change in calibrated speeds and much numbers in the speed profile is neglected

(3) Earth considered as the spherical and non-rotational with no wind effects

(4) All calculations are done for the for the mission and do not considered blocks

(5) Aerodynamic data for modelled aircraft are adopted from the BADA database, therefore basic characteristics, dimensions and aircraft / propulsion system parameters remain unchanged as specified in the database. These include the aircraft mass and balance (maximum take-off weight – MTOW, maximum landing weight – MLW, maximum zero fuel weight – MZFW, operating empty weight – OEW, fuel capacity – FW, and maximum payload – MPW, number of passengers, mean centre of gravity position, maximum operational altitude, environmental envelop and aircraft dimensions)

4.4.2 Aircraft Model Validation and Verification

The aircraft and engine models were integrated and series of trajectory simulations were performed to validate/verify the performance of the aircraft models using payload range chart. The payload range chart defines the combined weights of the payload and fuel that may be allowed to achieve any particular range within the aircrafts' performance capability. The payload range diagram has four critical points; each point represents a load configuration in terms of payload weight and fuel weight with the maximum range aircraft can be flown. At point A, the aircraft is at maximum payload with no fuel on-board. This point shows the maximum volumetric payload carried by a particular aircraft, which keep the aircraft within its structural limitations. Point B represents the maximum range the aircraft can fly with maximum payload. Beyond point B payload is traded for fuel to attain greater range. At point C the maximum fuel volume capacity has been achieved with the expense of payload and represents the maximum range with full fuel tanks where a reasonable payload can be carried. Finally point D the aircraft is theoretically at the operator's empty weight with zero payload (OEW) and range flown at the point considered the maximum ferry range.

The Figure 4-10 and 4-12 indicate the payload range capability of short range aircraft - CUSA and long range aircraft – CULA simulated models compared to those of the aircraft are based on (Airbus 320-200 and A340-300 respectively). It is important to notice that all the simulations were performed to find required payload ranges similar to standard flight profiles found in BADA Reference and according to following assumptions; (a) Cruise conditions: ISA+10^0, Mach numbers -0.76/0.80, and altitude - 35 000/39 000 ft, (b) International Reserves: Enroute 10%, Flight Time overshoot (c) 200 nm (370 km) diversion, 30 minutes hold at 1500 ft approach and landing.

Also all missions were simulated with standard assumptions for hold, diversion and on board reserved fuel. Therefore at the end of the mission the fuel on-board include the; (a) fuel for 20 min hold, (b) fuel for 200nm diversion route which includes a climb to 2000ft, cruise at constant altitude and speed of 20000ft and Mach 0.6 and descent, (c) fuel for on-board reserves 5% of trip fuel consumed.

The Table 4-1 and Table 4-2 indicates the short range and long range mission specific data for the three simulated points (B, C, and D) in Figure 4-10 and Figure 4-11. Given the various assumptions made in modelling, flight profile of the trajectory and numerical errors, variations between the required and achieved ranges are observed. However, as this is an attempt to simulate the generic performance of a short and long range aircraft, the errors are considered small and hence deemed acceptable.

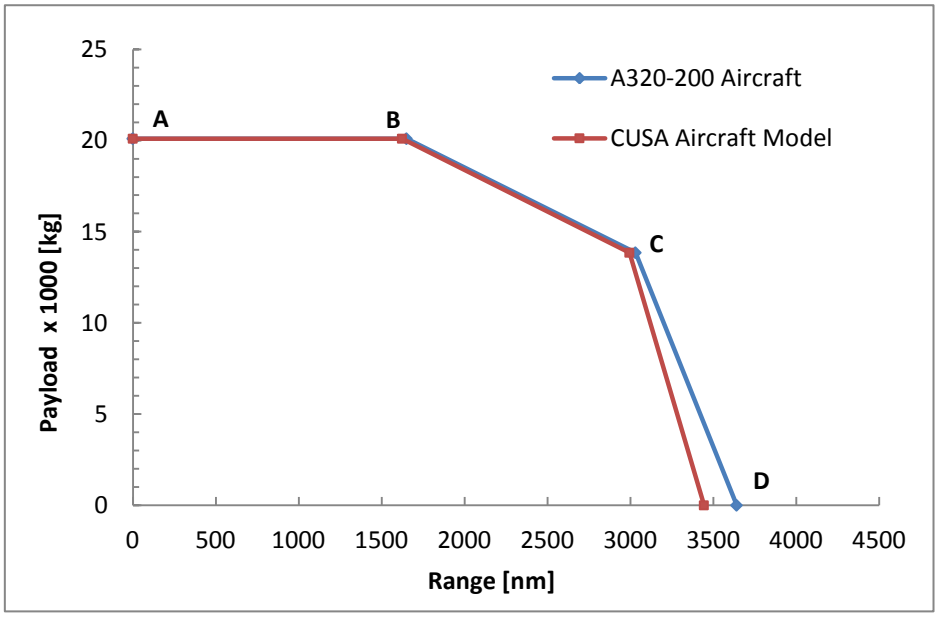

Figure 4-10 Payload Range Diagram for validation of short range aircraft model

Table 4-1 Payload Range validation of Short Range Aircraft CUSA

	Max Payload Range (B)	Max Fuel Range (C)	Max Ferry Range (D)
Max Take-off Weight (kg)	75500	75500	61650
Max Payload Weight (kg)	20100	13850	0
Operating Empty Weight (kg)	40900	40900	40900
Maximum fuel on-board (kg)	14500	20750	20750
Fuel for diversion - 200nm (kg)	1568	2354	2291
Contingency Fuel – 5% (kg)	616	876	879
Fuel consumed (kg)	12316	17520	17580
Range_Simulated Aircraft (nm)	1623	2994	3443
Range_Airbus A320 Aircraft (nm)	1650	3030	3640
Range Error (%) Ref. A320 data	1.4	1.2	5.4

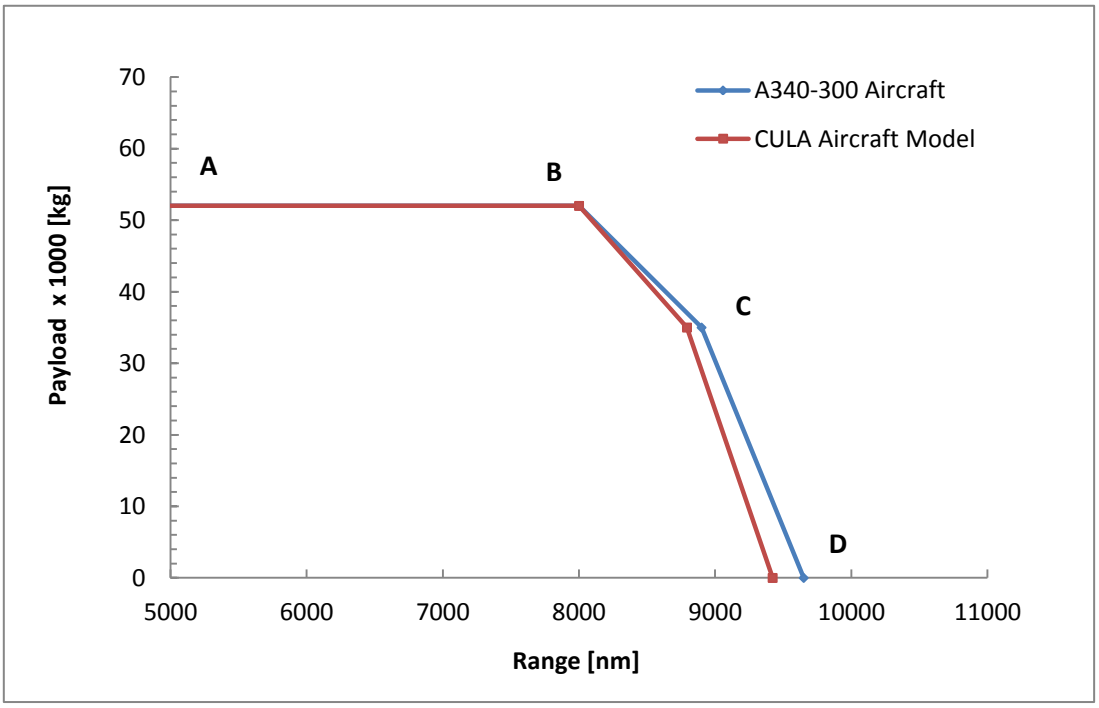

Figure 4-11 Payload Range Diagram for validation of long range aircraft model

Table 4-2 Payload Range validation of Short Range Aircraft CULA

	Max Payload Range (B)	Max Fuel Range (C)	Max Ferry Range (D)
Max Take-off Weight (kg)	275000	275000	239500
Max Payload Weight (kg)	52000	36500	0
Operating Empty Weight (kg)	130900	130900	130900
Maximum fuel on-board (kg)	92100	107600	107600
Fuel for Hold + Diversion (kg)	2854	3820	3480
Contingency Fuel – 5% (kg)	4264	4935	4958
Fuel consumed (kg)	85282	98830	99162
Range_Simulated Aircraft (nm)	6540	8793	9422
Range_Airbus A340 Aircraft (nm)	6600	8900	9650
Range Error (%) Ref. A340 data	0.92	1.2	2.4

4.5 Emission Prediction Model

There are three common methods available to predict gaseous emissions produced by gas turbine combustors; (a) the empirical correlation based method, (b) numerical simulations through CFD calculations, and (c) calculations based on stirred reactor models (physics based models) Celis and Moss (2009). Empirical correlation based models are typically less demanding in terms of computational resources and they are mainly suitable for existing engines with conventional combustors, where particular data is available. This means these models are adequate for predicting emissions such as CO_2, CO, NO_x, and HC etc., when there are pre-existing historical emission data certificates for that specific engine type (Pervier, 2013). The more sophisticated methods like stirred reactor method and complex numerical simulation based calculation models are generally computationally intensive, because of their high fidelity and level of detail combustion configurations. This makes them especially suitable for new combustor designs for which no historical data exists, but detailed information like combustor geometries and operating conditions are available Pervier (2013). For the purpose of aircraft trajectory analysis, where the engine and combustor design have been largely investigated in the past, an empirical correlation based model is expected to be satisfactory Celis (2009) and Pervier (2013).

4.5.1 Emission Prediction Model - NOx

The methodology used in this research to develop the emission prediction model is empirical correlation based P3T3 method. This method has been selected as the combustors considered in the selected engines have no design change and with available test data. The model comprises of an empirical correlations to predict NO_x emissions at altitude using publicly available engine performance data from ground level testing. These calculations require sensitive engine component data such as compressor exit pressure (designated as P3) and temperature (designated as T3) as well as the fuel air ratio (FAR) and the fuel flow (FF) both at altitude and at ground level. These data is taken from the engine performance models which are created using TURBOMATCH as described in section 4.3.1 and 4.3.2 and fed into the emissions prediction model. The summary of the P3T3 methodology is shown in Figure 4.12. The compressor exit temperature at altitude is used for ground level correlation of EINOx. An EINOx altitude correction for compressor exit pressure and FAR is performed. In addition, a humidity correction is included to account for the change in air properties at high altitudes, as the altitude increases from sea level ISA, the air become drier Norman, P.D., et al. (2003).

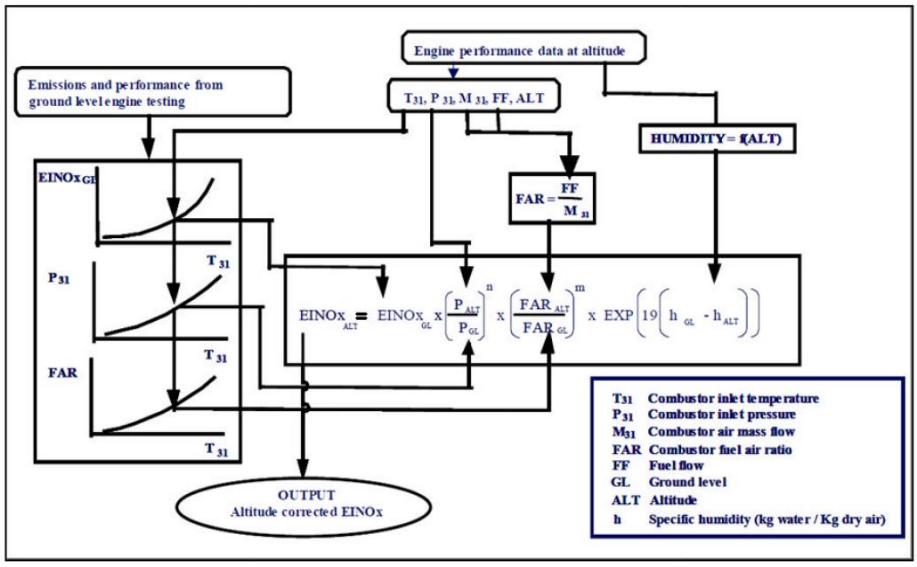

Figure 4-12 Flowchart of P3T3 methodology for NOx prediction (Norman 2003)

Furthermore, the emission indices (EI) of the specific pollutant for each engine required in order to correct them to the various flight conditions. The International Civil Aviation Organisation (ICAO) host an exhaust emission data base of various produced engines which

incorporates information from engine test certificates provided by the engine manufacturers. This data is based on established emission measurement procedures and compliance standards for gaseous pollutants. In order to characterise the operational conditions of an engines in terms of their emission performance a standard Landing and Take-Off Cycle (LTO) was defined. An extract of the emission performance data for the CFM56-5B4 and CFM56-5C4 engine type are shown in Table 4-3 and 4-4. Also it should be noted that the LTO cycle only assesses the emissions below 915m (3000 feet) and therefore may not be suitable for comparing the emissions of different engines in other flight modes such as full climb, cruise etc.

The P3T3 model utilises both, engine model performance data as well as the ground level emissions data published by the engine manufacturers to establish the emissions indices at certain altitudes and flight speeds. The resulting total NO_x emissions in kilograms can then be calculated using the below formula. For this study, only the emissions index (EI) for the NO_x emissions is of interest and other pollutants are not considered.

$$NOx = (W_f \; X \; Time) \; X \; EINOx \qquad (4.1)$$

This is where W_f is the fuel flow given in kilogram per second, Time is given in seconds and EINOx in grams/kilogram

Table 4-3 ICAO data base - exhaust emissions of CFM56-5B4 engine

Mode	Power Setting [% of TO Thrust]	Time [min]	Fuel Flow [kg/s]	Emission Indices [g/kg]		
				HC	CO	NOx
Take-off	100	0.7	1.260	0.1	1.40	28.7
Climb-out	85	2.2	1.030	0.2	3.60	23.3
Approach	30	4.0	0.370	5.3	1.40	10.0
Idle	7	26.0	0.120	3.6	35.65	3.9

Table 4-4 ICAO data base - exhaust emissions of CFM56-5C4 engine

Mode	Power Setting [% of TO Thrust]	Time [min]	Fuel Flow [kg/s]	Emission Indices [g/kg]		
				HC	CO	NOx
Take-off	100	0.7	1.456	0.008	1.00	37.67
Climb-out	85	2.2	1.195	0.008	0.85	29.05
Approach	30	4.0	0.386	0.065	1.40	10.67
Idle	7	26.0	0.124	5.000	30.93	4.28

4.5.2 Emission Prediction Model – CO_2 and H_2O

The calculation of CO_2 is an easier process than calculating NOx as it is considered to be in equilibrium and can readily be calculated from balancing of the chemical equations. The model uses the Fuel Composition Method (FCM) to calculate the emissions of CO_2 and H_2O. As these emissions are a product of combustion they are considered independent of operating parameters and modelled as proportionate to fuel burn and fuel composition. Assuming the combustion to be stoichiometric and the composition of fuel is represented as $C_xH_yS_z$, the emission indices (EI) in terms of grams of pollutant per 1000 grams of fuel can be computed as follows:

$$x = \frac{X}{12.011} \tag{4.2}$$

$$y = \frac{Y}{12.011} \tag{4.3}$$

$$z = \frac{Z}{12.011} \tag{4.4}$$

$$EICO_2 = \frac{1000\ X\ (x)\ X\ [12.011+(\ 2\ X\ 15.994\ )]}{[(x)\ X\ 12.11\ ]+[\ (y)\ X\ 1.0079\ ]+[\ (z)\ X\ 32.06\ ]} \tag{4.5}$$

$$EIH_2O = \frac{1000\ X\ (y/2)\ X\ [2\ X\ 1.0079\ +(\ 2\ X\ 15.994\ )]}{[(x)\ X\ 12.11\ ]+[\ (y)\ X\ 1.0079\ ]+[\ (z)\ X\ 32.06\ ]} \tag{4.6}$$

Where x = Carbon coefficient in chemical formula for fuel (in moles)
y = Hydrogen coefficient in chemical formula for fuel (in moles)
z = Sulphur coefficient in chemical formula for fuel (in moles)

$$C_{12}H_{24} + 18\ (\ O_2 + \frac{79}{21}N_2\ ) \rightarrow \quad 12CO_2 + 12\ H_2O + 18\left(\frac{79}{21}\right)N_2 \tag{4.7}$$

Note: CO_2 and H_2O have not been considered as an optimisation objective due to the scope of the project. However, fuel burn has been considered as an objective in order to understand the CO_2 emissions as it directly proportionate to fuel burn.

4.5.3 Key assumptions and limitations

(i) Compressor exit temperature (T3) and pressure (P3) have been considered as the inlet temperature and pressure of the combustor with zero losses

(ii) Combustion process considered to be complete in all phases of the flight

(ii) No impact of pollution formation on combustion heat

(iii) Emissions calculations of degraded engine are based on the P3 and T3 values obtained from the simulated engine models instead of real degraded engine data obtained for CFM56-5B4 and CFM56-5C4

4.5.4 Emission model validation

In order to verify the performance of the emission prediction model, ICAO data base was compared. The fuel flow and NO_x index of the four discrete power settings provided in ICAO data base for the particular engines of CFM56-5B4 and CFM56-5C4 have been used as target values to match the engine performance of the created engine model. The data from the previously performed engine off-design studies was used to find the respective fuel flow and EINOx at the different power settings of engines by controlling TET. As discussed in the model descriptor, the corresponding values of the burner inlet temperature (T3) and burner inlet pressure (P3) as well as the fuel-air ration (FAR) have been used as input parameters for the emissions calculations of the model. Figure 4.13 and 4.14 shows the calculated EINOx comparison with the ICAO data and the engine model at three different power settings (100%, 85% and 30%). It can be noted that engine model results at take-off, climb, approach, and idle power settings are generally following the trend of the ICAO data and hence model can be considered acceptable for the purpose of this study. The results at idle power setting however limited validity, due to limitations of the created engine model at very low power settings (ICAO (2013).

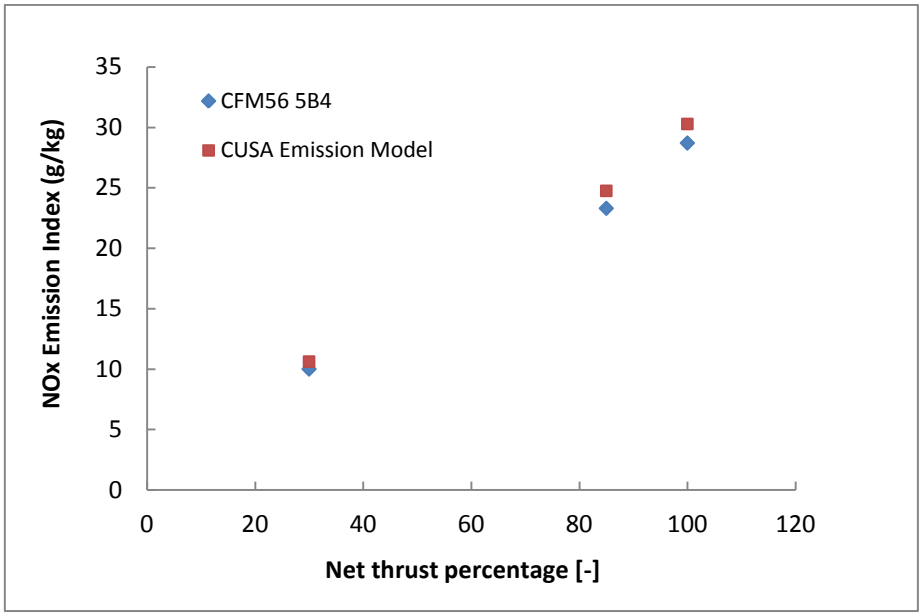

Figure 4-13 Comparison of EINOx variations against net thrust percentage of short range engine

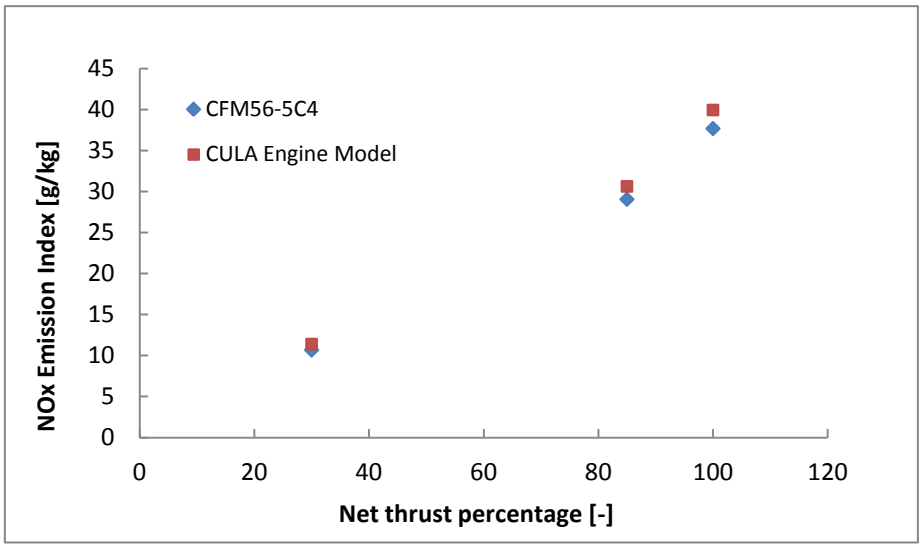

Figure 4-14 Comparison of EINOx variation against net thrust percentage of long range engine

4.6 The Contrail Model

The contrail formation process is fairly well established and can be described as follows. An aircraft engine produces hot air at the engine exhaust with high water content due to the reaction of complete combustion in the combustor. This hot and moist air mixes with the colder and drier ambient atmospheric air in the upper atmosphere. As shown in Figure 4-15, if the water partial

pressure exceeds the saturation pressure with respect to water, then according to Appleman (1953) methodology condensation will occur and a contrail is expected to be form. Depending on the final local atmospheric conditions, two cases can arise. If the mixing between the plume and the ambient air do not lead to saturation, with respect to ice, then the water is immediately evaporate and the contrails disappear within a short period of time. On the other hand if saturation with respect to ice is attained, then the contrails will persist. In this case they are called persistent contrails and can last for hours as long as atmospheric conditions remain ice saturated.

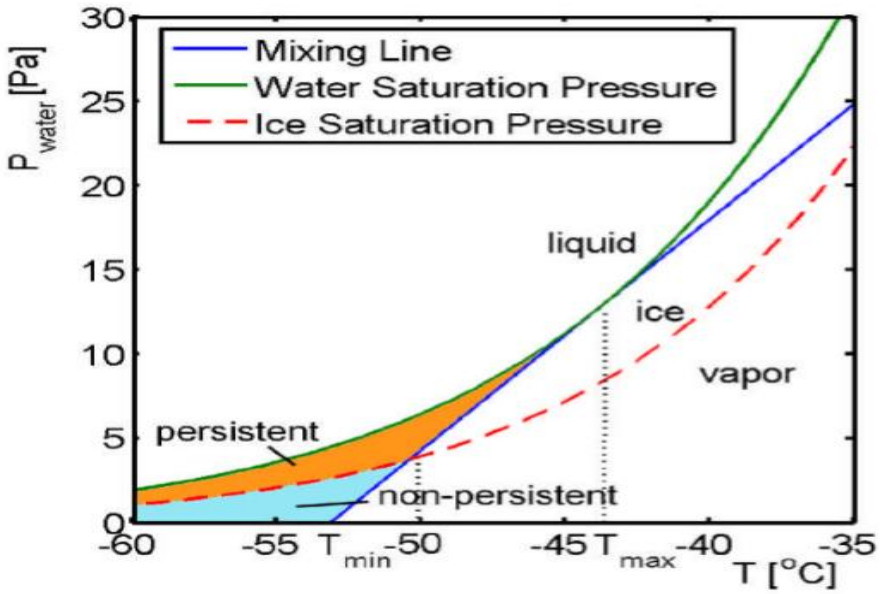

Figure 4-15 Phase diagram of contrail formation (Appleman, 1953)

The contrail prediction model for this work has been adopted from the model developed for the Clean Sky project by Camilari and Pervier (2012). The model was developed based on the above mentioned methodology (Appleman 1953) and the modifications brought by Schumann (1996). The model is able to predict the formation of persistent contrails so that based on the aircraft segment length; it will be possible to derive the number of kilometres of persistent contrails generated by an aircraft flying a given trajectory with known atmospheric conditions such as pressure, temperature and relative humidity. This value will subsequently be used as an objective for the aircraft trajectory optimisation framework. The detail description of the model specification can be found in the Camilari and Pervier (2013) for the reader's reference.

The schematic of the integrated contrail model is shown in Figure 4.16. Basically, it is consists of two main modules, the atmospheric module and the contrails module. The contrail module provides the contrail formation in every small flight segment in which the trajectory is divided during the trajectory execution. The contrail formation requires several atmospheric data (T_{amb}, P_{amb}, RH) and aircraft engine/emission parameters (emission index for water -$EI_{H2O,}$ Overall engine efficiency- η, specific heat capacity of exhaust gas C_{pg}, and molar mass ratio- MMR) which are provided by the atmospheric module, engine model, emission model and aircraft performance model respectively. The contrail module calculates the total length of the persistent and non-persistent contrails produced along the flight.

Once the value for temperature, pressure and relative humidity are received by the atmospheric module, they are passed as inputs for the contrail module along with the molar mass ratio of water and air, and other aircraft-engine related parameters (EI_{H20}, η, $C_{pg,}$) as shown in the Figure 4.16. Based on the input data, contrail module first evaluates whether the engine is producing any contrails. If it is producing any contrails, then module decides whether formation of contrails is persistent or non-persistent for the each segment in which the trajectory is divided. If some contrails are forecasted, the length of the corresponding segment is added to the total length of the persistent contrails, depending on the case, and then same procedure and all the calculations are repeated for the next segment. At the end of the calculations, the derived total length is given in a console window, while a detail of the segments in which the contrails forecasted is provided. Atmospheric data for the short range mission between London – Amsterdam and long range missions between London – Colombo are obtained from the geometric maps.

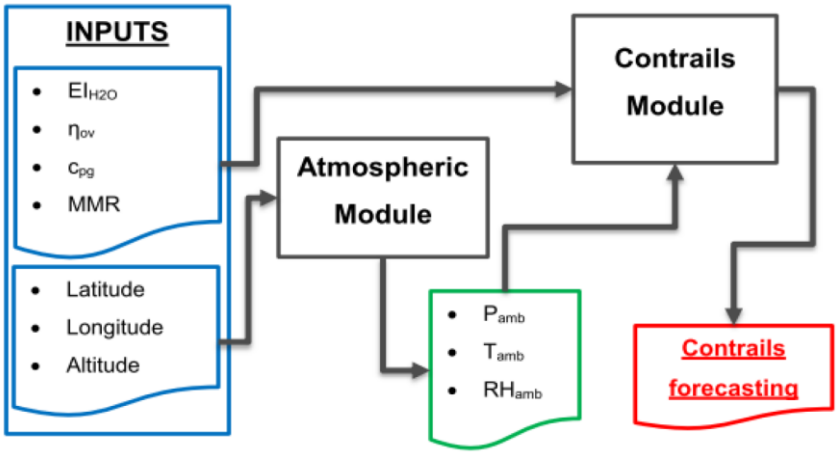

Figure 4-16 Schematic of the Contrail Model (Pervier 2012)

4.6.1 Key assumptions and limitations

The main assumption and limitation come from the water saturation curve. The equation and the curve are only valid for the range of -45^0C to -90^0C. The contrail formation occurs only when the atmospheric temperatures lie within these limits. If the any temperatures fall outside of the limit, code provides an error which has no effect on the rest of the calculations of the code. But, will assume no contrail formation for that particular segment of the mission.

4.6.2 Contrail model validation and verification

The contrail model validation is not a straight forward process. The validation of the model was done by the Camilari and Pervier (2012) against data found in Shull (1998). The work contains data gathered from the observation of actual aircraft at different altitudes including typical atmospheric conditions and contrail observations. Shull (1998) also carried out a comparison of these actual observations with predictions from the Air Force Weather Agency JETRAX Contrail Forecast Model. Therefore, this data provided the possibility to validate the model against a sophisticated third part tool in addition to assessing its ability to predict the formation of contrails based on actual observations. A summary of the results can be found in Pervier (2013).

The contrail prediction tool has given acceptable results, correctly predicting formation or non-formation of contrails with a hit rate of 81% on available data. Shull (1998), reported that other algorithms such as those based on Schrader and Schuman (1996) have given the hit rate of 79% and 81% respectively. Therefore, it has given confidence that the methodology has been correctly implemented and contrail prediction also in the same level of accuracy.

4.7 Optimiser used in the framework

The optimisation module used in this work utilises genetic algorithm based multi objective optimiser. The optimiser was developed as a requirement of Clean Sky project for trajectory optimisation at Cranfield University. It is a modified version of the Non-dominated Sorting Genetic Algorithm (NSGAII) created by Deb (2002) and Deb (2007). The initial development of this optimiser was conducted as a collaborative effort between Cranfield University and Airbus France which is a deliverable of the Sub-work Package 3.2 – Theoretical Transversal Optimisation and Trajectory Definition in Work Package 3.0 - Management of Trajectory and Mission (MTM), Clean Sky (2010). The author was responsible for the testing and benchmarking of the optimiser performance against several mathematical functions (ZDT

functions) and MOTS optimiser as a part of validation and verification process of the optimiser Benchmarking Report (Patra and Navaratne, 2010). The validation and verification of the optimiser will be discussed in the later part of this chapter.

4.7.1 Selection of GA based NSGAMO-II for trajectory optimisation

A number of optimisation methods have been developed in the past, many of which are customised to solve a specific problem. Most important optimisation methods can be grouped under three broad categories, (Schwefel 1981). (1) Hill Climbing Methods (Direct search methods, Gradient methods, and Newton methods); (2) Random Search methods, (3) Evolutionary methods (Evolutionary programming, Evolutionary strategies, Genetic programming, and Genetic Algorithms – GAs). A detail review of these methods can be found in Celis (2010). Betts (1998) considered evolutionary methods are not adequate to solve trajectory optimisation problems and are computationally inferior when compared to methods that use gradient information. However, recent work carried out by Celis (2010), found that GAs are indeed well suitable for this class of problems. Especially aircraft trajectory optimisation involving multi-model integration, where the characteristics of the functions interacting inputs to outputs are unknown, algorithms of this type seems to be the only practical alternative. A number of reasons that help to support the selection of GA based NSGAMO-II for this work are listed below;

- GAs do not use specific knowledge of the optimisation problem domain. Instead of using previously known domain – specific information to guide each step, they make random changes in their candidate solutions and then use the fitness function to determine whether those changes results are both model and problem independent, and they allow the users to (simultaneously) run different models for simulating different disciplines, they appear to be ideal and effective.
- GAs are well suitable to solve problems where the fitness landscape is complex (discontinuous and multi-model), number of constraints and objectives are involved and the space of all potential solutions is large (particular characteristics of nonlinear problems)
- GAs make use of parallel process of search for the optimum, which means that they can explore the solution space in multiple directions at once. If one path turns out to be a

dead end, they can easily eliminate it and progress in more promising directions thereby increasing the chance of finding the optimal solution.

Therefore GA based NSGAMO-II has been chosen for this work, because of large number of previous successful applications worldwide, Betts (1998), Bramlette (1991), Al-Garni (2007) Qing (1997) Miki ((2002), including those once worked on similar studies in aircraft trajectory optimisation Gu and Navaratne (2012), Navaratne (2013), Pervier (2013) and Nalianda (2012)

4.7.2 NSGAMO optimiser

The optimisation algorithm used in this work is NSGAMO-II (Non Dominated Sorting Genetic Algorithm Multi Objective - II) optimiser. This optimizer is able to perform multi objective optimisation with two objectives with or without constraints. Figure 4.17 shows the sequential steps of the NSGAMO-II. As shown in the flowchart, at the first step an initial population of the test case (i.e. candidate trajectories) is created randomly. The size of the initial population determined by the product of the prescribed population size with an initialization factor (>=1). A larger initial population size increases the probability of the optimizer converging to the global optimum point but slows down the optimization process. The optimizer then sends all the cases to the GATAC framework for the evaluation handler to evaluate and return the results (optimization objective) to the optimizer. On receipt of the results, the optimizer performs fitness evaluation on the data (i.e. qualifies the population). As optimum point is identified on the first generation, a second generation population is created and the process repeated. The process is repeated until convergence criteria are met (either a maximum number of generations will have been generated and evaluated or Pareto convergence will have been reached). In order to reduce the computational time of subsequent generations, the population size of the subsequent generations is reduced to prescribed population size. To achieve this, only the best solutions of the previous population are selected to create the next generation. New generations are created using different methods such as stochastic universal sampling, random selection and genetic operators (crossover and mutation). In the case of single objective optimization the result is the best-case while for a multi-objective optimization, the final result is a Pareto Front. The implementation of the NSGAMO algorithm allows, for via a text file, the user definition of the various parameters associated with the optimization, which include population size, mutation and crossover ratio, selection method and type of mutation and crossover and other parameters. A detailed description of the testing and benchmarking of the optimizer performance is presented in reference Patra and Navaratne (2012) and Tsotskas (2013)

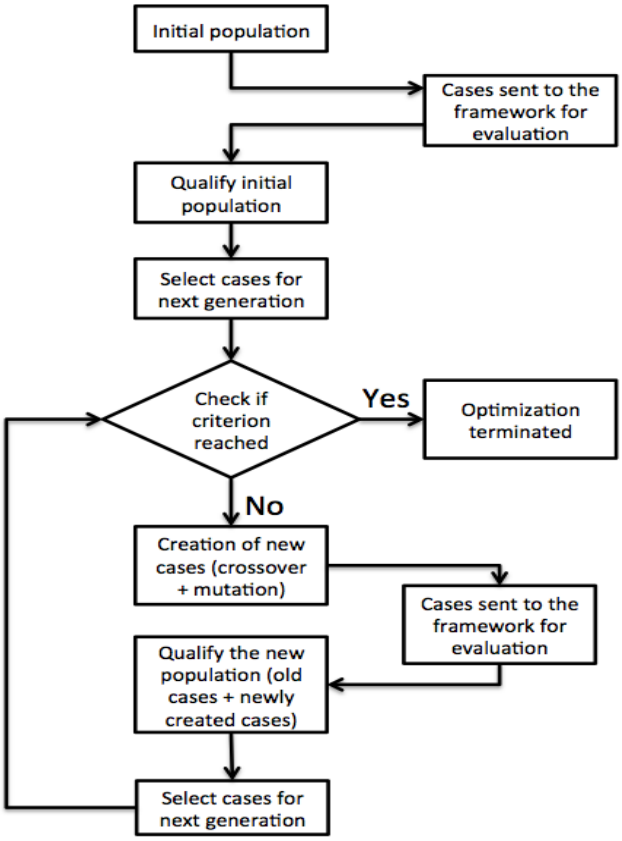

Figure 4-17 Optimisation flowchart (Navaratne 2013)

4.7.3 Optimiser validation and verification

Several benchmarking studies of the NSGAMO-II optimiser have been performed in the past to validate the performance for multi-objective aircraft trajectory optimisation problem. In order to verify the actual performance of a particular optimiser, predefined test problems must be used where the true Pareto optimal front is known. The results of the optimiser to be tested can then be compared to the known solutions. The common test functions which have been used in the past were standard ZDT (Zitzler, Deb and Thiele) mathematical functions. Different types of ZDT test functions have been established and are described in detail in (Pervier and Nalianda 2011, Patra and Navaratne 2012). The different ZDT functions aim at testing the ability of the optimiser to handle several or all of the following criteria while delivering a diverse set of solutions within the range of the Pareto optimal front: (1) Large number of decision variables, (2) Discontinuous Pareto fronts, (3) Minimum number of evaluations required by the algorithm to converge to Pareto optimal front, (4) Non-uniform diversity Pareto optimal with few solutions.

ZDT1, ZDT3 and ZDT6 have been utilised to benchmark the performance of the optimiser by Pervier and Nalianda 2011. As a part of this study NSGAMO-II optimiser was tested and benchmark by the author for its robustness against the ZDT4 and another well-established optimiser MOTS as standalone applications as well as within the GATAC optimisation framework. The performance indicators used to analyse the results are the convergence metric and divergence metric. The convergence metric is an indicator of how close the obtained solutions lie in relation to the known set of Pareto optimal solutions. The divergence metric measures the extent of spread achieved among the obtained solutions and is indicative of the extent to which a set of the solutions span the entire Pareto optimal front.

The results produced by the NSGAMO-II were very close to the true optimal curves in all ZDT functions including ZDT4. Thus the optimiser is behaving correctly and move towards the true optimal front. It was also noted that, compared to the MOTS optimiser, the NSGAMO-II within GATAC framework achieved the same or better results with a lesser number of evaluations. The comparisons of the NSGAMO-II and the ZDT4 true Pareto fronts generated within the optimisation framework and outside the framework are shown in Figure 4-18 and 4-19. The detail description of the benchmark study can be found in "Performance Assessment of NSGAMO-II and MOTS on ZDT functions Benchmarking Report (Patra and Navaratne 2012)

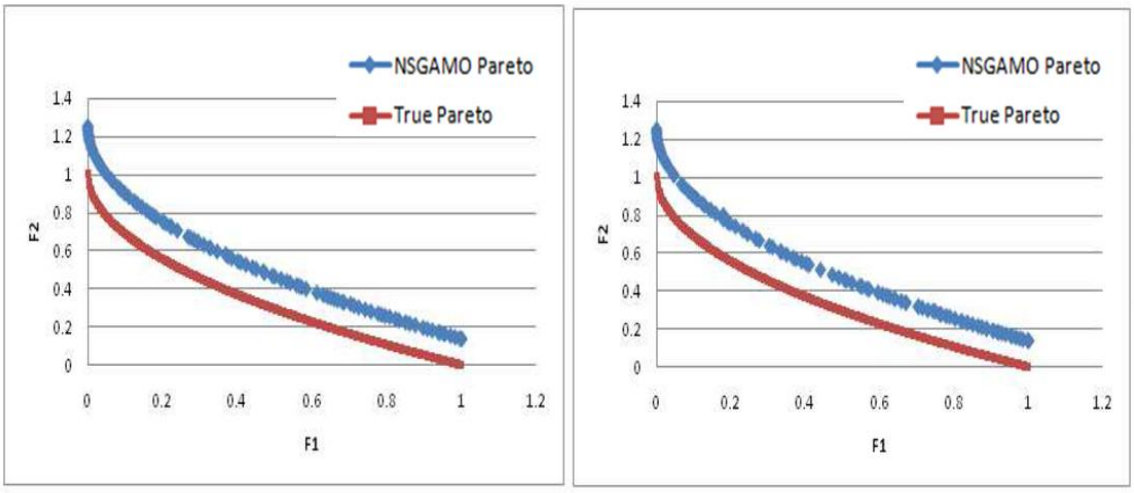

Figure 4-18 Comparison of NSGAMO-II with ZDT4 outside the framework

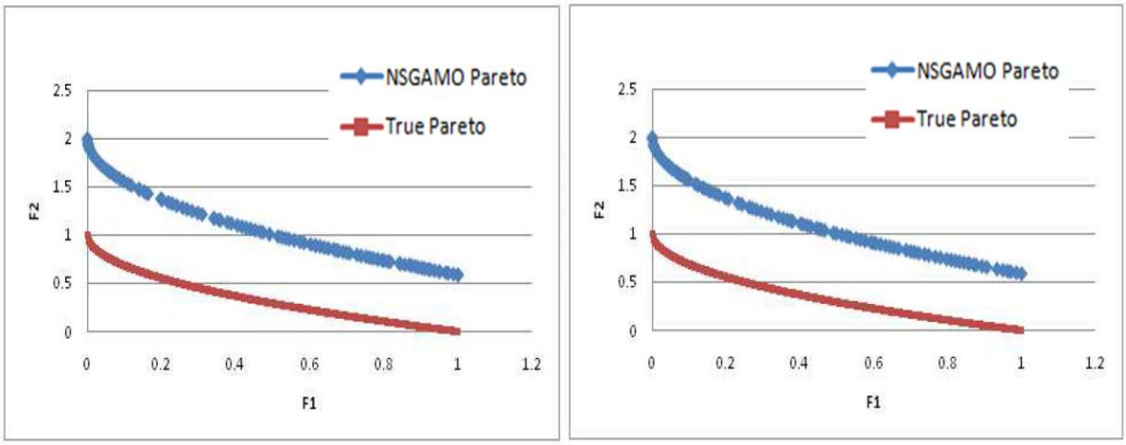

Figure 4-19 Comparison of NSGAMO-II with ZDT4 inside the framework

4.8 Aircraft trajectory simulation

A trajectory is defined by the area navigation (RNAV) method, which is based on longitude and latitude coordinates. Aircraft trajectory denotes the area navigation route and aircraft flies on while passing through specified geographical locations, which are called waypoints. It is assumed that the aircraft passes through a waypoint at a certain speed without deviation. The complete trajectory can be divided into various parts or segments – also known as phases of flight. The most usual phases are departure (which includes take off and initial climb), en-route (mainly cruise), and Arrival (including approach and landing). The departure and approach phases are the shortest parts of the flight and heavily depend on the current environmental conditions, such as ATM constraints for LTO cycle (imposed by the local authorities and legislation bodies) and pilot's operational decisions (Cook 2007). So, it is not necessary to optimise or automate the take-off and landing. However, other phases could be influenced by the optimisation as they are relatively large phases compare to take-off and landing. Therefore they attract higher interest since it is less intuitive for the operator to take into consideration all of the parameters and operate the aircraft in the most optimal way in terms of fuel consumption, minimum emissions and flight times. Hence, this work will focus on the main three phases of departure, en-route and approach of the complete flight.

The formulation of the trajectory, type and number of waypoints involved affects the complexity of the optimisation process. In reality, these trajectories are in 3D paths. As this project is focused on the real aircraft trajectory generation with real engine performance (representing real engines taking degradation into consideration), way point trajectory

generation approach has been employed. The considered trajectories are in 3D, hence vertical trajectories and range – distance flown for a given amount of fuel is split into small straight line segments. Each segment is defined between two waypoints. The target trajectory or mission route is formed by connecting these segments in a very special order so that the total energy at the boundaries of two adjacent segments is the same. Moreover the segments depend on the end of the previous one, as per the principles of control theory.

Considering from the waypoints and respective speed values they have been set for a single phase segment, the performance indices that characterise the flight are resolved by the Aircraft Dynamic Model (ADM), and Engine Performance Model (EPM). These models are coupled and applied on every single segment between two waypoints and the corresponding indices are aggregated for the whole phase. Depending on the aircraft performance characteristics of the selected aircraft for this study; ADM calculates the required thrust throughout the target segments and the respective flight time. Then the EPM invoked to calculate the fuel consumption of the particular engine used with aircraft over the same flight period or segment. This method is iteratively repeated for each and every segment considered between waypoints. It is important to mention that, at the end of the simulation of a single segment, the ADM calculates the exiting flight path angle and EPM compute the mass of the consumed fuel. These values will be used as input for the simulation of the following segment for the entering flight path angle and new total aircraft mass (reduced), respectively. Therefore, a single phase of the flight path has been simulated. In addition, EPM provide necessary input for the engine emission model (EEM) and Contrail Prediction Model (CPM) to calculate the gaseous emissions produced and contrail formation during the particular flight phase. This sequential process is automatically handled by the created GATAC framework. This will be repeated several times under different altitudes and speed values in order to obtain the optimum situation. The data flow between each model and optimiser within the GATAC framework will be discussed in the next section.

The number of segments to which the trajectory breaks down or number of way points is an important factor, which is related to the complexity of the case, as it increases the dimensionality (size of the problem). The trajectory simulation consists of two types of parameters; control and state parameters. The first type is initially defined variables such as aircraft weight, range, number of segments or waypoints) which are specified by the user. The other type is the control variables such as flight altitude, airspeed and thrust setting are systematically handled by the external algorithm which is the optimiser of the framework.

4.9 Multi objective aircraft trajectory optimisation

When calculating the optimal flight path, complex optimisation techniques have to be used. The optimisation of aircraft trajectories is a constrained, non-linear, multi-disciplinary and multi objective problem. The parameters uses are dynamic, deterministic, and real-valued. In addition, it involves principles of optimal control theory. In the majority of literature, flight paths are optimised by transforming the original problem into an optimal control problem such as, Betts (1998), Soler (2012), Jacobsen (2010), Torres (2011), and Liu (2011). Then the new problem is resolved by employing standard techniques used in optimal control theory. This method is partially chosen because it is easy to access the formulae that describe the problem which then turns out to be one of the numerical analysis problems. However, required information is not always available, mainly due to the complexity of the simulations and number of variables involved in the model. This research follows a different approach, which is more flexible and easily extendible to simulate a given real aircraft trajectory. The aforementioned APM, EPM, EEM and CPM models are coupled to gather and deliver the output metrics. Then the optimiser collects and handles this pair of inputs and output in an optimisation domain. Therefore this can be considered as the modular approach of the models, and which are managed by optimisation framework. Each part operates independently of the other part and can be manipulated separately. This has been discussed to a greater extend in the optimiser and optimisation framework section.

The aircraft is subjected to a number of constraints regarding its operational (e.g. speeds, maximum bank angle etc.) limitations and ATM (Air Traffic Management) restrictions (e.g. operate within certain speeds and altitude). All these constraints affect the range of components of the design vector. The lower and upper bound for both altitudes and speeds limit the design space, wherein optimiser should locate the best designs based on the objective values. In addition hard constraints are imposed by the APMs and EPMs whenever the design vector produces irregular trajectories. In the multi objective optimisation process, combination of the parameters (altitudes, speeds in waypoints) defines the design of the trajectory. Each component of the design varies within the continuous range of real numbers, which denotes the design space. In a similar way, objectives; mission fuel, mission time, gaseous emissions and contrails belongs to a different space, called objective space. The aim of the optimisation process is to try different combinations of these variables on the given simulation models and detect which areas express the best performance, defined by the objectives. Following a number of successful iterations through the optimisation phase, the best discovered Pareto Front is presented to choose the final design.

4.10 Frameworks and model interaction

In order to study the effects of engine degradation on optimum aircraft trajectories of short range and long range aircraft, two model setups have been developed using the created models [Aircraft Performance Models – Short Range (CUSA) and Long Range (CULA), Engine Performance Models – Short Range Engines: CUSE_0DL (clean), CUSE_1DL and CUSE_2DL (degraded), Long Range Engines: CULE_0DL (clean), CULE_1DL and CULE_2DL (degraded), Engine Emission Model (EEM) and Contrail Prediction Model (CPD)] within the GATAC environment. GA based NSGAMO-II optimiser also integrated within the framework. Apart from the optimiser, the framework is operating as a single integrated "sub-framework" within the main framework, but modular in structure. Generic framework with the models, optimiser and data interaction between them are shown in Figure 4.20. Developed framework has been used in next two Chapters to perform short range and long range aircraft trajectory optimisation with degraded engines.

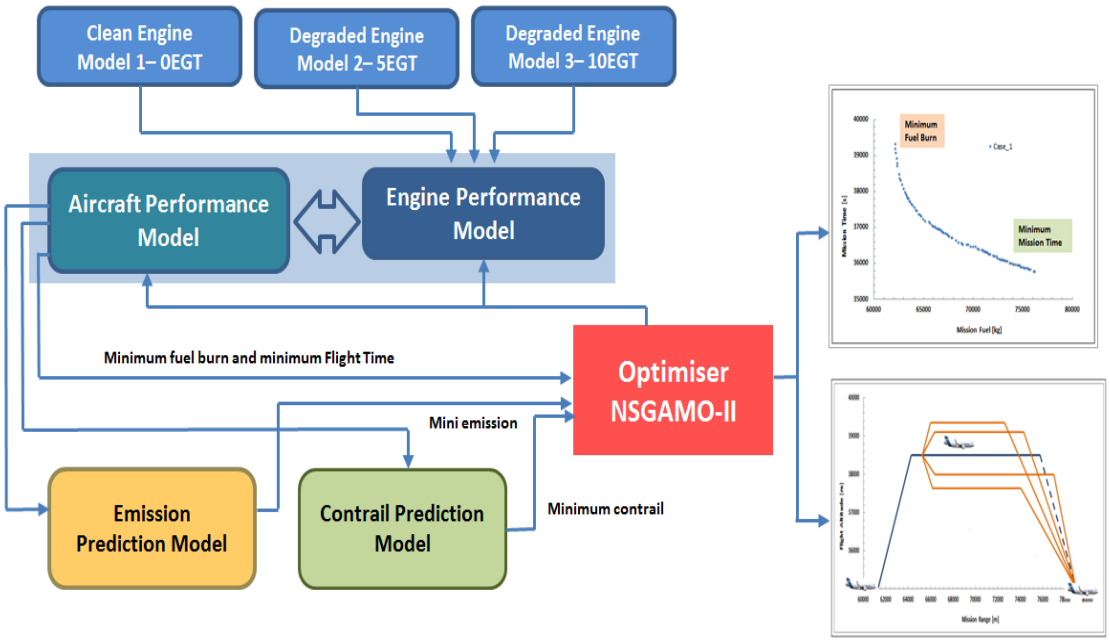

Figure 4-20 Optimisation framework developed for aircraft trajectory optimisation

4.11 Summary

This chapter concludes with an aim to provide the reader an understanding of the detail information of the framework and associated models required to perform trajectory optimisation studies of short range and long range aircraft with degraded engines. Having explained and establishing the requirements, capabilities and main assumptions with limitations of individual models and the optimiser, developed framework will be used to investigate the impact of degraded engine performance on optimum aircraft trajectories of short range and long range aircraft in the following two chapters.

5 Aircraft Trajectory Optimisation with degraded engines – Long range

5.1 Introduction

In order to truly understand the optimised environmental friendly trajectories that can be actually deployed by air lines, it is important to investigate the impact of degraded engine performance on real aircraft trajectories at a multi-disciplinary level. Therefore the aim of the work in this Chapter is to evaluate and quantify the effect of degraded engine performance on the overall flight mission and hence quantify the impact on the environment with regards the following objectives; fuel burn, NOx emissions and contrail formation. Then study further aims to identify the potential for implementing the optimised trajectories with respect to those objectives. A typical two spool high bypass ratio turbo fan engines (one clean and two degraded engines) and a typical wide body long range aircraft A340-300 have modelled as a basis for the study. An emission prediction model was developed to assess the NOx formation during the LTO cycle and the upper atmosphere. The contrail prediction model was adopted from previous studies. In addition, a multidisciplinary aircraft trajectory optimisation framework was developed and employed to analyse long range flight trajectories between London to Colombo under three cases. Case_1: Aircraft with clean engines, Case_2 and Case_3 are Aircraft with two levels of degraded engines. Three different optimisation studies were performed; (1) Fuel burn vs Flight time, (2) Fuel burn vs NOx emission, and (3) Fuel burn vs Contrails. Finally optimised trajectories generated with degraded engines were compared with the optimised trajectories generated with clean engines, as potential environmental trajectories for airline operation.

5.2 Problem definition

The problem is focused on the horizontal and vertical trajectory optimisation using the GATAC framework and associated models developed for the particular case of long haul flight between London Heathrow (EGLL/LHR) and Colombo International Airport (VCBI/CMB) – Sri Lanka. The distance and the current time for this scheduled route is 9027 km and take approximately 11.25 hours. The baseline aircraft is similar to the Airbus A340-300 (295 passenger variant) wide body aircraft with four engines. The engines are two spool high bypass turbofan engines similar to CFM56-5C4 engines. Three cases have been considered: Case_1: Aircraft with clean engine and Case_2 and Case_3 are, aircraft with two levels of degraded engines having 5% and 10% EGT increase. The Figure 5.1 shows a typical flight route of one ALK flights over European continent and Middle East as recorded by Flight Aware (2015).

Figure 5-1 London Heathrow (EGLL) - Colombo (VCBI) Flight Route (Flight Aware 2015)

Departure phase for the flight between London Heathrow (EGLL/LHR) and Colombo International Airport (VCBI/CMB) Sri Lanka is assessed based on the Dover (DVR) Standard Instrumental Departure (SID). For easterly departures, the current departure procedure requires the aircraft to flight onto Detling (DET) VOR R284 immediately after take-off with altitude bound to 600ft before reaching DET VOR/DME station and maintain the flight level until DVR

VOR/DME station, the last SID waypoint. Appendix A, shows the easterly departures for both northern runway, i.e. RWY09L (DVR 6K) and Southern runway i.e. RWY09R (DVR 6J) via Detling (DET) VOR/DME station and Dover (DVR) VOR/DME station as published in the UK AIP. A full SID chart of DET and DVR departure procedures can be seen in Appendix A.

For the en-route phase an effort is given on the assessment of the same objectives considered in departure phase. The test case studies of the en-route phase from the long haul flight between London-Heathrow (EGLL/LHR) and Colombo International Airport (VCBI/CMB) is defined to assess the trajectory optimisation for minimum fuel burn, flight time, NOx emissions and for contrail avoidance, hence ascertain an assessment on possible fuel penalty incorporation to the trajectory optimised for minimum fuel with different level of degraded engines. The minimum and maximum altitude and speed for the cruise was set to 10000/39000ft and 310/400kt respectively.

The aircraft arrival at Colombo International Airport (VCBI/CMB) the Civil Aviation Authority in Sri Lanka only mandates the aircraft to have a Noise Certification on board. This standard is a minimum requirement for Noise Abatement Procedures at any airport outside Europe. With this consideration, arrival phase is focuses on the conventional trajectory optimisation criteria of minimum fuel burn, minimum time and minimum NOx which is necessary to assess low level air pollution. The optimisation also attempts to enquire a better approach profile employing continuous descent approach profile as much as possible. The common standard instrument approach procedure at RWY04 is used in this study. The STAR Chart for RWY04 at Colombo International Airport (VCBI/CMB) can be seen in Appendix A-2

5.3 Mission Route

The mission route chosen for the study is take-off to landing from London Heathrow (LHR) airport to Colombo Bandaranaike International (CMB) airport. The ground track of the mission route is shown in Figure 5.2. The mission was divided into three flight phases (departure, en-route and arrival). The departure phase begins at 83ft above ground level (AGL) with the airspeed of 140kts and terminates at the end of the Standard Instrumental Departure (SID). The SID selected for the departure phase is DVR6K. The SID chart for London Heathrow is attached in Appendix A-1; London Heathrow SID Chart. The way points of the departure phase are given in Table 5-1

Figure 5-2 Long haul ground track: London Heathrow to Colombo (Flight Aware 2015)

Table 5-1 Departure Way Points and Constraints

WP	Latitude	Longitude	Altitude min/max [ft]	CAS min/max [kt]
WP1	51 27 53.33 N	000 27 20.46 W	83	140
WP2	51 27 52.94 N	000 23 50.68 W	83/10,000	140/310
WP3	51 26 36.05 N	000 20 05.61 W	83/10,000	140/310
WP4	51 18 14.00 N	000 35 50.00 E	83/10,000	140/310
WP5	51 09 45.00 N	000 21 33.00 E	10,000	310

The en-route phase starts after the aircraft has reached the London Heathrow (LHR) DVR/VOR waypoint and ends when the aircraft ends the Colombo Bandaranaike International airport STAR procedure. During this phase a minimum altitude of FL100 and a maximum of FL390 are used. These bounds give the optimiser the freedom of choosing an optimum flight level within both lower and upper airspaces. The speed during the en-route is limited by the CAS 310 for the lower boundary and by the maximum operation Mach number for the upper boundary. The route and waypoints selected for the en-route is shown in Table 5-2.

Table 5-2 En-route waypoints and constraints - long haul

WP	Latitude	Longitude	Altitude min/max [ft]	CAS min/max [kt]
DVR	51 09 45.00 N	001 21 33.00 E	10,000	310
WP6	51 05 40.86 N	002 39 05.85 E	10,000/39,000	310/400
WP7	50 30 53.10 N	005 37 25.00 E	10,000/39,000	310/400
WP8	49 14 10.37 N	010 22 59.33 E	10,000/39,000	310/400
WP9	47 25 39.41 N	016 35 58.95 E	10,000/39,000	310/400
WP10	41 27 12.00 N	032 59 35.00 E	10,000/39,000	310/400
WP11	38 42 29.80 N	039 13 26.70 E	10,000/39,000	310/400
WP12	29 52 31.00 N	048 29 44.00 E	10,000/39,000	310/400
WP13	25 37 00.00 N	054 55 34.00 E	10,000/39,000	310/400
WP14	20 37 00.00 N	060 57 00.00 E	10,000/39,000	310/400
WP15	12 15 47.20 N	074 16 06.20 E	10,000/39,000	310/400
WP16	11 08 05.50 N	075 57 17.50 E	10,000/39,000	310/400
WP17	09 49 51.90 N	078 05 20.50 E	10,000/39,000	310/400
WP18	08 17 06.30 N	078 35 55.30 E	10,000/39,000	310/400
ENRE	07 42 43.00 N	079 14 32.00 E	39,000	310

The third part of the mission route, arrival phase starts when the aircraft passes over ENRE and terminates at 100ft AGL at VOR/DME. The route waypoints and the related parameters for the arrival phase are listed in the Table 5.3.

Table 5-3 Arrival waypoints and constraints - long haul

WP	Latitude	Longitude	Altitude min/max [ft]	CAS min/max [kt]
ENRE	07 42 43 00 N	079 14 32.00 E	10,000	310
WP19	07 30 32.32 N	079 42 11.10 E	100/10,000	180/310
WP20	07 20 30.00 N	080 00 30.00 E	100/10,000	180/310
DME	07 09 41.00 N	079 52 07.00 E	100	180

5.4 Optimisation Framework

The trajectory optimisation framework was created based on the Generic Multi Disciplinary Optimisation framework GATAC developed in Chapter 3. The framework consists of; (1) Engine Performance Models (one clean engine CULE_0DL with 0% EGT increase and two levels of degraded engines CULE_1DL with 5% EGT increase and CULE_2DL with 10% EGT increase respectively). The full details of creating the degraded engine models are given in Chapter 4, (2) The long range aircraft performance model used in the framework is CULA – Cranfield University Long-range Aircraft model, (3) Engine Emission Prediction Model (EEM), (4) Contrail Formation Model (CFM), and (5) GA based Optimiser NSGAMO-II. The complete working sequence, development, testing and validation of all models and optimiser have already presented in Chapter 4. The interaction between models and optimiser within the framework to generate optimum aircraft trajectories are also discussed. The schematic of the optimisation framework with models and optimiser is shown in Figure 5-3.

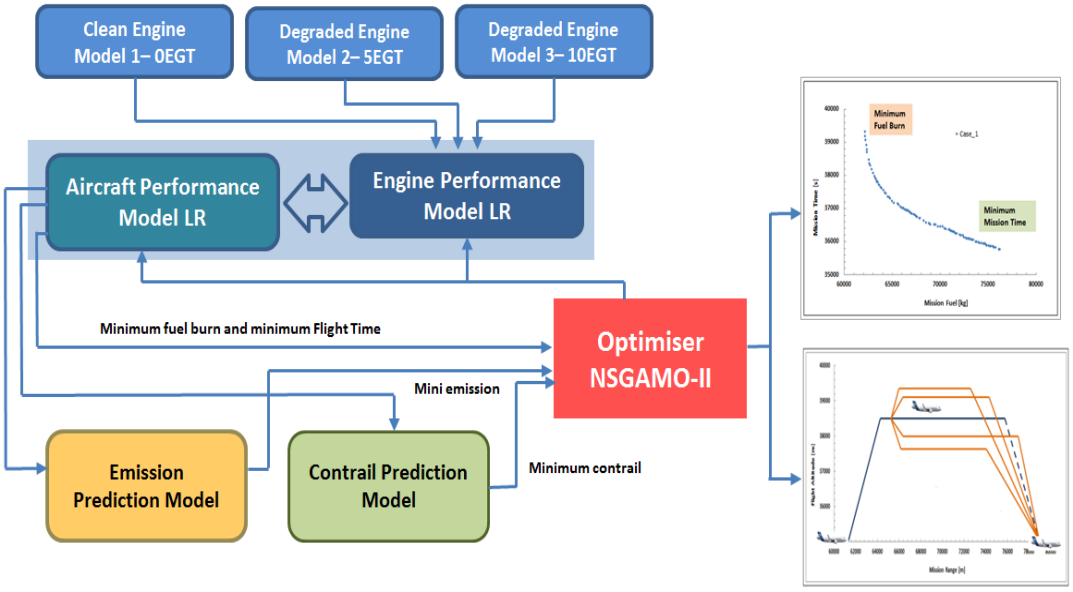

Figure 5-3 Optimisation framework developed for long range aircraft trajectory optimisation

5.5 Optimisation studies and trajectory analysis

The trajectory optimisation is performed to assess the impact of engine degradation on the long range optimum aircraft trajectories. Several objectives have been selected for the study. The traditional performance objectives include mission fuel and mission time, while the environmental objectives include NOx, and Contrails which produced over the mission as a result of fuel burn. These objectives are selected to investigate, how the optimised trajectories generated by degraded engines will differ in terms of operational parameters (speeds, altitudes, net thrust, SFC and EGTs) in comparison to the base line trajectories generated by the clean engines. Also to establish the environmental gains that may be achieved in terms of optimised objectives. Therefore in order to perform the trajectory optimisation, three cases have been considered: CASE_1 is aircraft with the clean engines (engines with 0% EGT increase), CASE_2 is aircraft with low degraded engines (engines with 5% EGT increase) and CASE_3 is aircraft with high degraded engines (engines with 10% EGT increase) as shown in Figure 5-4.

CASE	Aircraft	Engine	Level of Degradation
CASE_1	CULA	CULE_0DL	0 % EGT Increase
CASE_2	CULA	CULE_1DL	5 % EGT Increase
CASE_3	CULA	CULE_2DL	10 % EGT Increase

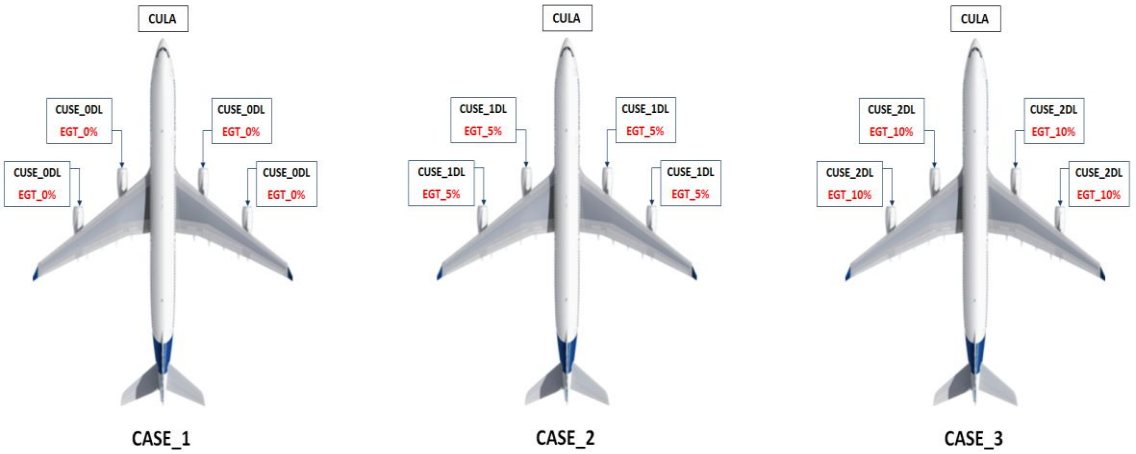

Figure 5-4 Cases considered for optimisation studies

5.5.1 Aircraft trajectory optimisation for fuel burn and flight time

The fuel burn and flight time are currently the key objectives considered for optimising the economic and environmental performance by the aviation industry. Also fuel burn can be directly used to calculate the amount of carbon dioxide emissions of the mission.

Optimisation set up

Minimum fuel and minimum time have been selected as the objective functions. The optimiser was set up for 250 generations. The population was selected as 100 and an initialisation ratio of 50. The number of evaluation was about 30,000.

Flight Phase	Objective 1	Objective 2	Generations	Population	In. Factor
Complete mission	Mission Fuel	Mission Time	250	100	50

.

5.5.1.1 CASE_1: Optimum aircraft trajectories generated with clean engines (engines with 0% EGT increase)

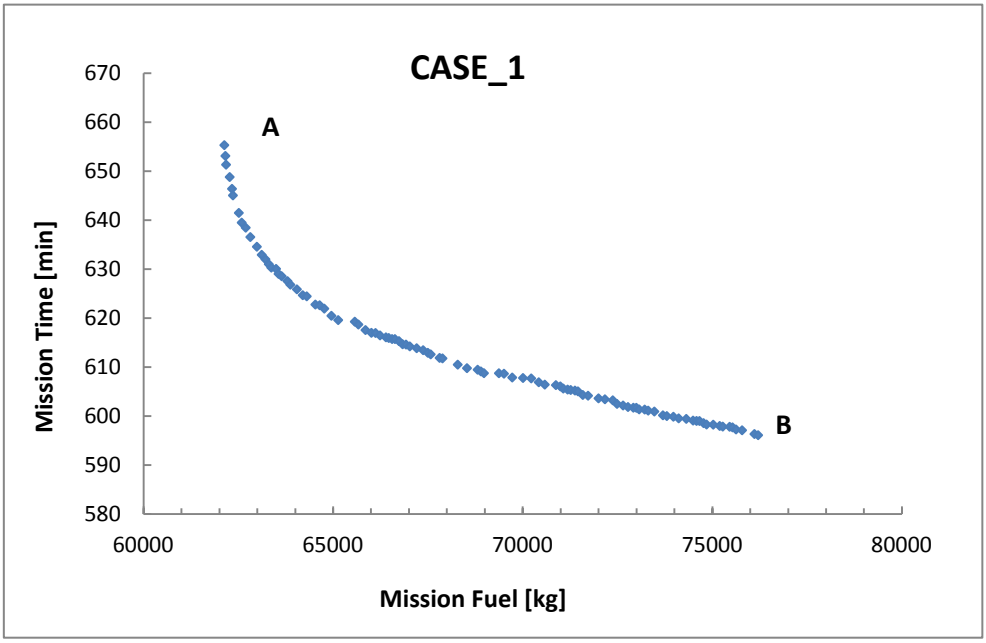

Figure 5-5 Pareto Front for minimum fuel and minimum time objectives

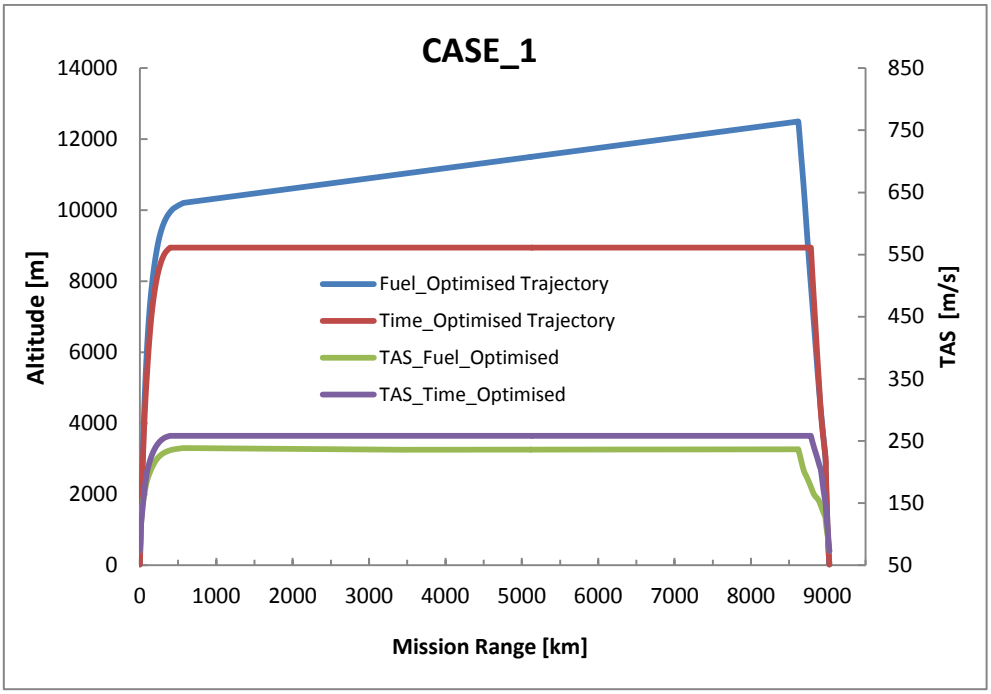

Figure 5-6 Minimum fuel and minimum time trajectories with TAS

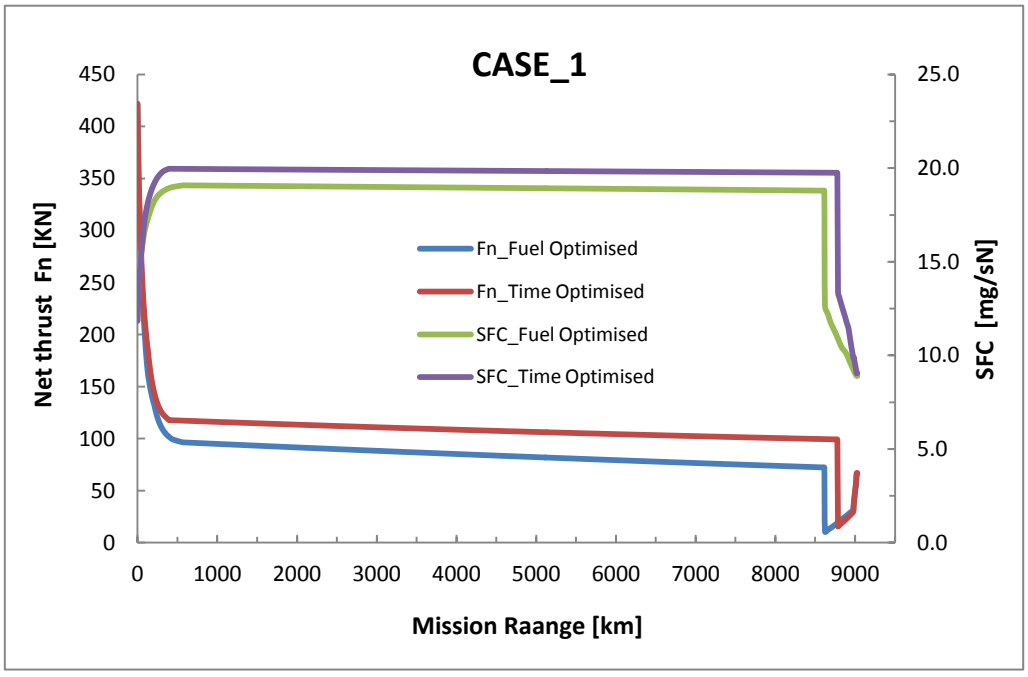

Figure 5-7 Net thrust and SFC variation for minimum fuel and minimum time trajectories

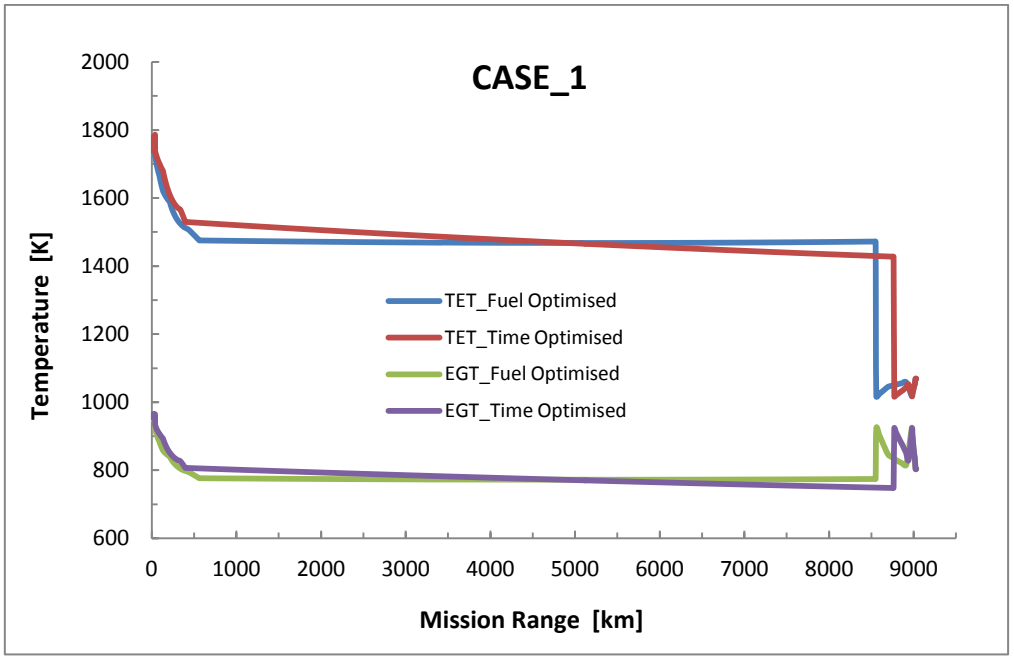

Figure 5-8 TET and EGT variation for minimum fuel and minimum time trajectories

5.5.1.2 CASE_2: Optimum aircraft trajectories generated with low degraded engines (engines with 5% EGT increase)

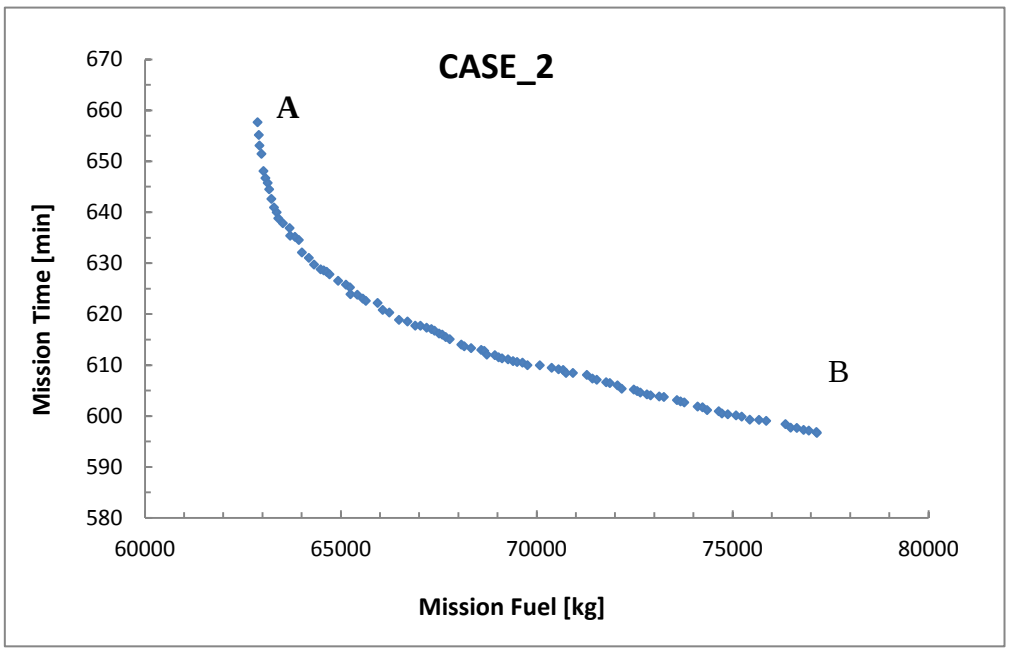

Figure 5-9 Pareto Front for minimum fuel and minimum time objectives

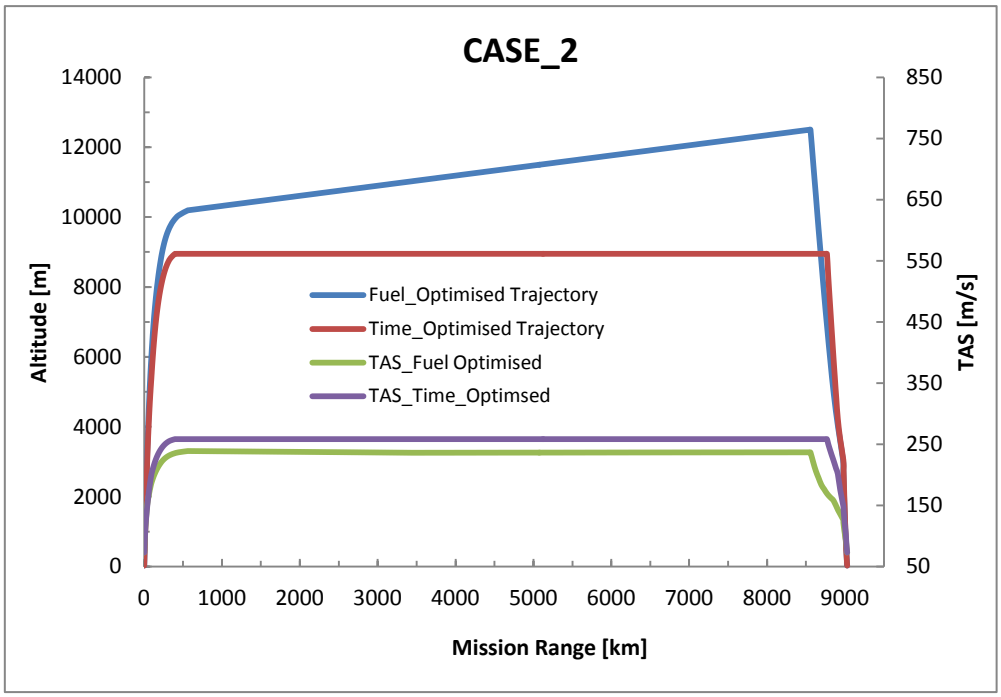

Figure 5-10 Minimum fuel and minimum time trajectories with TAS

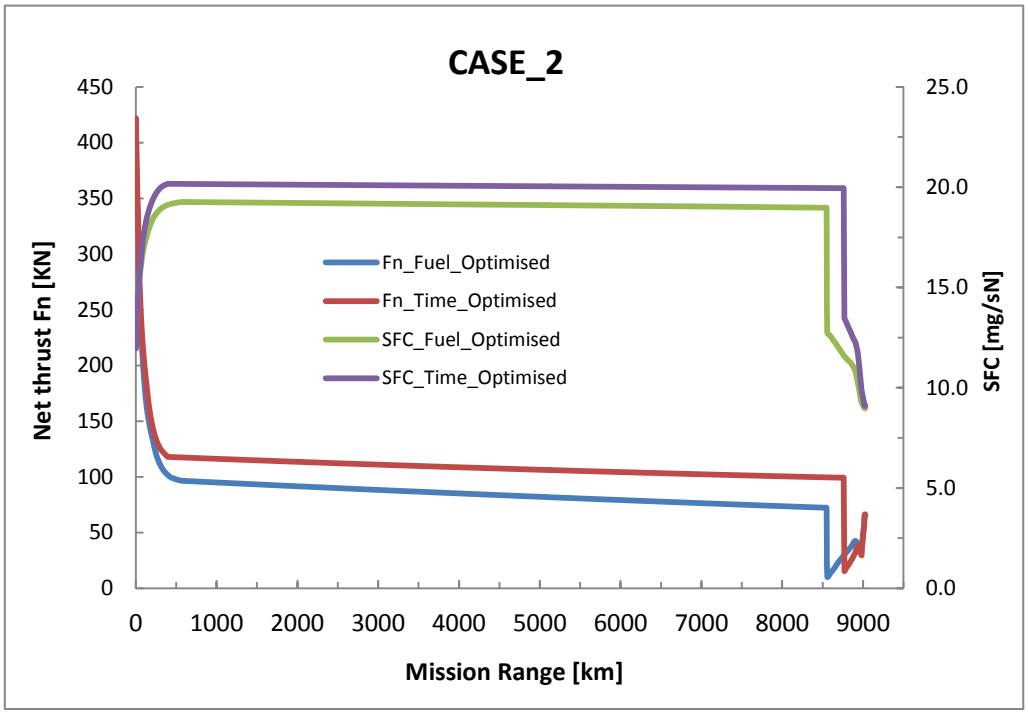

Figure 5-11 Net thrust and SFC variation for minimum fuel and minimum time trajectories

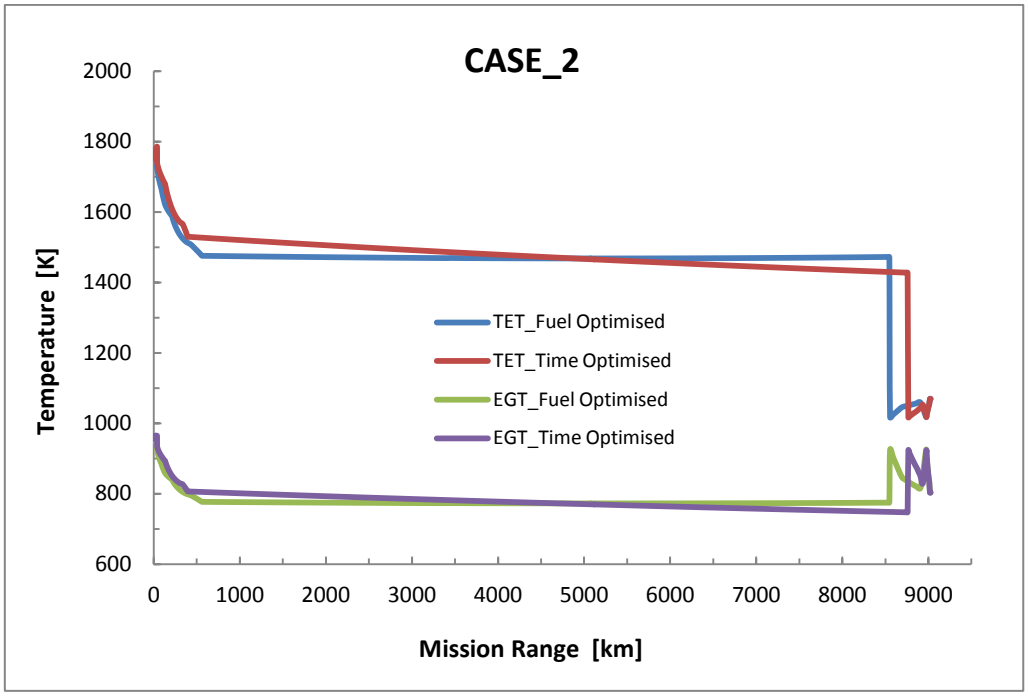

Figure 5-12 TET and EGT variation for minimum fuel and minimum time trajectories

5.5.1.3 CASE_3: Optimum aircraft trajectories generated with high degraded engines (engines with 10% EGT increase)

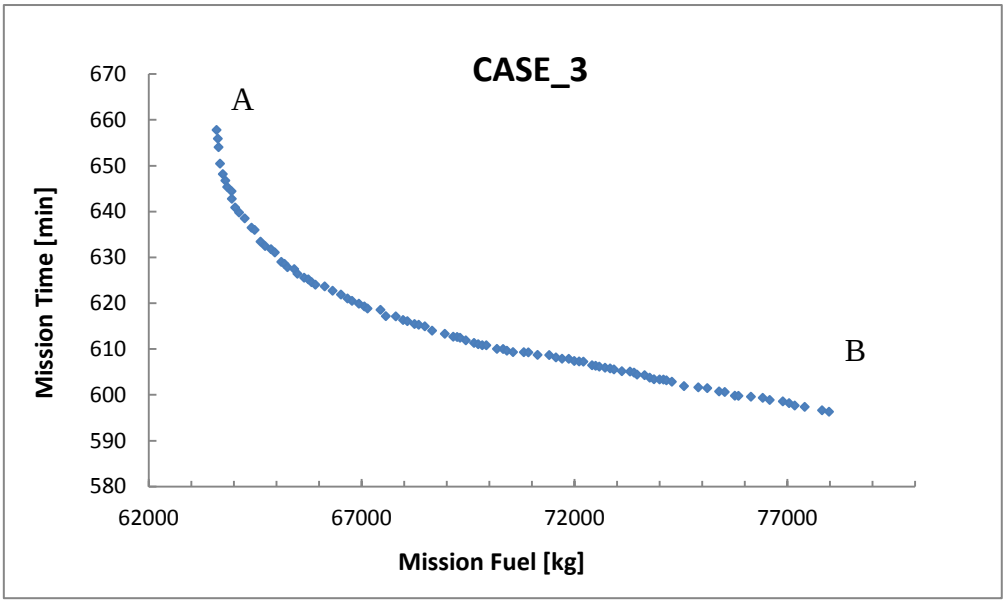

Figure 5-13 Pareto Front for minimum fuel and minimum time objectives

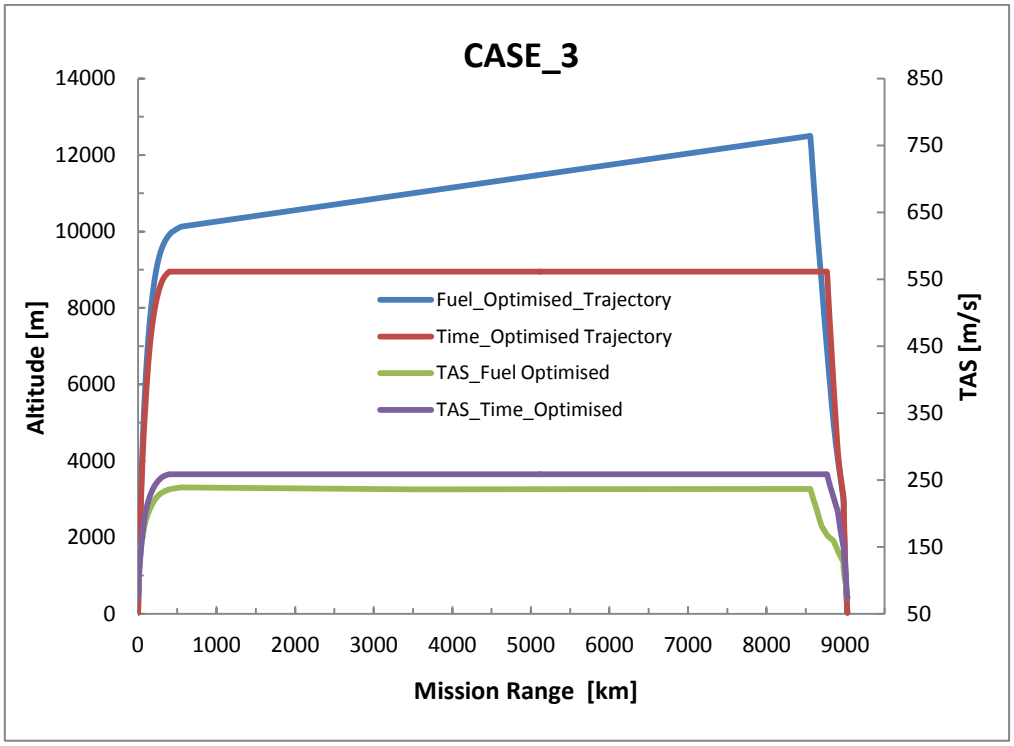

Figure 5-14 Minimum fuel and minimum time trajectories with TAS

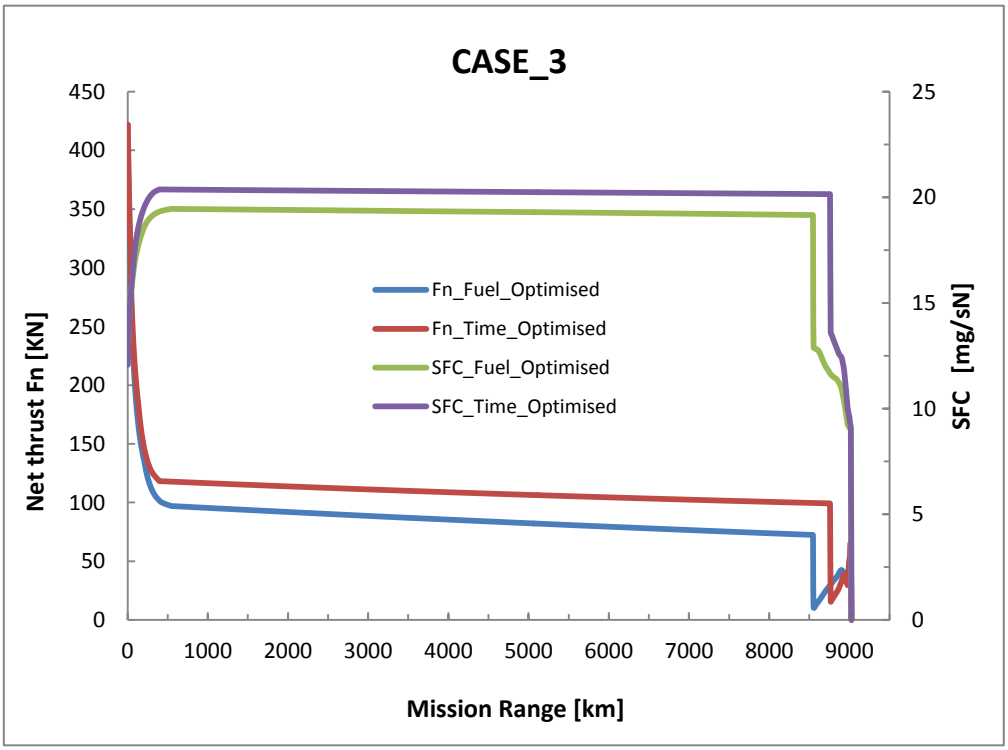

Figure 5-15 Net thrust and SFC variation for minimum fuel and minimum time trajectories

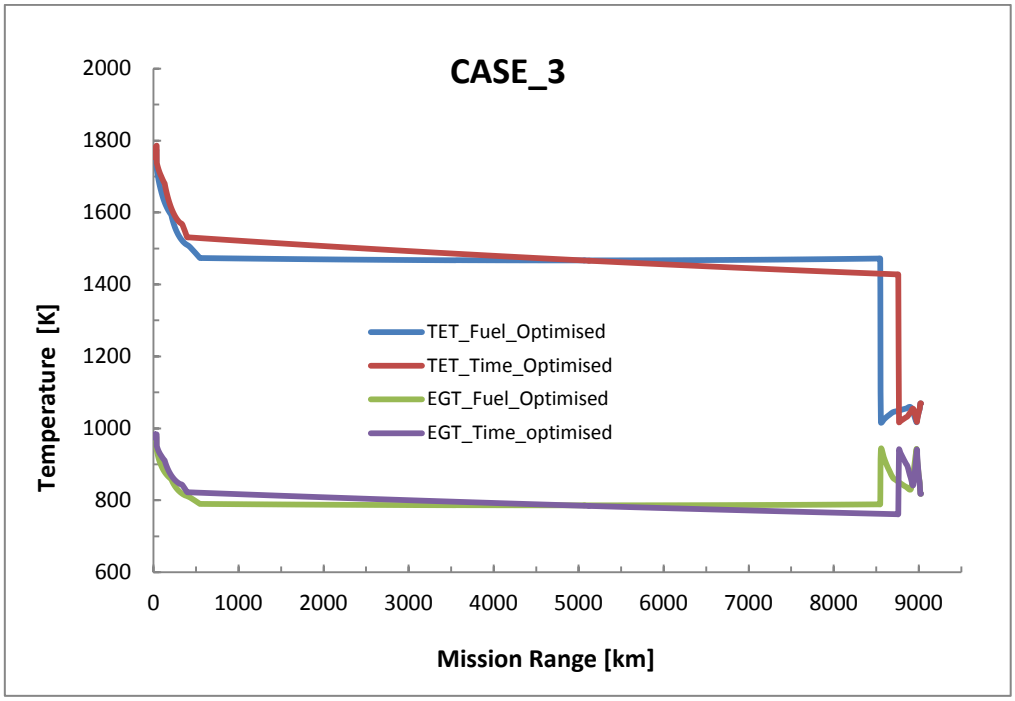

Figure 5-16 TET and EGT variation for minimum fuel and minimum time trajectories

Trajectories are optimised for the minimum fuel burn and minimum time objectives. Pareto fronts obtained from the long range aircraft with clean and two degraded engines are presented in Figure 5-5, 5-9 and 5-13. The Pareto fronts are formed by a series of points, where each point represents a trajectory. The two extreme points A and B represent the minimum fuel burn and minimum time (optimum) trajectories respectively. The remaining points are other intermediate trade off solutions. The complete profiles of the minimum fuel burn and minimum time trajectories with their TAS are shown in Figure 5-6, 5-10 and 5-14.

There is an optimum cruise altitude for minimum fuel burn. Therefore, optimal altitude is found where fuel consumption is minimised by flying at the most efficient speed and engine thrust setting. As fuel is burned and aircraft weight decreases, the amount of lift needed and consequently drag is reduced, which means required thrust is also become less. But, if throttle is reduced, then the engine is no longer operating at the most efficient setting. Therefore, the optimal procedure is to maintain the most efficient speed and power setting and use the excess thrust to gradually climb the aircraft continuously. The climb continued throughout the cruise (cruise climb) and ends at TOD when the optimum descent path is intercepted. This path is the result of descending continuously at minimum gradient (minimum drag) speed, which allows the aircraft to maximise the flown distance at idle thrust (or very low thrust). However, in

practice change in optimum cruise altitude is often taken into account by changing the cruise altitude in steps (step cruise). Step cruise is preferred as it is easier to manage from an air traffic control perspective.

An aircraft with degraded engines are heavier and therefore will tend to reach the optimum altitude early in the flight (lower altitude than the clean engine) and continues along the cruise climb which maintains an optimum altitude as the aircraft weight reduces. Therefore aircraft tends to follow the same continuous climb approach, but towards TOD the aircraft weight will approach that of a clean engine and therefore the altitudes tend to converge.

For the minimum time, the aircraft (for any mission type) must fly at the crossover altitude. The cross over altitude is the altitude at which the CAS (Calibrated Air Speed) limit and Mach number limit are equal in terms of TAS. Above this altitude TAS will fall at a fix Mach number due to reducing ambient air temperature. Below this altitude TAS will also fall at a fixed CAS. Therefore the maximum TAS is at the crossover altitude which the aircraft to achieve minimum time. When the engines are degraded TAS started reducing and as result minimum time increased. However it is important to notice that increase in minimum time for both degraded engines are marginal compared to aircraft with clean engines.

The variation of the net thrust, and SFC, for the minimum fuel burn and minimum time trajectories are given in Figure 5-7, 5-11 and 5-15. The variations of TET and EGT of all three cases are also presented in Figure 5-8, 5-12 and 5-16. Summary of the minimum fuel burn and minimum flight time for clean and two degraded engines are presented in Table 5-4 and Figures 5-19 and 5-20. When analysing the optimum trajectories it can be seen, both fuel optimised and time optimised trajectories demonstrated a significant trade-off between fuel burn and flight time. The fuel optimised trajectory of the clean engine has achieved a minimum fuel burn of 62137 kg with a flight time of 39301s (10hrs and 55min). Time optimised trajectory has achieved a minimum flight time of 35214s (09 hrs and 47 min) with a fuel burn of 76214kg. Therefore fuel optimised trajectory has achieved 22.6% of reduction in fuel burn compared to time optimised trajectory, but with a compromise of 11.6% flight time.

The optimum trajectories with low degraded engines (CULE_1DL) show a similar trade-off between fuel burn and flight time, but with a increased fuel burn and flight time. The fuel optimised trajectory has achieved a minimum fuel burn of 62875kg with a flight time of 39456s (10hrs and 58min). Comparing to the CASE_1, fuel burn and flight time has increased by 738kg and 155s (2.6min) i.e. 1.19% and 0.39% respectively. Time optimised trajectory has achieved a minimum flight time of 35365s (09hrs and 49min) with a fuel burn of 77151kg. But

comparing to the CASE_1, minimum time and minimum fuel has increased by 151s (2.52min) and 937kg, i.e. 0.43% and 1.23% respectively. Therefore looking at the both optimum trajectories, fuel optimised trajectory has achieved 18.5% of reduction in fuel burn compared to time optimised trajectory, but with 11.6% compromise of flight time.

Optimum trajectories with highly degraded engines (CULE_2DL) also show a similar trade-off between fuel burn and flight time. The fuel optimised trajectory has achieved a minimum fuel burn of 63598kg with a flight time of 39627s (11hrs). But comparing to the CASE_1, minimum fuel burn and minimum flight time has increased by 1461kg and 326s (5.4min) i.e. 2.35% and 0.83% respectively. Also comparing to the CASE_2, fuel burn and flight time have increased by 723kg and 171s (2.9min), i.e. 1.15% and 0.43% respectively. Whereas, time optimised trajectory has achieved a minimum flight time of 35517s (09hrs and 52min) with a fuel burn of 78081kg. But comparing to the CASE_1, minimum flight time and minimum fuel has increased by 303s (5.1min) and 1867kg, i.e. 0.86% and 2.45% respectively. Also comparing to the CASE_2, minimum flight time and minimum fuel burn have increased by 152s (2.5min) and 930kg, i.e. 0.42% and 1.2% respectively. Therefore looking at the both optimum trajectories, fuel optimised trajectory has achieved 18.5% of reduction in fuel burn compared to time optimised trajectory, but with 11.6% compromise of flight time.

The Table 5-4, Figure 5-17 and Figure 5-18 summarise the results of minimum fuel burn and minimum time optimised trajectories generated by the long range aircraft with clean engine (CASE_1) and aircraft with two levels of degraded engines (CASE_2 and CASE_3).

Table 5-4 Summary of optimisation results

	Fuel Optimised				Time Optimised			
Case	Fuel [Kg]	Time [Sec]	Del Fuel [%]	Del Time [%]	Fuel [kg]	Time [Sec]	Del Fuel [%]	Del Time [%]
Case 1	62137	39301	0.00	0.00	76214	35214	0.0	0.0
Case 2	62875	39456	1.19	0.39	77151	35365	1.23	0.43
Case 3	63598	39627	2.35	0.83	78081	35517	2.45	0.86

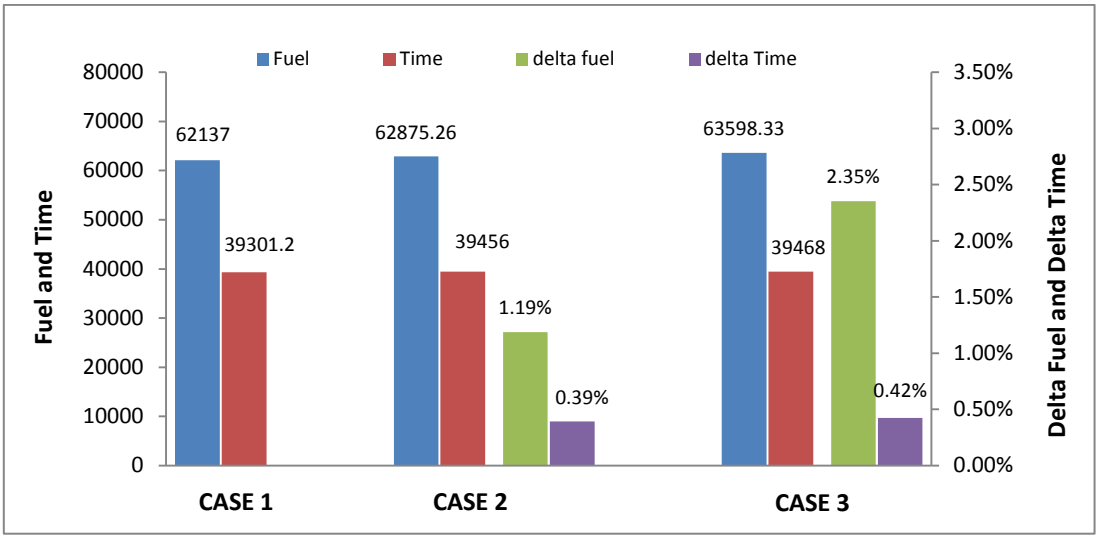

Figure 5-17 Fuel and Time penalty for fuel optimised trajectories

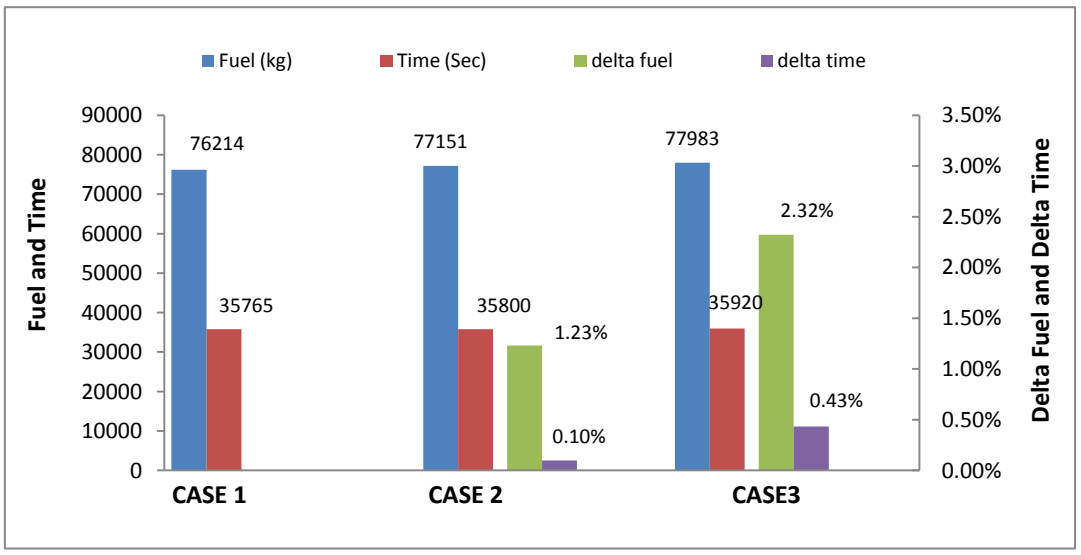

Figure 5-18 Fuel and Time penalty for time optimised trajectories

5.5.1.4 Impact of flying clean/degraded optimised trajectories with clean/degraded engines on fuel burn

Table 5-5 Fuel burn of optimum aircraft trajectories with clean/degraded engines

Long range aircraft with clean and low degraded engines	
Clean engines flying on trajectories optimised for clean engines (CE+COT)	62137 kg
Deg. engines flying on trajectories optimised for clean engines (DE+COT)	63127 kg
Delta Fuel Burn of (DE+COT) Reference to (CE+COT)	+990 kg (1.59%)
Deg. engines flying on trajectories optimised for deg. engines (DE+DOT)	62875 kg
Delta Fuel Burn of (DE+DOT) Reference to (DE+COT)	-252 kg (-0.40%)
Long range aircraft with clean and highly degraded engines	
Clean engines flying on trajectories optimised for clean engines (CE+COT)	62137 kg
Deg. engines flying on trajectories optimised for clean engines (DE+COT)	63982 kg
Delta Fuel Burn of (DE+COT) Reference to (CE+COT)	+1845 kg (2.9%)
Deg. engines flying on trajectories optimised for deg. engines (DE+DOT)	63598 kg
Delta Fuel Burn of (DE+DOT) Reference to (DE+COT)	-384 kg (-0.6%)

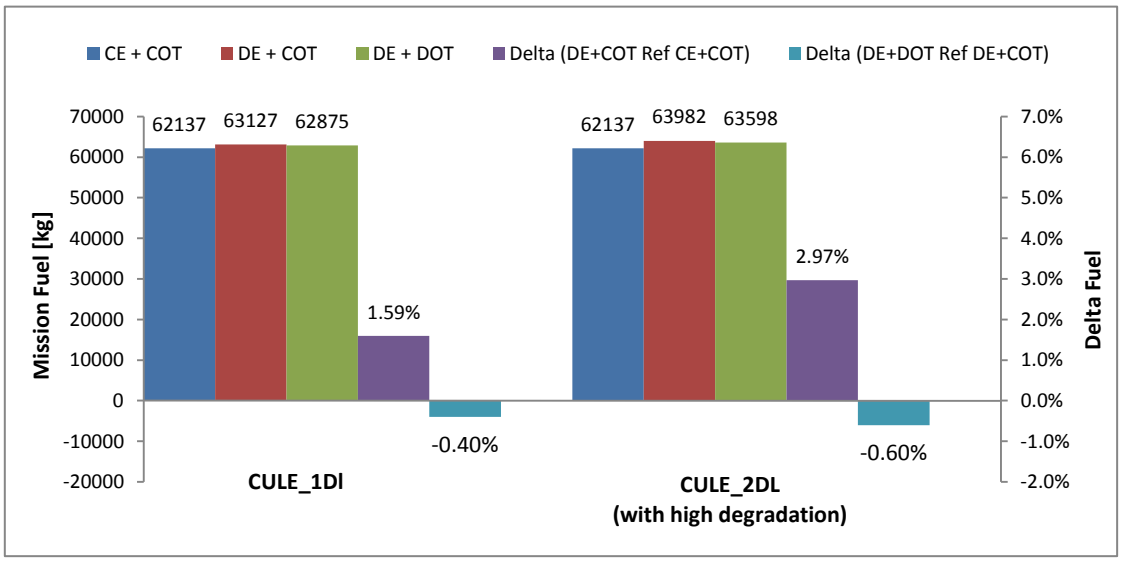

Figure 5-19 Fuel burn of aircraft trajectories with clean/degraded engines

5.5.1.5 Impact of flying clean/degraded optimised trajectories with clean/degraded engines on flight time

Table 5-6 Flight time of optimum aircraft trajectories with clean/degraded engines

Long range aircraft with clean and low degraded engines	
Clean engines flying on trajectories optimised for clean engines (CE+COT)	587 min
Deg. engines flying on trajectories optimised for clean engines (DE+COT)	591 min
Delta Flight Time of (DE+COT) Reference to (CE+COT)	+3.9 min (0.6%)
Deg. engines flying on trajectories optimised for deg. engines (DE+DOT)	589 min
Delta Flight Time of (DE+DOT) Reference to (DE+COT)	-1.4 min (-0.2%)
Long range aircraft with clean and highly degraded engines	
Clean engines flying on trajectories optimised for clean engines (CE+COT)	587 min
Deg. engines flying on trajectories optimised for clean engines (DE+COT)	594 min
Delta Flight Time of (DE+COT) Reference to (CE+COT)	+7.6 min (1.3%)
Deg. engines flying on trajectories optimised for deg. engines (DE+DOT)	592 min
Delta Flight Time of (DE+DOT) Reference to (DE+COT)	-1.4 min (-0.4%)

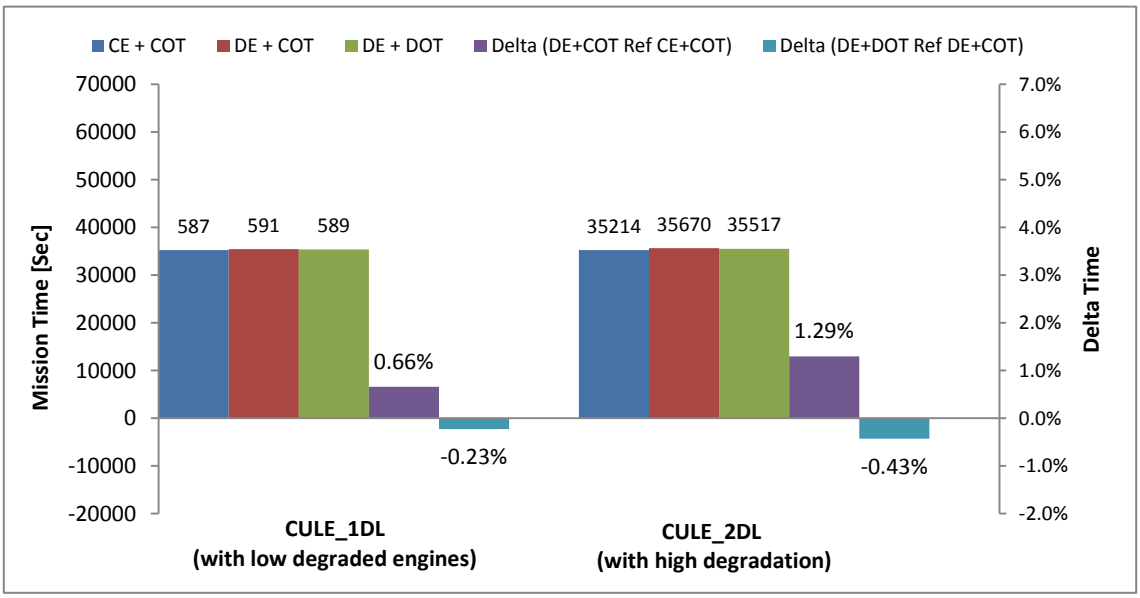

Figure 5-20 Flight time of aircraft trajectories with clean/degraded engines

Optimum trajectories demonstrate a significant trade-off between minimum fuel burn and minimum time for all three cases. Therefore it is important to investigate the impact on fuel burn and flight time, when the aircraft with degraded engines are flying on the trajectory which has been optimised for clean engines. Table 5-5 and Figure 5-19 shows the fuel burn of optimum trajectories of the aircraft with clean and degraded engines, also the fuel burn of the aircraft with two levels of degraded engines are flying on the same optimum trajectory of the clean engines.

Fuel optimised trajectory has achieved a minimum fuel burn of 62137kg with the clean engines. But when the aircraft is flying on the same trajectory with the degraded engines of 5% and 10% EGT increase, fuel burn has increased by 1.59% (i.e. 990kg) and 2.9% (i.e. 1845kg) comparing to the clean engine optimised trajectory (CE+COT). However, it is interesting to notice that fuel burn can be reduced by 0.4% (i.e. 252kg) and 0.6% (i.e. 384kg) with the degraded engines when the aircraft trajectories are specifically optimised for degraded engines.

However with the time optimum trajectories there are no significant differences. Table 5-6 and Figure 5-20 shows the flight times of the aircraft with clean and degraded engines, in addition to aircraft flying on the clean engine optimised trajectory. Time optimised trajectory has achieved a minimum flight time of 587min with the clean engines. But when the aircraft is flying on the same trajectory with the degraded engines of 5% and 10% EGT increase, flight time has increased by 0.6% (i.e. 3.9min) and 1.3% (i.e. 7.6min) comparing to the clean engine optimised trajectory (CE+COT). However, flight time can be reduced by 0.2% (i.e. 1.4min) and 0.4% (i.e. 2.6min), when the aircraft trajectories are specifically optimised for degraded engines.

5.5.2 Aircraft trajectory optimisation for fuel burn and NOx emissions

Oxides of Nitrogen (NOx) emissions continue to be the primary focus of environmental concerns with regards to aircraft emissions. The amount of NOx produced is calculated for the whole mission. Thus it includes the NOx generated during the LTO cycle but also the NOx generated at cruise level. Current legislations does not imposed any limitations on NOx produced during the cruise phase, however it is interesting to assess the amount of NOx is emitted in the upper atmosphere as its impact on climate change could be severer. Therefore aim of this study is to investigate the impact of engine

degradation on the NOx optimised trajectory and fuel optimised trajectory as they trade-off each other. Also to calculate the amount of NOx emission reduction could be achieve by optimising the trajectories specifically for degraded engines.

Optimisation set up

Minimum fuel and minimum NOx have been selected as the objective functions. The optimiser was set up for 250 generations. The population was selected as 100 and initialisation ratio of 50. The number of evaluation was about 30,000.

Flight Phase	Objective 1	Objective 2	Generations	Population	In. Factor
Complete mission	Mission Fuel	Mission NOx	250	100	50

5.5.2.1 Optimum trajectories generated from the aircraft with clean engines (Engines with 0% EGT increase)

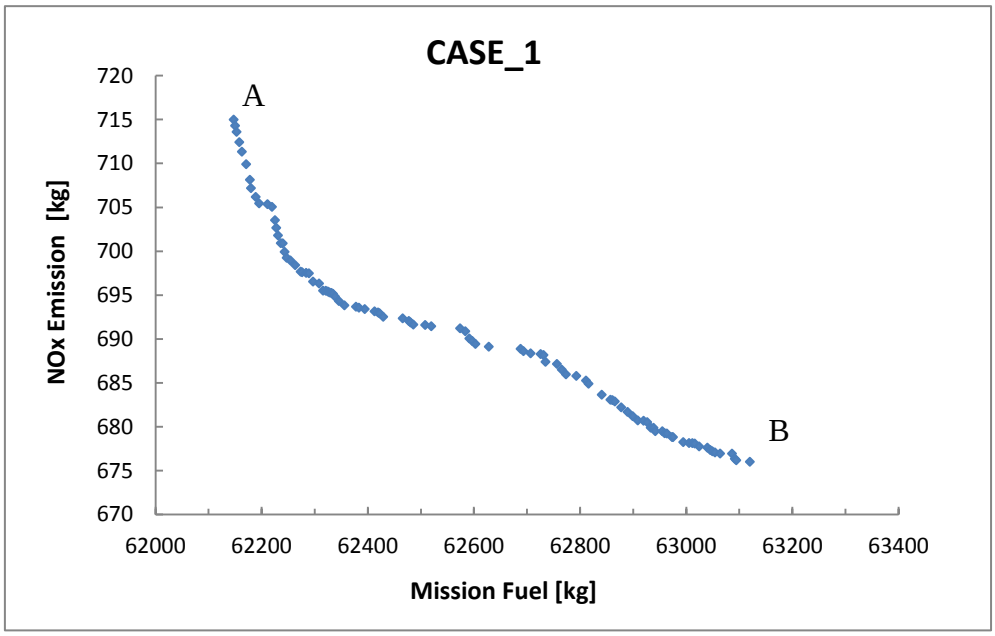

Figure 5-21 Pareto front for minimum fuel and minimum NOx emissions

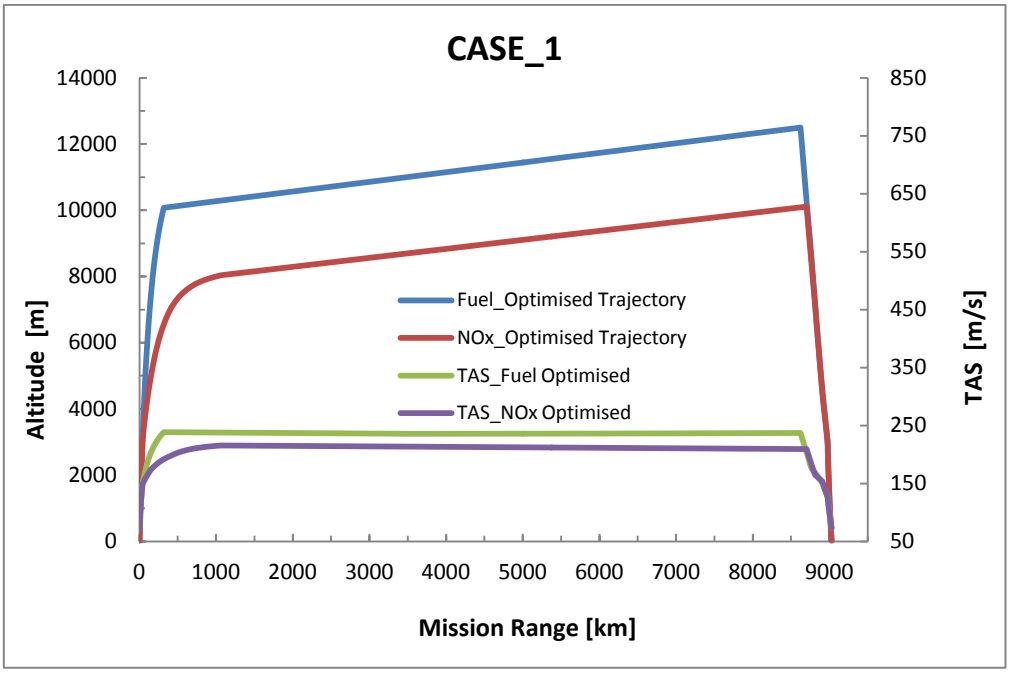

Figure 5-22 Minimum fuel and minimum NOx trajectories with TAS

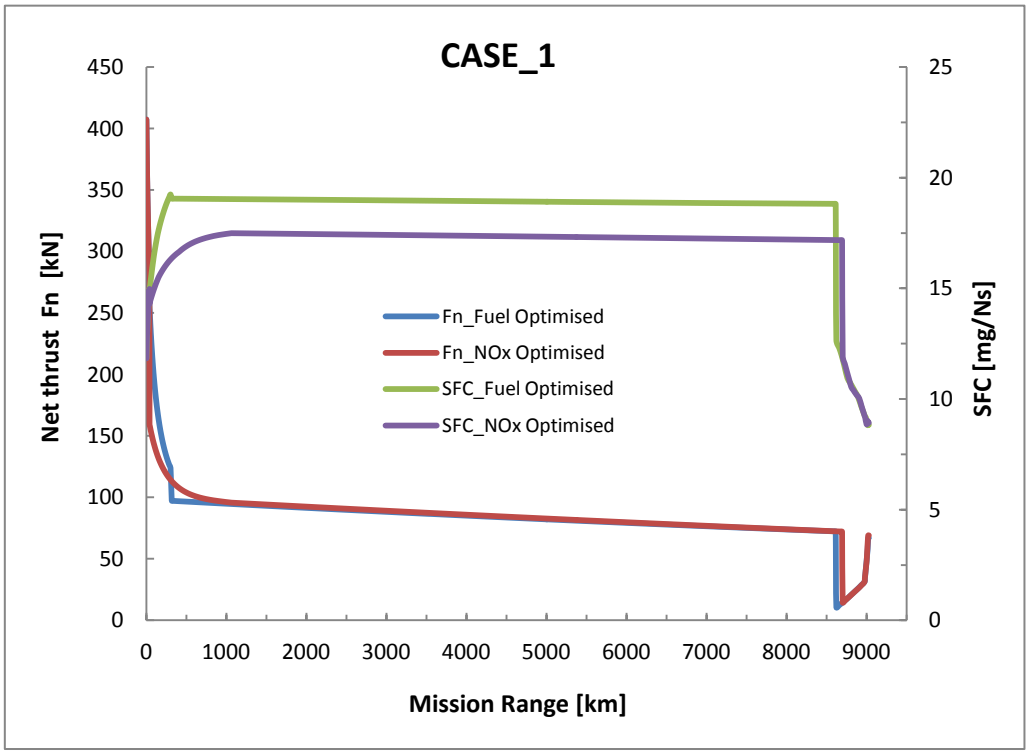

Figure 5-23 Net thrust and SFC variation for minimum fuel and minimum NOx

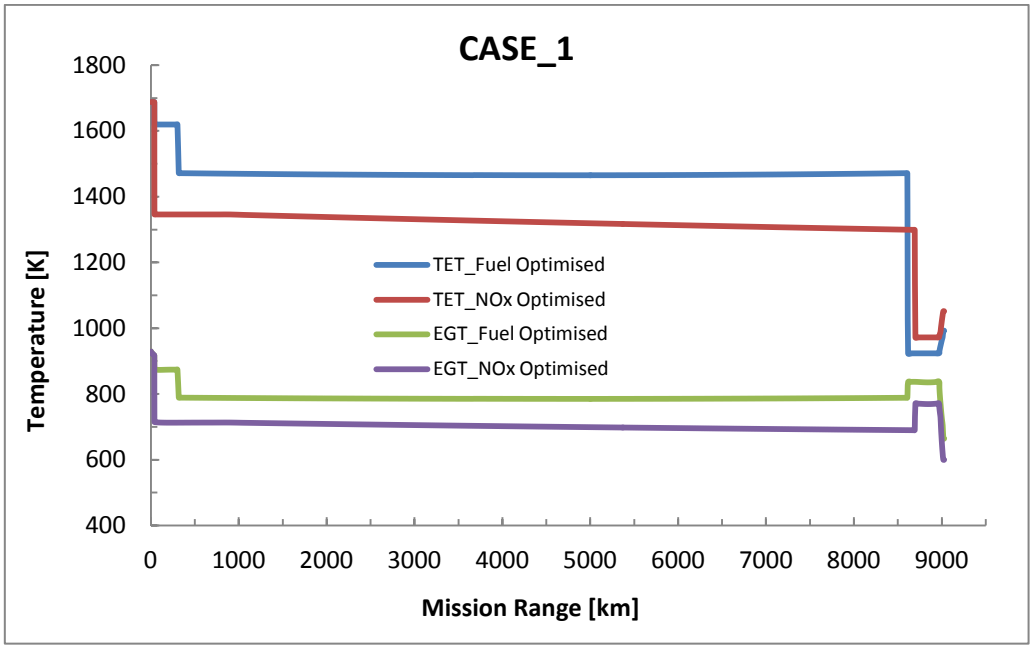

Figure 5-24 TET and EGT variation for minimum fuel and minimum NOx

5.5.2.2 CASE_2: Optimum aircraft trajectories generated from the aircraft with low degraded engines (engines with 5% EGT increase)

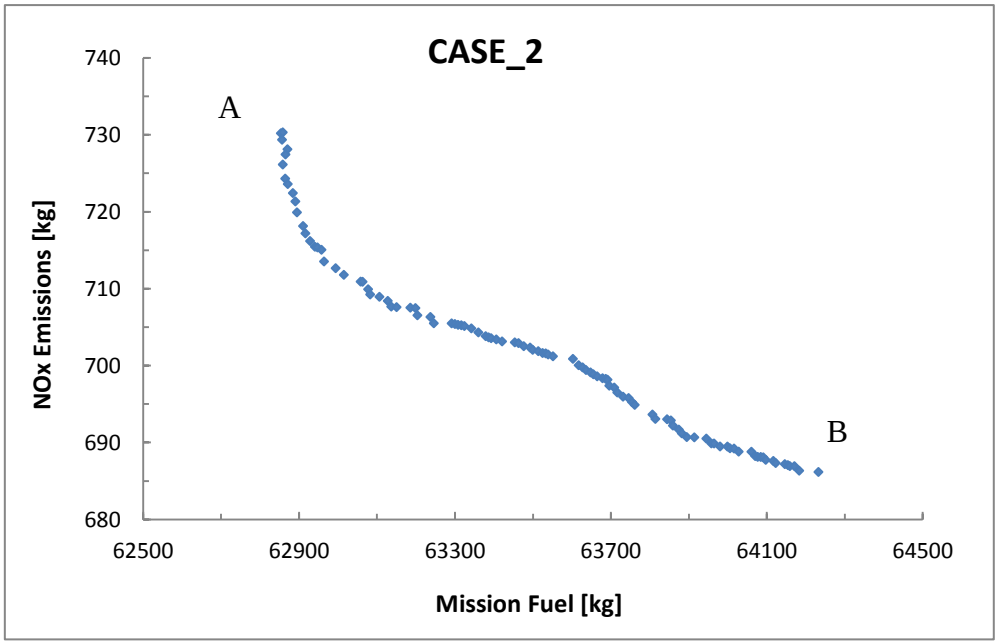

Figure 5-25 Pareto front for minimum fuel and minimum NOx emissions

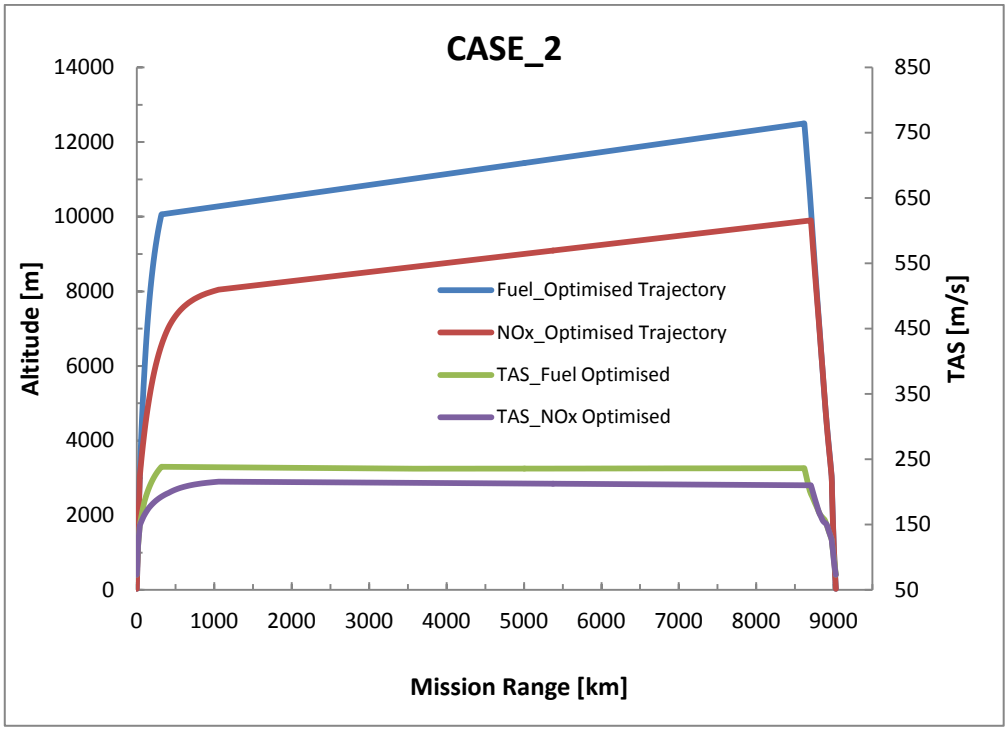

Figure 5-26 Minimum fuel and minimum NOx trajectories with TAS

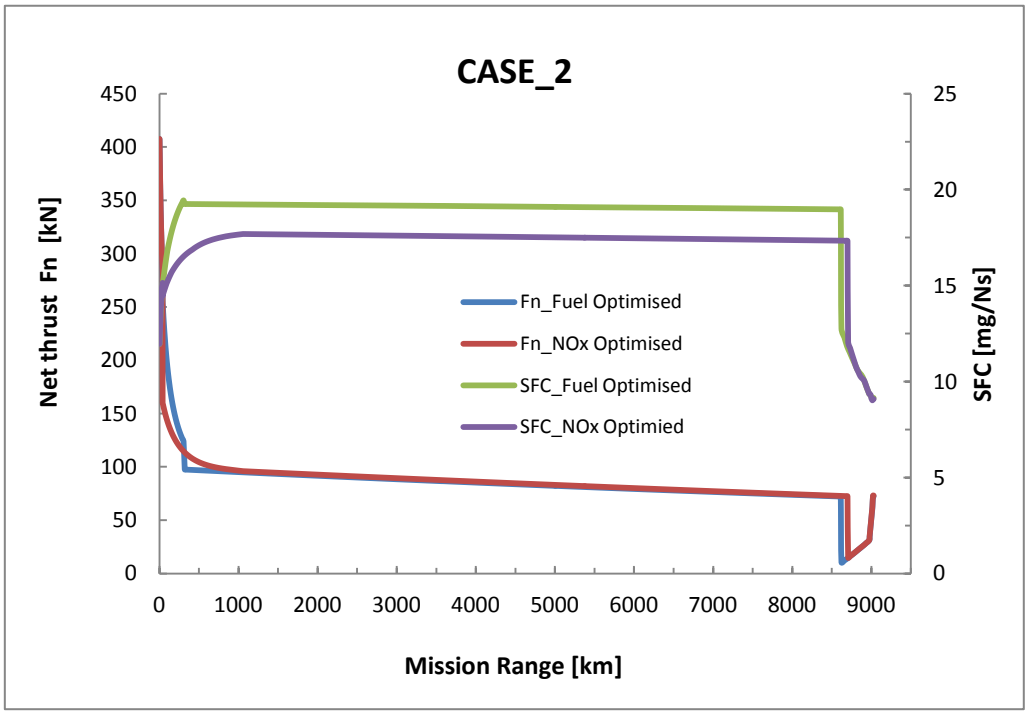

Figure 5-27 **Net thrust and SFC variation for minimum fuel and minimum NOx**

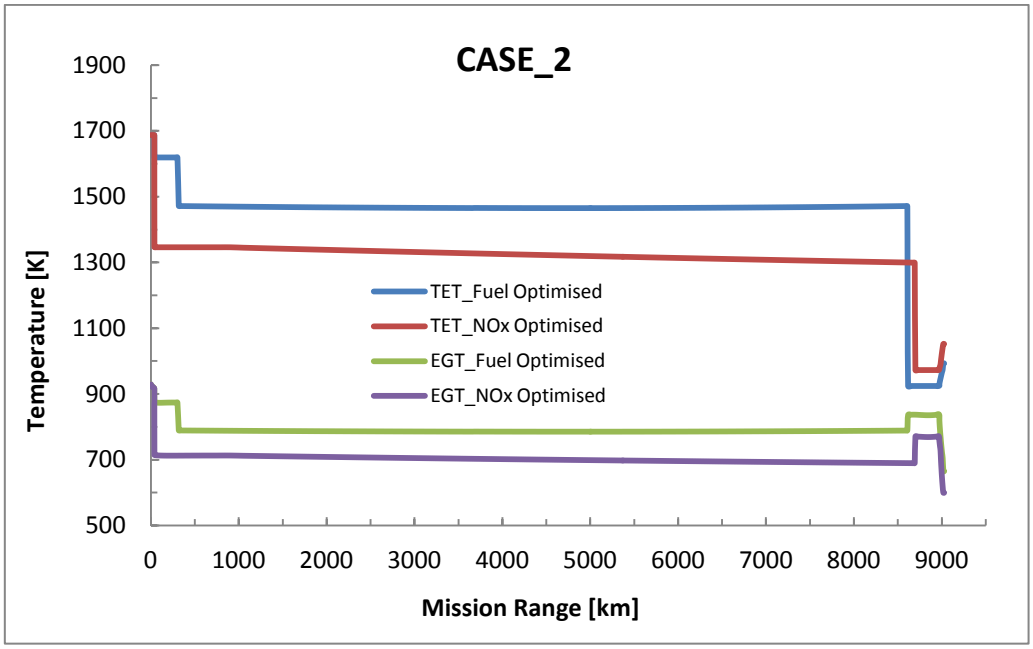

Figure 5-28 TET and EGT variation for minimum fuel and minimum NOx

5.5.2.3 CASE_3: Optimum aircraft trajectories generated from the aircraft with high degraded engines (engines with 10% EGT increase)

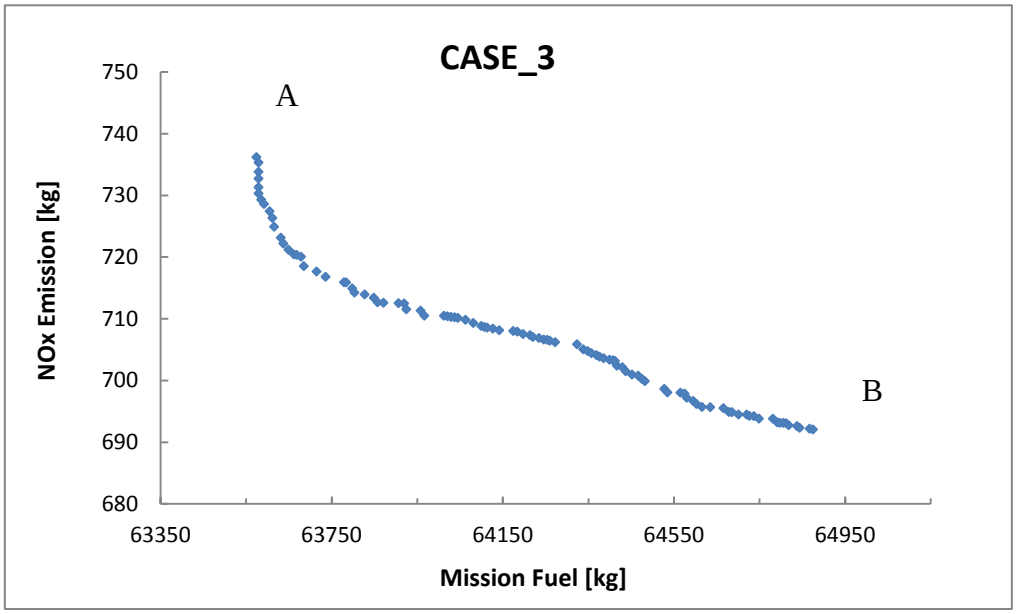

Figure 5-29 Pareto front for minimum fuel and minimum NOx emissions

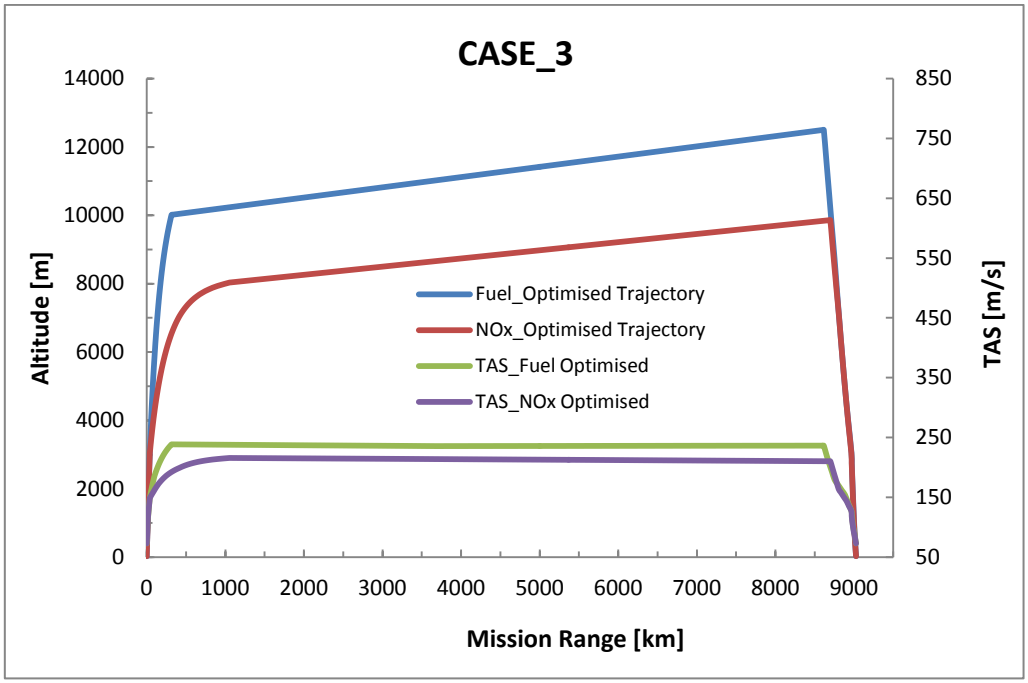

Figure 5-30 Minimum fuel and minimum NOx trajectories with TAS

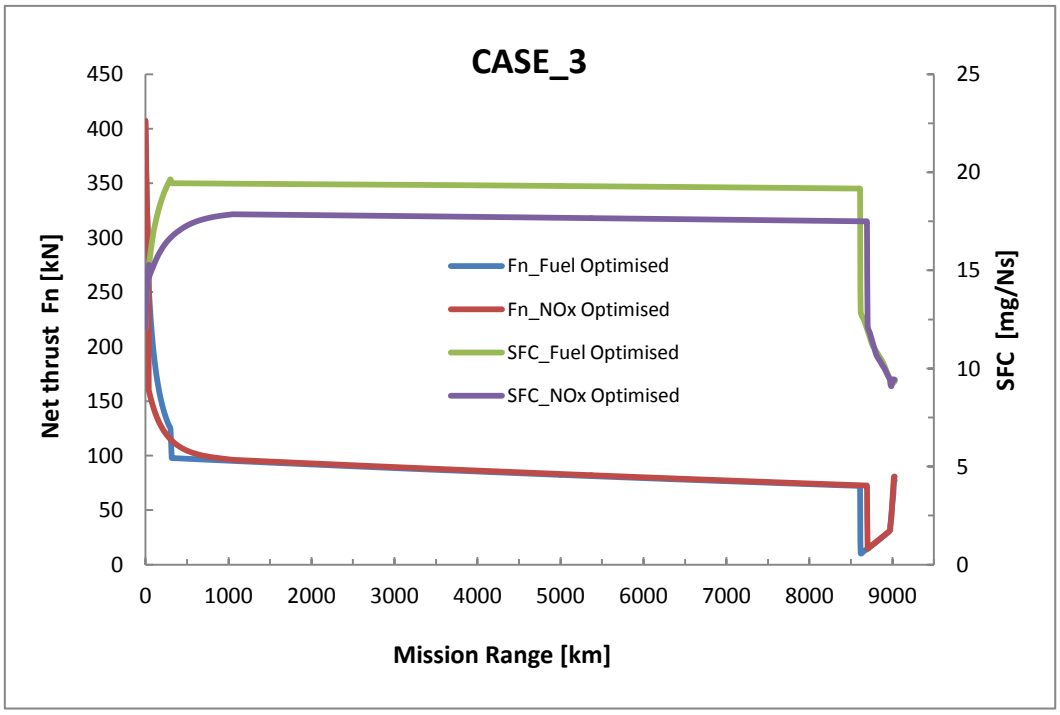

Figure 5-31 Net thrust and SFC variation for minimum fuel and minimum NOx

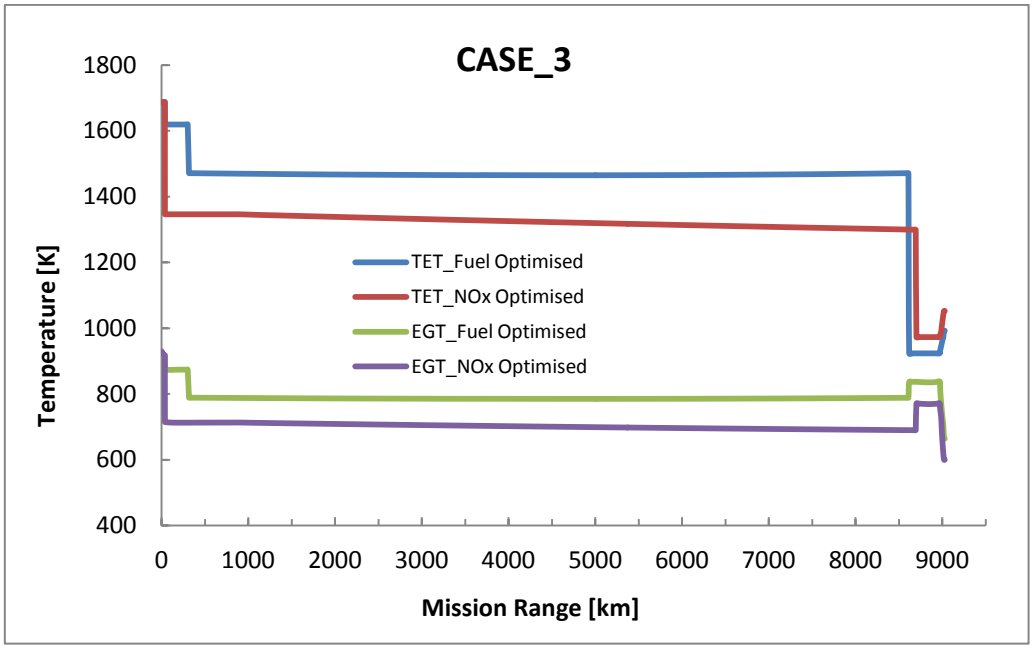

Figure 5-32 TET and EGT variation for minimum fuel and minimum NOx

Table 5-7 Summary of optimisation results

	Fuel Optimised				NOx Optimised			
Case	**Fuel [Kg]**	**NOx [kg]**	**Del Fuel [%]**	**Del NOx [%]**	**Fuel [kg]**	**NOx [kg]**	**Del Fuel [%]**	**Del NOx [%]**
Case 1	62137	715.2	0.00	0.00	63120	676.8	0.0	0.0
Case 2	62875	731.2	1.20	1.39	64233	686.2	1.76	1.40
Case 3	63595	735.3	2.34	2.80	64905	696.3	2.83	2.90

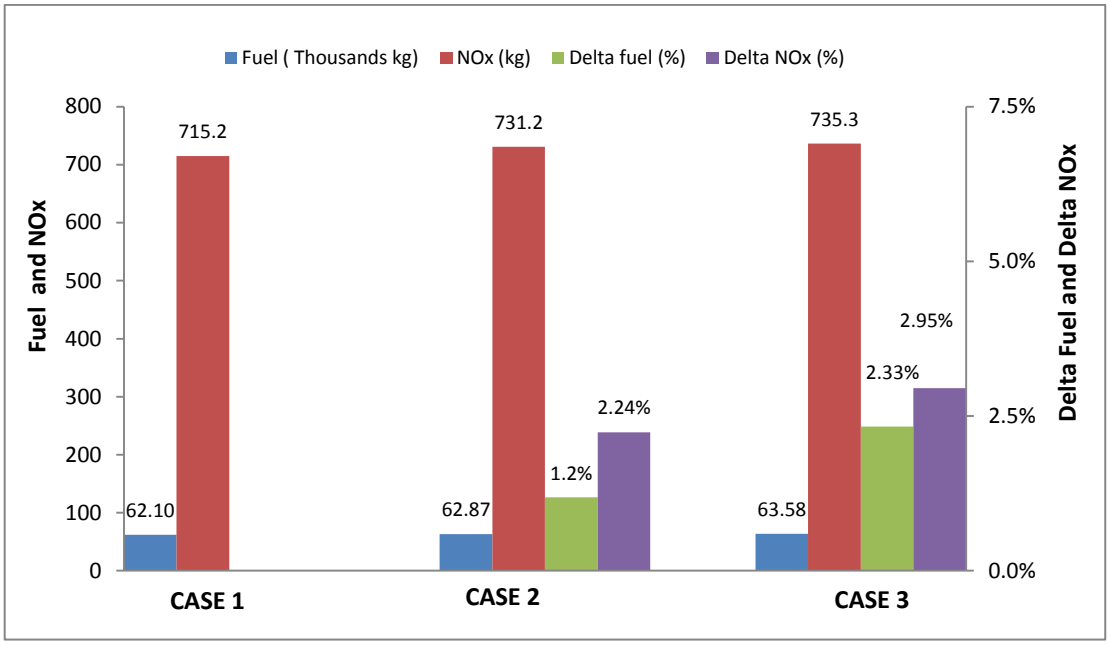

Figure 5-33 Fuel and NOx penalty for fuel optimised trajectory

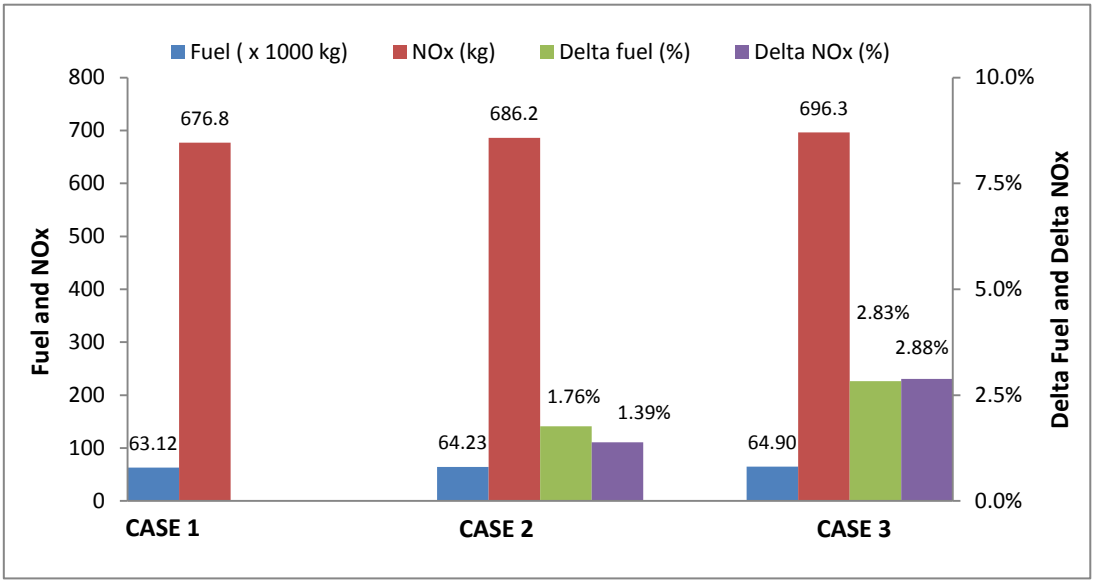

Figure 5-34 Fuel and NOx penalty for NOx optimised trajectory

Trajectories were optimised for the minimum fuel burn and minimum NOx objectives. Pareto fronts obtained from the long range aircraft with clean and two degraded engines are presented in Figure 5-21, 5-25 and 5-29. Diversity of the results on the Pareto fronts appears to be acceptable. The two extreme points A and B represent the min fuel burn and min NOx emission

(i.e. optimum) trajectories respectively. The remaining points are other intermediate trade off solutions. The complete profiles of the minimum fuel burn and minimum NOx trajectories with their TAS of three cases are shown in Figure 5-22, 5-26 and 5-30.

As in the previous case, there is an optimum cruise altitude for minimum fuel burn. Therefore, optimal altitude is found where fuel consumption is minimised by flying at the most efficient speed and engine thrust setting. As fuel is burned and aircraft become lighter, then amount of lift needed is less and consequently drag is reduced. As a result, required thrust is also become less. However, in order to reduce the fuel burn, if throttle is reduced, then the engine is no longer operating at the most efficient thrust setting. Therefore, the optimal procedure is to maintain the most efficient speed and power setting and use the excess thrust to gradually climb the aircraft continuously. The climb continued throughout the cruise (cruise climb) and ends at TOD when the optimum descent path is intercepted. But, as explained in practice change in optimum cruise altitude is achieved by changing the cruise altitude in steps (step cruise), because it is easier to manage with the air traffic controls. Aircraft with degraded engines are heavier and therefore will tend to reach the optimum altitude early in the flight (lower altitude than the clean engine) and continues along the cruise climb which maintains an optimum altitude as the aircraft weight reduces. Therefore aircraft tends to follow the same continuous climb approach as clean engine case until meet the TOD, where the aircraft weight is almost similar to clean engine. Therefore the altitudes tend to converge.

For the minimum NOx, the aircraft must reduce the combustion temperatures (TET) and fuel burn. To reduce the fuel burn aircraft will approach the minimum fuel trajectory. Also above the tropopause the ambient air temperature remains constant and therefore does not affect the NOx emissions. However, to reduce the combustion temperatures the aircraft must fly at a lower altitude than the minimum fuel altitude, so as to reduce the TET for a given thrust due to an increase in air density. Of course an increase in air density will also increase drag and hence the thrust requirement and therefore this strategy is limited. When the engine degrades, it starts reducing the thrust comparing to the clean engine. The thrust drop is compensated by the increasing the TET, which intern increase the formation of NOx. However, optimiser suggests aircraft to lower the flying altitude to keep the NOx emissions in optimum level.

The variation of the net thrust, and SFC, for the minimum fuel burn and minimum NOx trajectories are given in Figure 5-23, 5-27 and 5-31. The variations of TET and EGT of all three cases are also presented in Figure 5-24, 5-28 and 5-32. Summary of the minimum fuel burn and minimum NOx emissions for clean and two degraded engines are presented in Table 5-7 and Figures 5-33 and 5-34. When analysing the optimum trajectories it can be seen, both fuel

optimised and NOx optimised trajectories demonstrated a significant trade-off between fuel burn and NOx emissions. The fuel optimised trajectory of the clean engine (CASE_1) has achieved a minimum fuel burn of 62137kg with NOx emissions of 715kg. NOx optimised trajectory has achieved a minimum NOx emissions of 676.8kg with a fuel burn of 63120kg. Therefore NOx optimised trajectory has achieved 5.3% of reduction in NOx emissions compared to fuel optimised trajectory, but with a compromise of 1.6% fuel burn.

The optimum trajectories with low degraded engines (CULE_1DL) show a similar trade-off between fuel burn and NOx, but with an increased fuel burn and NOx emissions. The fuel optimised trajectory has achieved a minimum fuel burn of 62875kg with NOx emissions of 731.2kg. Comparing to the CASE_1, fuel burn and NOx has increased by 738kg and 16.2kg i.e. 1.2% and 1.39% respectively. NOx optimised trajectory has achieved a NOx emissions of 686.2kg with a fuel burn of 64233kg. But comparing to the CASE_1, minimum NOx and minimum fuel has increased by 9.4kg and 1113kg, i.e. 1.76% and 1.4% respectively. Therefore looking at the both optimum trajectories, NOx optimised trajectory has achieved 6.1% of reduction in NOx compared to fuel optimised trajectory, but with 2.2% compromise of fuel burn.

Optimum trajectories with highly degraded engines (CULE_2DL) also show a similar trade-off between fuel burn and NOx. The fuel optimised trajectory has achieved a minimum fuel burn of 63598kg with a NOx emission of 735.3kg. But comparing to the CASE_1, minimum fuel burn and minimum NOx has increased by 1458kg and 20.3kg i.e. 2.34% and 2.8% respectively. Also comparing to the CASE_2, fuel burn and NOx have increased by 720kg and 4.1kg, i.e. 1.14% and 0.56% respectively. Whereas, NOx optimised trajectory has achieved a minimum NOx of 696.3kg with a fuel burn of 64905kg. But comparing to the CASE_1, minimum flight time and minimum fuel has increased by 19.5kg and 1785kg, i.e. 2.9% and 2.8% respectively. Also comparing to the CASE_2, minimum NOx and minimum fuel burn have increased by 10.1kg and 672kg, i.e. 1.5% and 1% respectively. Therefore looking at the both optimum trajectories, NOx optimised trajectory has achieved 5.3% of reduction in NOx emissions compared to fuel optimised trajectory, but with 2.1% compromise of fuel burn.

The Table 5-7, Figure 5-33 and Figure 5-34 summarise the results of minimum fuel burn and minimum NOx optimised trajectories generated by the long range aircraft with clean engine (CASE_1) and aircraft with two levels of degraded engines (CASE_2 and CASE_3).

5.5.2.4 Impact of flying clean/degraded optimised trajectories with clean/degraded engines on NOx emissions

Table 5-8 NOx emissions of optimum aircraft trajectories with clean/degraded engines

Long range aircraft with clean and low degraded engines	
Clean engines flying on trajectories optimised for clean engines (CE+COT)	676.8 kg
Deg. engines flying on trajectories optimised for clean engines (DE+COT)	691.4 kg
Delta NOx of (DE+COT) Reference to (CE+COT)	+14.6 kg (2.2%)
Deg. engines flying on trajectories optimised for deg. engines (DE+DOT)	686.2 kg
Delta NOx of (DE+DOT) Reference to (DE+COT)	-5.3 kg (-0.7%)
Long range aircraft with clean and highly degraded engines	
Clean engines flying on trajectories optimised for clean engines (CE+COT)	676.8 kg
Deg. engines flying on trajectories optimised for clean engines (DE+COT)	704.7 kg
Delta NOx of (DE+COT) Reference to (CE+COT)	+27.9 kg (4.1%)
Deg. engines flying on trajectories optimised for deg. engines (DE+DOT)	696.3 kg
Delta NOx of (DE+DOT) Reference to (DE+COT)	-8.4 kg (-1.2%)

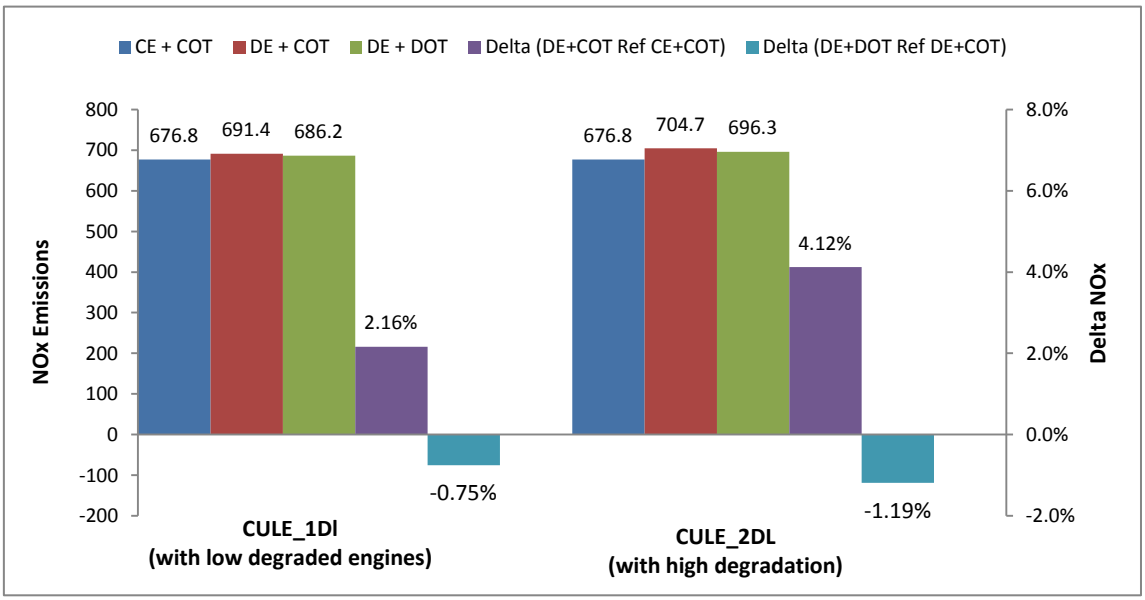

Figure 5-35 NOx emissions of optimum aircraft trajectories with clean/degraded engines

Optimum trajectories demonstrate a significant trade-off between minimum fuel burn and minimum NOx emissions for all three cases. Therefore it is important to investigate the impact on fuel burn and NOx emissions, when the aircraft with degraded engines are flying on the trajectory which has been optimised for clean engines. Table 5-8 and Figure 5-35 shows the NOx emissions for optimum trajectories of the aircraft with clean and degraded engines, also the NOx emissions of the aircraft with two levels of degraded engines are flying on the trajectory optimised for clean engines.

NOx optimised trajectory has achieved minimum NOx emissions of 676.8kg with clean engines. But when the aircraft is flying on the same trajectory with the degraded engines of 5% and 10% EGT increase, NOx emissions has increased by 2.2% (i.e.+14.6kg) and 4.1% (i.e. 27.9kg) comparing to the clean engine optimised trajectory (CE+COT). However, it is interesting to notice that fuel burn can be reduced by 0.7% (i.e. 5.3kg) and 1.2% (i.e. 8.4kg) with the low and high degraded engines respectively, when the aircraft trajectories are specifically optimised for degraded engines.

5.5.3 Aircraft trajectory optimisation for fuel burn and contrails

Contrails appear along the aircraft's trajectory at high altitude where the ambient temperature is very low. Contrails persist in the regions of atmosphere where the relative humidity with respect to ice is greater than 100%. Therefore it is tempting to avoid or re-route the aircraft to prevent forming persistent contrails. This may result in longer flight time, more fuel burn and increase other emissions. Therefore, optimising the trajectory for fuel burn and persistent contrails can develop alternative flight paths to enable trade-off between persistent contrails mitigation and fuel consumption for airlines to take operational decisions. Also it is important to investigate the impact of degraded engine performance on these optimum trajectories, as all engines in operation are degraded. Therefore this part of the study is focus to optimise the trajectories for minimum contrails and minimum fuel burn with clean and two levels of degraded engines. Thereby calculate the difference in fuel burn for zero contrails when the aircraft with degraded engines are flying on a trajectory optimised for clean engines and trajectories specifically optimised for degraded engines.

Optimisation set up

Minimum fuel and minimum Contrails have been selected as the objective functions. The optimiser was set up for 250 generations. The population was selected as 100 and initialisation ratio of 50. The number of evaluation was about 30,000.

Flight Phase	Objective 1	Objective 2	Generations	Population	In. Factor
Complete mission	Mission Fuel	Contrails	250	100	50

5.5.3.1 CASE_1: Optimum aircraft trajectories generated from the aircraft with clean engines (engines with 0% EGT increase)

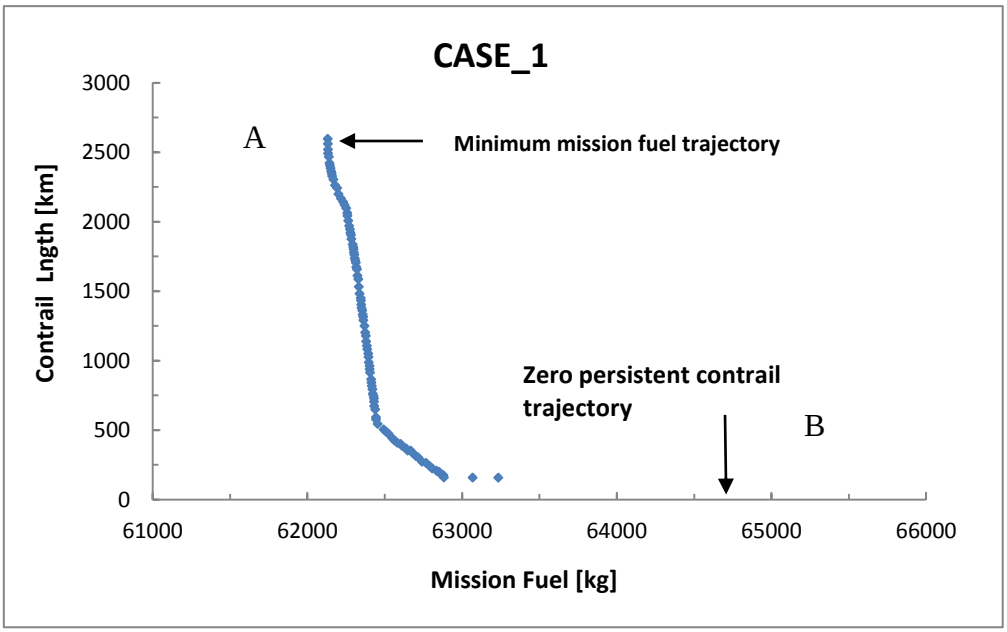

Figure 5-36 Pareto front for minimum fuel and minimum contrails

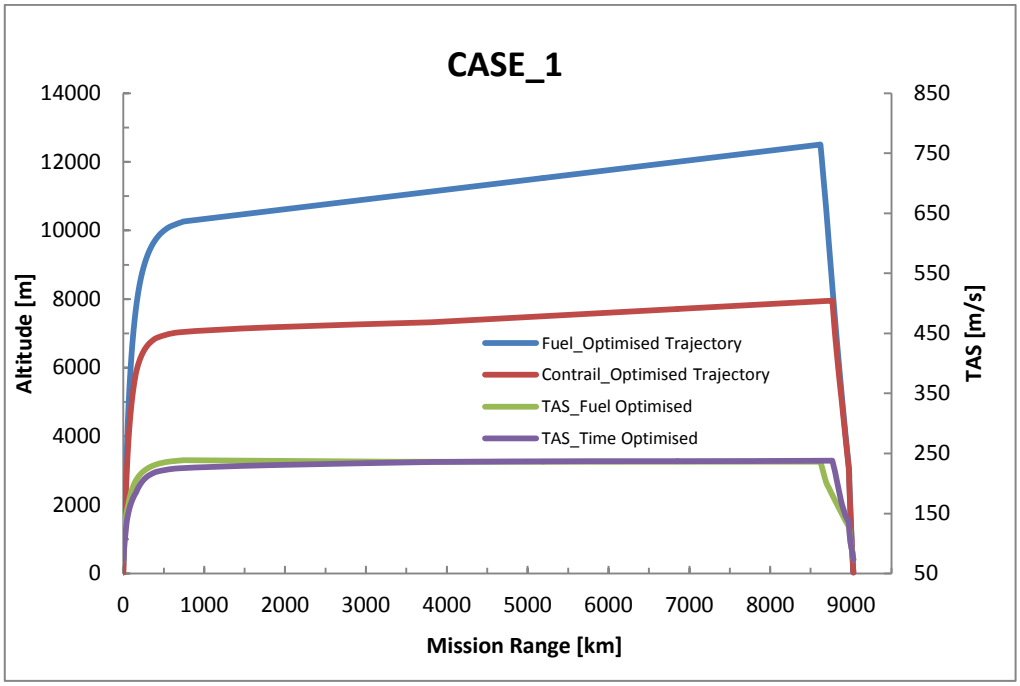

Figure 5-37 Minimum fuel and minimum contrail trajectories with TAS

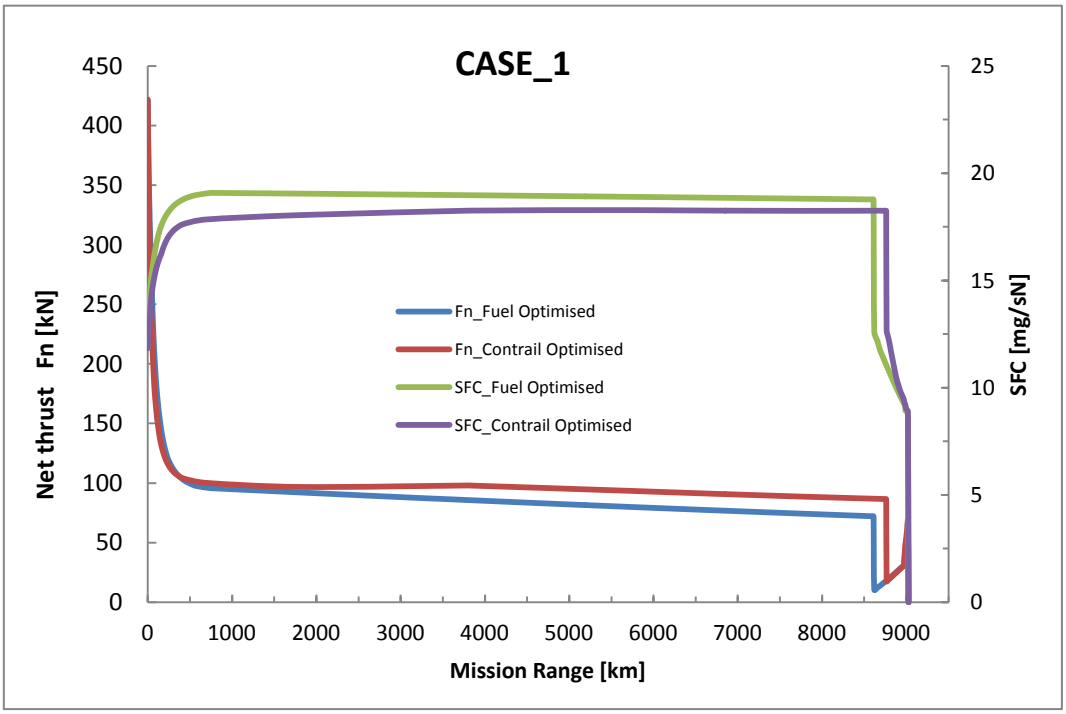

Figure 5-38 Net thrust and SFC variation for minimum fuel and minimum contrails

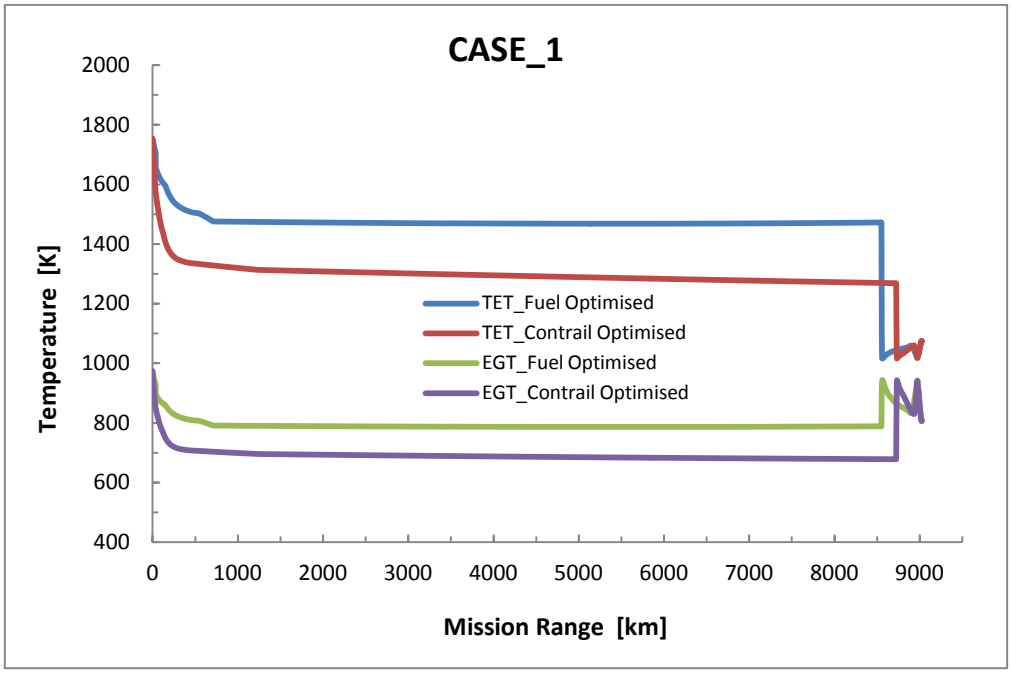

Figure 5-39 TET and EGT variation for minimum fuel and minimum contrails

5.5.3.2 CASE_2: Optimum aircraft trajectories generated from the aircraft with low degraded engines (engines with 5% EGT increase)

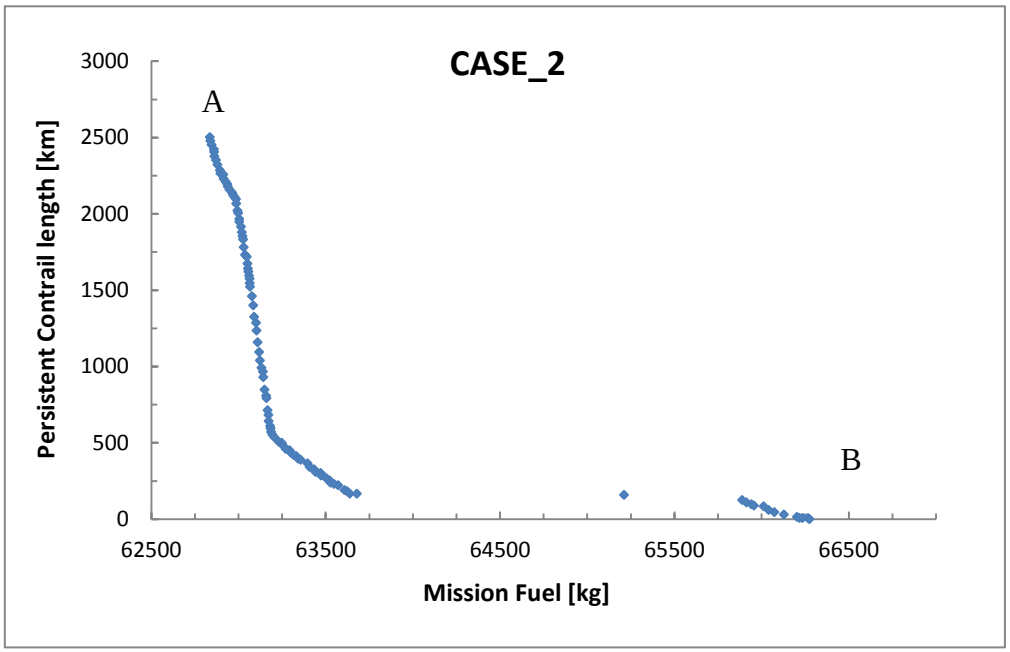

Figure 5-40 Pareto front for minimum fuel and minimum contrails

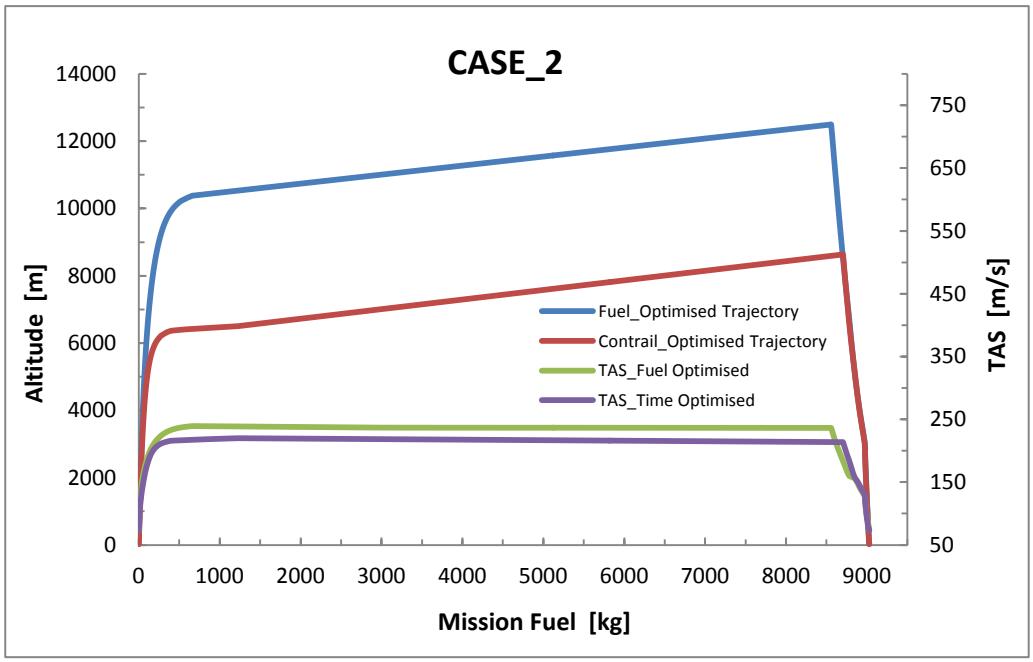

Figure 5-41 Minimum fuel and minimum contrail trajectories with TAS

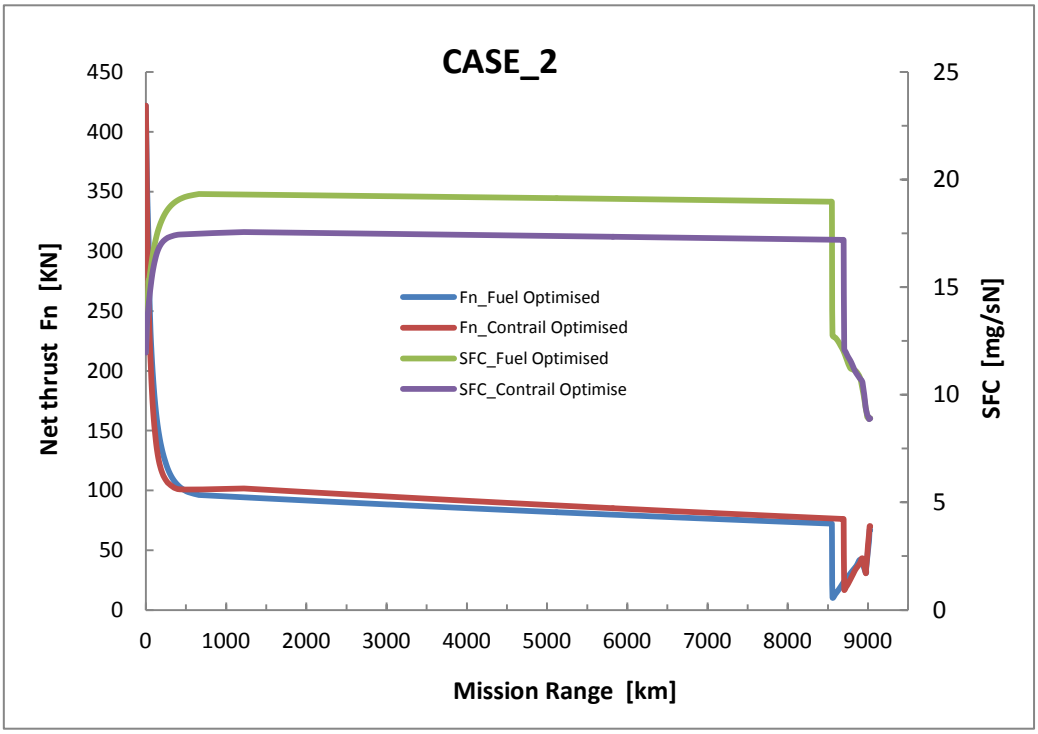

Figure 5-42 Net thrust and SFC variation for minimum fuel and minimum contrails

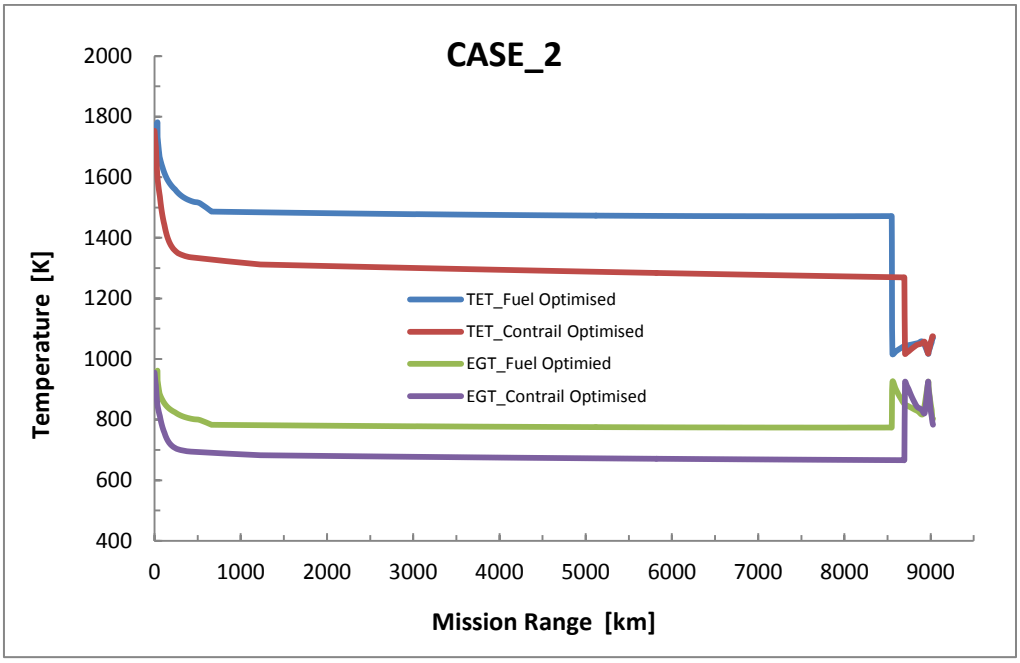

Figure 5-43 TET and EGT variation for minimum fuel and minimum contrails

5.5.3.3 CASE_3: Optimum aircraft trajectories generated from the aircraft with highly degraded engines (engines with 10% EGT increase)

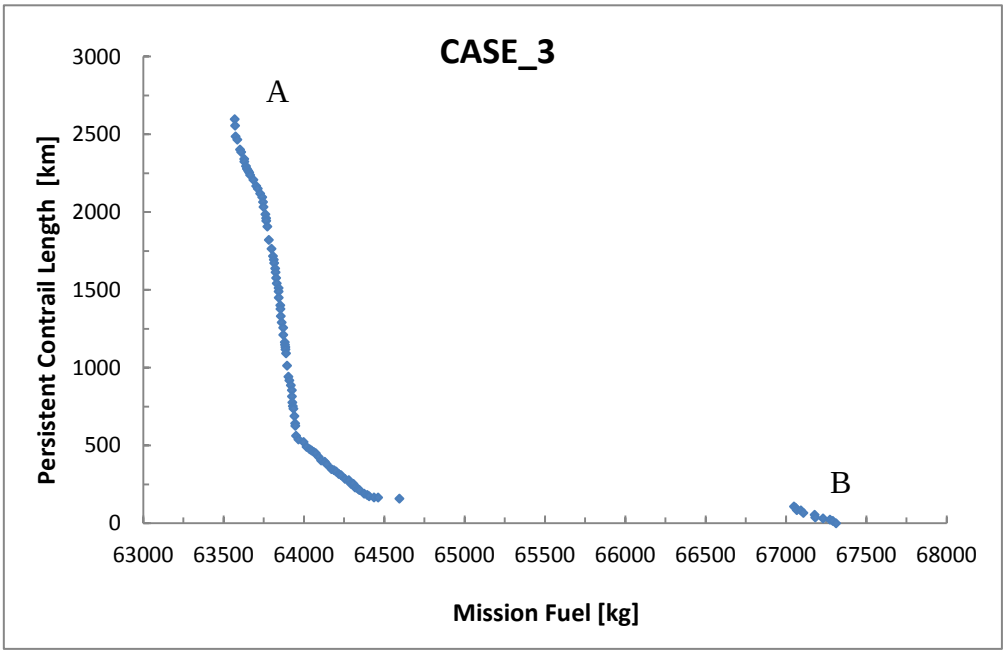

Figure 5-44 Pareto front for minimum fuel and minimum contrails

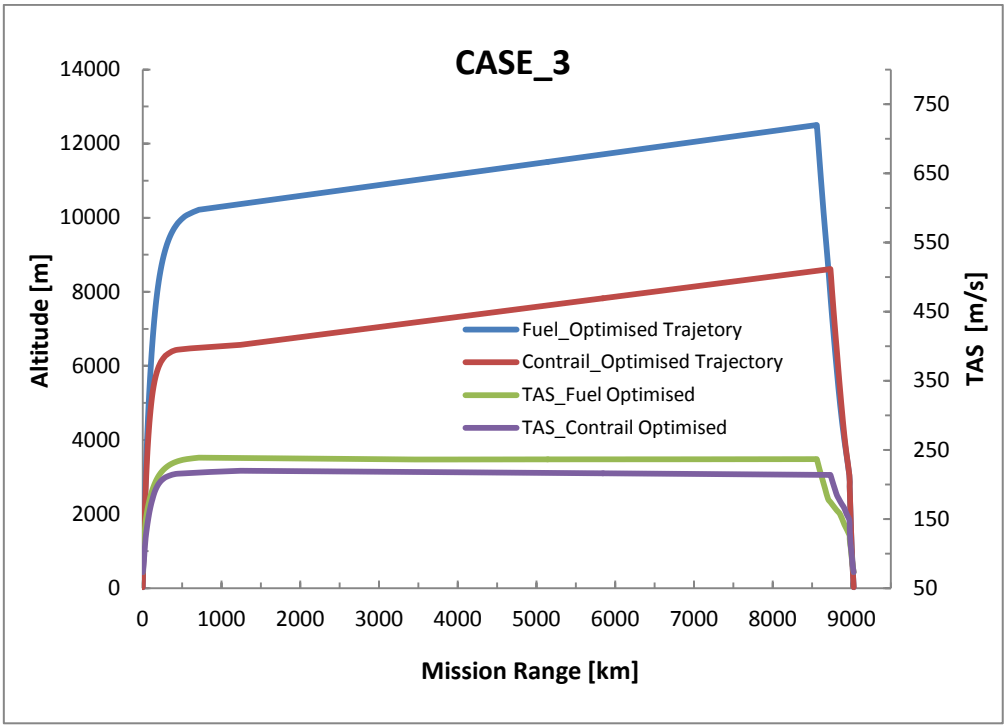

Figure 5-45 Minimum fuel and minimum contrail trajectories with TAS

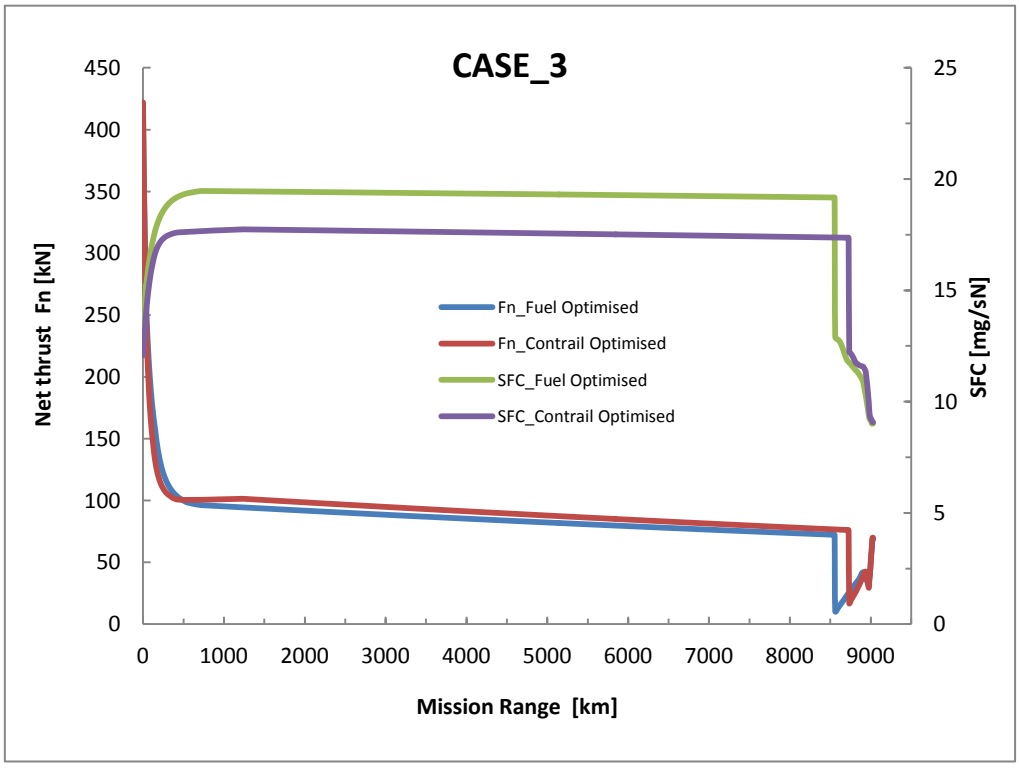

Figure 5-46 Net thrust and SFC variation for minimum fuel and minimum contrails

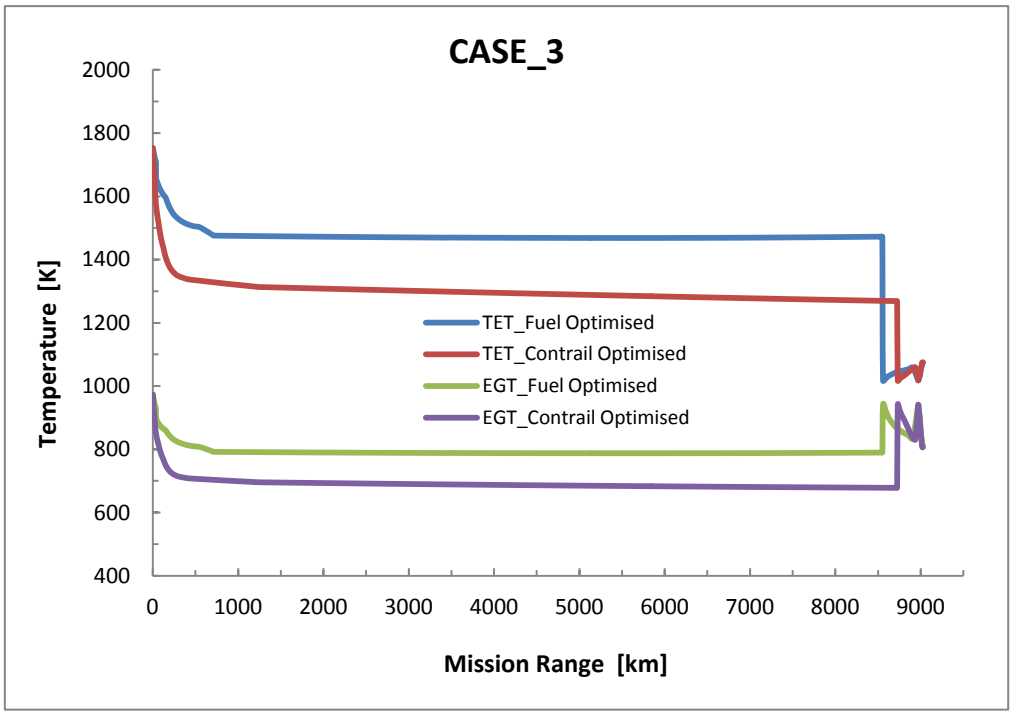

Figure 5-47 TET and EGT variation for minimum fuel and minimum contrails

Table 5-9 Summary of optimisation results

	Fuel Optimised				Contrail Optimised			
Case	**Fuel [Kg]**	**Contrails [km]**	**Delta Fuel [%]**	**Delta Contrails [%]**	**Fuel [kg]**	**Contrails [km]**	**Delta Fuel [%]**	**Delta Contrails [%]**
Case 1	62138.0	2495.3	0.0	0.0	64848	0.0	0.0	0.0
Case 2	62875.0	2508.5	1.20	0.52	66274	0.0	2.2	0.0
Case 3	63585.0	2526.2	2.40	1.23	67392	0.0	3.8	0.0

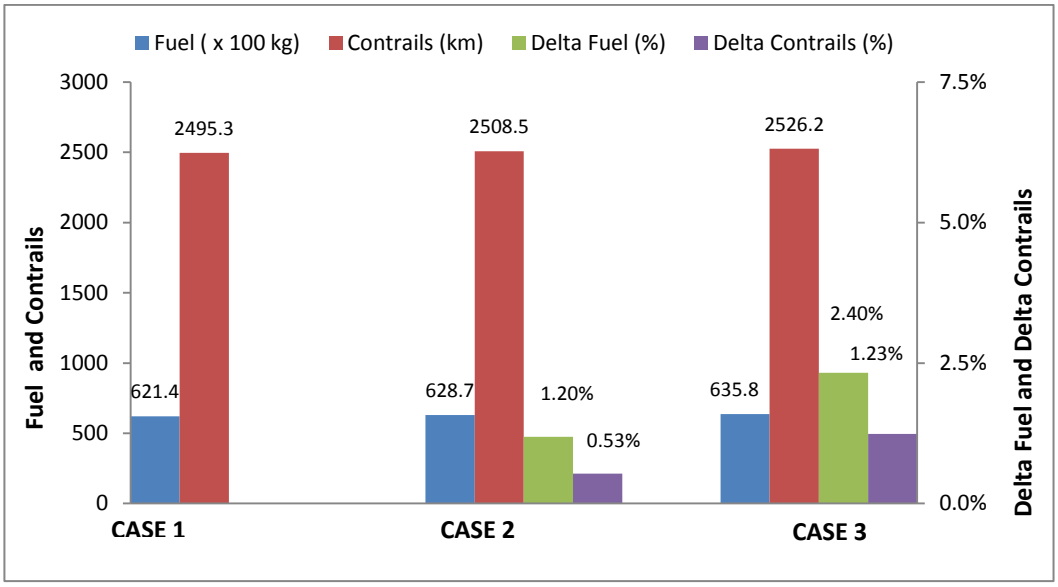

Figure 5-48 Fuel and contrail penalty for fuel optimised trajectory

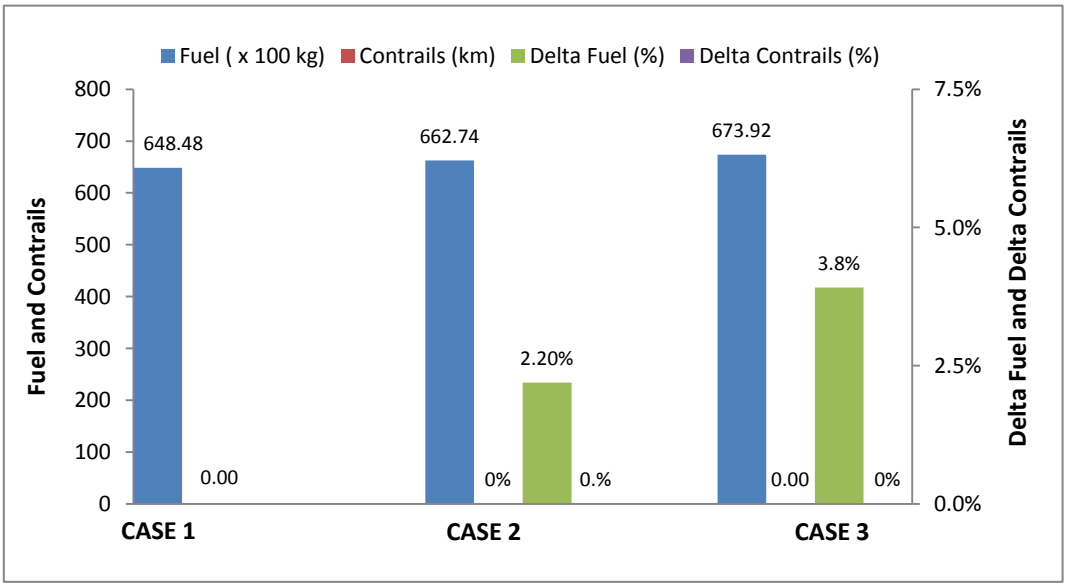

Figure 5-49 Fuel penalty for contrail optimised trajectory

The Pareto fronts generated for the minimum fuel burn and minimum contrails by the long range aircraft with the clean and two degraded engines are presented in Figures 5-36, 5-40 and 5-44. The respective trajectories of the minimum fuel burn and minimum contrails with the variation of true aircraft speed (TAS) are given in Figure 5-37, 5-41

and 5-45. The variation of the net thrust, SFC, for the minimum fuel burn and minimum contrail trajectories are given in Figure 5-38, 5-42 and 5-46. The variations of TET and EGT of all three cases are also presented in Figure 5-39, 5-43 and 5-47.

The Table 5-9 and the Figure 5-48 and 5-49 indicate the summary of the minimum fuel burn and contrail optimisation results. The solutions found in all three cases for the minimum fuel burn trajectories are similar to the other optimised trajectories generated for the minimum fuel burn. The fuel burn optimised trajectory has achieved minimum fuel burn of 62138kg with the expense of 2495.3 km of persistent contrails. However, the trajectories generated with the degraded engines, CASE_2 and CASE_3 have optimised the fuel burn with an increase of 1.2% and 2.4% at the expense of 0.52% and 1.23 % increase in contrail formation. The lengths of the respective contrails formed by the degraded engines are 2508.5 km and 2526.2 km.

With regards to the contrail optimised trajectories, contrail emissions can be reduced by increasing cruise altitude. At higher altitudes the atmospheric humidity typically declines. Contrails tend to persist at relative humidity levels above approximately 70% which are less likely at higher altitudes. However, for this case persistent contrails could not be eliminated completely by an increase in cruise altitude alone.

To eliminate contrails completely a low cruise altitude has to be adopted (6000m to 8000m). At these levels the atmospheric temperature is too warm for contrails to persist. However, impacts on fuel burn in severe. To avoid contrails completely, aircraft with clean engine has to increase the fuel burn by 4.4% and whereas aircraft with degraded engines have to increase the fuel burn by 5.4% and 5.9% with respect to their fuel optimised trajectories. It is also important notice that degraded engines will consume more fuel in all cases. More efficient engines tend to have higher contrail emissions due to lower exhaust temperatures (EGTs). However, the effect is secondary and no impact has been observed from these results.

5.5.3.4 Impact of flying clean/degraded optimised trajectories with clean/degraded engines on fuel burn to avoid contrails

Table 5-10 Fuel burn for zero contrail aircraft trajectories with clean/degraded engines

Long range aircraft with clean and low degraded engines	
Clean engines flying on trajectories optimised for clean engines (CE+COT)	64848 kg
Deg. engines flying on trajectories optimised for clean engines (DE+COT)	66507 kg
Delta Fuel Burn of (DE+COT) Reference to (CE+COT)	+1659 kg (2.5%)
Deg. engines flying on trajectories optimised for deg. engines (DE+DOT)	66274 kg
Delta Fuel Burn of (DE+DOT) Reference to (DE+COT)	-233 kg (-0.3%)
Long range aircraft with clean and highly degraded engines	
Clean engines flying on trajectories optimised for clean engines (CE+COT)	64848 kg
Deg. engines flying on trajectories optimised for clean engines (DE+COT)	67935 kg
Delta Fuel Burn of (DE+COT) Reference to (CE+COT)	+3087 kg (4.7%)
Deg. engines flying on trajectories optimised for deg. engines (DE+DOT)	67392 kg
Delta Fuel Burn of (DE+DOT) Reference to (DE+COT)	-543 kg (-0.8%)

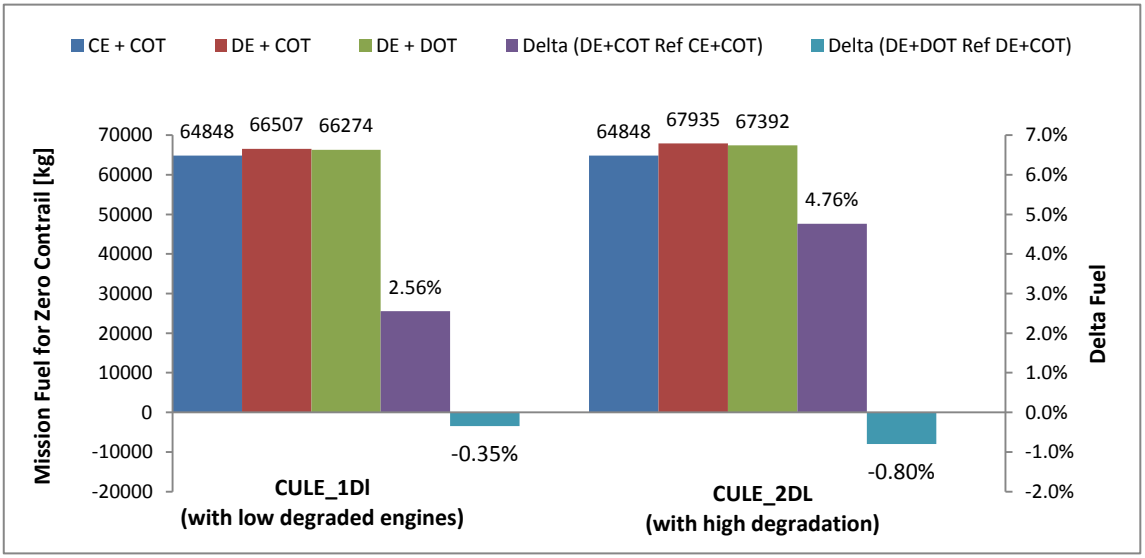

Figure 5-50 Fuel burn for zero contrail trajectories with clean/degraded engines

Optimum trajectories demonstrate a significant trade-off between minimum fuel burn and minimum (zero) Contrails for all three cases. Therefore it is important to investigate the impact on fuel burn and contrail formation, when the aircraft with degraded engines are flying on the trajectory which has been optimised for clean engines. Table 5-10 and Figure 5-50 shows the fuel burn of optimum trajectories of the aircraft with clean and degraded engines, also the fuel burn of the aircraft with two levels of degraded engines are flying on the trajectory optimised for clean engines.

Contrail optimised trajectory has achieved zero contrails with a fuel burn of 64848kg for aircraft with clean engines. But when the aircraft is flying on the same trajectory with degraded engines of 5% and 10% EGT increase, in order to avoid contrails (for zero contrails) fuel burn has increased by 2.5% (i.e. 1659kg) and 4.7% (i.e. 3087kg) comparing to the clean engine optimised trajectory (CE+COT). However, it is important to notice that fuel burn for zero contrails can be reduced by 0.3% (i.e. 233kg) and 0.8% (i.e. 543kg) with the low and high degraded engines respectively, when the aircraft trajectories are specifically optimised for degraded engines.

5.6 Summary

The aim of this chapter was to investigate the impact of engine degradation on long range aircraft trajectories. For the purpose of this study, multi-disciplinary optimisation framework developed in Chapter 4 was employed to optimise the trajectories between London to Colombo with clean and two levels of degraded engines. Fuel burn, flight time, NOx and contrails have selected as conflicting objectives. Three different optimisation studies were performed and impact of engine degradation on optimum trajectories were investigated. Finally, trajectories were compared to quantify the difference in fuel burn, NOx emissions and contrails produced, when the aircraft with degraded engines are flying on the trajectory optimised for clean engines and flying on the trajectories specifically optimised for degraded engines. The reduction in fuel burn, NOx and contrails were presented.

6 Aircraft Trajectory Optimisation with Degraded Engines – Short Range

6.1 Introduction

Aircraft flight profile or trajectory can be represented by the ratio of the "aircraft flight time to flight cycles", terms hours-to-cycle ratio which is often used to describe an aircraft operational profile. Short range aircraft flight profiles are completely different to long range flights as they have low hour-to-cycle ratios. Therefore it is important to investigate the impact of engine degradation on short range flight trajectories and quantify the impact on the environment in terms of fuel burn, NOx emissions and contrail formation. The aim of this Chapter is to evaluate and quantify the effect of degraded engine performance on the overall flight mission and hence quantify the impact on the environment with regards the following objectives; fuel burn, NOx emissions and contrail formation. Then study further aims at identify the potential for implementing the optimised trajectories with respect to those objectives. A typical two spool high bypass ratio turbo fan engines (one clean and two degraded engines) and a typical narrow body short range aircraft A320-200 have modelled as a basis for the study. An emission prediction model was developed to assess the NOx formation during the complete mission. The contrail prediction model was adopted from previous studies. In addition, a multidisciplinary aircraft trajectory optimisation framework was developed and employed to analyse short range flight trajectories between London to Amsterdam under three cases. Case_1: Aircraft with Clean Engines, Case_2 and Case_3 are Aircraft with low and highly degraded engines respectively. Three different optimisation studies were performed; (1) Fuel burn vs Flight time, (2) Fuel burn vs NOx emission, and (3) Fuel burn vs Contrails. Finally optimised trajectories generated with degraded engines were compared with the optimised trajectories generated with clean engines, as potential environmental trajectories for airline operations.

6.2 Problem definition

The problem is focused on the horizontal and vertical trajectory optimisation using the GATAC framework and associated models developed for the particular case of short range flight between London Heathrow (EGLL/LHR) and Amsterdam Schiphol (AMS) International Airport. The distance and the current time for this scheduled route is 450 km and take approximately 50min. The baseline aircraft is similar to Airbus A320-200 (120 passenger variant) narrow body single aisle aircraft with two engines. The engines are two spool high bypass turbofan engines similar to CFM56-5B4 engines. Three cases have been considered: Case_1: Aircraft flying with clean engines and Case_2 and Case_3 are considered aircraft with two levels of degraded engines (5% and 10% EGT increase). The complete mission from London Heathrow to Schiphol Amsterdam is defined to assess the trajectories optimised for minimum fuel burn, minimum time, minimum NOx and for contrail avoidance, hence ascertain and assessment of possible fuel penalties incorporated with the optimum trajectories generated from the clean and degraded engines. The Figure 6.1 shows a typical flight route of a flight from London to Amsterdam recorded by Flight Aware (2015).

Figure 6-1 London Heathrow (EGLL) – Schiphol (AMS) Flight Route (Flight Aware 2015)

Departure phase for the flight between London Heathrow (EGLL/LHR) and Amsterdam is assessed based on the Dover (DVR) Standard Instrumental Departure (SID). For easterly departures, the current departure procedure requires the aircraft to flight onto Detling (DET) VOR R284 immediately after take-off with altitude bound to 600ft before reaching DET VOR/DME station and maintain the flight level until DVR VOR/DME station, the last SID waypoint. Appendix A-3 shows the easterly departures for both northern runway, i.e. RWY09L (DVR 6K) and Southern runway i.e. RWY09R (DVR 6J) via Detling (DET) VOR/DME station and Dover (DVR) VOR/DME station as published in the UK AIP. A full SID chart of DET and DVR departure procedures can be seen in Appendix A-3

The aircraft arrival at Schiphol Amsterdam is under the standard requirements of Noise Abatement Procedures at any airport required within Europe. With this arrival phase is focuses on the conventional trajectory optimisation criteria of minimum fuel, minimum time and minimum NOx which is necessary to assess low level air pollutions. The optimisation also attempts to enquire a better approach profile employing continuous descent approach profile as much as possible. The common standard instrument approach procedure at RWY04 is used in this study. The STAR Chart for Schiphol Amsterdam can be seen in Appendix A-4

6.3 Mission Route

Figure 6-2 Short haul ground track

The mission route chosen for the study is take-off to landing from London Heathrow (LHR) airport to Amsterdam Schiphol (AMS) airport. The ground track of the mission route is shown in Figure (6-1). The mission was divided into three flight phases (departure, en-route and arrival). Departure phase begins at 83 ft above ground level (AGL) with an air speed of 140 kts and terminates at the end of the Standard Instrumental Departure (SID). The SID selected for the departure phase is BPK7G. The way points of the departure phase are given in Table (6-1)

Table 6-1 Departure Way Points and Constraints

WP	Latitude	Longitude	Altitude min/max [ft]	CAS min/max [kt]
WP1	51 27 53.25 N	000 28 54.99 W	83	140
WP2	51 27 52.51 N	000 31 35.75 W	83/10,000	140/310
WP3	51 31 08.00 N	000 40 38.00 W	83/10,000	140/310
WP4	51 35 07.13 N	000 36 29.69 W	83/10,000	140/310
WP5	51 37 23.00 N	000 31 07.00 W	83/10,000	140/310
BPK	51 44 59.00 N	000 06 24.00 W	10,000	310

v

The en-route phase starts after the aircraft has reached the London Heathrow (LHR) BPK/VOR waypoint and ends when the aircraft ends the Amsterdam Schiphol International airport STAR procedure. During this phase a minimum altitude of FL100 and a maximum of FL390 are used. These bounds give the optimiser the freedom of choosing an optimum flight level within both lower and upper airspaces. The air speed during the en-route is limited by the KCAS 310 for the lower boundary and by the maximum operation Mach number for the upper boundary. The route and waypoints selected for the en-route is shown in Table 6-2.

Table 6-2 En-route way points and constraints

WP	Latitude	Longitude	Altitude min/max (ft)	CAS min/max (kt)
BPK	51 44 59.00 N	000 06 24.00 W	10,000	310
WP6	51 46 30.00 N	000 11 48.00 E	10,000/39,000	310/350
WP7	51 46 45.00 N	000 15 00.00 E	10,000/39,000	310/350
WP8	51 48 40.00 N	000 39 06.00 E	10,000/39,000	310/350

WP9	51 49 19.00 N	000 47 39.00 E	10,000/39,000	310/350
WP10	51 50 55.00 N	001 08 51.00 E	10,000/39,000	310/350
WP11	51 54 19.00 N	001 25 33.00 E	10,000/39,000	310/350
WP12	52 06 52.51 N	002 29 16.61 E	10,000/39,000	310/350
WP13	52 26 52.00 N	003 25 15.00 E	10,000/39,000	310/350
SUGOL	52 31 31.00 N	003 58 02.00 E	10,000	310

The third part of the mission route, arrival phase starts when the aircraft passes over SUGOL and terminates at 100ft AGL. The STAR used in this phase for Amsterdam Schiphol airport is RNAV RWY06 and the entry altitude is set to FL100. The route and related procedures for the arrival phase are listed in Table 6-3.The aerodrome charts are attached in Appendix A-3 London-Heathrow SID charts.

Table 6-3 Arrival waypoints and constraints

WP	Latitude	Longitude	Altitude min/max (ft)	CAS min/max (kt)
SUGOL	52 31 31.00 N	003 58 02.00 E	10,000	310
WP14	52 25 20.00 N	004 23 16.00 E	100/10,000	150/310
WP15	52 14 14.00 N	004 21 51.00 E	100/10,000	150/310
WP16	52 12 33.00 N	004 27 45.00 E	100/10,000	150/310
WP17	52 12 28.00 N	004 31 35.00 E	100/10,000	150/310
WP18	52 13 14.00 N	004 33 27.00 E	100	150

6.4 Models and Framework

The trajectory optimisation framework was created based on the Generic Optimisation framework GATAC developed in Chapter 4. The framework consists of: (1) A short range aircraft performance model CUSA developed based on the Airbus short range narrow body single aisle aircraft A320-200 with twin engines, (2) Engine Performance Models (one clean engine CUSE_0DL with 0% increase of EGT and two degraded engines having low and high degradation levels CUSE_1DL with 5% EGT increase and 10% EGT increase respectively, (3) Emission Prediction Model (EEM) and (4) Contrail Prediction Model (CPM), and (5) GA based NSGAMO-II which have been already used

for the long range aircraft study. The detail description of individual models, optimiser and framework, including their interaction between optimiser can be found in Chapter 4. The model and optimiser testing and validation are also included in the same Chapter. The schematic of the specific optimisation framework is shown in Figure 6-3.

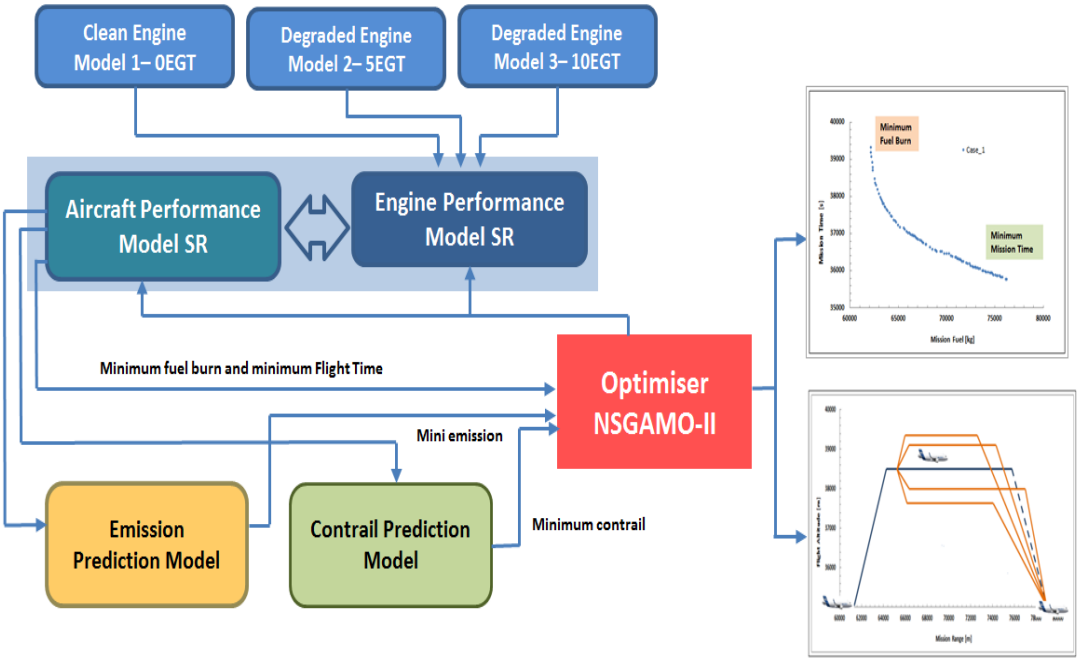

Figure 6-3 Short range aircraft trajectory optimisation framework

6.5 Optimisation studies and Trajectory Analysis

Trajectory optimisation is performed in order to assess the impact of engine degradation on optimum aircraft trajectories generated by a short range aircraft. Several objectives have been selected for the study. The traditional objectives include mission fuel burn and mission time, while the environmental objectives include NOx emissions and Contrails produced over the mission. The objectives have been carefully selected to understand, how the optimised trajectories generated by different levels of degraded engines differ in terms of operational parameters (speeds, altitudes, thrust settings, SFC and EGTs), compared to the optimum trajectories generated by the aircraft with clean engines (base line trajectories). Also to establish the gains that may be achieved in terms of optimised objectives. Three cases have been

considered for the analysis; CASE_1: short range aircraft with clean engines (with EGT increase of 0%), CASE_2: same aircraft with low degraded engines (with 5% EGT increase) and CASE_3: aircraft with highly degraded engines (EGT increase of 10%) as described in Figure 6-4.

CASE	Aircraft	Engine	Level of Degradation
CASE_1	CUSA	CUSE_0DL	0 % EGT Increase
CASE_2	CUSA	CUSE_1DL	5 % EGT Increase
CASE_3	CUSA	CUSE_2DL	10 % EGT Increase

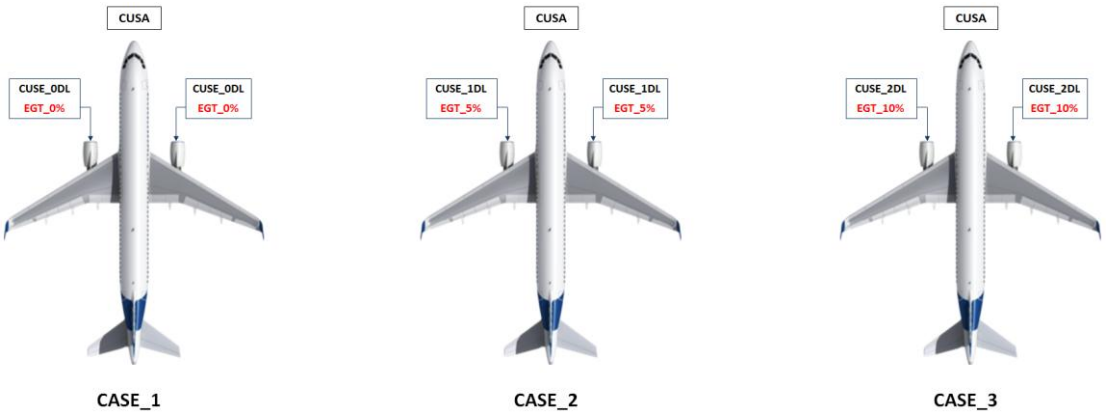

Figure 6-4 Cases considered for optimisation studies

6.5.1 Trajectory optimisation for fuel burn and flight time

Optimisation set up

Minimum fuel and minimum time have been selected as the objective functions. The optimiser was set up for 250 generations. The population was selected as 100 and an initialisation ratio of 50. The number of evaluation was about 30,000.

Flight Phase	Objective 1	Objective 2	Generations	Population	In. Factor
Complete mission	Mission Fuel	Mission Time	250	100	50

6.5.1.1 CASE_1: Optimum short range aircraft trajectories generated with clean engines (Engines with 0% EGT increase)

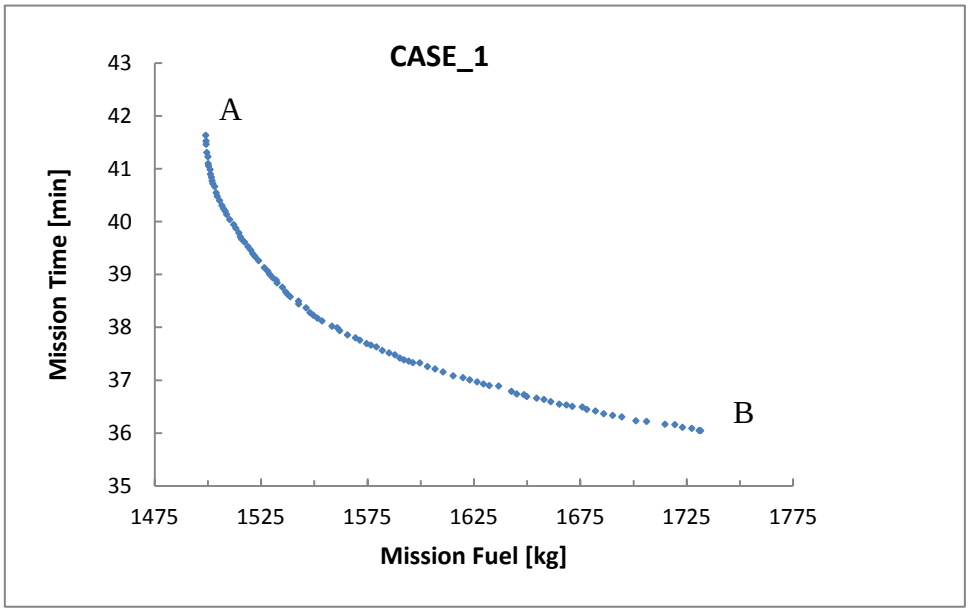

Figure 6-5 Pareto front of fuel burn and flight time objectives

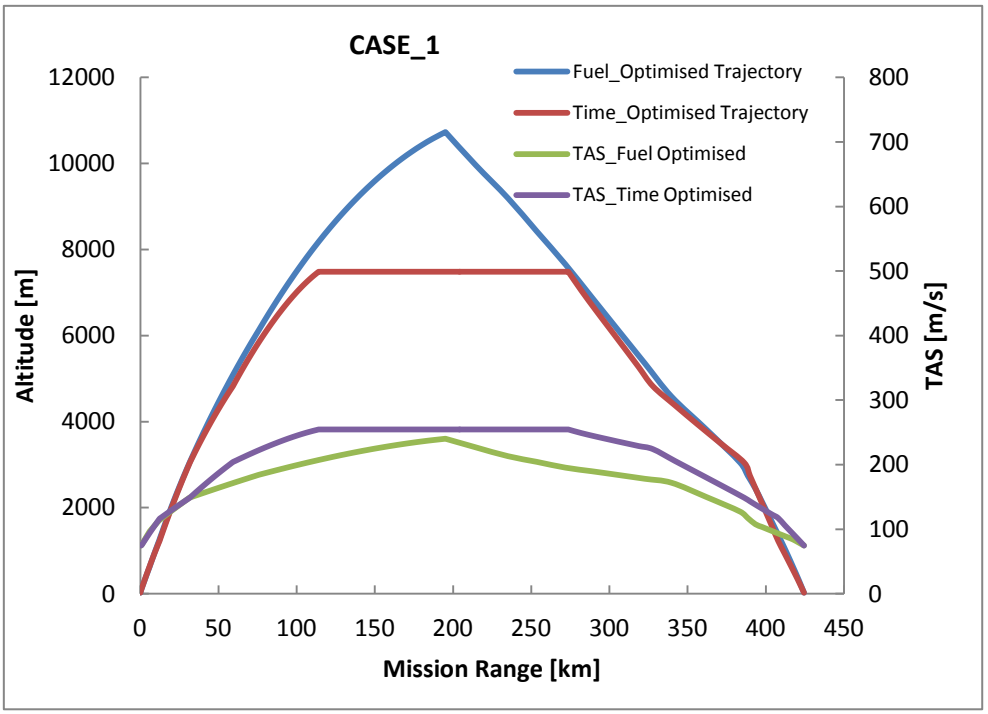

Figure 6-6 Minimum fuel and minimum time trajectories with TAS

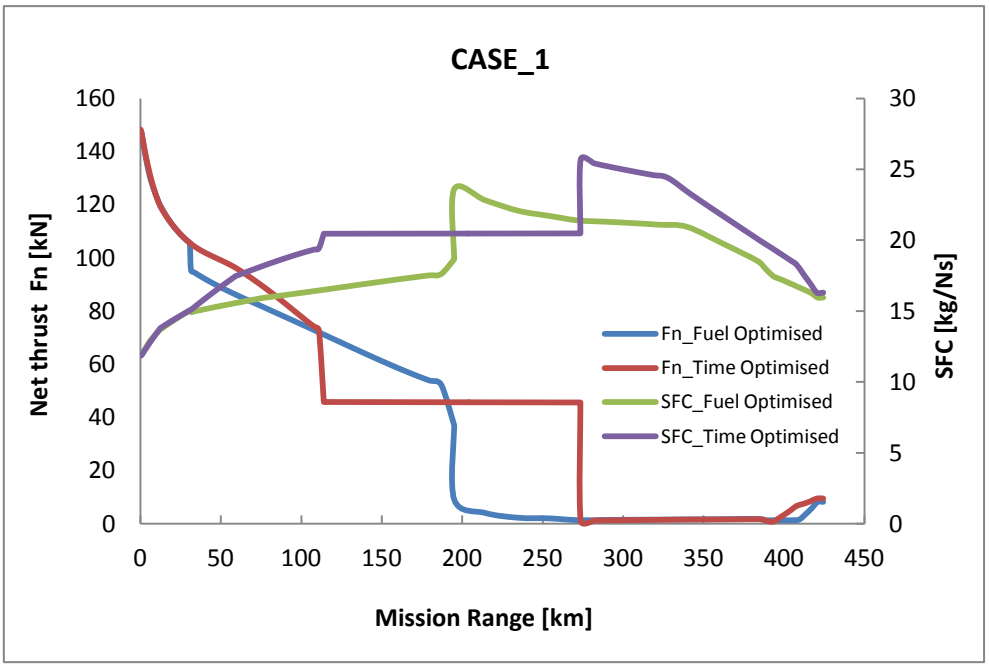

Figure 6-7 Net thrust and SFC variation of optimum trajectories

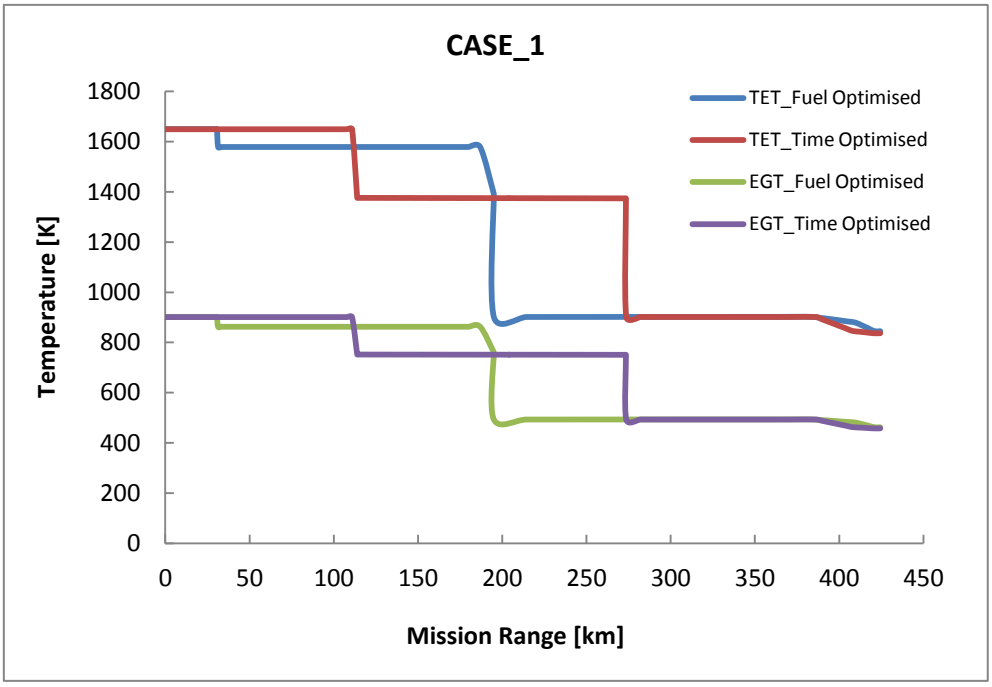

Figure 6-8 TET and EGT variation of optimum trajectories

6.5.1.2 CASE_2: Optimum short range aircraft trajectories generated with low degraded engines (Engines with 5% EGT increase)

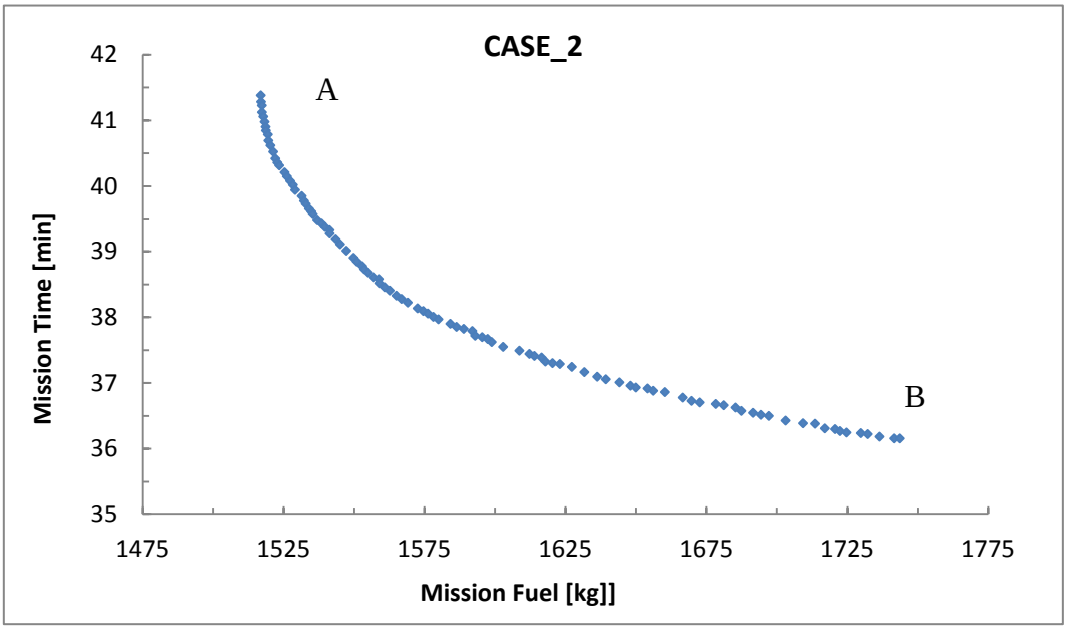

Figure 6-9 Pareto front of fuel burn and flight time objectives

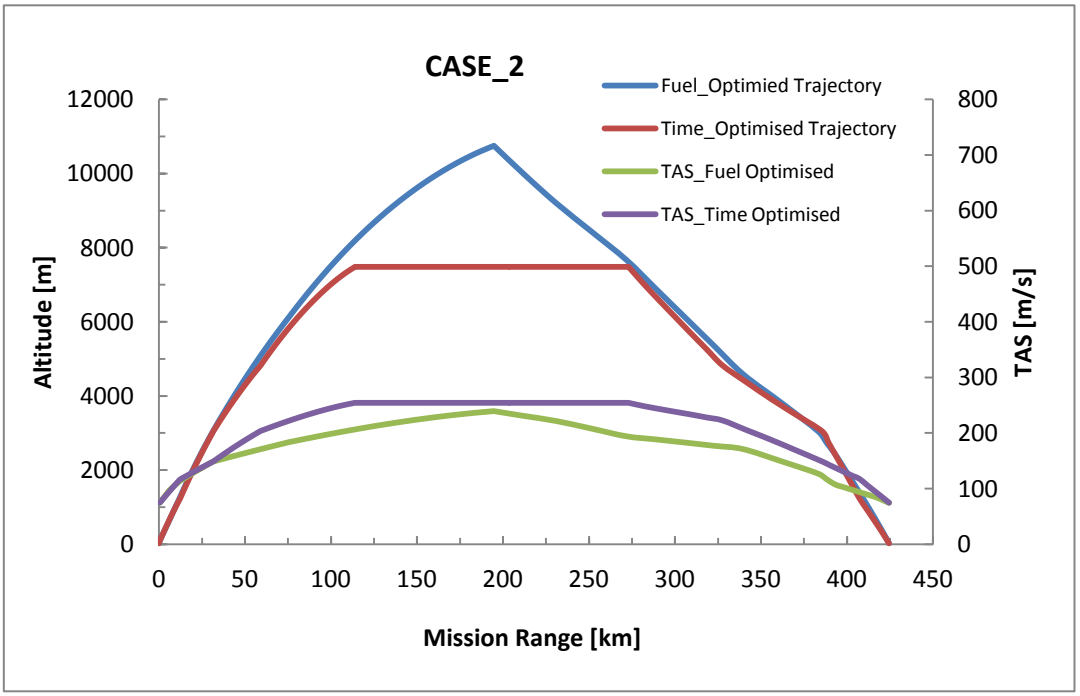

Figure 6-10 Optimum trajectories and TAS

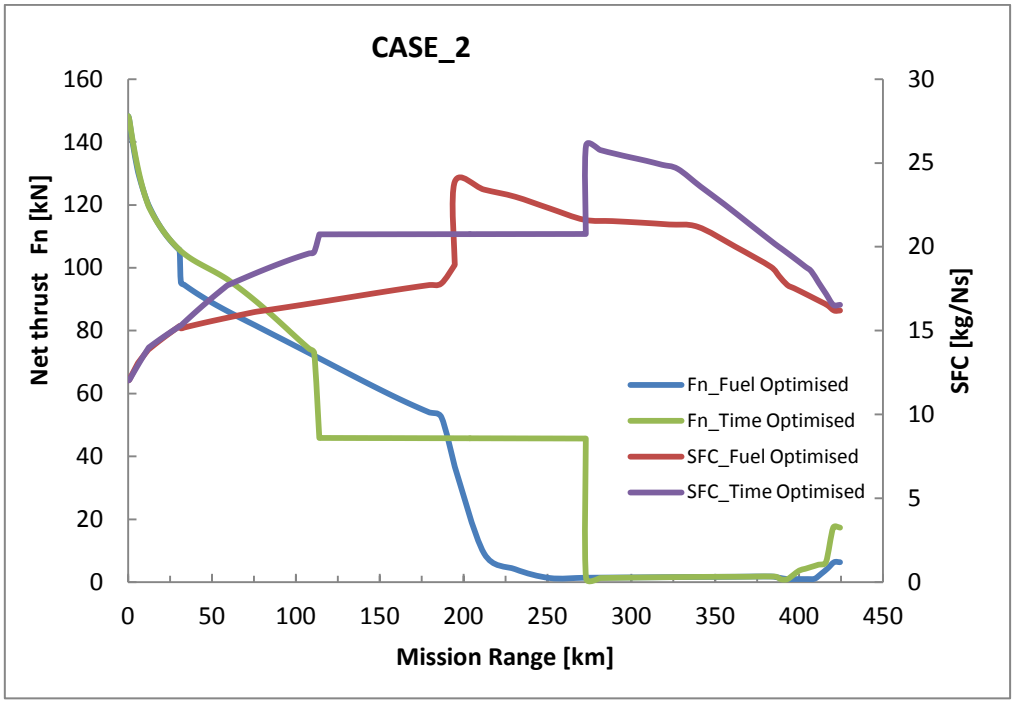

Figure 6-11 Net thrust and SFC variation of optimum trajectories

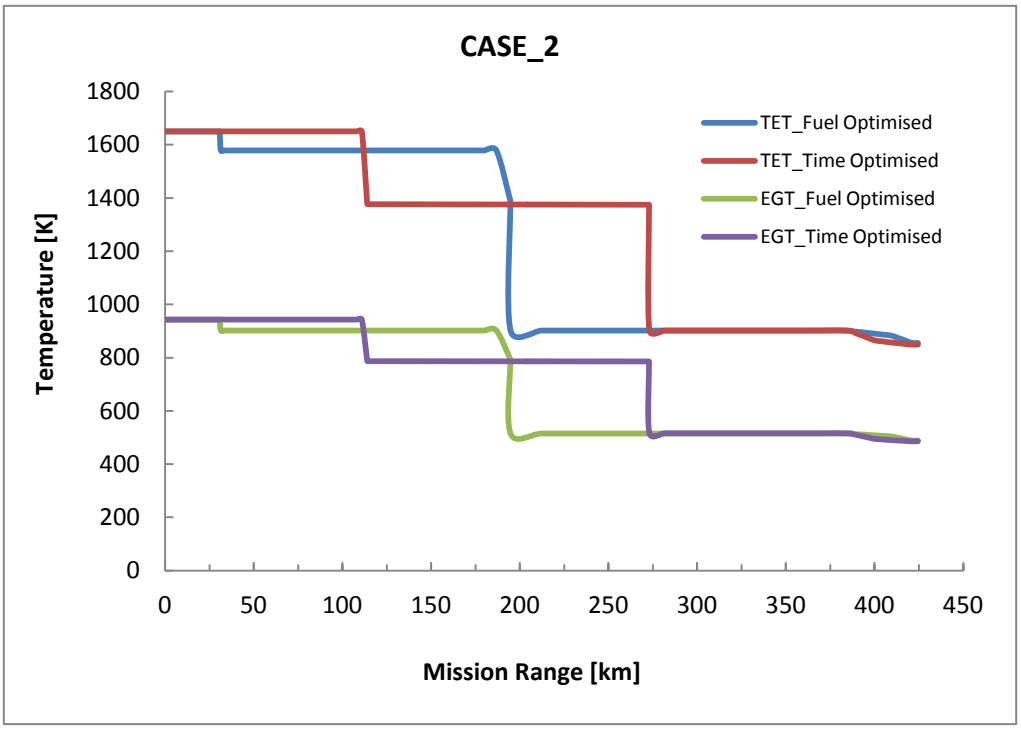

Figure 6-12 TET and EGT variation of Optimum trajectories

6.5.1.3 CASE_3: Optimum short range aircraft trajectories generated with highly degraded engines (Engines with 10% EGT increase)

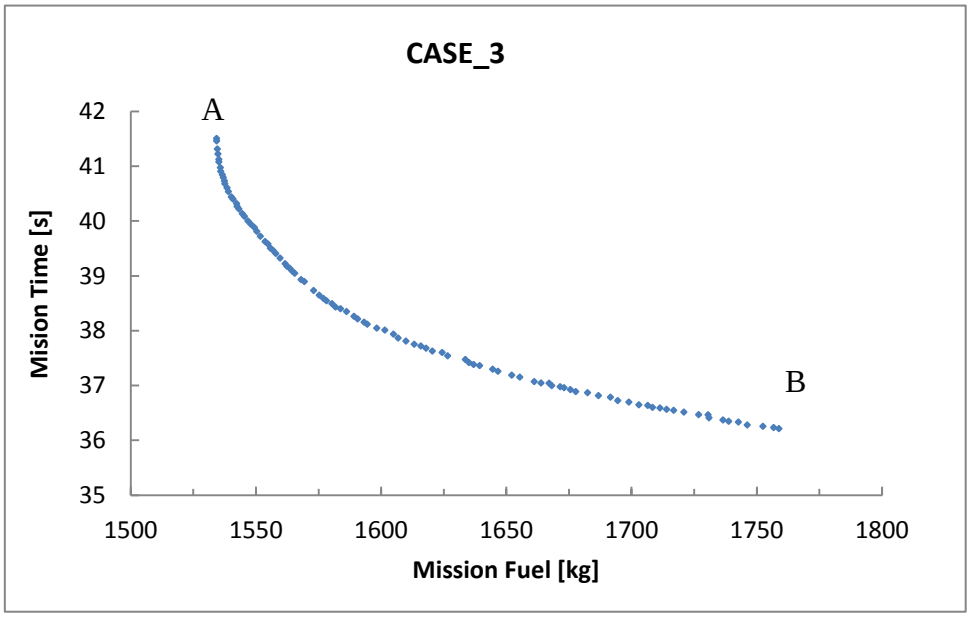

Figure 6-13 Pareto front of fuel burn and flight time as objectives

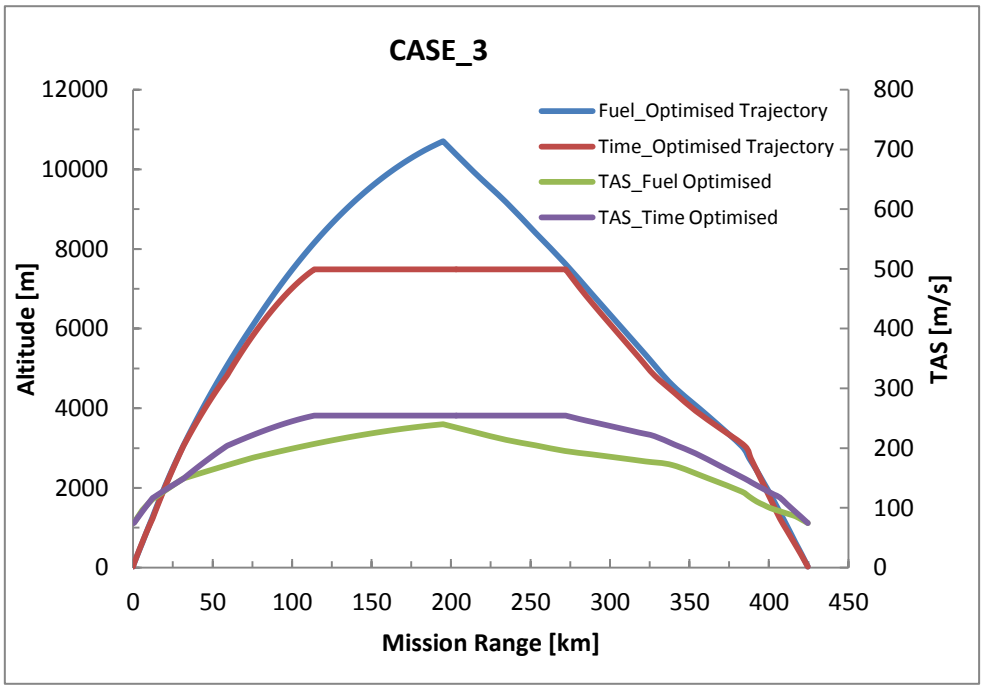

Figure 6-14 Optimum trajectories and TAS

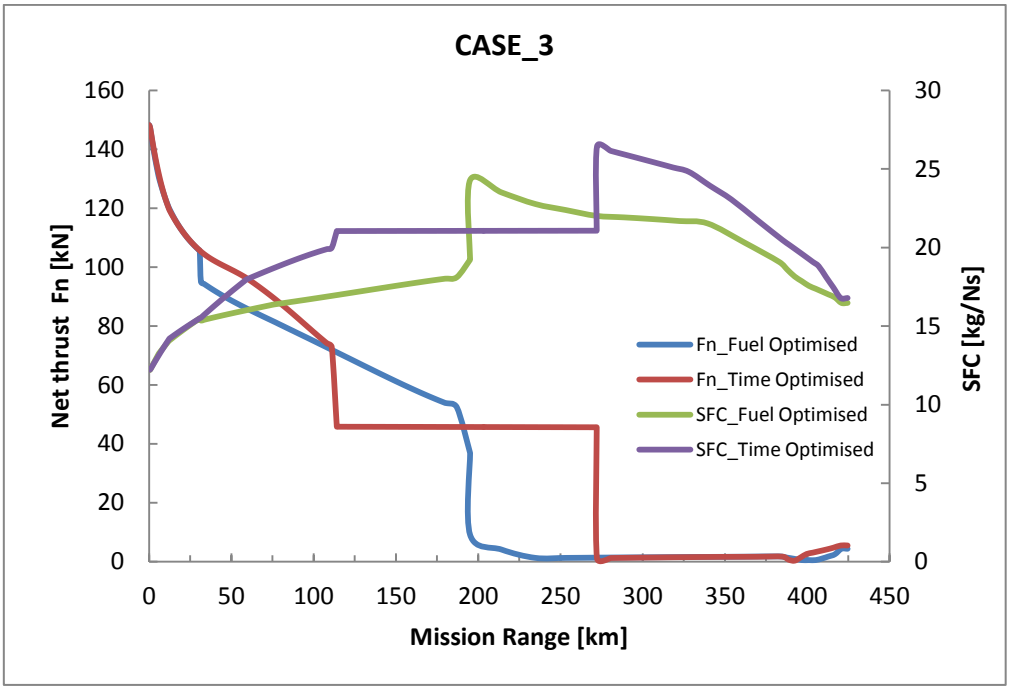

Figure 6-15 Net thrust and SFC variation of optimum trajectories

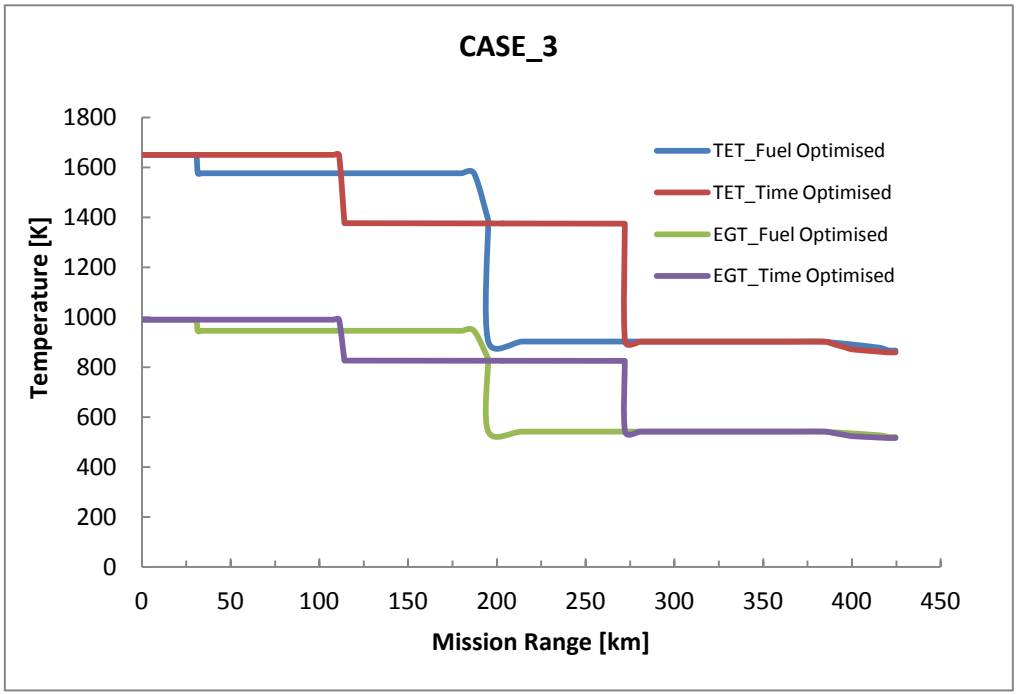

Figure 6-16 TET and EGT variation of optimum trajectories

Trajectories are optimised for the minimum fuel burn and minimum time objectives. Pareto fronts obtained from the short range aircraft with clean and two degraded engines are presented in Figure 6-5, 6-9 and 6-13. The Pareto fronts are formed by a series of points, where each point represents a trajectory. The two extreme points A and B represent the minimum fuel burn and minimum time (i.e. optimum) trajectories respectively. The remaining points are other intermediate trade off solutions. The complete profiles of the minimum fuel burn and minimum time trajectories with their TAS are shown in Figure 6-6, 6-10 and 6-14.

There is an optimum cruise altitude for minimum fuel burn. Therefore, optimal altitude is found where fuel consumption is minimised by flying at the most efficient speed and engine thrust setting. In another, words lowest possible speed and highest possible altitude. When the fuel is burned and aircraft weight decreases, the amount of lift needed and consequently drag is reduced, which means required thrust is also become less. But, if throttle is reduced, then the engine is no longer operating at the most efficient setting. Therefore, the optimal procedure is to maintain the most efficient speed and power setting and use the excess thrust to gradually climb the aircraft continuously throughout the cruise (cruise climb) until meet the TOD. However in this short mission there is not clear cruise phase, as it meets the TOD immediately finishing the climb phase. TOD is the point, which allows the aircraft to maximise the flown distance at idle thrust (or very low thrust). However, in practice change in optimum cruise altitude is often taken into account by changing the altitude in steps (step cruise). As explained in long range mission, step cruise is preferred as it is easier to manage from an air traffic control perspective.

On the other hand aircraft with degraded engines are heavier and therefore will tend to reach the optimum altitude early in the flight (lower altitude than the clean engine) and continues the climb which maintains an optimum altitude as the aircraft weight reduces. Therefore aircraft tends to follow the same continuous climb approach, but towards TOD the aircraft weight will approach that of a clean engine and therefore the altitudes tend to converge.

For the minimum time, optimiser suggests aircraft to fly at the highest speed and lowest altitude as possible. Therefore aircraft (for any mission type) must fly at the crossover altitude. The cross over altitude is the altitude at which the CAS (Calibrated Air Speed) limit and Mach number limit are equal in terms of TAS. Above this altitude TAS will fall at a fixed Mach number due to reducing ambient air temperature. Below this altitude TAS will also fall at a fixed CAS. Therefore the maximum TAS is at the crossover altitude which the aircraft to achieve the maximum speed and minimum time. When the engines are degraded TAS started reduce and as result minimum time increased. However But most of the time has been recovered by compensating the thrust drop by increasing the spool speed and TET. It is important to notice

that increase in minimum time for both degraded engines are marginal compared to aircraft with clean engines.

The variation of the net thrust, and SFC, for the minimum fuel burn and minimum time trajectories are given in Figure 6-7, 6-11 and 6-15. The variations of TET and EGT of all three cases are also presented in Figure 6-8, 6-12 and 6-16. Summary of the minimum fuel burn and minimum flight time for clean and two degraded engines are presented in Table 6-4 and Figures 6-19 and 6-20. When analysing the optimum trajectories it can be seen, both fuel optimised and time optimised trajectories demonstrated considerably low trade-off between fuel burn and flight time. The fuel optimised trajectory of the clean engine has achieved a minimum fuel burn of 1499kg with a flight time of 2483s (41.38min). Time optimised trajectory has achieved a minimum flight time of 2163s (36.1 min) with a fuel burn of 1732kg. Therefore fuel optimised trajectory has achieved 13.4% of reduction in fuel burn compared to time optimised trajectory, but with a compromise of 14.8% flight time.

The optimum trajectories with low degraded engines (CUSE_1DL) show a similar trade-off between fuel burn and flight time, but with an increased fuel burn and marginal flight time. The fuel optimised trajectory has achieved a minimum fuel burn of 1523kg with a flight time of 2498s (41.6min). Comparing to the CASE_1, fuel burn and flight time has increased by 24kg and 15s (0.25min) i.e. 1.6% and 0.6% respectively. Time optimised trajectory has achieved a minimum flight time of 2172s (36.2min) with a fuel burn of 1744kg. But comparing to the CASE_1, minimum time and minimum fuel has increased only by 9s (0.15min) and 12kg, i.e. 0.42% and 0.69% respectively. Therefore looking at the both optimum trajectories, fuel optimised trajectory has achieved 12.7% of reduction in fuel burn compared to time optimised trajectory, but with 15% compromise of flight time.

Optimum trajectories with highly degraded engines (CUSE_2DL) also show a similar trade-off between fuel burn and flight time. The fuel optimised trajectory has achieved a minimum fuel burn of 1542kg with a flight time of 2503s (41.7min). But comparing to the CASE_1, minimum fuel burn and minimum flight time has increased by 43kg and 20s (0.33min) i.e. 2.9% and 0.8% respectively. Also comparing to the CASE_2, fuel burn and flight time have increased by 19kg and 5s (0.01min), i.e. 1.2% and 0.2% respectively. Whereas, time optimised trajectory has achieved a minimum flight time of 2177s (36.3min) with a fuel burn of 1758kg. But comparing to the CASE_1, minimum flight time and minimum fuel has increased by 14s (0.23min) and 26kg, i.e. 0.65% and 1.5% respectively. Also comparing to the CASE_2, minimum flight time and minimum fuel burn have increased by 5s (0.08min) and 14kg, i.e. 0.23% and 0.8% respectively. Therefore looking at the both optimum trajectories, fuel

optimised trajectory has achieved 14% of reduction in fuel burn compared to time optimised trajectory, but with 14.9% compromise of flight time.

The Table 6-4, Figure 6-17 and Figure 6-18 summarise the results of minimum fuel burn and minimum time optimised trajectories generated by the short range aircraft with clean engine (CASE_1) and aircraft with two levels of degraded engines (CASE_2 and CASE_3).

Table 6-4 Summary of fuel and time optimised trajectories

	Fuel Optimised				Time Optimised			
Case	Fuel [Kg]	Time [Sec]	Del Fuel [%]	Del Time [%]	Time [Sec]	Fuel [Kg]	Del Time [%]	Del Fuel [%]
Case 1	1499	2483	Ref	Ref	2163	1732	Ref	Ref
Case 2	1523	2498	1.60	0.61	2172	1744	0.40	0.69
Case 3	1542	2503	2.90	0.80	2177	1758	0.65	1.50

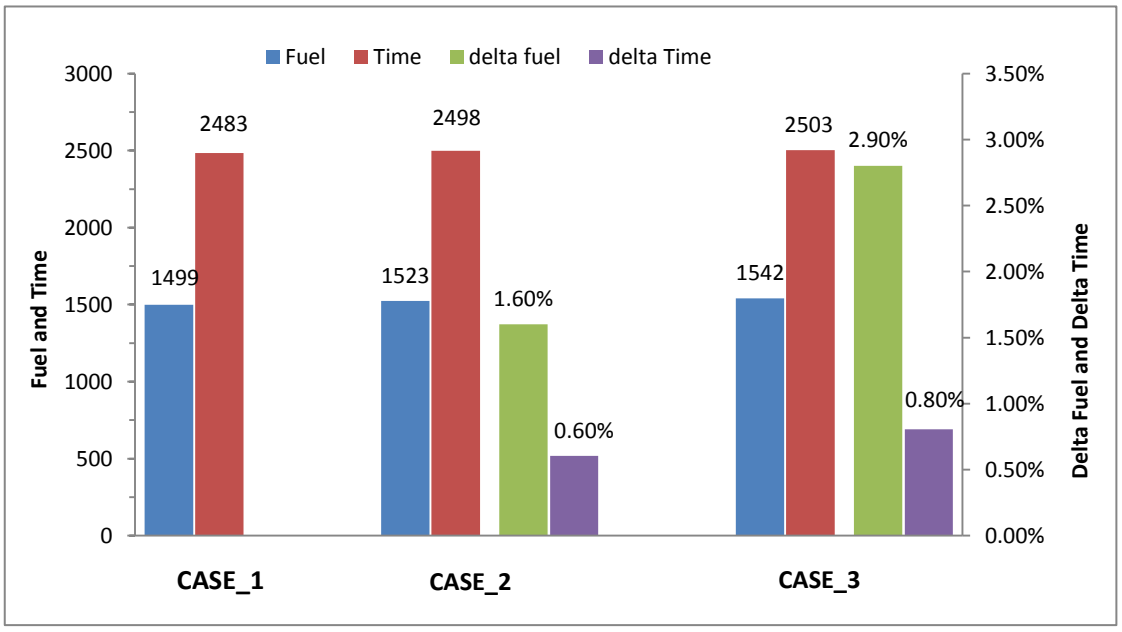

Figure 6-17 Fuel and time penalties for fuel optimised trajectories

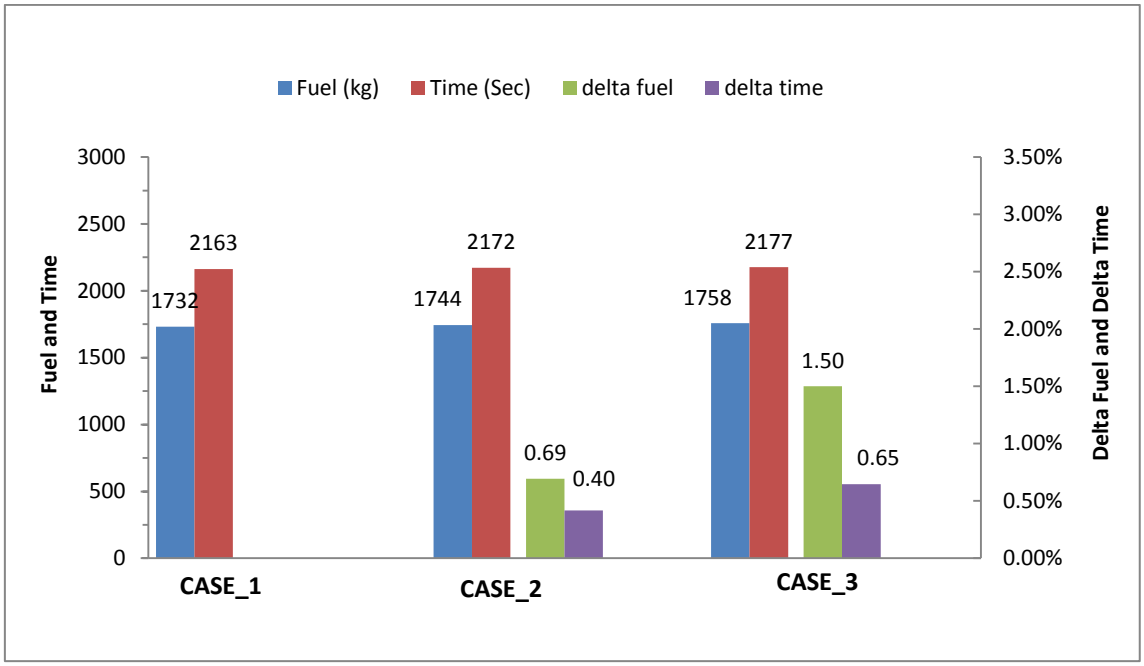

Figure 6-18 Fuel and time penalties for time optimised trajectories

6.5.1.4 Impact of flying clean/degraded optimised trajectories with clean/degraded engines on fuel burn

Table 6-5 Fuel burn of optimum aircraft trajectories with clean/degraded engines

Short range aircraft with clean and low degraded engines	
Clean engines flying on trajectories optimised for clean engines (CE+COT)	1499 kg
Deg. engines flying on trajectories optimised for clean engines (DE+COT)	1537 kg
Delta Fuel Burn of (DE+COT) Reference to (CE+COT)	+38 kg (2.5%)
Deg. engines flying on trajectories optimised for deg. engines (DE+DOT)	1523 kg
Delta Fuel Burn of (DE+DOT) Reference to (DE+COT)	-14 kg (-0.9%)
Short range aircraft with clean and highly degraded engines	
Clean engines flying on trajectories optimised for clean engines (CE+COT)	1499 kg
Deg. engines flying on trajectories optimised for clean engines (DE+COT)	1559 kg
Delta Fuel Burn of (DE+COT) Reference to (CE+COT)	+60 kg (4.0%)
Deg. engines flying on trajectories optimised for deg. engines (DE+DOT)	1542 kg
Delta Fuel Burn of (DE+DOT) Reference to (DE+COT)	-17 kg (-1.1%)

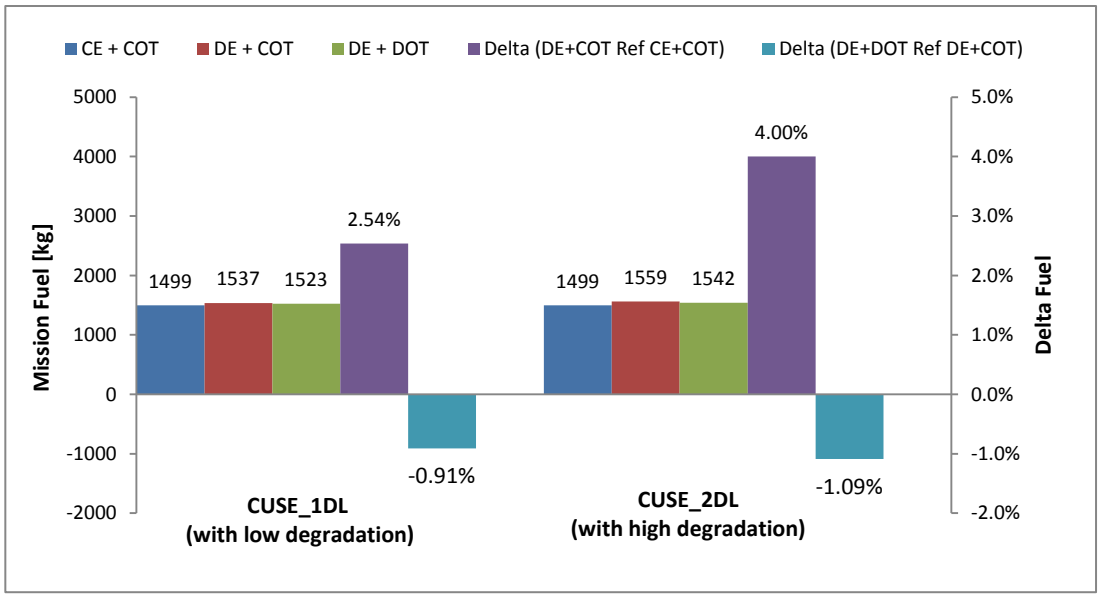

Figure 6-19 Fuel burn of optimum aircraft trajectories with clean/degraded engines

6.5.1.5 Impact of flying clean/degraded optimised trajectories with clean/degraded engines on flight time

Table 6-6 Flight time of optimum aircraft trajectories with clean/degraded engines

Short range aircraft with clean and low degraded engines	
Clean engines flying on trajectories optimised for clean engines (CE+COT)	36.05 min
Deg. engines flying on trajectories optimised for clean engines (DE+COT)	36.35 min
Delta Flight Time of (DE+COT) Reference to (CE+COT)	+0.3 min (0.8%)
Deg. engines flying on trajectories optimised for deg. engines (DE+DOT)	36.2 min
Delta Flight Time of (DE+DOT) Reference to (DE+COT)	-0.15 min (-0.4%)
Short range aircraft with clean and highly degraded engines	
Clean engines flying on trajectories optimised for clean engines (CE+COT)	36.05 min
Deg. engines flying on trajectories optimised for clean engines (DE+COT)	36.5 min
Delta Flight Time of (DE+COT) Reference to (CE+COT)	+0.45 min (1.2%)
Deg. engines flying on trajectories optimised for deg. engines (DE+DOT)	36.28 min
Delta Flight Time of (DE+DOT) Reference to (DE+COT)	-0.22 min (-0.6%)

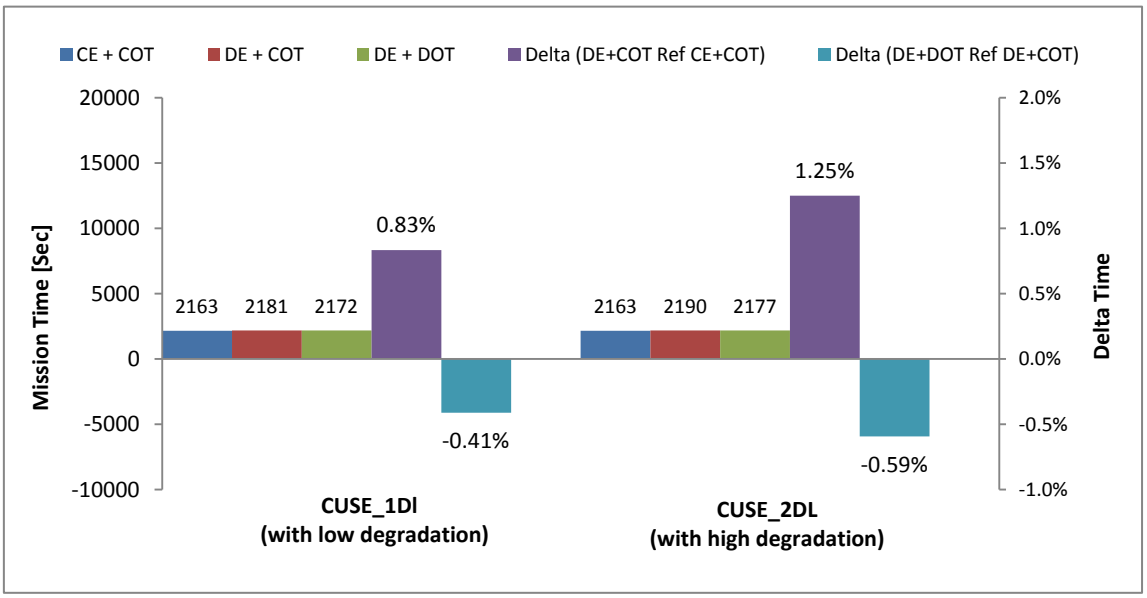

Figure 6-20 Flight time of optimum aircraft trajectories with clean/degraded engines

Optimum trajectories demonstrate a significant trade-off between minimum fuel burn and minimum time for all three cases. Therefore it is important to investigate the impact on fuel burn and flight time, when the aircraft with degraded engines are flying on the trajectory which has been optimised for clean engines. Table 6-5 and Figure 6-19 shows the fuel burn of optimum trajectories of the aircraft with clean and degraded engines, also the fuel burn of the aircraft with two levels of degraded engines are flying on the same optimum trajectory of the clean engines.

Fuel optimised trajectory has achieved a minimum fuel burn of 1499kg with the clean engines. But when the aircraft is flying on the same trajectory with the degraded engines of 5% and 10% EGT increase, fuel burn has increased by 2.5% (i.e. +38kg) and 4% (i.e. 60kg) comparing to the clean engine optimised trajectory (CE+COT). However, it is interesting to notice that fuel burn can be reduced by 0.9% (i.e. -14kg) and 1.1% (i.e. -17kg) with the degraded engines when the aircraft trajectories are specifically optimised for degraded engines.

Similar to the long range aircraft, with the time optimum trajectories there are no significant differences. Table 6-6 and Figure 6-20 shows the flight times of the trajectories optimised for aircraft with clean engines and degraded engines, in addition to aircraft with degraded engines are flying on the trajectory optimised for clean engines. Time optimised trajectory has achieved a minimum flight time of 36.05min with the clean engines. But when the aircraft is flying on the same trajectory with the degraded engines of 5% and 10% EGT increase, flight time has increased by 0.8% (i.e. 0.3min) and 1.2% (i.e. 0.45min) comparing to the clean engine optimised trajectory (CE+COT). However, flight time can be reduced by 0.4% (i.e. 0.15min) and 0.6% (i.e. 0.22min), when the aircraft trajectories are specifically optimised for degraded engines.

6.5.2 Trajectory optimisation for fuel burn and NOx emissions

Optimisation set up

Minimum fuel and minimum NOx have been selected as the objective functions. The optimiser was set up for 250 generations. The population was selected as 100 and an initialisation ratio of 50. The number of evaluation was about 30,000.

Flight Phase	Objective 1	Objective 2	Generations	Population	In. Factor
Complete mission	Mission Fuel	Mission NOx	250	100	50

6.5.2.1 CASE_1: Optimum short range aircraft trajectories generated with clean engines (Engines with 0% EGT increase)

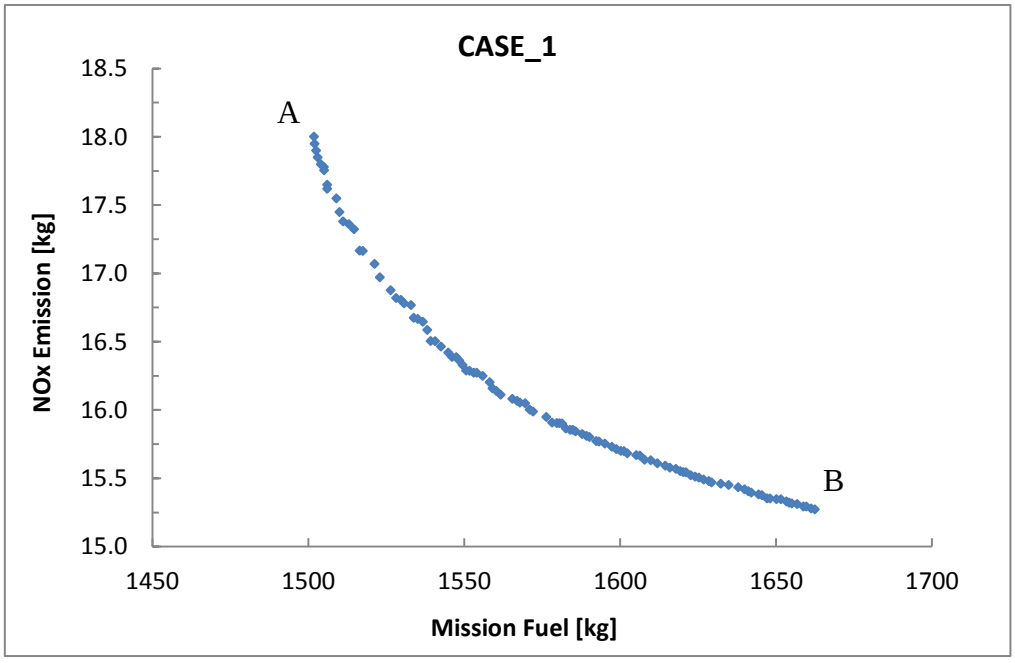

Figure 6-21 Pareto front of fuel burn and mission NOx as objectives

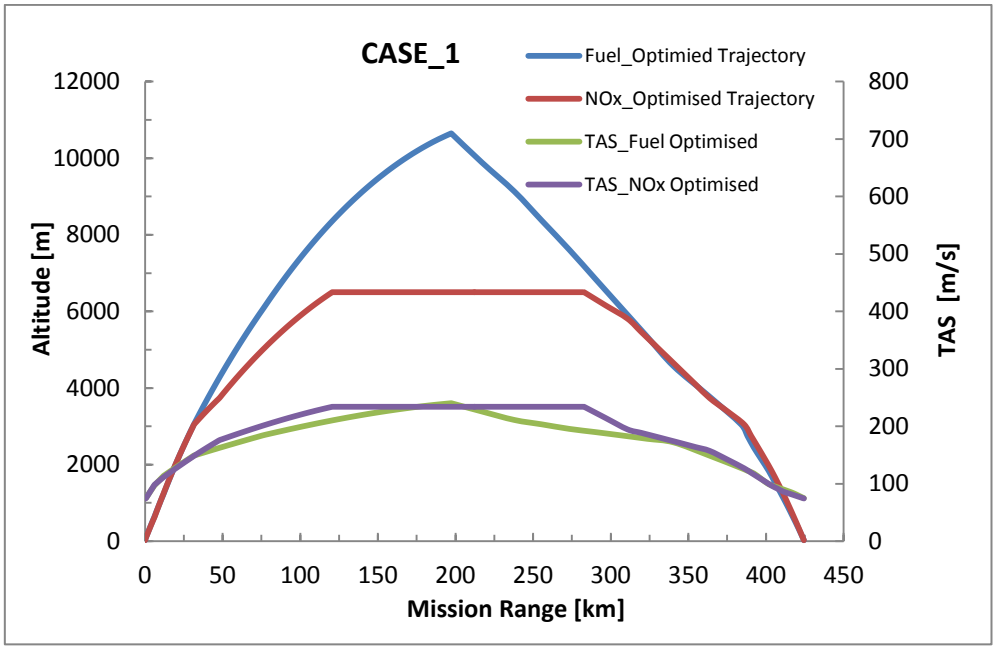

Figure 6-22 Optimum trajectories and TAS

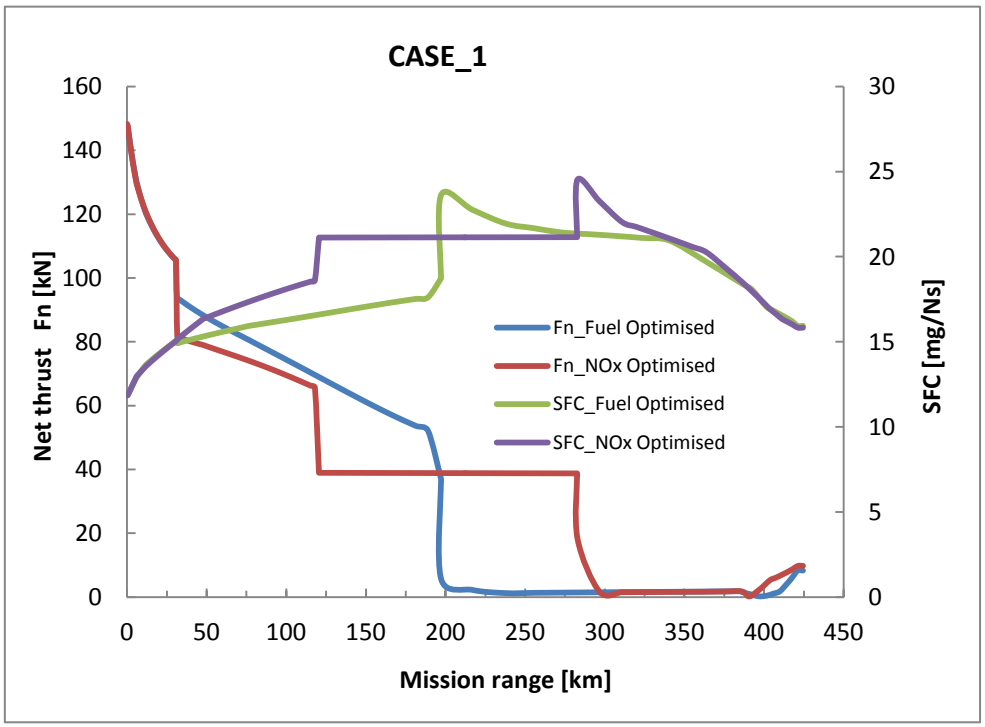

Figure 6-23 Net thrust and SFC variation of optimum trajectories

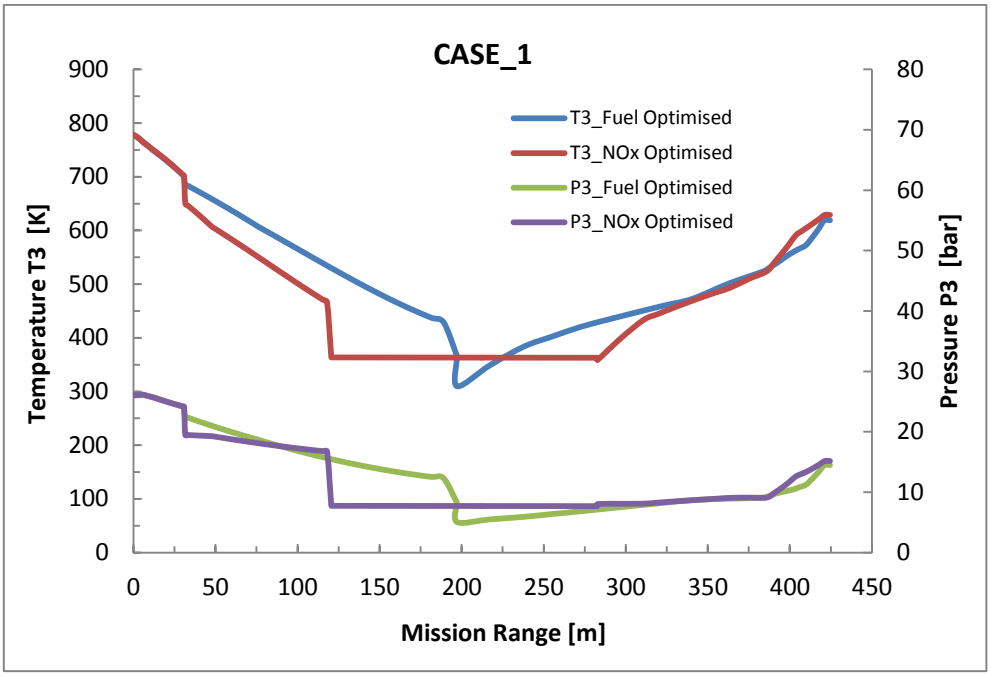

Figure 6-24 Combustor temperature T3 and Pressure P3 variation of optimum trajectories

6.5.2.2 CASE_2: Optimum short range aircraft trajectories generated with low degraded engines (Engines with 5% EGT increase)

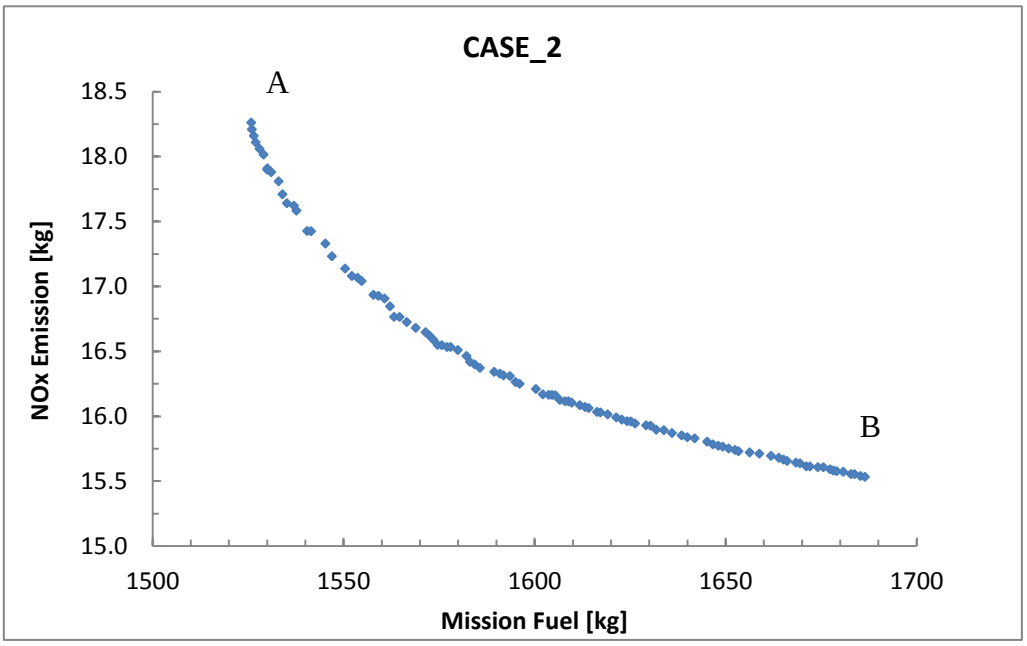

Figure 6-25 Pareto front of fuel burn and mission NOx as objectives

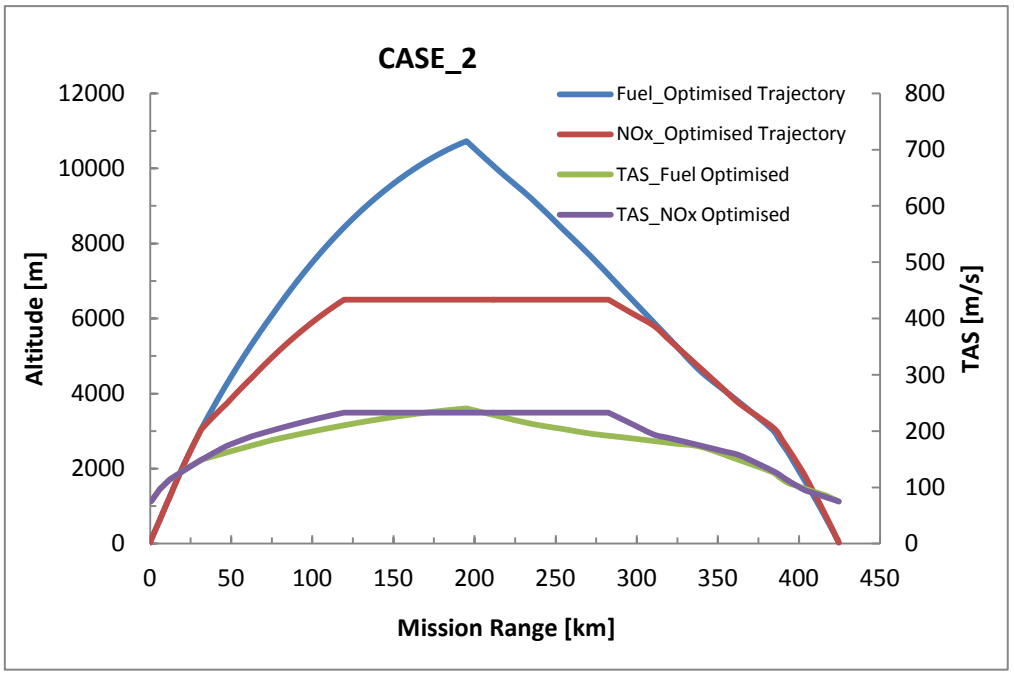

Figure 6-26 Optimum trajectories and TAS

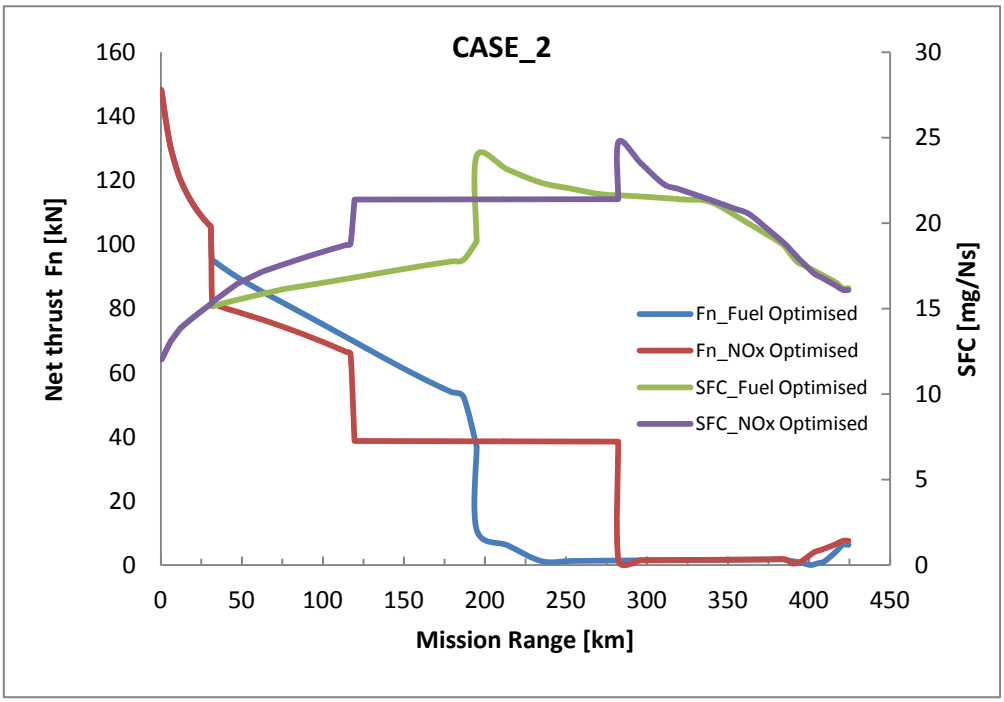

Figure 6-27 Net thrust and SFC variation of optimum trajectories

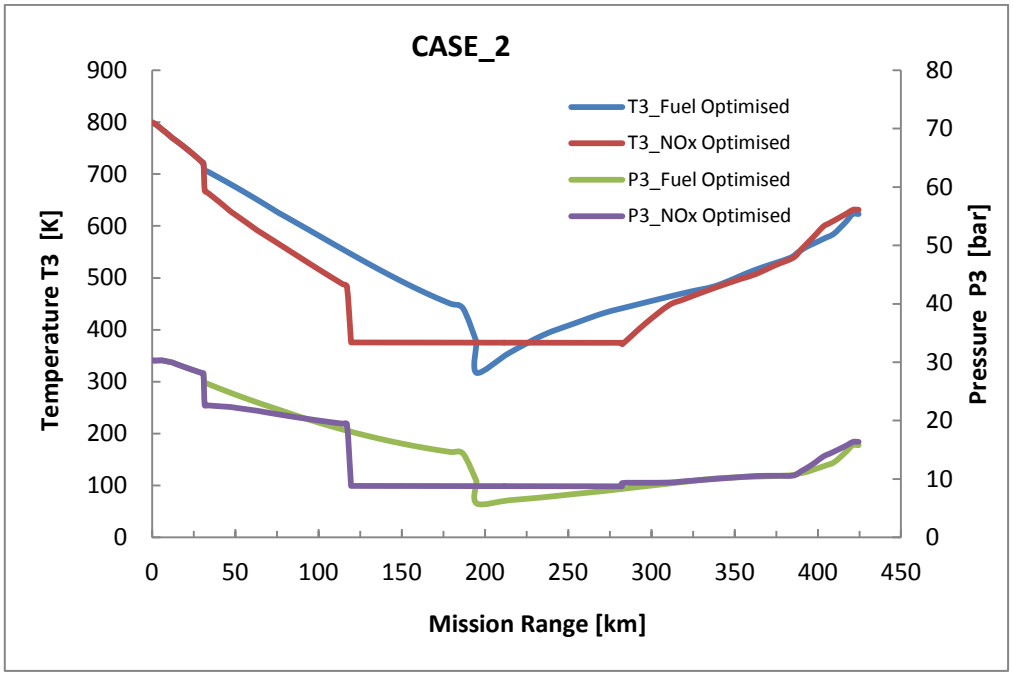

Figure 6-28 Temperature T3 and Pressure P3 variation of optimum trajectories

6.5.2.3 CASE_3: Optimum short range aircraft trajectories generated with highly degraded engines (Engines with 10% EGT increase)

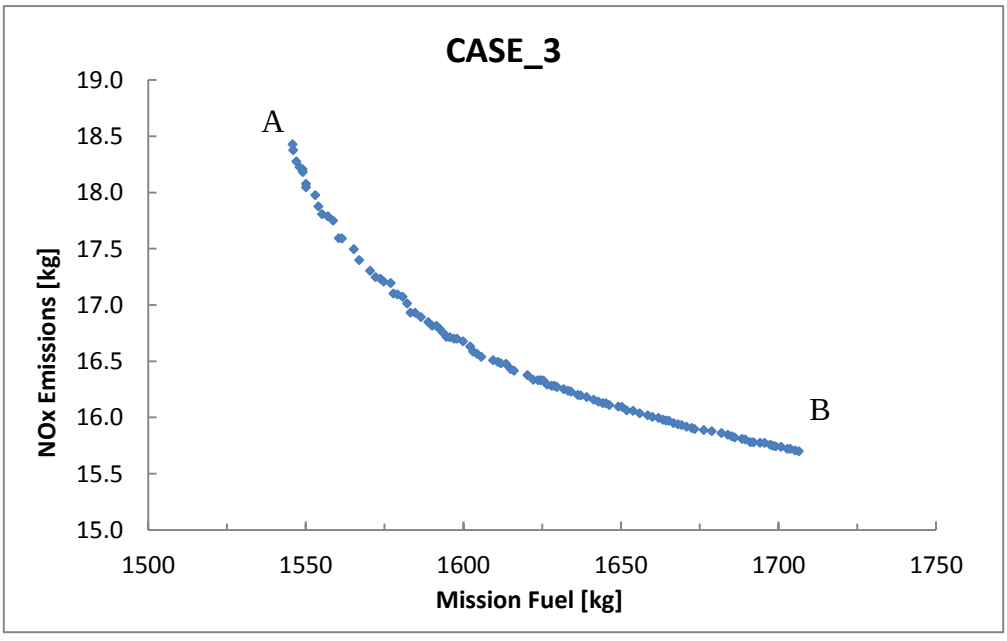

Figure 6-29 Pareto front of fuel burn and mission NOx as objectives

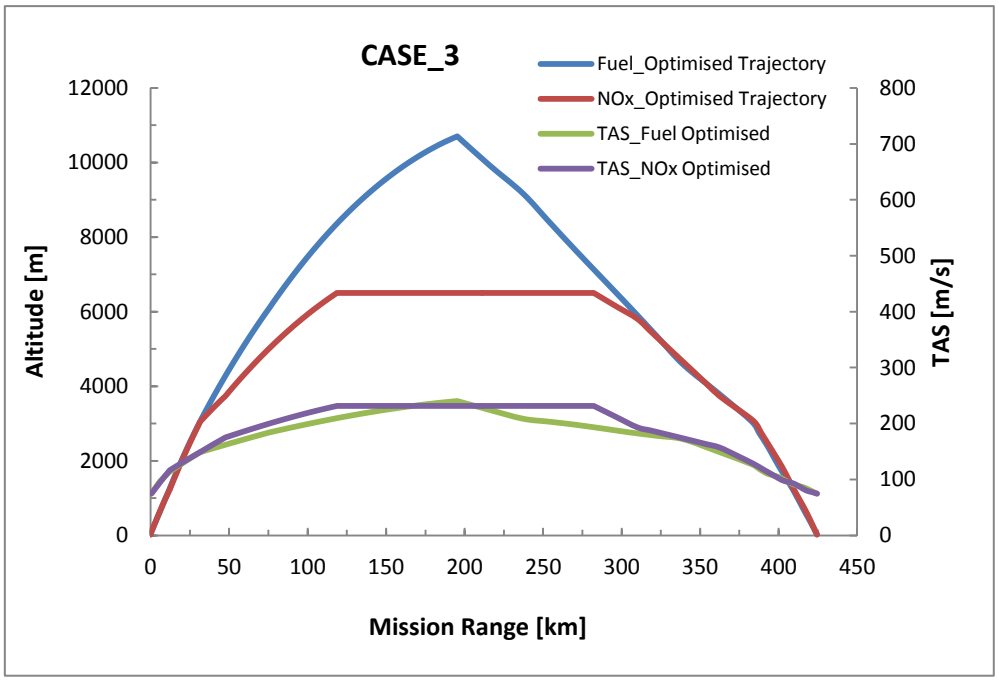

Figure 6-30 Optimum trajectories and TAS

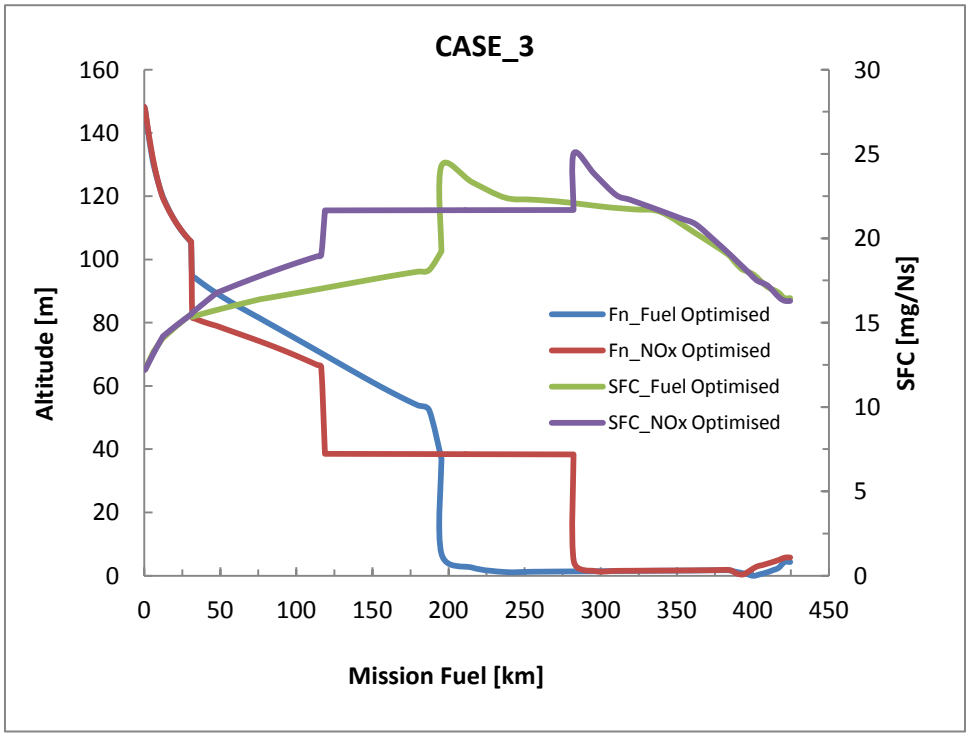

Figure 6-31 Net thrust and SFC variation of optimum trajectories

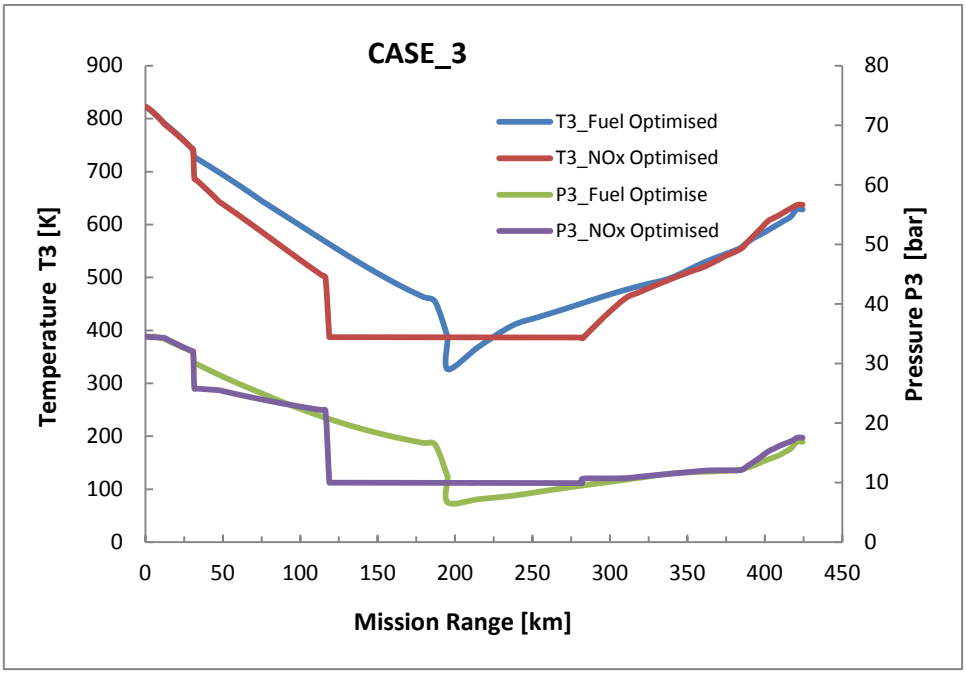

Figure 6-32 Temperature T3 and Pressure P3 variation of optimum trajectories

Trajectories were optimised for the minimum fuel burn and minimum NOx objectives. Pareto fronts obtained from the short range aircraft with clean and two degraded engines are presented in Figure 6-21, 6-25 and 6-29. Diversity of the results on the Pareto fronts appears to be acceptable. The two extreme points A and B represent the min fuel burn and min NOx emission trajectories respectively. The remaining points are other intermediate trade off solutions. The complete profiles of the minimum fuel burn and minimum NOx trajectories with their TAS of three cases are shown in Figure 6-22, 6-26 and 6-30.

As in the previous case, there is an optimum cruise altitude for minimum fuel burn. Therefore, optimal altitude is found where fuel consumption is minimized by flying at the most efficient speed and engine thrust setting. As fuel is burned and aircraft become lighter, then amount of lift needed is less and consequently drag is reduced. As a result, required thrust is also become less. However, as discussed in the long range aircraft, to reduce the fuel burn, if throttle is reduced, then the engine is no longer operating at the most efficient thrust setting. Therefore, the optimal procedure is to maintain the most efficient speed and power setting and use the excess thrust to gradually climb the aircraft continuously. In the short range aircraft there is no considerable cruise phase as the range is very short. The climb phase ends almost at the TOD and aircraft immediately start the descent phase to minimize the fuel burn. In the case of degraded engines, aircraft are heavier and therefore will tend to reach the optimum altitude

early in the flight (lower altitude than the clean engine) and aircraft tends to follow the same continuous climb approach as clean engine case until meet the TOD, where the aircraft weight is almost similar to clean engine. Therefore the altitudes tend to converge.

For the minimum NOx, the aircraft must reduce the combustion temperatures (TET) and fuel burn. To reduce the fuel burn aircraft will approach the minimum fuel trajectory. Also above the tropopause the ambient air temperature remains constant and therefore does not affect the NOx emissions much. However, to reduce the combustion temperatures the aircraft must fly at a lower altitude than the minimum fuel altitude, so as to reduce the TET for a given thrust due to an increase in air density. Increase in air density will also increase drag and hence the thrust requirement and therefore this strategy is limited in short range cases as well. When the engine degrades, it starts reducing the thrust comparing to the clean engine. The thrust drop is compensated by the increasing the TET, which intern increase the formation of NOx. However, optimiser suggests aircraft to lower the flying altitude to keep the NOx emissions in optimum level.

The variation of the net thrust, and SFC, for the minimum fuel burn and minimum NOx trajectories are given in Figure 6-23, 6-27 and 6-31. The variations of combustor inlet temperature (T3) and pressure (P3) of all three cases are also presented in Figure 6-24, 6-28 and 6-32. Summary of the minimum fuel burn and minimum flight time for clean and two degraded engines are presented in Table 6-7 and Figures 6-33 and 6-34. When analysing the optimum trajectories it can be seen, both fuel optimised and NOx optimised trajectories demonstrated a considerable trade-off between fuel burn and NOx emissions. The fuel optimised trajectory of the clean engine (CASE_1) has achieved a minimum fuel burn of 1501kg with NOx emissions of 18kg. NOx optimised trajectory has achieved a minimum NOx emissions of 15.3kg with a fuel burn of 1662.6kg. Therefore NOx optimised trajectory has achieved 15% of reduction in NOx emissions compared to fuel optimised trajectory, but with a compromise of 10.8% fuel burn.

The optimum trajectories with low degraded engines (CUSE_1DL) show a similar trade-off between fuel burn and NOx, but with an increased fuel burn and NOx emissions. The fuel optimised trajectory has achieved a minimum fuel burn of 1525kg with NOx emissions of 18.3kg. Comparing to the CASE_1, fuel burn and NOx has increased by 24kg and 0.3kg i.e. 1.6% and 1.7% respectively. NOx optimised trajectory has achieved a NOx emissions of 15.5kg with a fuel burn of 1686.5kg. But comparing to the CASE_1, minimum NOx and minimum fuel has increased by 0.2kg and 23.9kg, i.e. 1.3% and 1.4% respectively. Therefore looking at the

both optimum trajectories, NOx optimised trajectory has achieved 15.3% of reduction in NOx compared to fuel optimised trajectory, but with 10.6% compromise of fuel burn.

Optimum trajectories with highly degraded engines (CUSE_2DL) also show a similar trade-off between fuel burn and NOx. The fuel optimised trajectory has achieved a minimum fuel burn of 1545kg with a NOx emission of 18.5kg. But comparing to the CASE_1, minimum fuel burn and minimum NOx has increased by 44kg and 0.5kg i.e. 2.9% and 2.8% respectively. Also comparing to the CASE_2, fuel burn and NOx have increased by 20kg and 0.2kg, i.e. 1.3% and 1.1% respectively. Whereas, NOx optimised trajectory has achieved a minimum NOx of 15.7kg with a fuel burn of 1706.1kg. But comparing to the CASE_1, minimum NOx and minimum fuel has increased by 0.4kg and 43.5kg, i.e. 2.6% and 2.6% respectively. Also comparing to the CASE_2, minimum NOx and minimum fuel burn have increased by 0.2kg and 19.6kg, i.e. 1.3% and 1.2% respectively. Therefore looking at the both optimum trajectories, NOx optimised trajectory has achieved 15.1% of reduction in NOx emissions compared to fuel optimised trajectory, but with 10.4% compromise of fuel burn.

The Table 6-7, Figure 6-33 and Figure 6-34 summarized the results of minimum fuel burn and minimum NOx optimised trajectories generated by the long range aircraft with clean engine (CASE_1) and aircraft with two levels of degraded engines (CASE_2 and CASE_3).

Table 6-7 Summary of fuel and time optimised trajectories

	Fuel Optimised				NOx Optimised			
Case	Fuel [Kg]	NOx [kg]	Del Fuel [%]	Del NOx [%]	NOx [kg]	Fuel [Kg]	Del NOx [%]	Del Fuel [%]
Case 1	1501.0	18.0	Ref	Ref	15.3	1662.6	Ref	Ref
Case 2	1525.0	18.3	1.60	1.70	15.5	1686.5	1.31	1.44
Case 3	1545.0	18.5	2.90	2.78	15.7	1706.1	2.61	2.62

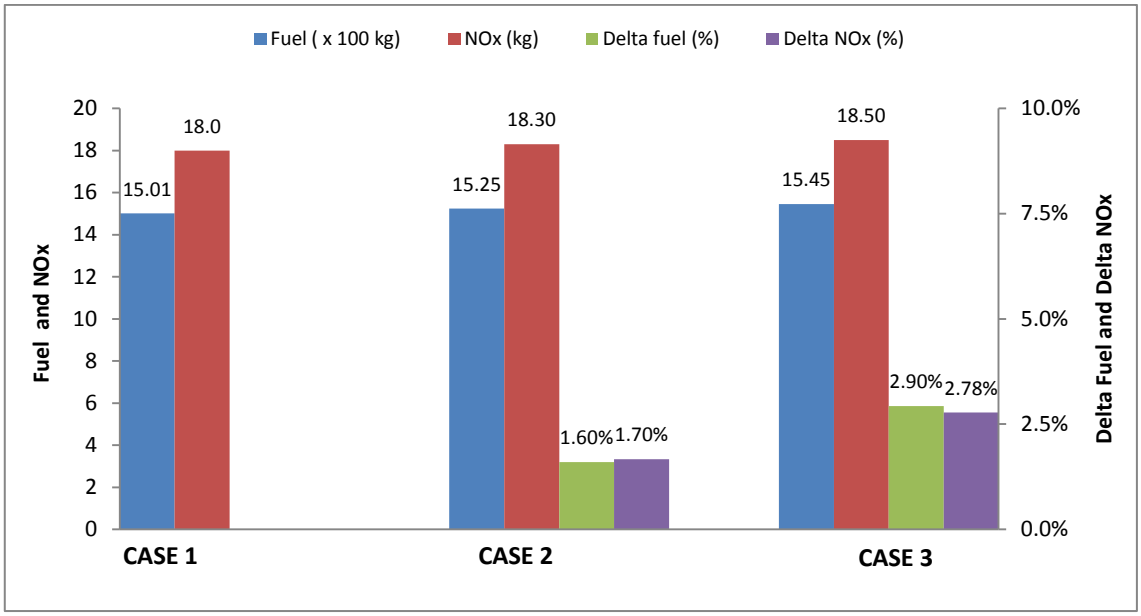

Figure 6-33 Fuel and NOx penalties for fuel optimised trajectories

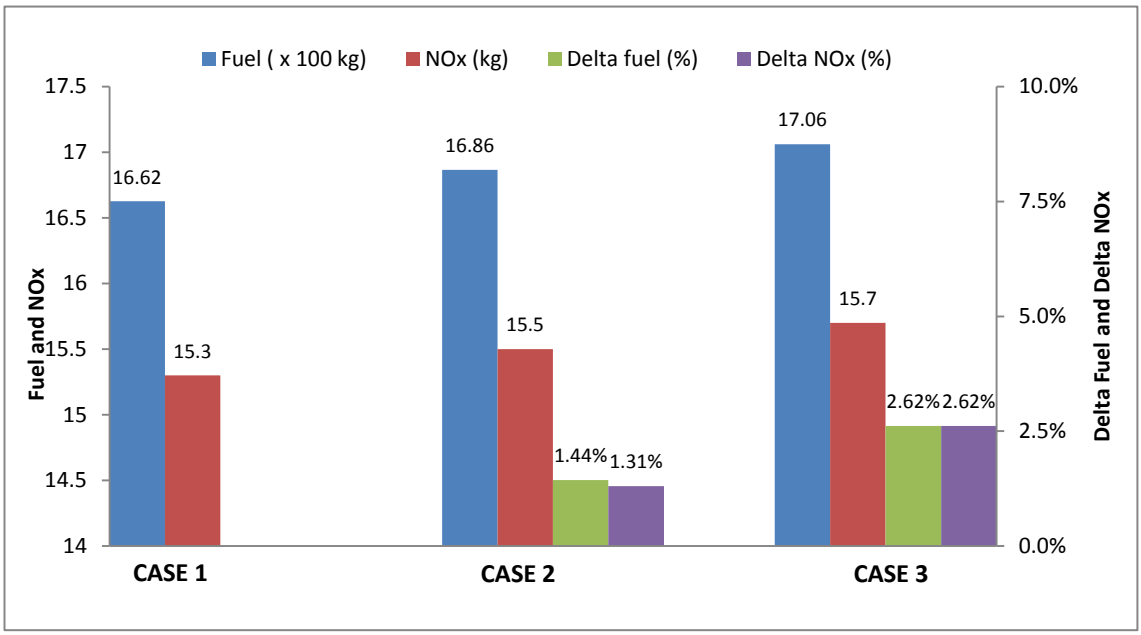

Figure 6-34 Fuel and NOx penalties for NOx optimised trajectories

6.5.2.4 Impact of flying clean/degraded optimised trajectories with clean/degraded engines on NOx emissions

Table 6-8 NOx emissions of optimum aircraft trajectories with clean/degraded engines

Short range aircraft with clean and low degraded engines	
Clean engines flying on trajectories optimised for clean engines (CE+COT)	15.3 kg
Deg. engines flying on trajectories optimised for clean engines (DE+COT)	15.7 kg
Delta NOx of (DE+COT) Reference to (CE+COT)	+0.4 kg (2.6%)
Deg. engines flying on trajectories optimised for deg. engines (DE+DOT)	15.5 kg
Delta NOx of (DE+DOT) Reference to (DE+COT)	-0.2 kg (-1.2%)
Short range aircraft with clean and highly degraded engines	
Clean engines flying on trajectories optimised for clean engines (CE+COT)	15.3 kg
Deg. engines flying on trajectories optimised for clean engines (DE+COT)	16.0 kg
Delta NOx of (DE+COT) Reference to (CE+COT)	+0.7 kg (4.5%)
Deg. engines flying on trajectories optimised for deg. engines (DE+DOT)	15.7 kg
Delta NOx of (DE+DOT) Reference to (DE+COT)	-0.3 kg (-1.9%)

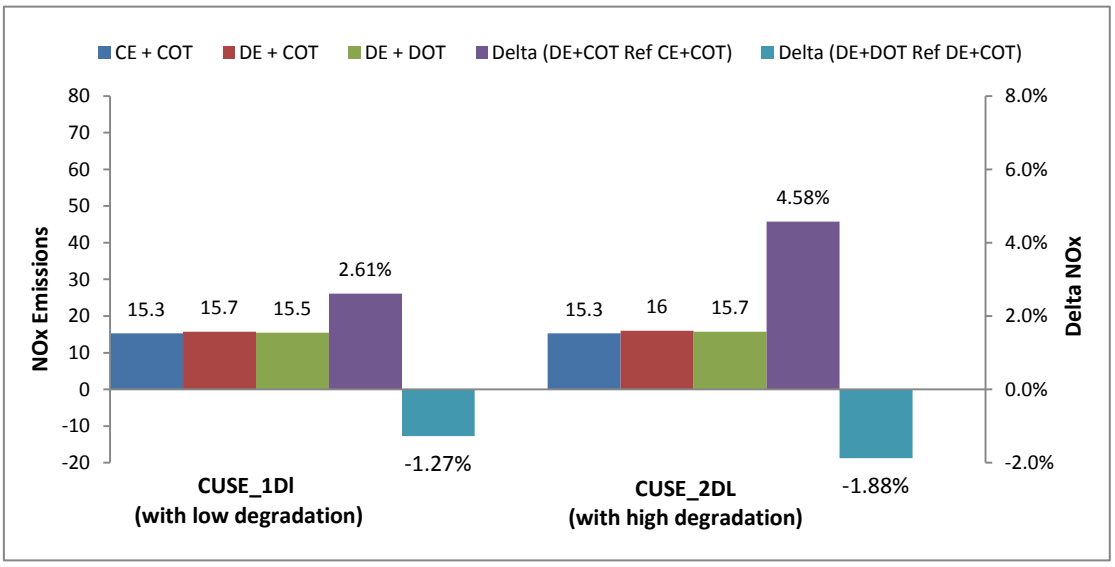

Figure 6-35 NOx emissions of optimum aircraft trajectories with clean/degraded engines

Optimum trajectories demonstrate a significant trade-off between minimum fuel burn and minimum NOx emissions for all three cases. Therefore it is important to investigate the impact on fuel burn and NOx emissions, when the aircraft with degraded engines are flying on the trajectory which has been optimised for clean engines. Table 6-8 and Figure 6-35 shows the NOx emission optimum trajectories of the aircraft with clean and degraded engines, also the NOx emissions for the aircraft with two levels of degraded engines are flying on the trajectory optimised for clean engines.

NOx optimised trajectory has achieved minimum NOx emissions of 15.5kg with clean engines. But when the aircraft is flying on the same trajectory with the degraded engines of 5% and 10% EGT increase, NOx emissions has increased by 2.6% (i.e. 0.4kg) and 4.5% (i.e. 0.7kg) comparing to the clean engine optimised trajectory (CE+COT). However, it is interesting to notice that NOx emissions can be reduced by 1.2% (i.e. 0.2kg) and 1.9% (i.e. 0.3kg) with the low and high degraded engines respectively, when the aircraft are flying on the trajectories specifically optimised for degraded engines.

6.5.3 Trajectory optimisation for fuel burn and Contrails

Optimisation set up

Minimum fuel and minimum Contrails have been selected as the objective functions. The optimiser was set up for 250 generations. The population was selected as 100 and initialisation ratio of 50. The number of evaluation was about 30,000.

Flight Phase	Objective 1	Objective 2	Generations	Population	In. Factor
Complete mission	Mission Fuel	Contrails	250	100	50

6.5.3.1 CASE_1: Optimum short range aircraft trajectories generated with clean engines (Engines with 0% EGT increase)

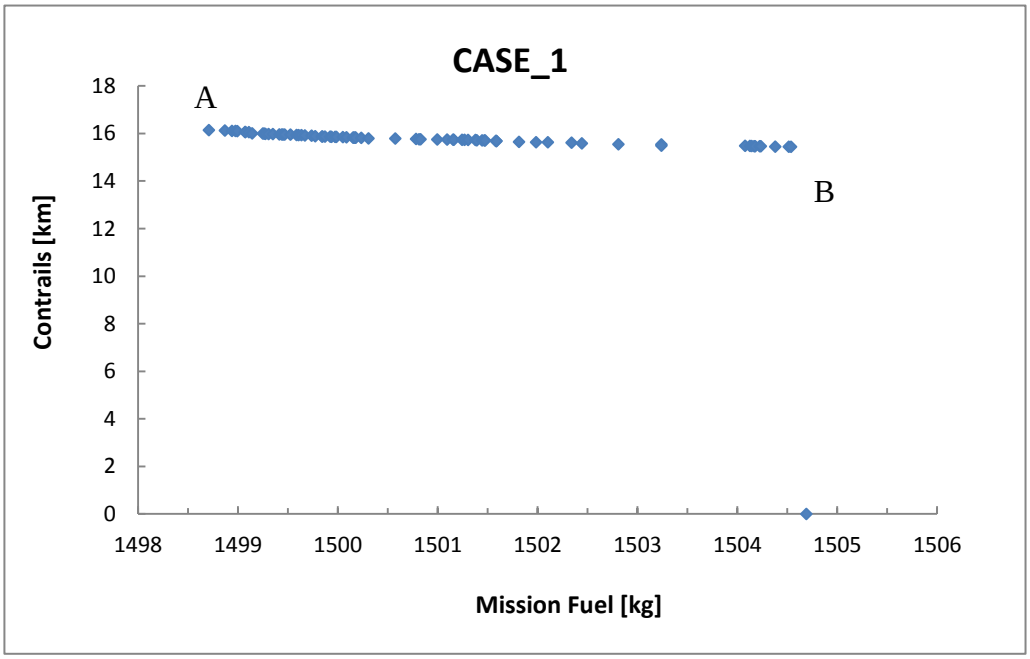

Figure 6-36 Pareto front of fuel burn and contrails as objectives

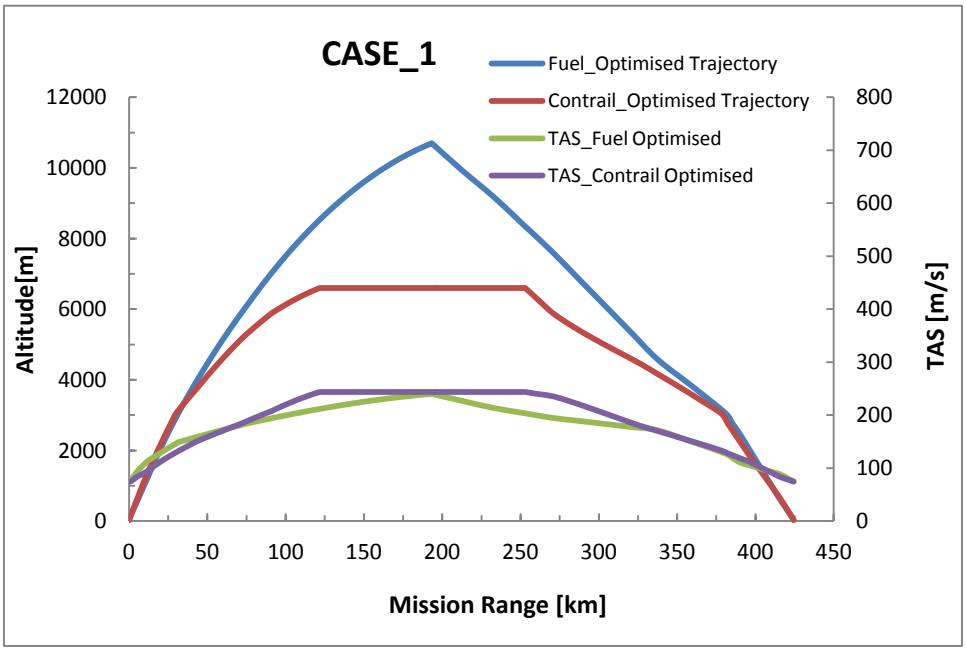

Figure 6-37 Optimum trajectories and TAS

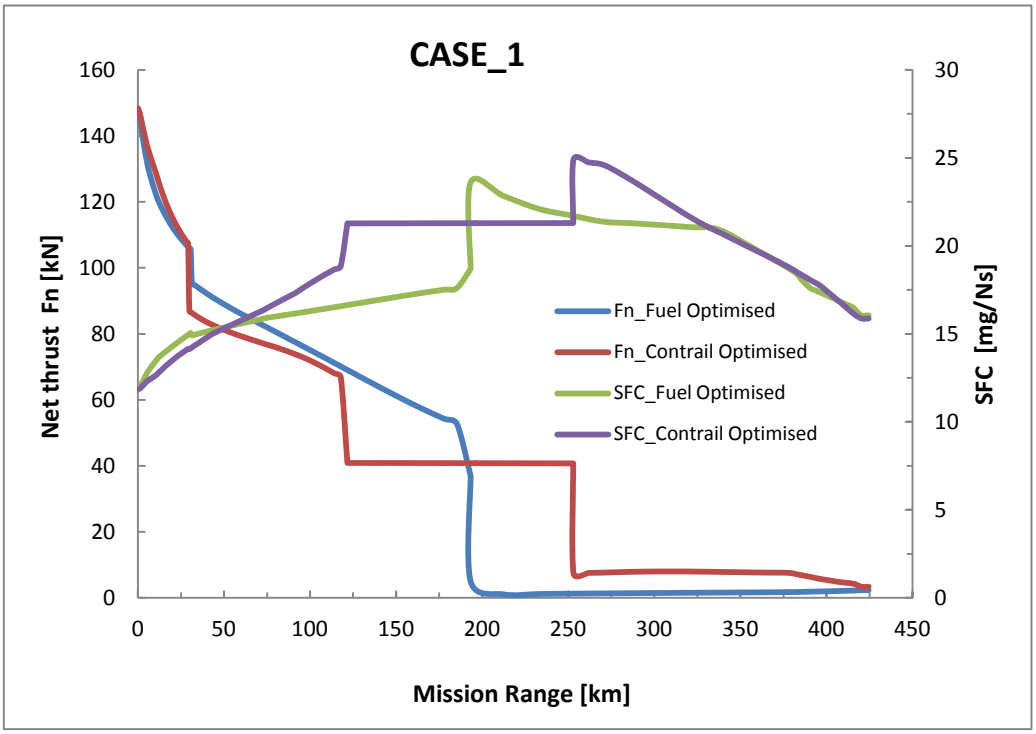

Figure 6-38 Net thrust and SFC variation of optimum trajectories

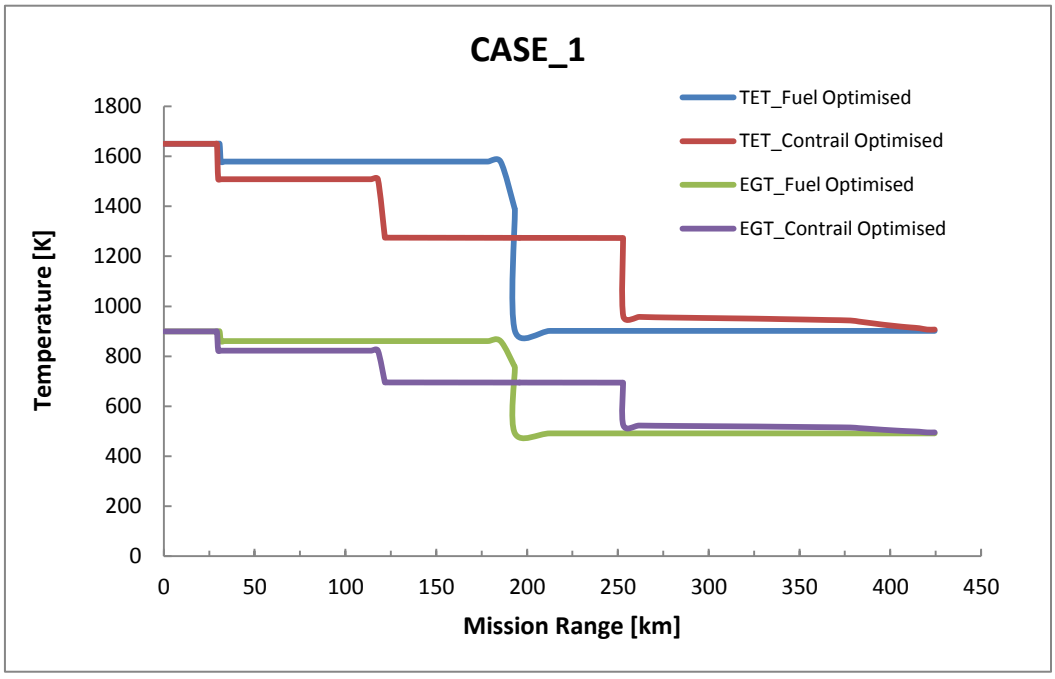

Figure 6-39 TET and EGT variation of optimum trajectories

6.5.3.2 CASE_2: Optimum short range aircraft trajectories generated with low degraded engines (Engines with 5% EGT increase)

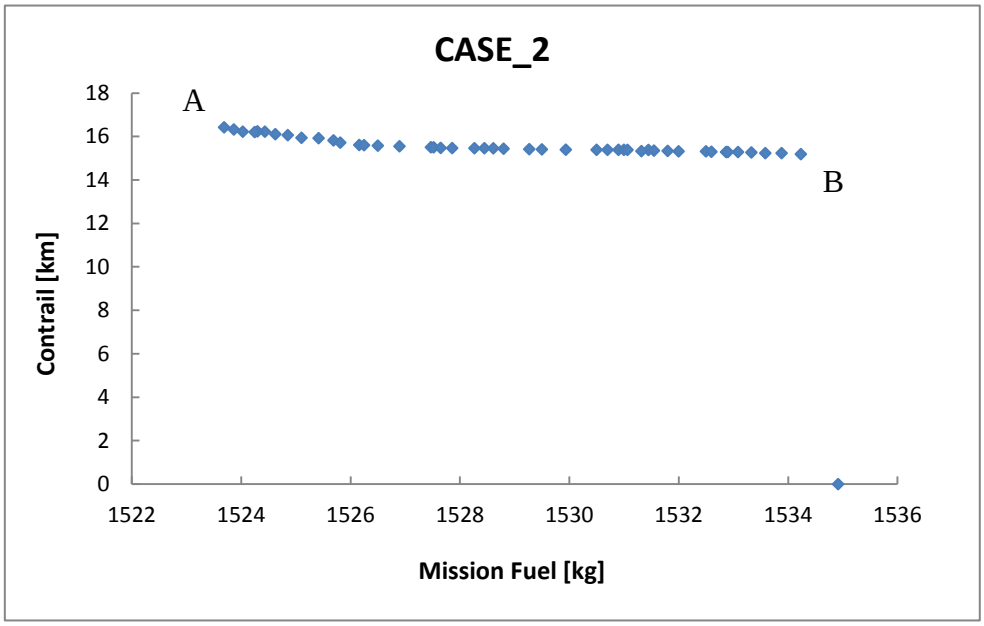

Figure 6-40 Pareto front of fuel burn and contrails as objectives

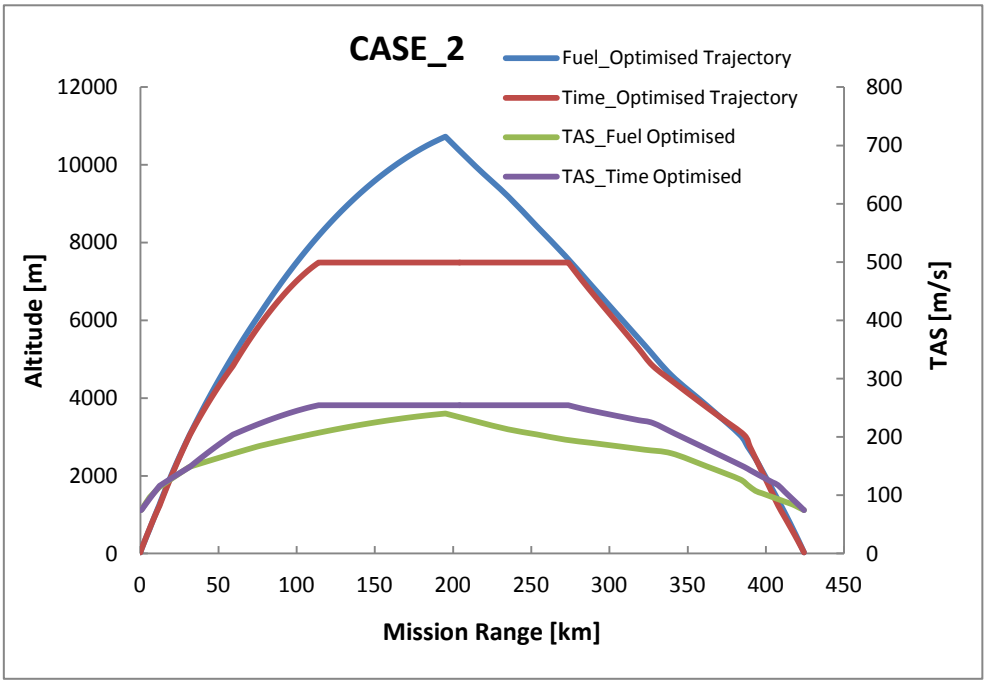

Figure 6-41 Optimum trajectories and TAS

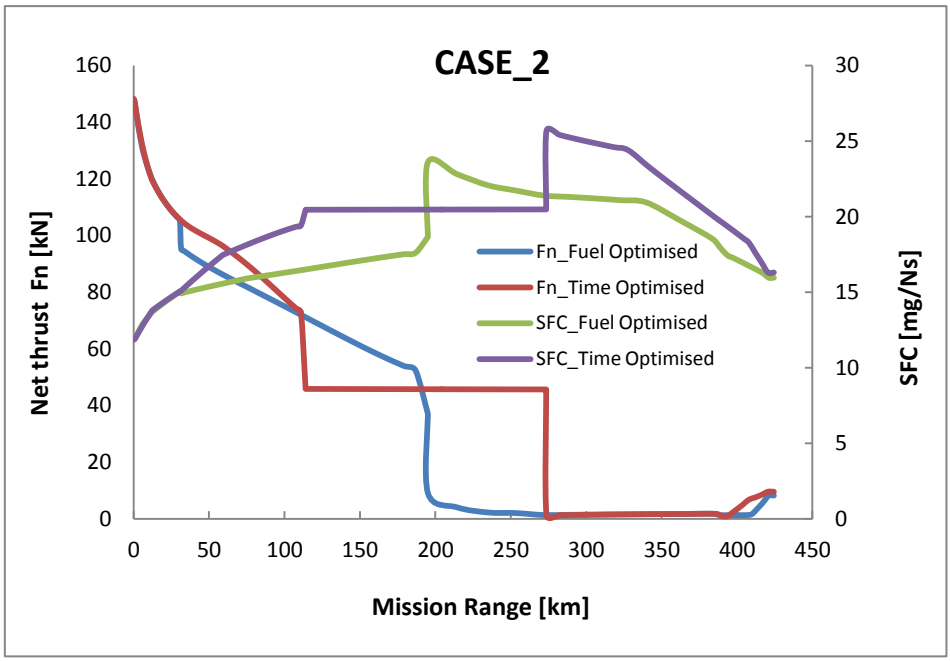

Figure 6-42 Net thrust and SFC variation of optimum trajectories

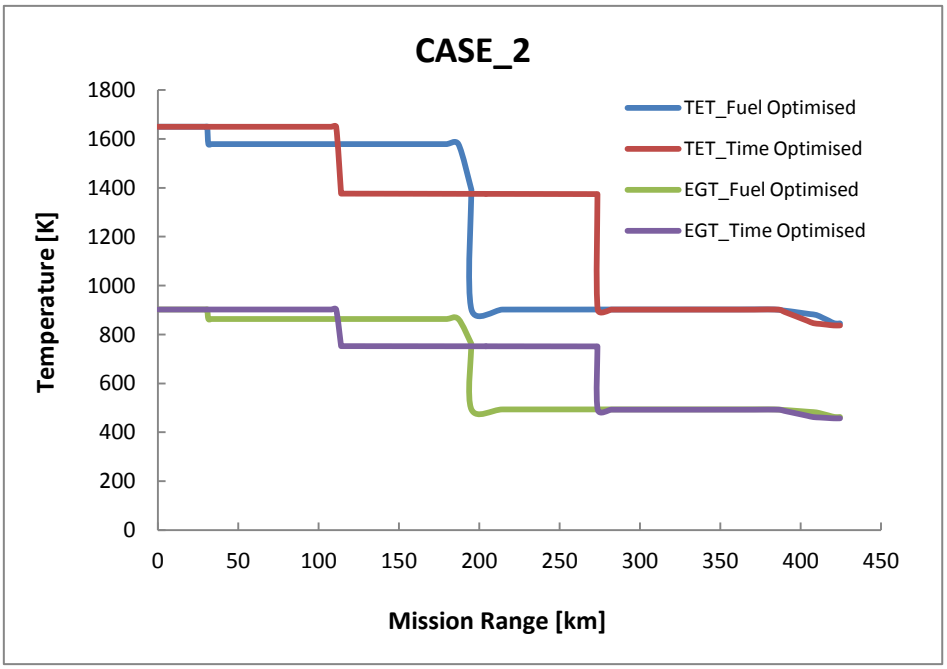

Figure 6-43 TET and EGT variation of optimum trajectories

6.5.3.3 CASE_3: Optimum short range aircraft trajectories generated with highly degraded engines (Engines with 10% EGT increase)

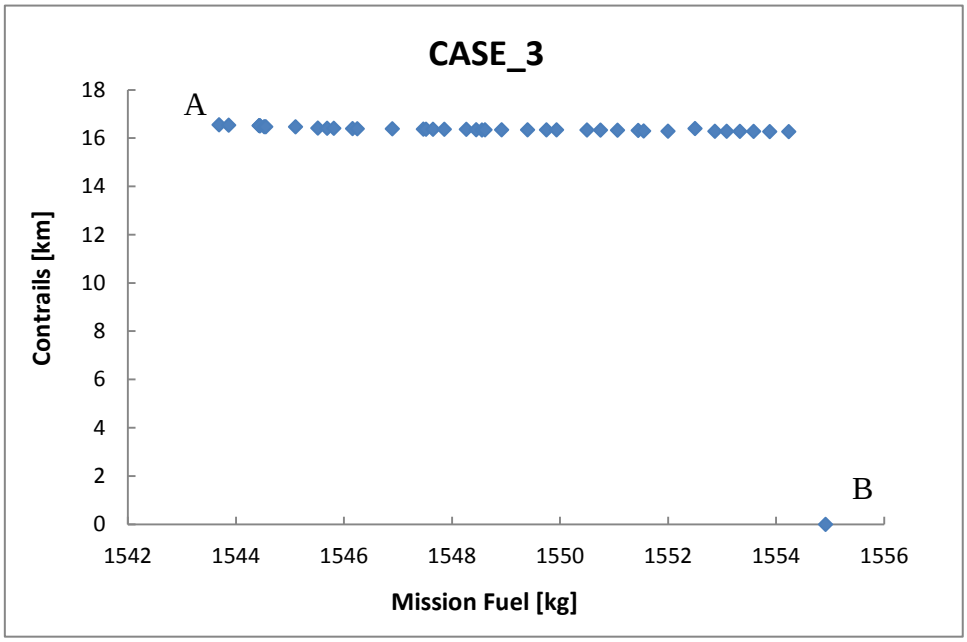

Figure 6-44 Pareto front of fuel burn and contrails as objectives

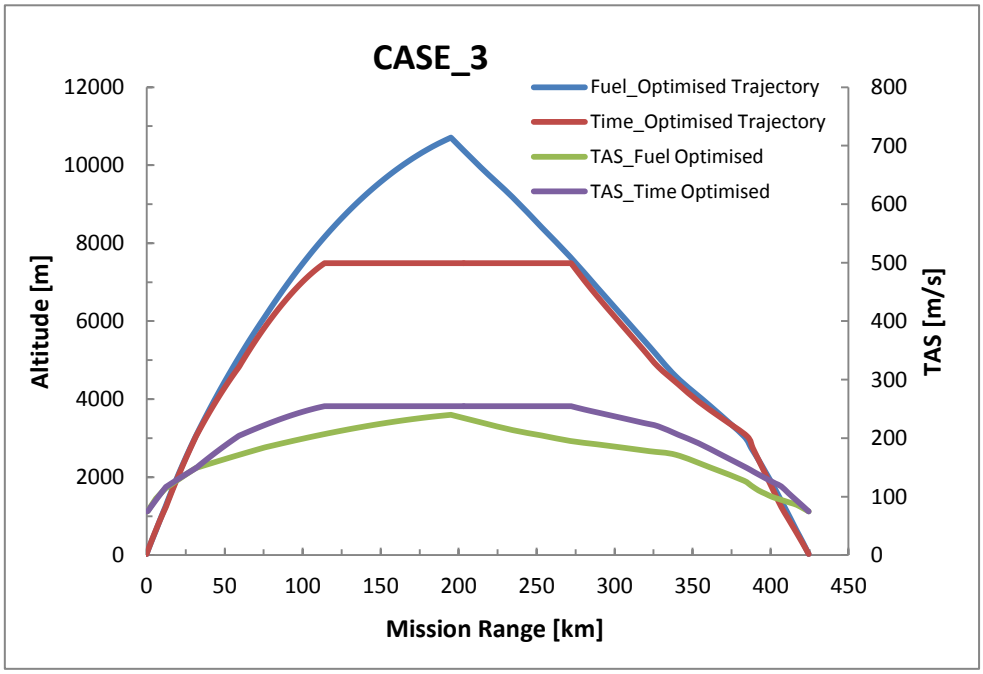

Figure 6-45 Optimum trajectories and TAS

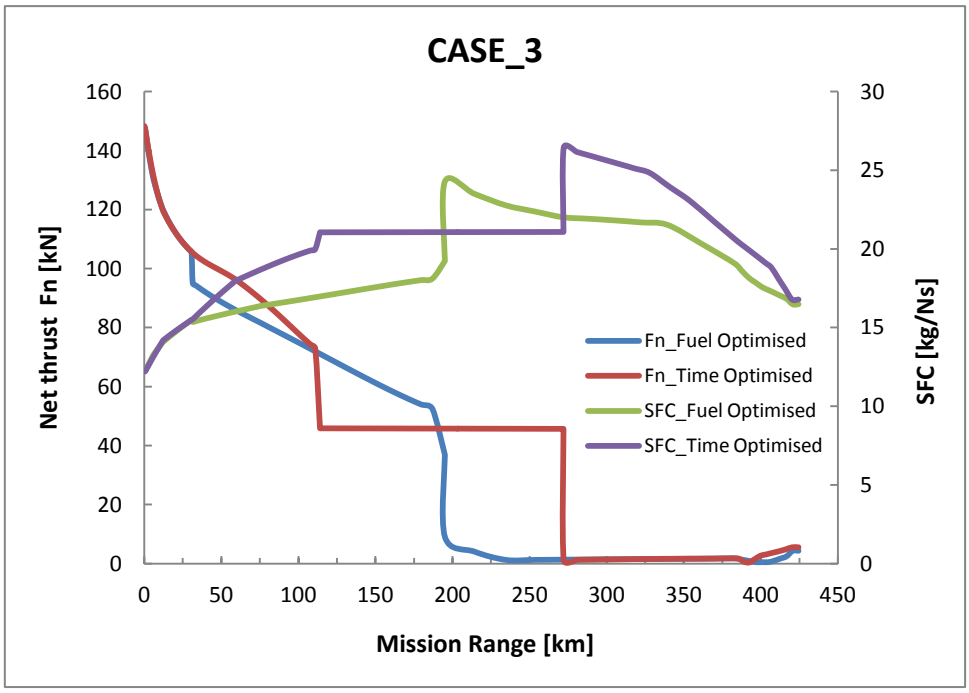

Figure 6-46 Net thrust and SFC variation of optimum trajectories

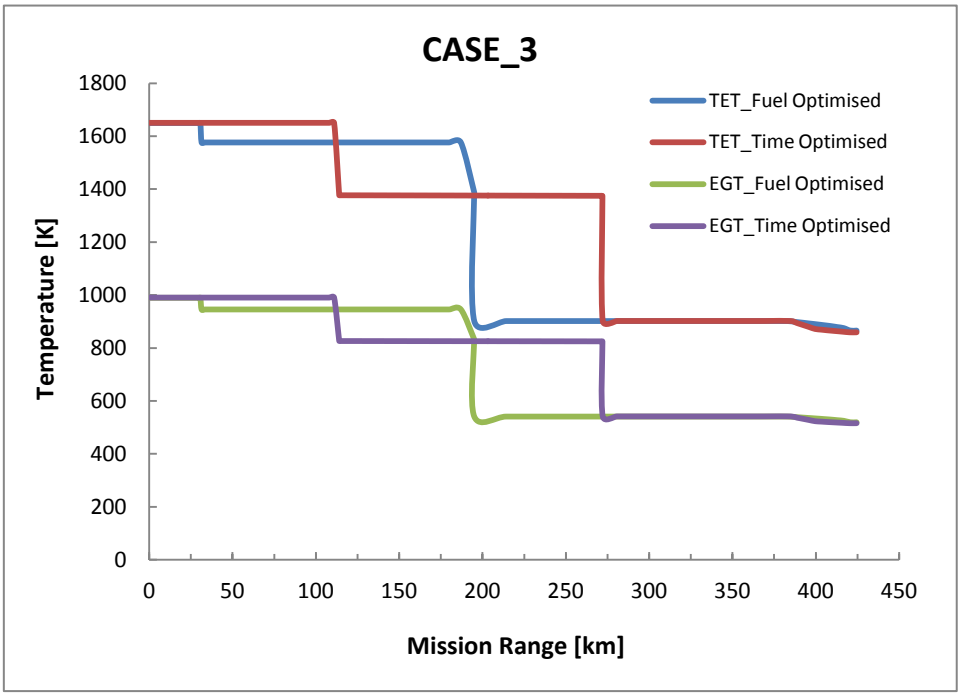

Figure 6-47 TET and EGT variation of optimum trajectories

The Pareto fronts generated for the minimum fuel burn and minimum contrails by the short range aircraft with the clean and two degraded engines are presented in Figures 6-36, 6-40 and 6-44. The respective trajectories of the minimum fuel burn and minimum contrails with the variation of true aircraft speed (TAS) are given in Figure 6-37, 6-41 and 6-45. The variation of the net thrust, SFC, for the minimum fuel burn and minimum contrail trajectories are given in Figure 6-38, 6-42 and 6-46. The variations of TET and EGT of all three cases are also presented in Figure 6-39, 6-43 and 6-47.

The Table 6-9 and the Figure 6-48 and 6-49 indicate the summary of the minimum fuel burn and contrail optimisation results. The solutions found in all three cases for the minimum fuel burn trajectories are similar to the other optimised trajectories generated for the minimum fuel burn. The fuel burn optimised trajectory for clean engines (CASE_1) has achieved minimum fuel burn of 1499.1kg with the formation 16.14km of persistent contrails. However, the trajectories generated with the degraded engines, CASE_2 and CASE_3 have optimised the fuel burn with an increase of 1.6% 9i.e. 24.6kg) and 2.9% (44.3kg) with the increase of 1.73% (0.28km) and 2.6% (0.42) contrail formation. The lengths of the respective contrails formed by the degraded engines are 16.42km and 16.56km.

With regards to the contrail optimised trajectories, contrail emissions can be reduced by increasing cruise altitude. At higher altitudes the atmospheric humidity typically declines. Contrails tend to persist at relative humidity levels above approximately 70% which are less likely at higher altitudes. However, for this case persistent contrails could not be eliminated completely by an increase in cruise altitude alone.

To eliminate contrails completely a low cruise altitude has to be adopted. At low flight altitudes the atmospheric temperature is too warm for contrails to persist. However, at low altitudes aircraft has to operate with a high drag due to increase in density, therefore impacts on fuel burn in sever. To avoid contrails completely, aircraft with clean engine has to increase the fuel burn by 0.34% which is 5.1 kg of fuel. Whereas aircraft with degraded engines of 5% and 10% EGT increase, have to increase the fuel burn by 2.1% (i.e. 31.2kg) and 3.42% (51.4kg) with respect to the contrail optimised trajectory with clean engines. It is also important notice that degraded engines will consume more fuel in all cases. More efficient engines tend to have higher

contrail emissions due to lower exhaust temperatures (EGTs). However, the effect is secondary and no impact has been observed from these results.

Table 6-9 Summary of fuel and contrail optimisation

	Fuel Optimised				Contrail Optimised			
Case	**Fuel [Kg]**	**Contrails [km]**	**Del Fuel [%]**	**Del Cont [%]**	**Contrails [km]**	**Fuel [Kg]**	**Del Cont [%]**	**Del Fuel [%]**
Case 1	1499.1	16.14	Ref	Ref	0	1504.2	Ref	Ref
Case 2	1523.7	16.42	1.60	1.73	0	1535.4	0.00	2.10
Case 3	1543.4	16.56	2.90	2.60	0	1555.6	0.00	3.42

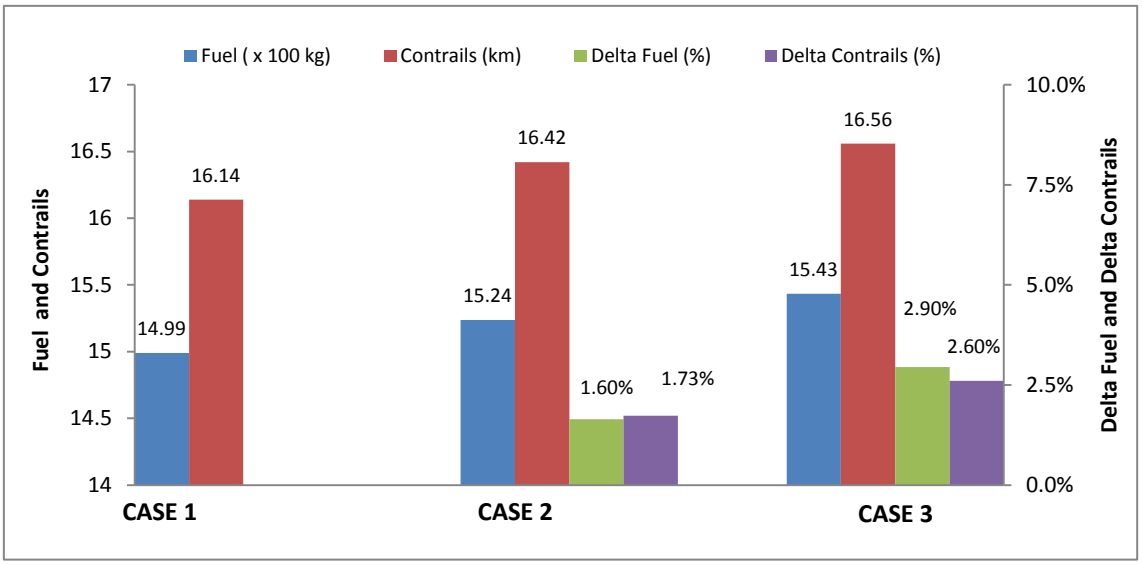

Figure 6-48 Fuel and contrail penalties for fuel optimised trajectories

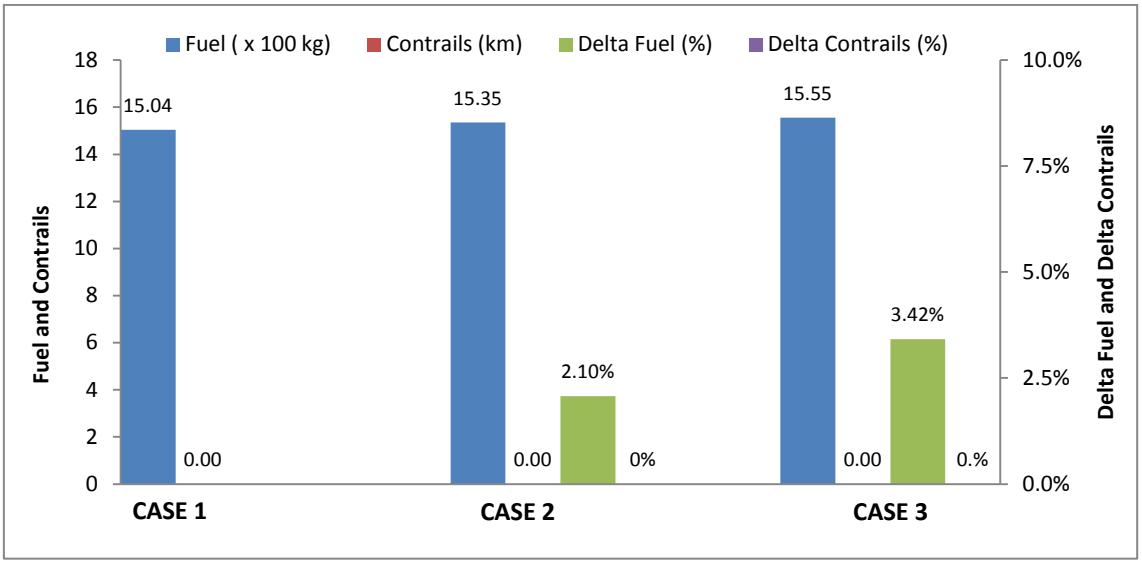

Figure 6-49 Fuel and contrail penalties for contrail optimised trajectories

6.5.3.4 Impact of flying clean/degraded optimised trajectories with clean/degraded engines on fuel burn to avoid contrails

Table 6-10 Fuel burn for zero contrail aircraft trajectories with clean/degraded engines

Short range aircraft with clean and low degraded engines	
Clean engines flying on trajectories optimised for clean engines (CE+COT)	1504 kg
Deg. engines flying on trajectories optimised for clean engines (DE+COT)	1544 kg
Delta Fuel Burn of (DE+COT) Reference to (CE+COT) for zero contrails	+40 kg (2.6%)
Deg. engines flying on trajectories optimised for deg. engines (DE+DOT)	1535 kg
Delta Fuel Burn of (DE+DOT) Reference to (DE+COT) for zero contrails	-9 kg (-0.6%)
Short range aircraft with clean and highly degraded engines	
Clean engines flying on trajectories optimised for clean engines (CE+COT)	1504 kg
Deg. engines flying on trajectories optimised for clean engines (DE+COT)	1570 kg
Delta Fuel Burn of (DE+COT) Reference to (CE+COT) for zero contrails	+66 kg (4.3%)
Deg. engines flying on trajectories optimised for deg. engines (DE+DOT)	1555 kg
Delta Fuel Burn of (DE+DOT) Reference to (DE+COT) for zero contrails	-16 kg (-1.0%)

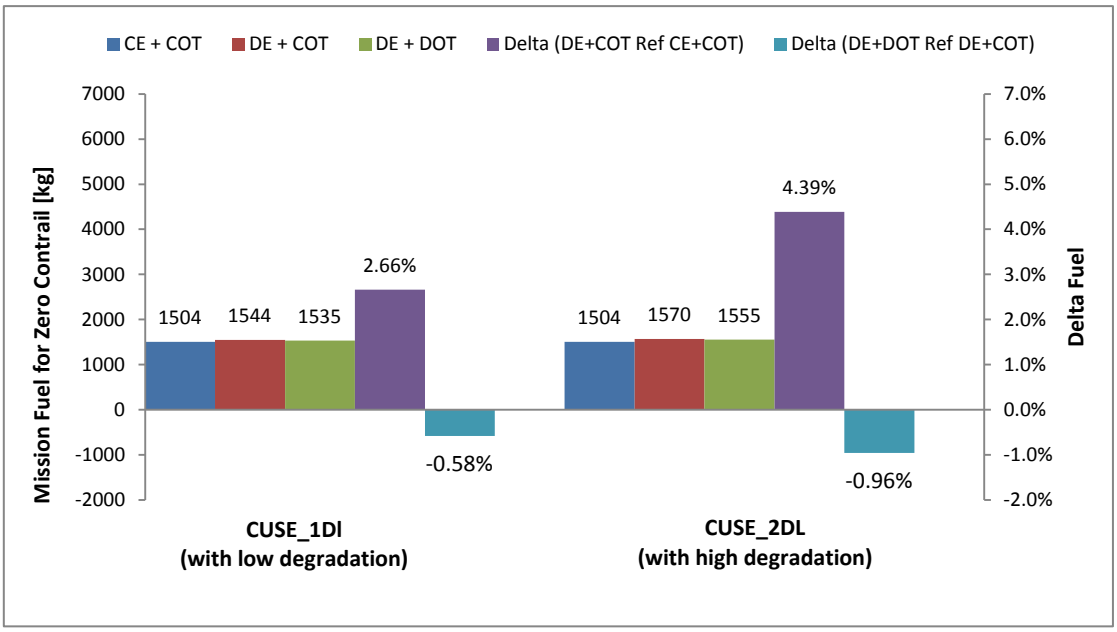

Figure 6-50 Fuel burn for zero contrail aircraft trajectories with clean/degraded engines

Optimum trajectories demonstrate a significant trade-off between minimum fuel burn and minimum (zero) Contrails for all three cases. Therefore it is important to investigate the impact on fuel burn and contrail formation, when the aircraft with degraded engines are flying on the trajectory which has been optimised for clean engines. Table 6-10 and Figure 6-50 shows the fuel burn of optimum trajectories of the aircraft with clean and degraded engines. Also the fuel burn of the aircraft with two levels of degraded engines is flying on the trajectory which has been optimised for clean engines.

Contrail optimised trajectory has achieved zero contrails with a fuel burn of 1505kg for aircraft with clean engines. But when the aircraft is flying on the same trajectory with degraded engines of 5% and 10% EGT increase, to avoid contrails (for zero contrails) fuel burn has increased by 2.6% (i.e. 40kg) and 4.3% (i.e. 66kg) comparing to the clean engine optimised trajectory (CE+COT). However, it is important to notice that fuel burn for zero contrails has been reduced by 0.6% (i.e. 9kg) and 1% (i.e. 16kg) with the low and high degraded engines, when the aircraft trajectories are specifically optimised for degraded engine

6.6 Summary

Profile of short range aircraft is completely different to long range aircraft trajectories. Therefore, this chapter was focused to understand the impact of engine degradation on short range aircraft trajectories. For the purpose of this study, multi-disciplinary optimisation framework developed in Chapter 4 was employed to optimise the trajectories between London to Amsterdam with clean and two levels of degraded engines similar to long range aircraft. Fuel burn, flight time, NOx and contrails have selected as conflicting objectives. Three different optimisation studies were performed and impact of engine degradation on optimum trajectories were investigated. Finally, trajectories were compared to quantify the difference in fuel burn, NOx emissions and contrails produced, when the aircraft with degraded engines are flying on the trajectory optimised for clean engines and flying on the trajectories specifically optimised for degraded engines. The reduction in fuel burn, NOx and contrails were presented.

7 Conclusion and Recommendations

The chapter summarises the overall conclusions of the work presented in each of the individual chapters. Author's contribution to knowledge in the area of environment friendly aircraft operational procedures and trajectory optimisation are presented. The main limitations of the research work are highlighted and recommendations for further work are appropriately made.

7.1 Conclusions

Trajectory optimisation is one of the identified solutions found to reduce environmental emissions of aviation and also a measure that can readily be implemented by airlines. Optimum trajectories generated with clean engines are different to the optimum trajectories generated by the aircraft with degraded engines. Therefore it is important to investigate the impact of degraded engine performance on optimum aircraft trajectories. This research quantify the difference in fuel burn and emissions (NOx and contrails), when flying a trajectory which has been specifically optimised for an aircraft with degraded engines and flying a trajectory which has been optimised for clean engines.

For the purpose of this study, models of a clean and two levels of degraded engines have been developed, that is similar to CFM56-5B4 and CFM56-5C4 engines used in short range and long range aircraft currently in service. Degradation levels have been assumed based on the deterioration levels of exhaust gas temperature (EGT) margin. Aircraft performance models have been developed for short range and long range aircraft (similar to A320-200 and A340-300) with the capability of simulating vertical and horizontal flight profiles with way points provides by the airlines. An emission prediction model was developed to assess NOx emissions of the mission. The contrail prediction model was adopted from previous studies to predict persistent contrail formation. All models have been tested and verified with publicly available data and information provided by Sri Lankan Airline in order to validate their suitability. GA based NAGAMO-II optimiser was selected as multi-objective optimiser, after benchmarking against ZDT functions and MOTS optimiser. A multidisciplinary aircraft trajectory optimisation framework was developed and employed to analyse short range flight trajectories between London and Amsterdam and long range flight trajectories between London and Colombo under three cases. Case_1: Aircraft with Clean Engines, Case_2 and Case_3 were Aircraft with two different levels of degraded engines having a 5% and 10% EGT increase respectively. Three different multi objective optimisation studies were performed for minimum fuel burn, minimum NOx, and minimum persistent contrails under three case studies. Finally fuel burn and emissions were quantified, when the aircraft with degraded engines are flying on the optimum trajectories customised for degraded engines, compared to the aircraft with degraded engines flying on the trajectories optimised for aircraft with clean engines.

The most significant results obtained relate to the fuel burn which indicates that; for the long range aircraft the fuel burn would be reduced by 0.4% (i.e. 252 kg) with engines having 5% EGT increase and 0.6% (i.e. 384kg) with highly degraded engines having 10% EGT increase. Whereas for short range aircraft the effect of the approach is greater and the aircraft would achieve 0.9% (i.e. 14kg) and 1.1% (i.e. 17kg), reductions in the fuel burn with the optimised trajectories when the engines are degraded by 5% and 10% EGT increases. These savings over a year with highly degraded engines would equate to more than 140 tons per aircraft over a long haul flight such as London to Colombo and 6.2 tons on a short haul flight such as London to Amsterdam. Figure 7-1 shows the reduction in fuel burn for long range and short range aircraft with different level of degraded engines, when flying on optimum trajectories compared to flying on optimum trajectories of clean engines.

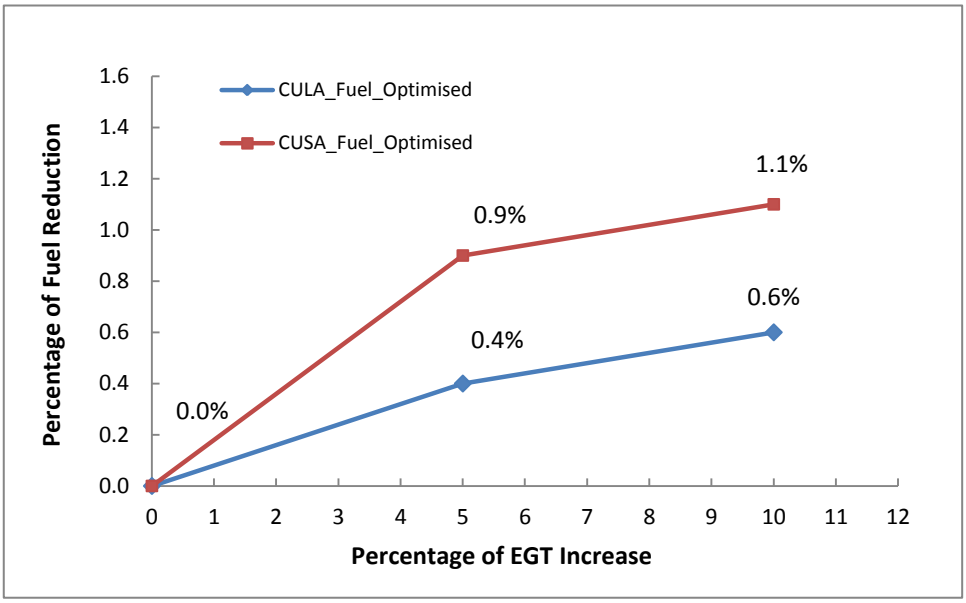

Figures 7-1 Reduction in fuel burn for different degraded engines compared to optimum trajectory of clean engine

Less significant were the optimisation of the trajectories to achieve a minimum flight time. For a long haul flight, the flight time was reduced by 0.23% (i.e. 1.4min) and 0.43% (i.e. 2.5min) and for short haul flight a reduction of 0.41% (i.e. 0.15 min) and 0.6% (0.22 min) when the engines are degraded by the same 5 and 10% levels. However it is important to notice that in both cases time reductions are very marginal. Figure 7-2 shows the reduction in flight time for long range and short range aircraft with different level of degraded engines, when flying on optimum trajectories compared to flying on optimum trajectories of clean engines.

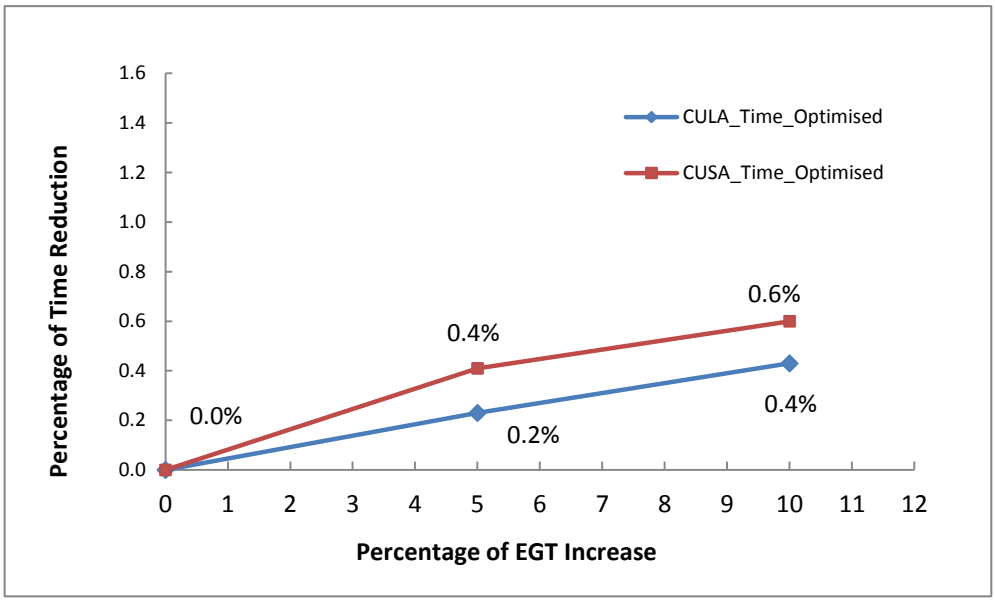

Figure 7-2 Reduction in flight time for different degraded engines compared to optimum trajectory of clean engine

NOx and contrails are a global concern, so it is interesting to observe that for the long range aircraft a significant reduction in the NOx formation by 0.7% and 1.2% was observed, whereas the short range aircraft achieved even greater reductions of 1.2% (i.e. 0.2kg) and 1.9% (i.e. 0.3kg) for the same EGT levels of degradation. NOx emission was assessed for the complete mission as it is important to understand the emission of NOx in the upper atmosphere in addition to LTO cycle. However NOx emission in LTO cycle was not separately calculated. Figure 7-3 shows the reduction in NOx emissions for long range and short range aircraft with different levels of degraded engines, when flying on optimum trajectories compared to flying on optimum trajectories of clean engines.

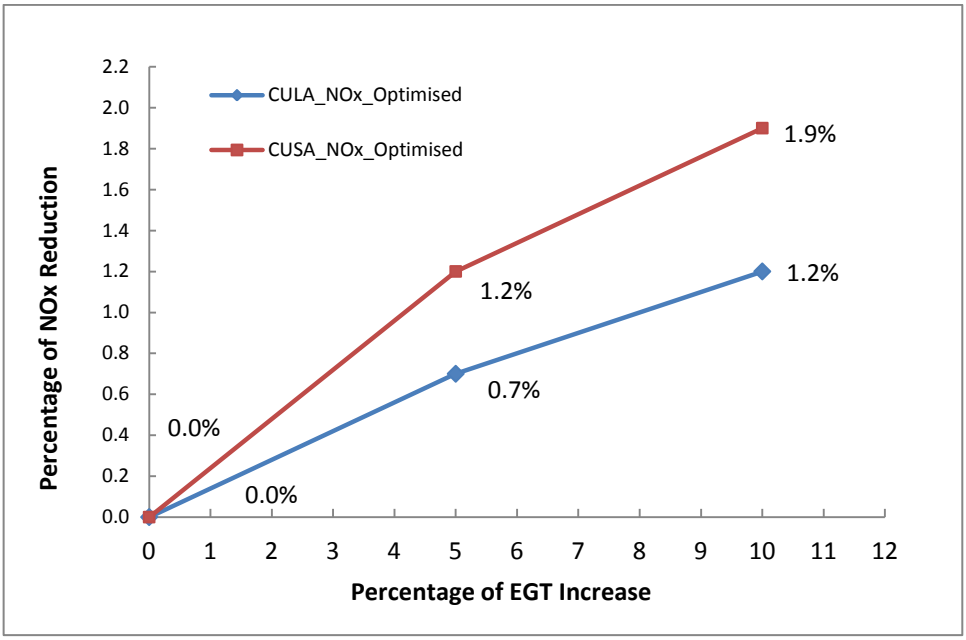

Figure 7-3 Reduction in NOx emissions for different degraded engines compared to optimum trajectory of clean engine

In all cases and based on the atmospheric profiles chosen, contrails were completely avoided by the both aircraft with a fuel penalty of 0.35% (233kg) and 0.8% (543kg) for long range and 0.6% (9kg) and 1% (16kg) for short range aircraft when engines were degraded by 5% and 10% EGT increase. Figure 7-4 shows the increase in fuel burn for zero contrails for long range and short range aircraft with different levels of degraded engines, when flying on optimum trajectories compared to flying on optimum trajectories of clean engines.

The overall results have shown the impact of engine degradation on optimum aircraft trajectories are significant and in order to reduce fuel burn and emissions, aircraft need to fly on an optimised trajectory customised for the degraded engine performance.

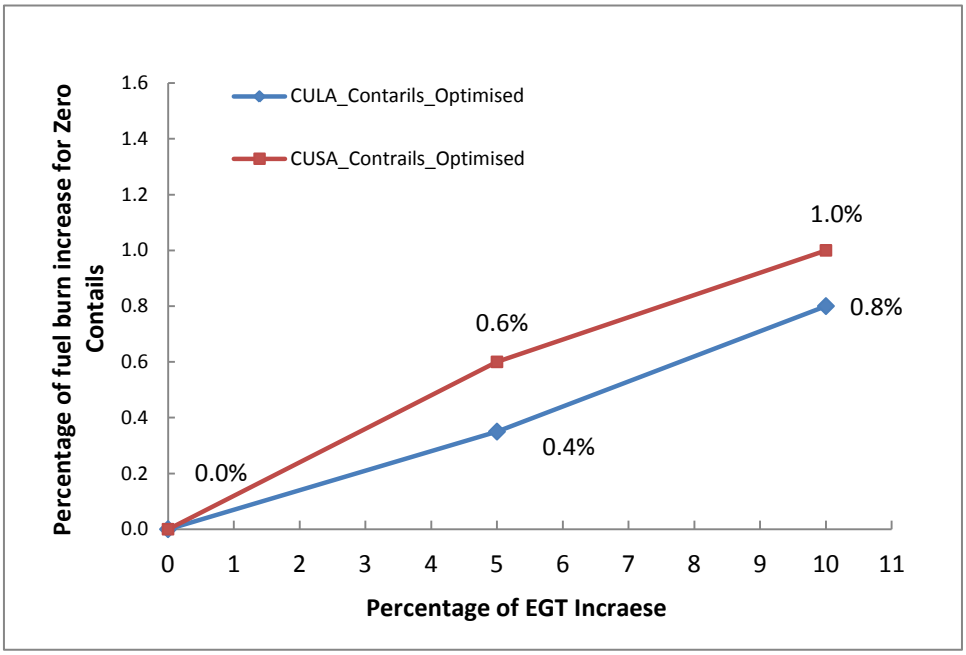

Figure 7-4 Increase in fuel burn for zero contrails with different degraded engines compared to optimum trajectory of clean engine

The main purpose of this research work and contribution to knowledge work was to provide a methodology to enhance the conventional approach of aircraft trajectory optimisation problem by including the degraded engine performance and real aircraft flight paths within the optimisation loop (framework) and thereby: assess the potential reduction of aircraft environmental impact in terms of fuel burn, NOx emissions and persistent contrail formation of aircraft in operation. Developed models, and integrated multi-disciplinary optimisation framework was successfully employed to assess the multi-objective aircraft trajectory optimisation problems to obtained the above results. Therefore work carried out proved the completion of the research objectives defined and set out in the introduction Chapter. Also the development of the multi-disciplinary optimisation framework with the approach of incorporating the degraded engine performance and real aircraft flight paths in optimisation provide an unique way of assessing the fuel burn, NOx and persistent contrails of aircraft currently in service.

7.2 Limitations and recommendations for further work

The results of the engine performance and trajectory analysis are subjected to several assumptions and limitations, which have been introduced in order to perform a feasible and comparable assessment. Therefore, recommendations from this research include the following;

7.2.1 Limitations of the current models and optimisation set up

- **Improving the engine performance model:** The code use for engine performance simulation TURBOMATCH provides many options to create variety of engine designs and architectures with extensive simulation capabilities. For the purpose of this study, the adopted engine models have been developed with many details as necessary to achieve practical representation of the desired real engines. However, no provisions have been made for advanced bleeds such as control bleeds, variable engine geometry or active clearance control which may allow for more realistic engine simulations, also in terms of transient engine performance. Therefore, developed engine models can produce only approximate results when simulating the engine off-design performance at very low thrust settings and idle conditions.

- **Improving the engine emission model:** The current emission prediction model incorporated within the framework uses the general P3T3 correlation based model to predict NOx emission. The other emissions such as CO, UHC have not been investigated. Even though this method has been well validated, it can be used only with for conventional combustor technology, where EINOx is established. If the framework use to investigate the emissions of aircraft engines with non-conventional combustors, a more sophisticated model such as physics based stirred reactor model needs to be incorporated.

- **Improving the optimiser:** The GA based optimiser used in this work has consistently provided efficient and good results for different setups and case studies in terms of convergence and diversity of solutions. However, when considering optimisation problems in which the number of variables is greatly increased may reveal limitations on the algorithm. Due to the inherent randomness of the search space of genetic algorithm (GA), increasing larger number of variables leads to require more evaluations to reach convergence to an optimum Pareto Front. Thus number of variables that can be changed will

depend on the computational resources available. Otherwise, improving the optimisation technique can help in scaling up the complexity of the optimisation problem. Techniques such as hybridisation of genetic algorithm with other classical search methods (in particular with direct search – gradient based methods) is one possible way forward. These hybrid techniques would take advantage of genetic algorithm to initially find for the most promising set of solutions, while the direct search , method would be used at a later stage to accelerate the converge to the final solution. In addition to the hybrid techniques there are possibilities of using other optimisation techniques. "Multi-Objective Tabu Search (MOTS)", and "Intelligent GA" are some other optimisation technique suitable for handling multi-objective optimisation problems with larger number of design space variables and it is an optimiser already tested and used within Clean Sky project for trajectory optimisation problems.

- **Multi-Objective Optimisation:** Another area need to be considered, is selection of number of objectives in the optimisation process. As the current study is focused on understanding and implementation of environmental friendly optimised trajectories, it is necessary to simultaneously consider the combined effects of fuel burn, gaseous emissions (NOx, CO_2), Contrails, Noise etc. Therefore more than two objectives need to be considered as conflicting objectives in the optimisation process of selecting the most suitable trajectory to be implemented in real operations.

7.2.2 Extending the Multidisciplinary optimisation framework with additional models

Additional models can further introduce some practical and new constraints to the trajectory optimisation problems of interest. Especially through models such as aircraft noise prediction model, weather model, engine life assessment model, aircraft maintenance, and economic (direct operating cost models).

- **Noise Prediction Model:** One of the Clean Sky objectives is to reduce noise generation from aircraft and engines. Therefore it would be interesting to perform an optimisation study with extending the aircraft trajectory optimisation setup with a noise model and optimise the trajectories for minimum noise as one of the objectives. This will help to assess the impact of aircraft noise in the vicinity of airport during landing and take-off cycles (i.e. LTO cycle). Further this noise model integrated framework can be used to analyse any trade-off that may be pertinent in terms of selecting the most environment friendly trajectories.

- **Global weather model / Climate model:** Aircraft are affected by the various weather conditions such as wind effects (head wind and tail wind) and adverse weather conditions. In adverse weather conditions aircraft are required to necessarily avoid weather patterns and hence fly sub optimal trajectories. Therefore in order to accommodate these complexities, framework may also incorporate a global weather or climate model. This will enable identifying the effects of various weather patterns may have constraints in achieving environmentally optimal trajectories and hence establish in terms of excess fuel burn or environmental impact (emissions).

- **Engine life prediction model:** Any aircraft engine demonstrates engine degradation from the time it commence operation due to various mechanisms. These mechanisms deteriorate the engine performance and affect the engine life and eventually lead to component failures. Thus it is important to investigate, the effect of engine degradation on engine life and fuel burn, by considering engine life as an optimisation objective. Also it is important to understand the implications of engine life when aircraft trajectories are optimised for other environmental objectives. Therefore author recommend to incorporating a life prediction model in the optimisation framework.

- **Economical Model / Direct Operating Cost (DOC) Model:** DOC is another important objective any airline wants to investigate. A key drive to lower the operating cost is a considerable reduction in fuel burn. But maintenance cost will inevitably rise with engine degradation and engine life deterioration which are main components of DOC. Further study of the trade-off between emissions and DOC is therefore recommended.

- **Real time Optimisation:** At the moment the above aircraft trajectory optimisations carried out are not in real time. A new methodology or framework can be built which allows real time optimisation without updates or modifications to the original flight plans due to any possible changes in flight constraints including unexpected changes in weather, air traffic control or delays in flight landing and operations.

REFERENCES

Acker, F., Saravanamuttoo, H. I. H., (1987), "Predicting of gas turbine performance degradation due to compressor fouling using computer simulation techniques", ASME 88-GT 206, USA

Airbus Report (2004), "Bird Strike Threat Awareness: Flight Operational Environments," Airbus Customer Service, October 2004

Airplane Characteristics – A320-200 (2005), Technical Data Support and Services, Issue Sep. 30/85, Rev. Sep. 01/10, Airbus Group France

Airplane Characteristics – A340-300 (2005), Technical Data Support and Services, Issue Mar. 30/05, Rev. Nov. 01/11, Airbus Group France

Aker, G.F., and Saravanamuttoo, H.I.H., "Predicting Gas Turbine Performance Degradation due to Compressor Fouling Using Computer Simulation Techniques," Transactions of the ASME: Journal of Engineering for Gas Turbine and Power, Vol. 111, pp. 343-350, 1989

Al-Gani, A., Kassem, A.H., (2007), "On the Optimisation of Aerospace Plane Ascent Trajectory", No. 168, Transaction of the Japanese Society of Aeronautical and Space Science, Vol. 50, p113

Appleman, H., (1953), "The formation of exhaust contrails by jet aircraft," Bulletin of American Meteorological Society, pp. 14 – 20, 1953

Audet, C., and Dennis, J. E. Jr., (2006), "Mesh Adaptive Direct Search Algorithms for Constrained Optimisation," SIAM Journal on optimisation, Vol 17, No. 1, pp. 188-217

Betts, T. J., (1998), Survey of Numerical Methods for Trajectory Optimisation, Journal of Guidance, Control and Dnamics, Vol. 21, No. 2, March-April 1998

Bramlette, M.F., and Bouchard, E.E., (1991), Genetic Algorithms in Parametric Design of aircraft, Lawrence Davis (ed), Handbook of Genetic Algorithms 1991, pp. 109-123

Boyle, R. J., Senyitko, R. G., (2003), "Measurements and Predictions of Surface Roughness Effects on Turbine Vane Aerodynamics", Proceedings of ASME Turbo Expo 2003, GT2003-38580 Atlanta, GA

Brasseur, G. P., et. al., (1998), European Scientific Assessment of the Atmosphere Effect of Aircraft Emissions, Atmospheric Environment Vol. 32, No. 13, pp. 2329 - 2418

Brun, K., and Nored, M., (2011), "Particles Transport Analysis of Sand Ingestion in Gas Turbine Engines", Proceedings of ASME Turbo Expo 2011, Jun 6-10, Canada GT2011-45057

Bunday, B. D., (1984), Basic Optimisation Methods, Edward Arnold, London UK

Camilari, W., and Pervier, H., (2012), Specifications of contrail model, WP3.1 Report O_3.1_25-a/SGO-WP3.1-CU-OUT-0248-A of SGO-ITD Clean Sky, Cranfield University, UK

Celis, C., (2010), Evaluation and Optimisation of Environmentally Friendly Aircraft Propulsion Systems, PhD, School of Engineering, Cranfield University, UK

Celis, C., (2014), Theoretical Optimal Trajectories for Reducing the Environmental Impact of Commercial Aircraft Operations, Journal of Aerospace Tech. Mang Vol. 6, No. 1, pp. 29-42 Jan-March 2014

Celis, C., (2009), Gaseous Emission Formation Model, Clean Sky Systems for Green Operations, ITD WP3.1 Deliverable Report D3.1.2_1

Celis, C., Moss, B., Pilidis, P., (2009), "Emission Modelling for the Optimisation of Green Aircraft Operations", Proceedings of ASME Turbo Expo 2009, Power for Land, Sea and Air, Orlando, Florida, USA GT2009-59211

CFM (2011) CFM Technical specification engine database, available at: http://www.cfm56.com/products/cfm-technical-data, sourced on 26 April 2011

CFM (2014) CFM56-5B4 and CFM56-5C4 Engine Performance Data Report, Engineering and Flight Operations, Sri Lankan Airlines

Chandran, S., (2013), "Effects of engine degradation on engine and aircraft performance, MSc Thesis, School of Engineering Cranfield University UK

Chen, X., and Hutchinson, J. W., (2002), "Particle Impact on Metal Substrates with application to Foreign Object Damage to Aircraft Engines", Journal of Mechanics and Physics of Solids, 50 (2002) 2667-2690

Chircop, K., Xuereb, M., Zammit-Mangion, D., (2010), "A Generic Framework for Multi-Parameter Optimisation of Flight Trajectories", 27th Int. Conference of the Aeronautical Sciences 2010

Clark, J. P., (2003), "The role of advanced air traffic management in reducing the impact of air craft noise and enabling aviation growth", Journal of Air Transport Management, 9(3), 161-165 (2003)

Clean Sky (2010), Description of Work, WP3 Mission and Trajectory Management, Systems for Green Operation ITD, Clean Sky Project Framework Programme 7

Clean Sky SGO-ITD (2013), Model Description of Aircraft Dynamic Model for 3D Trajectories, WP 3.1Model and Tools, Systems for Green Operations, Clean Sky

Cook, A., (2007), European Air Traffic Management: Principles, Practices and Research, Ashgate, Aldershot ISBN: 978-0754672951

Deb, Kalyanmoy (2010), Optimisation for Engineering Design, Algorithms and Examples, by PHI Learning, New Delhi

Deb Kalyanmoy (2002), Multi Objective Optimisation using Evolutionary Algorithms, John Wiley and Sons, New York USA

Deb, K., Pratap, A., Agrawal, S., and Meyarivam, T., (2002), "A Fast and Elite Multiobjective Genetic Algorithm: NSGA11, IEEE Transactions on Evolutionary Computation, pp. 2:182-197

Deb, K., Pratap, A., Agrawal, S., and Meyarivan, T., (2007), A fast and Elitist Multiobjective Genetic Algorithm: NSGA-II, IEEE Transactions on Evolutionary Computations, Vol. 6., November 2002., pp 182-197

DuBois, D., and Paynter, G. C., "Fuel Flow Method II for Estimating Aircraft Emissions," Society of Automotive Engineers TP 2006-01-1987, Warrendale PA, Aug. 2006

Dunn, M. G., Padova, C., Moller, J. G., and Adams, R. M., "Performance Deterioration of Turbofan and a Turbojet Engine upon Exposure to Dust Environment," Journal of Engineering for Gas Turbine and Power, Vol. 109, No. 2, 1987, pp. 336-343

Eliaz, N., Shemesh, G., and Latanision, R. M., (2002), "Hot corrosion in gas turbine components", Journal of Engineering Failure Analysis 9 (2002) 31-43

Epstein, A., (2013), "Why the environment need gas turbine engines", Key Note Speech, International Gas Turbine Conference, ASME IGTI, June 2013 San Antonio, Texas

European Commission (2010), Aeronautical and Air Transport Research, 7th Framework Programme 2007-2013, Project Synopsys, Vol. 1 Office, Directorate – Com. Unit Brussels

Fletcher, R., (1987), "Practical Methods of Optimisation", Second Edition, John Willy, Chichester, United Kingdom

Flight Aware (2015), "Flight Aware Live Flight Tracking", August 2015, Online Available; http:/uk.flightaware.com, Accessed August 2015

Fonseca, C. M., Fleming, P. J., (1993) "Genetic Algorithms for Multi Objective Optimisation Formulation, Discussion and Generalisation of Genetic Algorithm", Proceedings of the Fifth International Conference (S. Forrest, ed.), San Mateo, CA: Morgon Kaufmann, July 1993

Gas Turbine Engineering Group, 2008 "The TURBOMATCH Scheme", TURBOMATCH, User's Manual, School of Engineering – Cranfield University

Giannakakis, P., (2009), Hermes V5 and TurbomatchCalls V3 User manual, Department of Power and Propulsion, Cranfield University, UK

Green, J. E., (2003), "Civil Aviation and the Environmental Challenge", The Aeronautical Journal, June 2003, pp. 281 – 299

Gu, W., (2013), "Evaluation of optimised flight trajectories for conventional and novel aircraft and engine integrated systems," PhD Thesis, Department pf Power and Propulsion, School of Engineering, Cranfield University UK

Gu, W., Navaratne, R., Quaglia, D.,Sethi, V., Zammi-Mangion, D., (2012), Towards Development of a Multi-Disciplinary Flight Trajectory Optimisation Tool – GATAC, Proceedings of ASME Turbo Expo GT2012-69862, June 11-15, 2012, Denmark

Hamed, A., Tabakoff, W., (2006), "Erosion and Deposition in Turbomachinery", Journal of Propulsion and Power, Vo. 22, No. 2, March – April 2006

Hartjes, S., Quaglia,D., Madani, I., Nalianda, D., Sammut, M., (2011), Performance Analysis of Optimised Trajectories, Report SGO-WP-3.2.2-C-U-DEL-0039-B1, Clean Sky SGO ITD

Holland, J. H., (1975) Adaptationin Natural and Artificial Systems, First Edition, University of Michigan Press, Michigan, USA

ICAO (2006), International Civil Aviation Organisation, Procedures for Aircraft Navigation Services – Aircraft Operations – Flight Procedures – Volume 1, 5th Edition 2006

ICAO (2006), International Civil Aviation Organisation, Procedures for Aircraft Navigation Services – Aircraft Operations – Flight Procedures – Volume 2, 5th Edition 2006

ICAO (2010), Presentation by the ICAO Environmental Branch at ICAO Technology Goals process for Aviation Environmental Protection, ICAO Montreal, Canada, Available at www.icao.int/CLO10/Docs/3 Jahangir_icao.pdf, accessed on 20 July 2012

ICAO (2013), International Civil Aviation Organisation Engine emission Certificate of CFM engines (CFM56-5B4 and CFM56-5C4) available on Engine Exhaust Emission Data Bank, Ref 09/04/2013

Jacobsen, M., Ringertz, T., (2010), "Airspace Constraints in Aircraft Emission Trajectory Optimisation", Journal of Aircraft, Vol. 47, No. 4, July – August 2010

Kelaidis M., Aretakis, N., Tsalavoutas, A., and Mathioudakis, K., (2009), "Optimal mission analysis accounting for engine aging and emissions," Journal of Engineering for Turbine and Power (ASME), Vol. 131, January 2009

Khun, M., (2010), ICAO to examine timeline for aircraft CO2 standard, Available at http://www.flightglobal.com/articles/2010/02/22/338681/icao-to-examine-timeline-for-aircraft-co2-standard.htmi (accessed on August 2011)

Kurz, R., and Burn, K., (2001), "Degradation in Gas Turbine Systems", Journal of Engineering for gas Turbine and Power, January 2001 Vol. 123/77

Lattime, S. B., Steinetz, B. M., (2002), "Turbine Engine Clearance Control System: Current Practice and Future Directions", NASA Report AIAA-2002-3790

Lee, D. S., et al., (2009) Aviation and Global Climate Change in the 21st Century, Atmospheric Environment, Vol. 43, Issue 22-23, July 2009 pp. 3520-3537

Leylekian, L., Lebrun, M., Lempereur, P., (2014), "An Overview of Aircraft Noise Reduction Technologies", Journal of Aerospace, Issue 7, June 2014, pp. 1-15

Liu, W., and Hwang, I., (2011), "Probabilistic Trajectory Prediction and Control Detection for Air Traffic Control", Journal of Guidance, Control and Dynamics, Vol. 34, N. 6, November – December 20111

Lukachko, S.P., and Waitz, A., (1997), "Effects of engine aging on aircraft NOx emissions", International Gas Turbine & Aeroengine Congress, 97-GT-386, June 2-5, 1997, Florida

MacMillan, W., (1974) "Development of a modular type computer program for the calculation of gas turbine off design performance", PhD Thesis, School of Engineering, Cranfield University, UK

Mao, R. H., Meguid, S. A., and Ng, T. Y., (2009), "Effects of Incident Angle in Bird Strokes on Integrity of Aero Engine Fan Blade" International Journal of Crashworthiness 14(4), 295-308

Mattingly, J. D., (1996), "Elements of gas turbine propulsion", McGrow Hill Series in Aeronautical and Aerospace Eng. McGrow Hill Books Co., Singapore

Miki, S., Takano, H., Baba, Y., (2002), Trajectory Optimisation for an Aircraft with Genetic Algorithm, Proceedings of Aircraft Symposium, Vol. 40, pp. 119-122

Mund, F. C., and Pilidis, P., (2006), "Gas turbine compressor washing; Historical development, trends and main design parameters for online system", Journal of Engineering for Gas Turbine and Power 128(2), 344-353

Naeem, M., (2008), Impact of Low Pressure (LP) Compressor Fouling of a Turbofan upon Operational effectiveness of a Military Aircraft", Journal of Applied Energy 85 (2008), 243-270

Naeem, M., (1999), "Impact of Aero Engine Deterioration for Military Aircraft's Performance", PhD Thesis, School of Engineering, Cranfield University, UK

Nalianda, D., (2012), Impact of Environmental Taxation Policies on Civil Aviation – A Techn_Economic Environmental Risk Assessment, PhD Thesis, Cranfield University UK

Navaratne, R., Tessaro, M., Gu, W., Sethi, V., Pilidis, P., Sabatini, R., (2013), Generic Framework for Multi-disciplinary Trajectory Optimisation of Aircraft and Power Plant Integrated Systems, Journal of Aeronautics and Aerospace Engineering, Vol. 2:1, 2013

Navaratne, R., Camilleri, W., Sethi, V., Pilidis, P., (2013), Preliminary Aero Engine Life Assessment Via Techno-economic Environmental Risk Assessment, Proceedings of ASME Turbo Expo 2013, GT2013-94830, June 3 – 7, 2013, Texas USA

Norman, P. D., (2003), Development of technical basis for a new Emissions Parameter covering the whole AIRcraft operation: NEPAIR, Final Technical Report NEPAIR/WP4/WPR/01, "Competitive and Sustainable Growth" Programme (1998-2002), UK

Norvig, P., and Russell, S., (2003), Artificial Intelligence: A Mordern Approach, Second Edition, New Jersey, Prentice Hall, 2003

Nqobile, K., (2014), "Influence of airport factors and mission fuel burn optimised trajectories on severity and engine life," PhD Thesis, School of Aerospace, Transport and Manufacturing, Cranfield University UK

Nuice, A., (2012) "User Manual for Base of Aircraft Data (BADA) revision 3.10," Eurocontrol, 2012

Palmer J. R., and Pachidis V., (2005) "The turbomatch scheme: for aero/industrial gas turbine engine design point/off design performance calculations", Cranfield University, UK

Patra, K., (2014), Multi-Disciplinary Aircraft Trajectory Optimisation using a Hybrid Based Optimiser, PhD Thesis, School of Engineering, Cranfield University, UK

Patra, K., Navaratne, R., (2012), "Performance Assessment of NSGAMO2 and MOTS on ZDT Functions – Benchmarking Report," WP3.2, SGO-ITD, Clean Sky

Penner, J. E., Lister, D. H., Griggs, D. J., and McFarland, M., (1999), "Aviation and Global Atmosphere", A Special Report, IPCC Working Groups I and III, 1999

Pervier, H., Nalianda, D., Espi, R., Sethi, V., Zammit-Mangion, D., Jean-Michel, R., Entz, R., (2011), "Application of Genetic Algorithm for Preliminary Trajectory Optimisation", SAE International Journal of Aerospace, Vol. 4. Issue 2, November 2011

Pervier, H., (2013) PhD Thesis, Emission Modelling for Engine Cycle and Aircraft Trajectory Optimisation, Department of Power and Propulsion, School of Engineering, Cranfield University, UK

Peters, J. O., and Ritchie, R. O., (2000), "Influence of Foreign Object Damage on Crack Initiation and Early Crack Growth during high cycle fatigue of Ti-6Al-4V", Journal of Engineering Fracture Mechanics 67 (2000) 193-207

Qing, L.,Wei, G., Yuping, L., and Chunlin, S., (1997), Aircrfat Route Optimisation using Genetic Algorithms, Genetic Algorithms in Engineering Systems: Innovations and Applications, 2 – 4 September 1997, Glasgow, UK

Quagliarella, D., (1998), Genetic Algorithms and Evolution Strategy in Engineering and Computer Science, Recent Advances and Industrial Applications, John Wiley, Chichester, UK

Rao, S. S., (1996), Engineering Optimisation: Theory and Practice, Third Edition John Wiley, New York, 1996

Schumann, U., (1996), “On conditions for contrails formation from aircraft exhaust”, Meteorol. Zeitschrift, vol. 5, pp. 4-23, February 1996

Saravanamuttoo, H.I.H., (2009), “Gas Turbine Theory”, 6th Edition, Pearson Education Limited, England

Schwefel, H. P., (1981), Numerical Optimisation of Computer Models, John Wiley, Chichester, United Kingdom

Segovia Blat C. M., (2012), “Effect of Engine Degradation on Fuel Burn Optimum Civil Aircraft Trajectories, MSc Thesis, Cranfield University, UK

SESAR (2008), “SESAR (Single European Sky ATM Research) Consotium Master Pla, SESAR Definition Phase, Milestone Deliverable 5,” April 2008

Shull, J. D., (1998), “A validation study of the Air Force Weather Agency (AFWA), JETRAX Contrail Forecasting Algorithm,” Ohio, MSc Thesis, 1998

Singh, R., (2009), Gas Turbine Combustors Volume 1, School of Engineering, Department of Power and Propulsion, Cranfield University, UK

Soler, M., Olivers, A., Staffetti, E., and Zapata, D., (2012) “Framework for Aircraft Trajectory Planning Towards an Efficient Air Traffic Management,” Journal of Aircraft Vol. 49, No. 1, January-February 2012

Soler, M., Olivares, A., and Staffetti, E., (2012), “Hybrid Optimal Control Approach to Commercial Aircraft Trajectory Optimisation,” Journal of Guidance, Control and Dynamics, Vol 33, No. 3, May-June 2010

Sridhar, B., Ng, H. K., Chen, N. Y., (2011), “Aircraft Optimisation and Contrail Avoidance in the Presence of Winds”, Journal of Guidance, Control, and Dynamics, Vol. 34, No. 5, September – October 2011

Thrasher, T., (2010), Presentation by the ICAO Environmental Branch at ICAO Colloquium on Aviation and Climate Change (12th May 2010), Available at, www.icao.int/CLQ10/Docs/3_Jahangir_icao.pdf, accessed on 20th July 2011

Torres, R., Chaptal, J., (2011), “Optimal, Environmentally Friendly Departure Procedures for Civil Aircraft”, Journal of Aircraft, Vol. 48, No. 1, January – February 2011, pp. 11 – 22

Tsotskas, C., Kipouros, T., Savill, M., (2013) Biobjective Optimisation of Preliminary Aircraft Trajectories, R.C. Purshouse et al. (Eds.): EMO 2013, LNCS 7811, pp. 741–755, 2013.

Venediger B., (2013), Civil aircraft trajectory analysis – Impact of engine degradation on fuel burn and emissions, MSc Thesis, School of Engineering, Cranfield University, UK

Visser, H. and Wijnen, R., (2001), "Optimization of Noise Abatement Arrival Trajectories". Journal of Aircraft, 38(4), pp. 620-627

Walsh, G. P., (1975), Methods of Optimisation, John Wiley, London, UK

Yokoyama, N., (2001), Flight Trajectory Optimisation Using Genetic Algorithm Combined with Gradient Method, Journal of Information Technology for Economics and Management, Vol. 1, No 1, 2001 Paper 10, 2001

Yupu, G., Wei, C., Deping, G., (2008), "Foreign Object Damage to Fan Rotor Blades of Aero-engine Part II: Numerical Simulation of Bird Impact", Chinese Journal of Aeronautics 21(2008) 328-334

APPENDICES

Appendix A – Standard Instrument Departure and Arrival Charts

Appendix A-1 Standard Departure Instrument Chart (SID) – London Heathrow

Appendix A-2: Standard Instrument Arrival Chart of CBI Airport Sri Lanka

Appendix A-3: Standard Instrument Departure London Heathrow Brookmans Park

Appendix A-4: Standard RNAV Instrument Arrival Chart AIP Netherlands

Appendix A-5: Standard Instrument Approach Chart Schiphol Netherlands

Appendix B – Publications

Appendix B-1: Preliminary aero engine life assessment via Techno-economic Environmental Risk Analysis

Appendix B-2: Generic Framework for Multi-Disciplinary Trajectory Optimisation of Aircraft and Power Plant Integrated Systems

Appendix B-3: Towards the Development of a Multi-disciplinary Flight Trajectory Optimization Tool — GATAC

Appendix B-4: Full Trajectory Optimisation of a Commercial Aircraft Considering Three-Objectives

Appendix A-1 Standard Departure Instrument Chart (SID) – London Heathrow

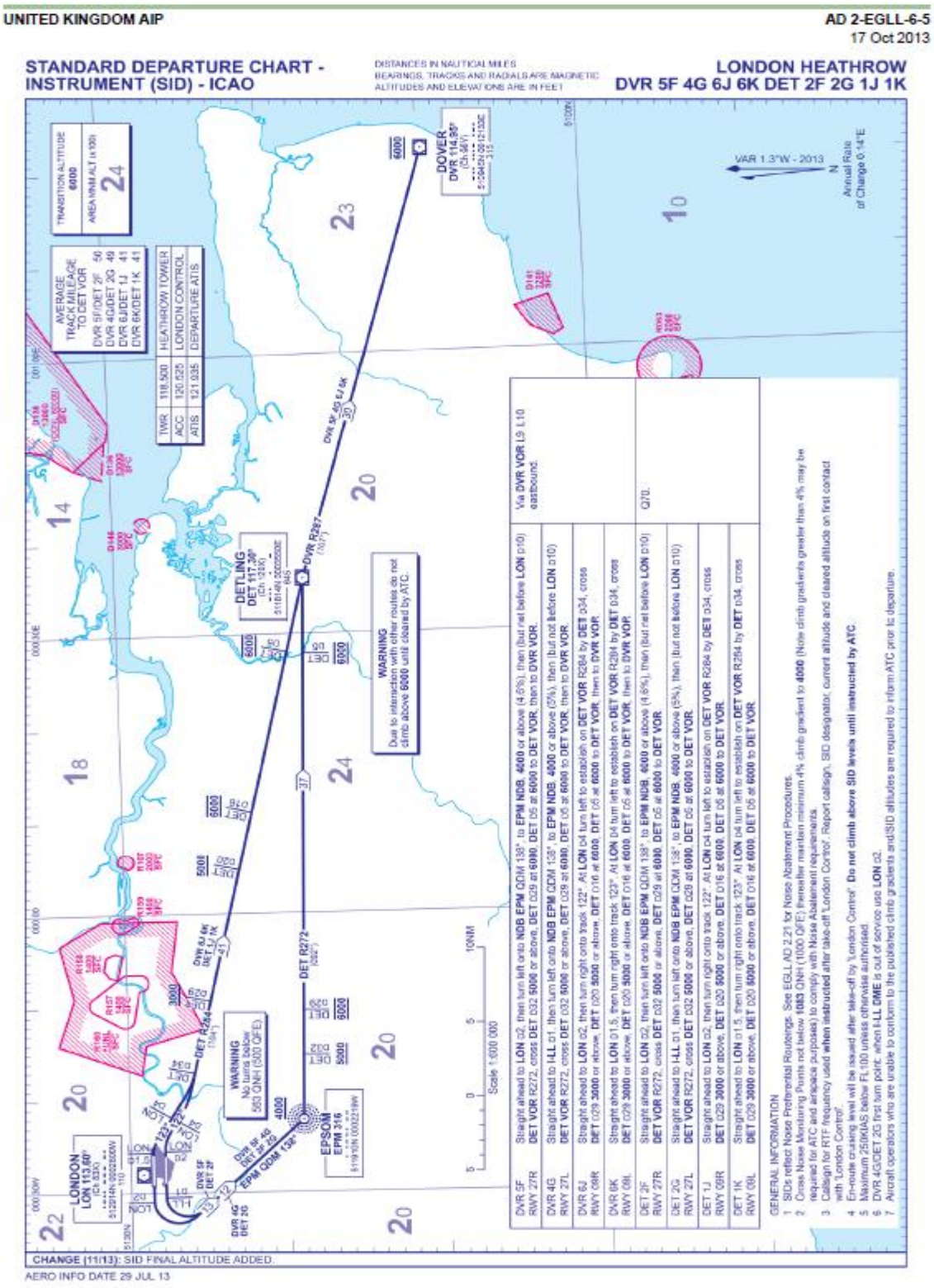

Appendix A-2: Standard Instrument Arrival Chart of CBI Sri Lanka

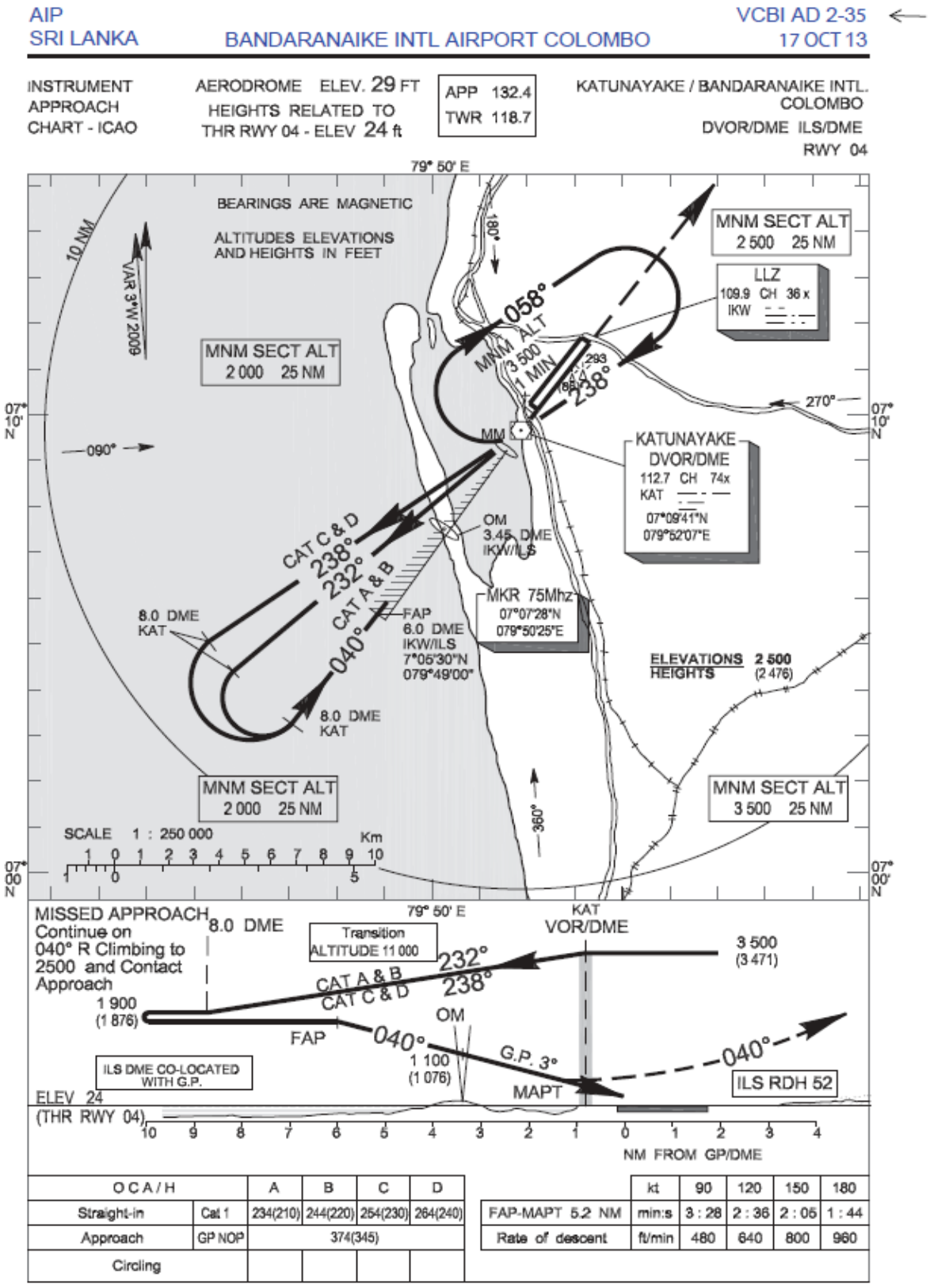

Appendix A-3: Standard Instrument Departure Chart – London Heathrow

Brookmans Park

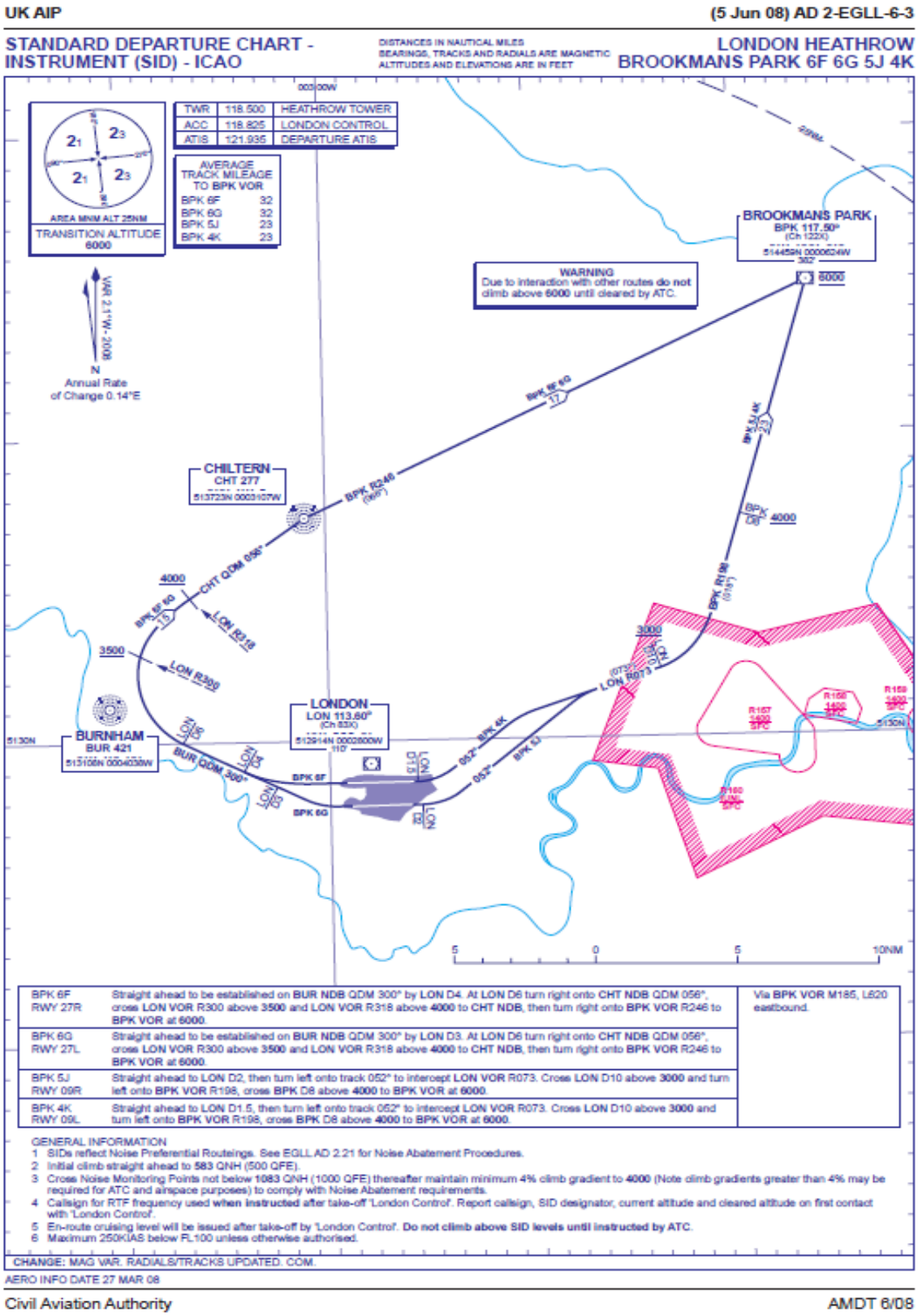

Appendix A-4: Standard RNAV Instrument Arrival Chart AIP Netherlands

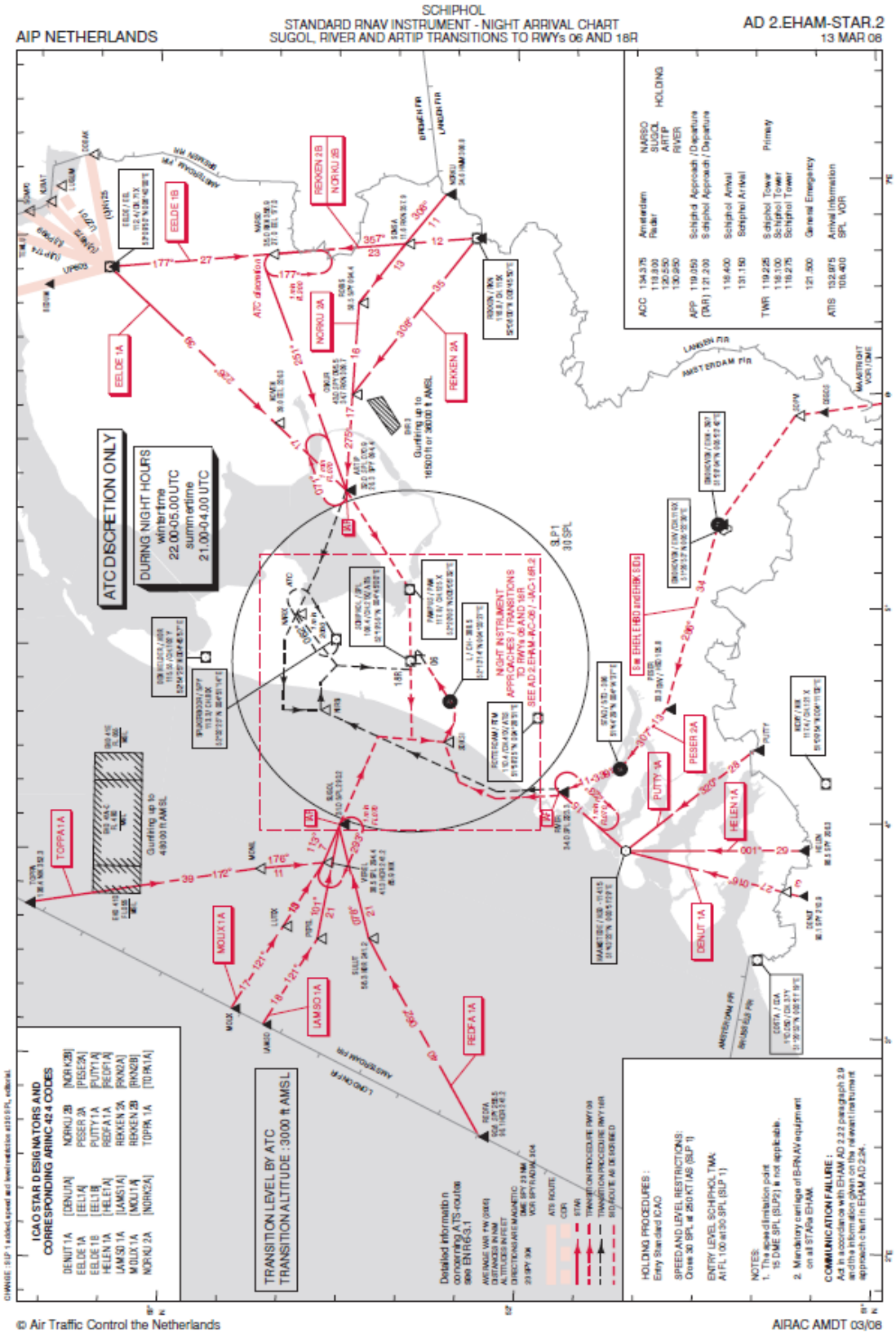

Appendix A-5: Standard Instrument Approach Chart Schiphol

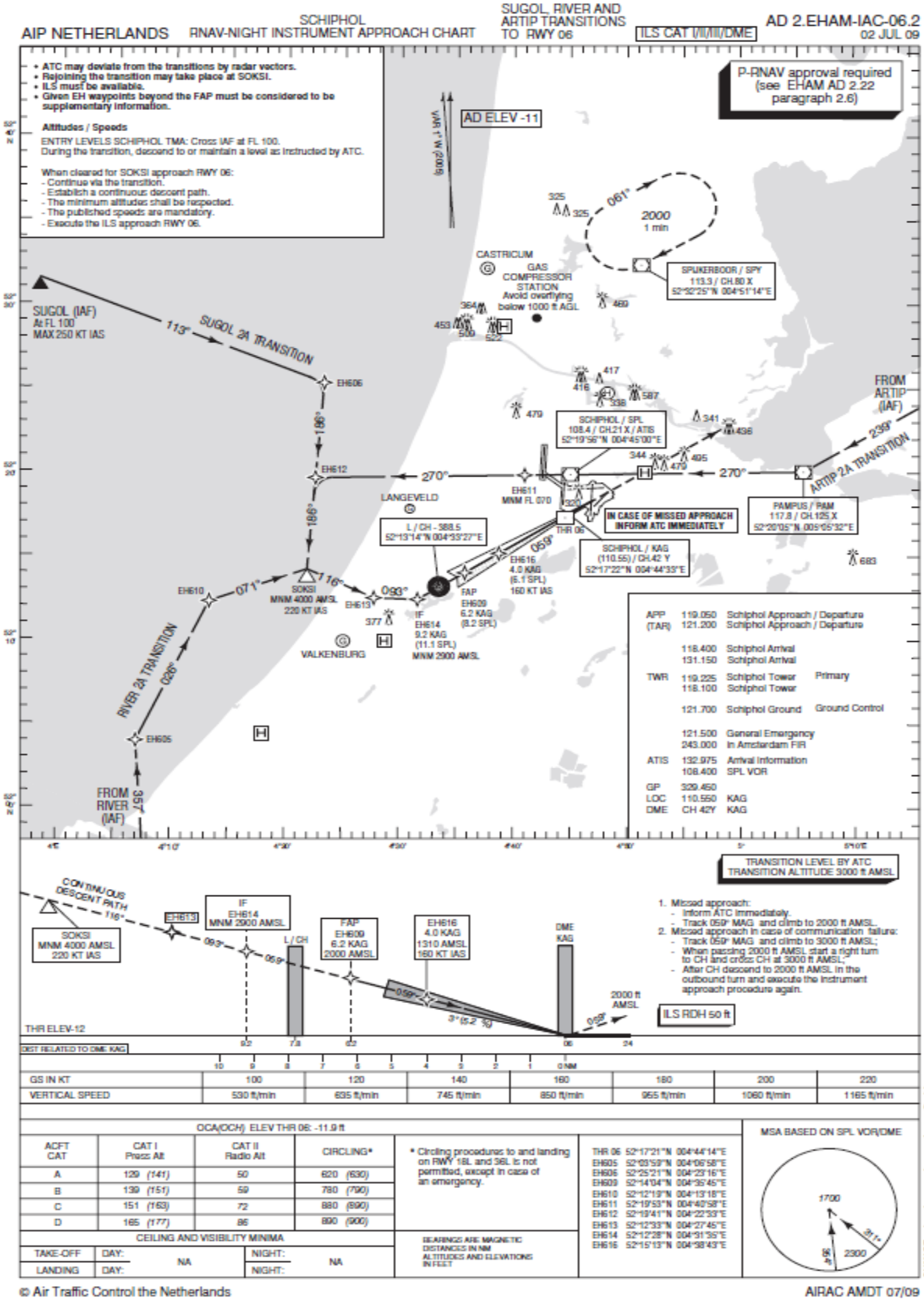

Appendix B-1

Proceedings of ASME Turbo Expo 2013
GT2013
June 3-7, 2013, San Antonio, Texas, USA

GT2013-94830

Preliminary Aero Engine Life Assessment via Techno-Economic Environmental Risk Assessment

Rukshan Navaratne, William Camilleri, Vishal Sethi, Pericles Pilidis
Department of Power and Propulsion
School of Engineering, Cranfield University, UK

Abstract

Significant progress has been made towards the improvement of engine efficiency through the increase in overall pressure ratio (OPR) and reduction in specific thrust (SFN). The implications of engine design extend beyond thermodynamics and should include the consideration of multi-disciplinary aspects related to operation, emissions, lifing and cost. This paper explores the relationship between fuel burn and engine life across the design space of a typical aircraft engine integrated system.

In this context the Cranfield University Techno-economic Environmental Risk Analysis (TERA) methodology allows for the assessment of environmental and economic risk when the design of an engine system is at its conceptual stage. It is essentially a multi-disciplinary optimization framework which can be used for design space exploration. Such an approach is necessary in order to assess the trade-off between asset life and powerplant efficiency at the preliminary stage of the design process.

A parametric study was conducted in order to assess the sensitivity of major design parameters on engine life and specific fuel consumption (SFC) for a given engine type. The principal failure modes of creep, fatigue and oxidation, were considered for engine life estimation. In addition an optimization study was carried out in order to investigate the trade-off between fuel burn and engine life as Time Between Overhaul (TBO). This was accomplished by integrating aircraft performance, engine performance and lifing models in the TERA Framework.

An increase in turbine entry temperature (TET) is required to maintain efficiency at OPR. However, as TET has a strong influence on engine life there is an important trade-off to be made against engine efficiency. The parametric study outlined in this work explores the design space both with respect to engine life as well as efficiency. The optimization study showed that a penalty of 1.42kg additional fuel is required per additional hour of TBO. The fuel penalty is a consequence of sub-optimal design parameters with respect to engine efficiency and is applicable for the presented engine aircraft combination.

Appendix B-2

Journal of Aeronautics and Aerospace Engineering

Vol. 2, Issue 1 pp. 1-14. Issue 1, 2013, ISSN: 2168-9792 DOI: 1000103

Generic Framework for Multi-Disciplinary Trajectory Optimisation of Aircraft and Power Plant Integrated Systems

Rukshan Navaratne[1], Marco Tessaro[1], Vishal Sethi1, Pericles Pilidis[1],

Department of Power and Propulsion,

Roberto Sabatini[2] David Zammit-Mangion[2]

Department of Aerospace Engineering, Cranfield University, UK

Abstract

Engineering improvements, technology enhancements and advanced operations have an important role to play in reducing aviation fuel consumption and environmental emissions. Currently several organisations worldwide are focussing their efforts towards large collaborative projects whose main objective is to identify the best technologies or routes to reduce the environmental impact and fuel efficiency of aircraft operations. The paper describes the capability of a multi-disciplinary optimisation framework named GATAC (Green Aircraft Trajectories under ATM Constrains) developed as part of the Clean Sky project to identify the potential cleaner and quieter aircraft trajectories.

The main objective of the framework is to integrate a set of specific models and perform multi-objective optimisation of flight trajectories according to predetermined operational and environmental constraints. The models considered for this study include the Aircraft Performance Model, Engine Performance Simulation Model and the Gaseous Emissions Model. The paper, further discusses the results of a test case to demonstrate trade-offs between fuel consumption, flight time and NOx emissions that the trajectory optimization activity achieves at a primary level. It thereby forms the basis of a complete reference base-line trajectory which will be used to determine more accurate environmental gains that can be expected through optimisation with the integration of more models within the framework in the future.

Appendix B-3

Proceedings of ASME Turbo Expo 2012
GT2012
June 11-15, 2012, Copenhagen, Denmark

GT2012-69862

Towards the Development of a Multi-disciplinary Flight Trajectory Optimization Tool — GATAC

Weiqun Gu①, **Rukshan Navaratne**① Daniele Quaglia①, Yang Yu①, Kenneth Chircop②, Irfan Madani①Huamin Jia①, Vishal Sethi①, Roberto Sabatini①, David Zammit-Mangion①②

① - Cranfield University, ② - University of Malta

Abstract

Reducing the impact on the environment and the associated commercial implications are two major challenges that the global commercial aviation industry is addressing with significant commitment today. In this respect, Clean Sky, which is a €1.6 billion Joint Technology Initiative part funded by the European Commission is the largest ever programme addressing the greening of air transportation in response to the Advisory Council for Aeronautics Research in Europe (ACARE) goals of reducing CO_2 and perceived noise emissions by 50% and NO_x by 80% by 2020 compared to 2000 condition. This paper presents research work carried out within the "Systems for Green Operations", Integrated Technology Demonstrator (ITD) of Clean Sky Project, which is associated with GATAC, a trajectory and route planning tool to enable the multi-objective optimization of flight trajectories and missions. The design and operational methodology of the tool, the optimization algorithms and models are discussed and the results of a preliminary application for a long-range commercial flight are presented.

Appendix B-4

Full Trajectory Optimisation of a Commercial Aircraft Considering Three-Objectives

Abstract

Protection of the environment is a great concern in the 21st century. Considering the critical nature of the problem several solutions have been proposed and managing the trajectory and mission for existing aircraft is a promising approach. However most of the trajectory optimisation studies performed in this direction is limited to two objectives. Therefore this report investigates the trade-off of three objectives to minimise fuel burn, flight time and emissions which are conflicting by nature. These values are obtained by using a combination of well-established models under a common framework. The optimal trade surface is derived by employing a native multi objective optimiser: Multi Objective Tabu Search (MOTS-II). The results provide deeper insight into understanding how the trajectory schedule affects the trade-off between the objectives and how this knowledge should affect the future of aviation

1 Introduction

The concept of Aircraft Trajectory Optimisation (ATO) occurred since the beginning of aviation and still remains one of the hottest topics of the aviation industry. The main reasons are the excessive fuel consumption and the effects of pollutants in the atmosphere, which both affect the climate, environment, passengers and citizens. A number of significant initiatives have been set by the European Union and other large scale projects in order to reduce fuel burn and effects from the aircraft using multi-disciplinary optimisation of trajectories. However, it is noted that most of the trajectory optimisation studies is limited to two general mission tasks and limited to two objectives optimisation. To the best of author's knowledge, this is the first time a study involves three conflicting objectives is carried out and is still a matter of discussion. This will serve in better understanding of the implications among fuel burn, mission

time and emissions of a full trajectory by using a short range commercially available aircraft. This report will focus only on existing aircraft and the results obtained from this study have a twofold interpretation; on one hand, it is attempted to influence Air Traffic Control (ATC) in a sense to provide more flexibility for the flight plan, while securing aircraft separation – a major principle of ATC. The current ATC regulations should be adjusted so as to allow more space for aircraft to fly, and hence improve their overall performance under the given frame. In addition, the optimised trajectories can reshape the existing cost indexed trajectories or propose new (hopefully better) ones. On the other hand, given the current ATC envelop, the shape of the optimal trajectories can influence the current flight practices and /or affect the (re)design of certain parts of the aircraft in order to increase the flight performance. The proposed methodology is capable of simulating the trajectory performance of any defined aircraft configuration, within any defined mission. This is achieved by integrating aircraft performance model, engine performance model and emission prediction model along with multi objective optimiser under a common framework. The ultimate goal is to help in shaping the future of aviation by assessing the trade-off between, fuel burn, flight time and NOx emissions. The structure of the report as follows. The first section introduces all the tools and methods used to deliver environmentally friendly trajectories. Three models are described for a baseline aircraft and trajectory along with the optimisation settings and problem formulation. The next section presents the optimal aircraft trajectories obtained. These are compared each other and discussed.

2 Methodology

For the purpose of this study a number of models have been developed;

- The Aircraft Performance Model will be simulated by employing HERMES, which is configured to simulate the operation of an aircraft similar to Boeing 737-800. Also the schedule (speed and altitude values for different phases) of the trajectory is defined.
- TURBOMATCH will serve as an engine performance simulation code to develop the engine performance model similar to CFM56-7B27.
- The NOx emissions will be predicted by P3T3 Model, based on the same engine configuration and test performance data

- MOTS-II optimiser Multi Objective Tabu Search II algorithm was specifically turned for this trajectory optimisation case
- Coupling among the above models will achieved via a developed framework This will be linked with the following optimiser in order to carry out multi-objective optimisation of the performance metrics

2.1 Engine Performance Model

The engine performance model was developed based upon the CFM56-7B27 engine which is currently used to power the Boeing 737 twin engine single isle aircraft. The configuration of the model is two spool high bypass ratio turbofan engine with a booster stage, separate exhausts, custom bleeds and cooling bleed off-takes. The schematic of the engine is given in Figure 1 and while a summary of the main parameters are given in Table 1.

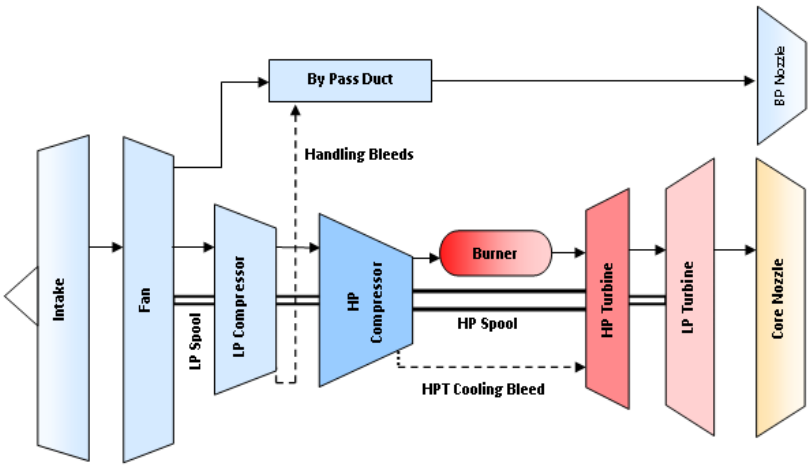

Figure 1 Schematic of the Engine model

The design point of the engine model was selected at top of climb (TOC) i.e. Alt: 10668 m, Mach number 0.8, and the pressure recovery of 0.99 under International Standard Atmospheric (ISA) conditions. Several iterations were performed using the model at design and off-design conditions to match the performance of the model with the data obtained from the public domain for the engine on which the design was based (CFM 2011, ICAO 2013)

The mass flow rate of the engine intake was estimated based on the measured nacelle area and assuming an average inlet Mach number of 0.55 – 0.65. The design point (at the top of climb) bypass ratio (BPR) and the turbine entry temperature (TET) were determined based on the overall pressure ratio (OPR) and the net trust at top of climb. The optimum fan pressure ratio (FPR) corresponding to the calculated TET, overall pressure ratio (OPR) and bypass pressure ratio (BPR) were also determined. In addition to the above, compressor pressure ratios, component efficiencies, and compressor bleeds for turbine cooling, custom bleeds, and other parameters, were guessed and iterated to match the required engine performance at design point and off-design (maximum take-off and cruise) conditions (CFM 2011, ICAO 2013). Finally, the model has been tested and validated against different off-design conditions such as several thrust ratings and corresponding fuel flow rates available in the public domain (CFM 2011, ICAO 2013). The validated engine model has been used to simulated many off-design conditions required by the aircraft performance model and emission model to calculate fuel burn and emissions for each flight segment as well as the full mission.

2.2 Aircraft Performance Model

The software that has been used to simulate the integrated aircraft-engine performance is called HERMES. It has been developed at Cranfield University in order to assess the performance of conventional aircraft and potential benefits of novel aircraft configurations (Hermes 2009). The code consists six different modules; (1) Input data, (2) Mission profile module, (3) Atmospheric module, (4) Engine data module, (5) Aerodynamic module, and (6) Aircraft performance module. The required input data comprises the basic information used to define the aircraft shape and the geometry, atmospheric data and finally the information of required mission profile (Hermes 2009). The user specified the climb schedule, cruise speed and altitude (including any stepped cruise requirements) and descent schedule of the aircraft. These input information passes to the atmospheric model and aerodynamic model to calculate the aerodynamic performances of the complete aircraft. The mission profile data is also used by the engine data model to determine the off-design operational conditions of the engine to calculate the engine performance required for various segments of the mission profile defined by the user. The information from the rest of the modules is passes to the aircraft performance module where the detailed figures are produced and the overall performance of the aircraft is computed. The output of the model includes, total fuel required to complete the given mission, flight duration, and distance covered for each flight segment. In addition, model is capable of producing components level engine performance parameters such as temperatures, pressures

and mass flows along with the overall engine thrust, and SFC (Giannakakis 2009). The baseline aircraft in this study is a short range, twin engine, and single aisle narrow body aircraft similar to Boeing 737-800 aircraft. A summary of the main characteristics are given in Table 2. The complete flow chart of the HERMES aircraft model is shown below in Figure 2.

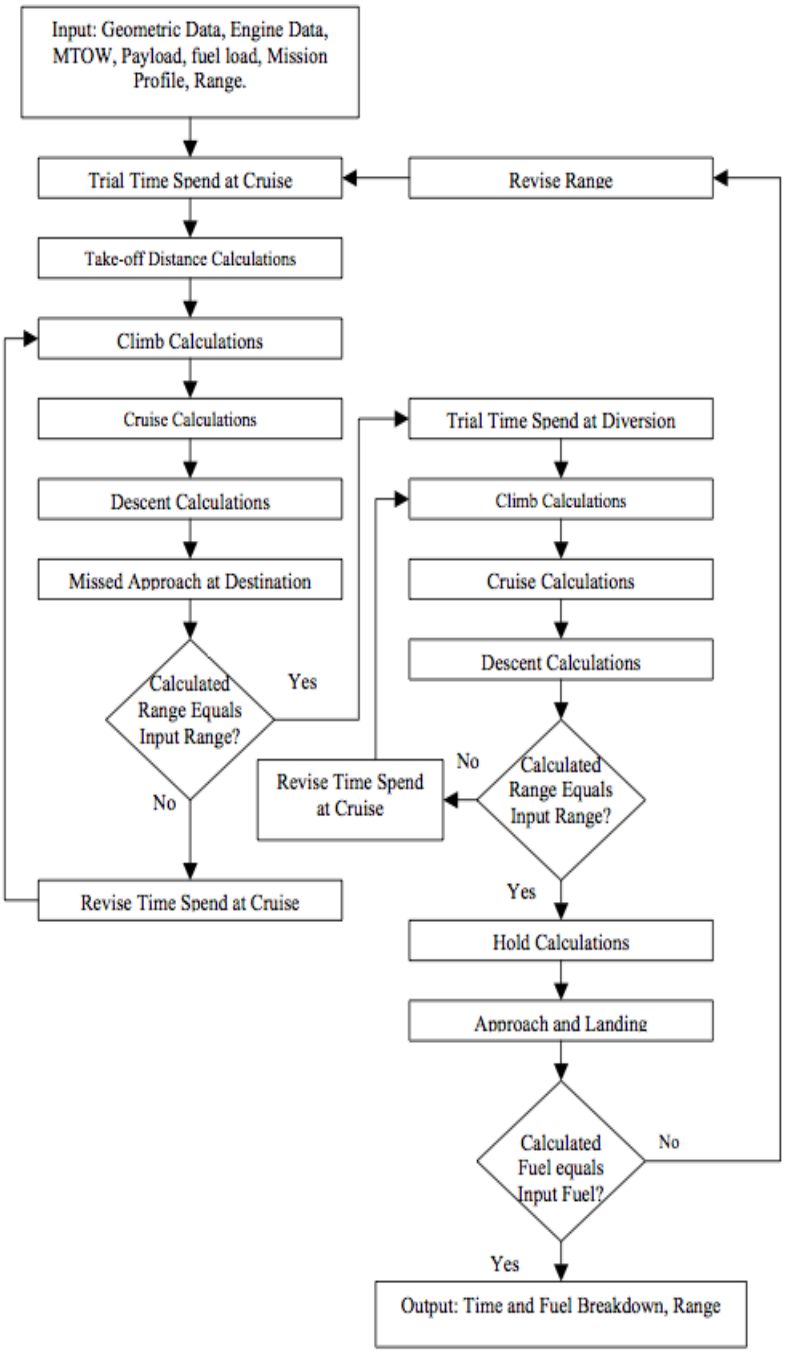

Figure 2: Hermes aircraft performance model flow chart

2.3 Emission Prediction Model

Emission prediction model use in this work is the P3T3 empirical correlation model. This model estimates the level of the emissions at altitude using a correlation with the emissions measured at ground level (ICAO 2010, Norman 2003). This methodology is straightforward. Firstly during the certification test of the engine the emission indexes are measured. Then, it is required to correct them to take into the combustion parameters for the operating condition at both ground level and altitude. These parameters are: burner inlet pressure (P3) and Temperatures (T3), fuel air ratio (FAR) and fuel flow (FF). In addition model takes into account the variation of humidity from the sea level to altitude. The model is capable of prediction of all the emissions and in this paper main focus given to NOx emissions only (Pervier 2013). Emission model sketch shows the calculation of the corrected emission index NOx (EINOx) at altitude (Norman at. el, 2003).

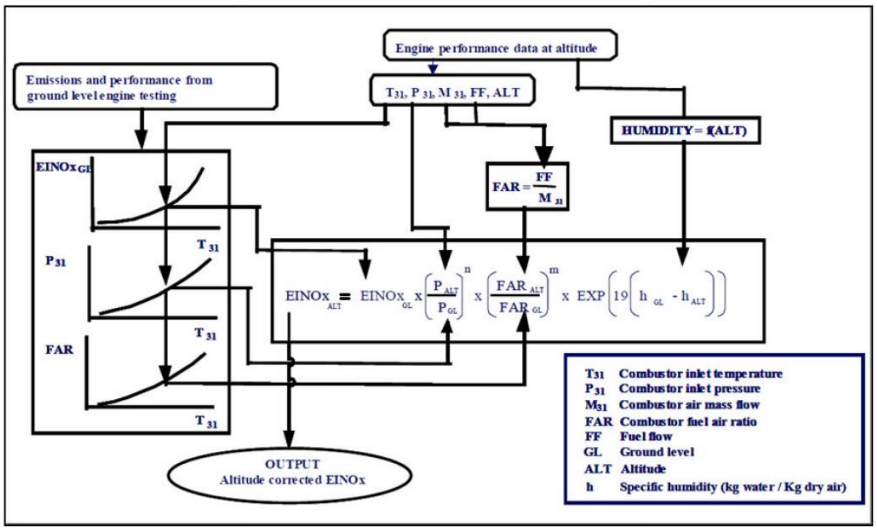

Figure 3: Flowchart of P3T3 methodology for NOx prediction

EINOx measurements at ground level are plotted for different combustor inlet temperatures. Moreover, as explained above, in order to calculate the emissions at certain flight altitude and speed, the combustor inlet temperatures. Inlet pressure and air mass flow have to be known. Even if these values are not measured during the ICAO tests they can be assessed using the gas turbine simulation software (TURBOMATCH) At this point similar to EINOx, burner inlet pressure and fuel air ratio are plotted for different burner inlet temperatures as shown in

Figure 3. Then, using the combustor inlet temperature at it is possible to obtain the respective value of EINOx at ground level from the specific plot. This value of EINOx is then corrected for taking into account the differences in FAR and inlet combustor pressure between ground level and altitude. The values of exponent "n" and "m" established the severity of the EINOx correlation. Finally, the correlation for the humidity influence is also taken into account. Having calculated the value of EINOx, the emitted NOx in kg is given by:

$$NOx = (FF\ .\ Time)\ .\ EINOx$$

where FF is the fuel flow in [kg/s], and Time in seconds.

The model is based on correlations and main advantage of using P3T3 model respect to other models such as Multi-stirred reactor emission model, is the low computational time. The required computational time is a key feature for a model that has to be used in aircraft multi-objective trajectory optimisation study considering the large amount of calculation involved in an optimisation study.

2.4 Problem Description

The simulated aircraft is Boeing 737-800 with engines CFM56-7B27 and flies from Heathrow (London) to Schiphol (Amsterdam). This is a very frequent flight, carried out daily by KLM airline with the same aircraft. Although the combination of aircraft, engines and city pair is very specific, the results can provide a trend for short-haul flights methodology can equally be applied on other combinations too. Airports London Amsterdam were chosen not only because they are very strategic airport for serving all the range of flights and one of the most frequently operated airports. Mission range has been selected as 210NM ground track. The trajectory is decomposed into a number of segments, which is related to the dimensionality of the optimisation problem. Only the three basic flight phases will be considered, since they represent more than 90% flight duration. More specifically, 18 segments for CLIMB, 10 segments for DESCENT are defined. The number of CRUISE segments is automatically resolved. For CLIMB altitude and speed values are specified. Throughout CRUISE only a single pair of speed and altitude values is set. When the aircraft reaches the Top Of Climb (TOC), it continues on CRUISE until it reaches the Top Of Descent (TOD), this is repeated for a multiple of fixed time-length segments. The DESCENT phase performs Continuous Descent Approach for the altitude values, which is the most optimal arrival way for an aircraft to approach the runway. For this phase, the altitude is automatically resolved and only speed values vary.

The design space is composed of 44 parameters which is combination of the trajectory altitude and speed values at various points. The three objectives to be minimised are Total Block Time – TIME – (in minutes), Total Block Fuel – FUEL- (in kg of burn fuel) and NOx (in kg of emitted pollutant). Optimiser settings are set to combine exploration and exploitation of the design space. Sensitivity analysis has been performed beforehand in order to resolved all the settings related with each parameter individually, such as the search-step and optimiser's configuration settings. The optimisation search is performed until it there is no significant improvement on the optimal set. In this approach every objective comes from a different model, which is considered as a black box. This has two advantages; it permits to interchangeable and alter different models of various fidelity without interrupting the others and different optimisers can be applied on any models' combination. The framework orchestrates the information exchanged by capturing and processing data before the execution of each model and finally feeding information back to the optimiser. The pipeline starts from HERMES, then feeds information to TURBOMATCH and finally comes P3T3. This is repeated whenever the optimiser requires evaluating a given set of parameters.

The whole trajectory of a single aircraft, without diversion, is resolved at once. All three flight phases are calculated one after the other. The take-off, early climb, approach and landing phases are not considered for the optimisation. They are very specific and subject to a number of conditions and parameters that cannot be modelled and/or controlled, such as weather, and also depend on ATM constrains of different airports. Also, the aircraft congestion will not affect the result at the current stage.

Shortly, the process is as follows. The optimiser settings are based on experience and earlier studies, where sensitivity analysis has also been performed. First, the progress of the optimisation process will be commented. Second, the results of the optimisation process that is the non-dominated or optimal of Pareto Front (PF) set will be presented. Since 3 objectives are involved, the parallel co-ordinates projection, also called ‖-coords, will be used. In addition the importance of variables and objectives' interplay will be analysed. Then the trajectories will be visualised and information from the flight path will be extracted. The discussion will be focused on the variables that correspond to the most extrema objectives, the datum design and, finally, the compromise design. In order to demonstrate the merits of the optimisation process, for each objective, the parameters that correspond to each minimum objective will be compared against the datum design and the compromise design. This serves the understanding how the shape of the trajectory alters depending on which performance criterion is considered as the most important.

2.5 Flight Restrictions

Due to noise restriction the speed of the aircraft near the airport area should be preserved under a certain threshold. In fact, this type of constraint affects the range of variability of the parameter. For the CLIMB phase, this is 250 knots CAS and for DESCENT the upper limit is initially 250 knots CAS and then drops to 220 and 160 knots CAS. Of course the lower limit is the operation threshold under which the aircraft cannot fly. Since in both cases it is not possible to precisely, a small safety margins have been added, which slightly widens the range of variability for the respective parameters. These constraints were extracted from official SID and STAR procedure diagrams.

ATM constraints are imposed to increase/secure minimum separation between aircraft. After the exit point from airport's airspace, both altitude and speed of CLIMB phased should only increase. By problem definition, during CRUISE level flight is performing. Speed values during DESCENT phase should be continuously decreasing. In addition, following ATC regulations, there are two main restrictions for cruise. First, aircraft can fly within a zone of 1000 ft. However, if it needs to move to another zone, this should be (multiples of) 2000 ft either higher or lower than the current one. Hence, all of the proposed trajectories can be considered as flyable. The aircraft, engine and their respective setting will be unaltered. Here, the focus is only on the flight schedule. This is actually the combination of altitude and speed values at certain points in 2-D space, called way-points. An abstract trajectory, as modelled, is illustrated in Figure 4. Under certain regulations some values will be fixed. Which will slightly reduced dimensionality of the problem.

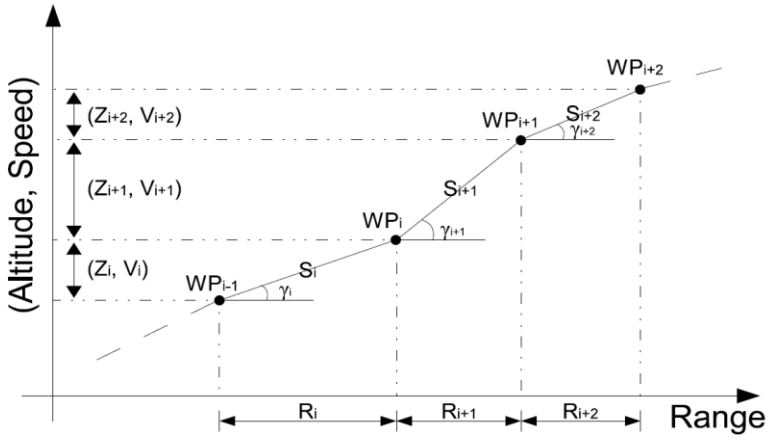

Figure 4 Abstract trajectory modelling

The trajectories studied in this work are in 2-D, however real trajectories are in 3-D. Adding the 3rd dimension affect aircraft dynamics models and the optimisation case. For future studies, required 3-D trajectories for the analysis, this will required to expand existing models in the third dimension and latter will increase the dimensionality of the problem to be optimised. Also more design parameters will be involved. This will be investigated in future studies. It is noteworthy that the ground distance of the visualised altitude and speed profiles, see Figure 9 (a) and 9 (b), is automatically resolved by HERMES in accordance to the respective speeds. So, the user (and to some extend the optimiser) can not directly set it. The main reason is that HERMES always delivers a flyable trajectory as appose to other approaches, where point mass model is used, and the user need to specify this information, too. Hence the overall range slightly different for each trajectory.

3 Discussions

3.1 Optimiser Progress

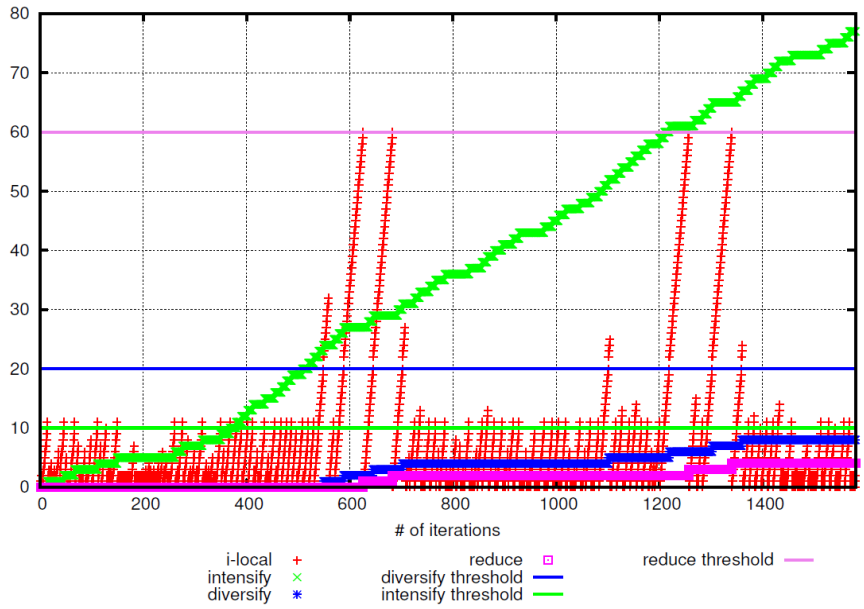

Figure 5: MOTS-II Search Progress

The optimiser carried out 1581 iterations and its progress is depicted in Figure 5. Initially, MOTS-II behaves as a local search optimiser, since it only performs the intensification move for the first third of its progress. Then, it diversifies the search and reduces the search step a couple of times, since finding a better design was not possible with the current search settings. Thereafter, it keeps again searching locally with sporadic calls to diversification and reduce

move until 1200th iteration, where diversification and reductions were consecutively called for a number of times to discover new designs. The latter means that again there was not improvement of the Pareto Front and a change to the search settings was required, which seems to be a correct choice because of the number of better designs discovered. For the remaining of its progress the local search scheme was used until the end of the computational budget. Primarily, by employing the local search move the optimal results were obtained, which proves the suitability of MOTS-II for this case.

The results of the optimisation are illustrated in Figure 6. For completeness, data since the start of the optimisation process, i.e. HISTORY, and the optimal ones are presented. By performing all the possible permutations between the axis that represent the objectives it is proven that all the objectives are negatively related to each other, and hence they are conflicting. Although this statement is more obvious in Figure 6a, it is not always true, which means that the objectives are conditionally conflicting in nature and it is interesting to notice under what circumstances they are in harmony. As it will be discussed later, the more the optimiser approaches the optimal set, the lesser conflicting the objectives will be. This is demonstrated by the non-intersecting lines connecting adjacent axis and by the scarcity of designs in the non-dominated set. Understanding how the optimiser advances through the objective space, as shown in Figure 6a, indicates the complexity of the problem. This figure presents the distinct performance (objective wise) of all the valid designs explored. By nature, all the objectives are conflicting, since the parallel co-ordinates projection informs the user that axis-parameters are negatively related.

For case of understanding the progress, HISTORY is linearly split in four mutually exclusive sets based on the number of evaluations, coloured differently. First comes the blue set, which is the most scattered, and then the other colours incrementally form the history progress. There is a wide range of designs discovered across a relatively large region of the objective space that are not within the optimal set. However, interestingly, several time-optimal solutions (as depicted in Figure 6b) were found from the early stage of the optimisation, which means that it is relatively easier to minimise time elapsed time. As the search step is refined, certain regions of the design space have been intensively explored, which yields a few thick bands of performance in the objective space. Gradually, the following performance areas are thinner than their predecessors and also lower, which means that the optimiser converges to the optimal region. Therefore, the last region, coloured in green, is significantly low, and contains most of the non-dominated designs in terms of FUEL and NO_X.

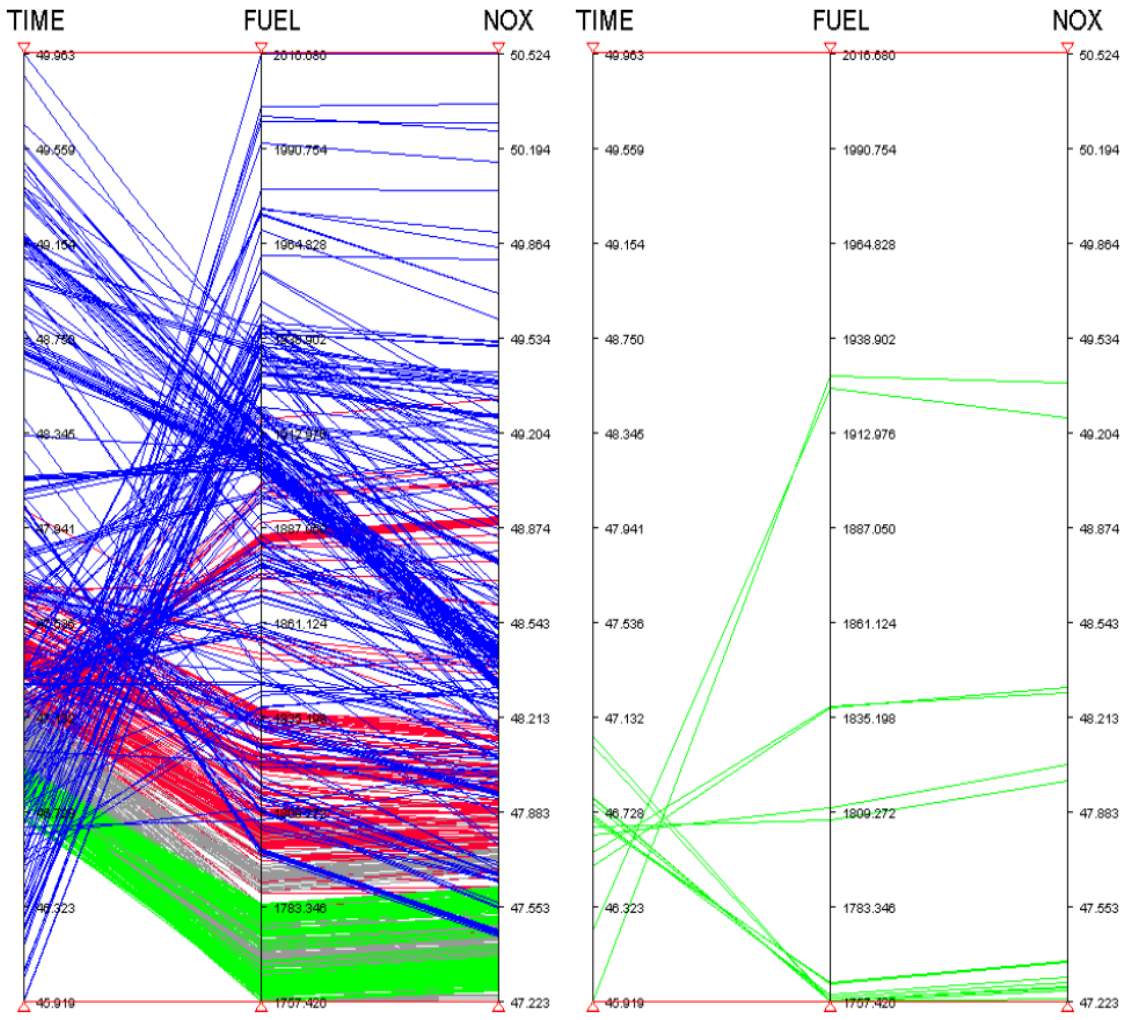

(a) (b)

(a) : Incremental history progress of valid designs, blue-13608 evaluation, red-31692 evaluations, gray-49821 evaluations, green-67851 evaluations

(b) : Optimal Set

Figure 6: ‖-coords projection of the objective space

Another metric of importance for the optimal objectives can be their interplay, see Figure 6b. More specifically, little change in the time axis yields significant performance difference of the other objectives. For instance, less than two minutes flight time can result in more than 170 kg of consumed fuel and 2 kg of NOx emitted in the atmosphere. This observation can be integrated into the optimiser's logic so as to speed-up and/or affect the whole process. First, understanding which objectives are easier to optimise, that means their minimum can be reached within a relatively small number of objective function evaluations, can advance the optimisation process. Second, the optimiser can focus on improving the performance of the

objective that presents the larger gap of performance between the extrema. Finally, this can be an indication about the ranking of importance of the objectives and this information can be particularly useful at the decision making stage.

Via using Il-coords interactively an interesting relationship among the objectives has been discovered. It was found that for the optimal designs both FUEL and NOx objectives mostly live in harmony, as already demonstrated in Figure 6b. They are not related linearly, but they increase and decrease together. However, during the initial and middle phase of the optimisation process all of the objectives conflict each other. Therefore, it is suggested to start a 3 objectives optimisation to guide the search and after a large number of iterations (more than 2/3 of the computational budget) the problem should switch to 2 objectives when the objectives start living in harmony. This functionality, which could potentially reduce problem's complexity, should be carried out within the optimiser's core.

3.2 Comparing the variables and objectives

Finding out which variables drive the optimisation process is crucial and certainly affects the speed and quality of the optimiser. Here, the same methodology is applied both on HISTORY and optimal set, since it was commented that they are both equally important. The Principal Component Analysis will be used for all the valid and optimal designs, separately. This is done in order to reduce the dimensionality of 44 parameters, while capturing more than 99% of the variability. The results are depicted in Figure 7.

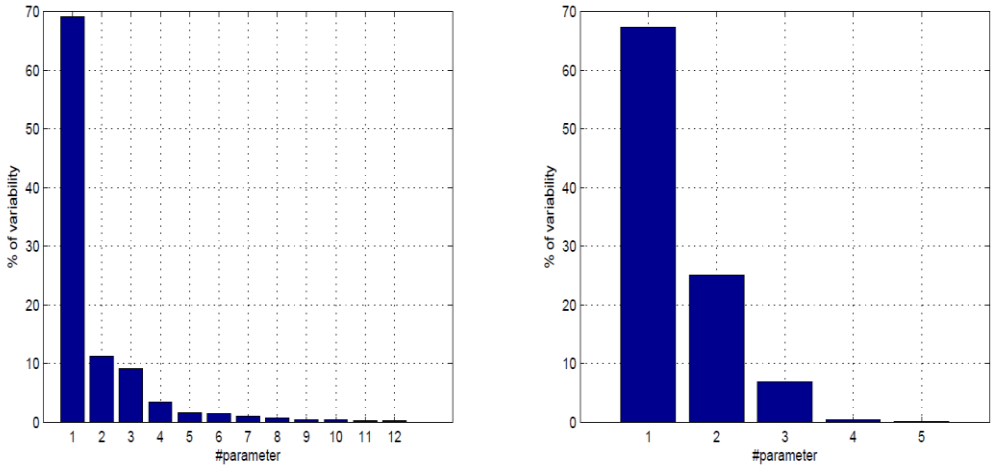

(a) (b)

Figure 7: Comparing the variability from history and optimal set

Table 3: Selected trajectories objectives

	TIME (min)	FUEL (kg)	NOx (kg)
Datum	44.50	1761.52	18.27
Minimum Time	41.28	1780.55	18.68
Minimum Fuel	42.06	1621.38	17.89
Minimum NOx	42.30	1621.64	17.82
Compromise	41.98	1626.14	17.92

Obviously, the first component of the set is by far the most significant since it accounts for more than 65% of problem's variability. This parameter corresponds to the first altitude value and it contributes to the first and second segment of the CLIMB phase. The rest of the parameters are lesser important in decreasing order. More specifically, the first 12 variables from HISTORY accommodate for 99% variability, whereas the top 5 of the optimal set accommodate for 99.9%. For the Pareto Front the second parameter gained importance and the third ones dropped. So, resolving accordingly the altitude waypoints during CLIMB will heavily affect all of the objectives.

Among the valid and optimal solutions a number of them were selected in order to demonstrate the practical progress of the optimisation process. This informs the user how each performance criterion affects the shape of the trajectory. The datum design represents the first solution, where the optimiser started from and will be used as a base-line against the other solutions. Since three objectives are optimised, one set of designs that includes the minimum from each objective will be selected, too. For the NOx objective, three solutions were found that correspond to the same performance set, but they only differ at the last CLIMB altitude parameter and the 14th CLIMB speed parameter. Without loss of generality, by sorting these solutions in ascending order, the middle solution was chosen. Finally, a compromise design has to be resolved, which stands among the objectives. This corresponds to the set of parameters whose performance is closer to the middle of each objective respectively. The performance of all the five solutions is presented in Table 3 and the normalised performance based on datum design is depicted in Figure 8. First of all, there is at least one objective for each solution that behaves better than the datum design, which proves that employing optimisation techniques is successful. Then, Minimum Time solution is the only solution that improves TIME by 7%, but at the same time delivers worse performance for FUEL and NOx. All the other solutions improve all of the objectives, especially FUEL, followed by TIME and then NOx. Practically, the optimisation process delivered environmentally-respectful solutions.

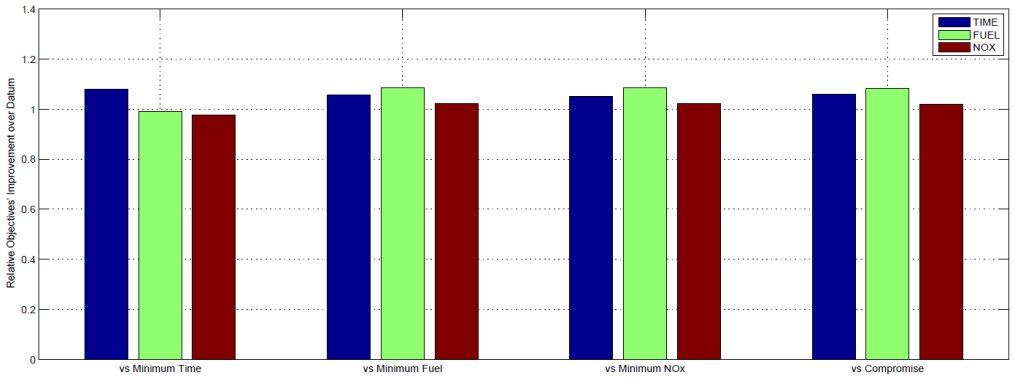

Figure 8: Relative objectives' improvement from datum (better above 1.0)

3.3 Aircraft Trajectories

The last part will visualise and discuss the actual (and optimised) trajectories. Effectively, a trajectory is a combination of waypoints, but for ease of illustration the altitude and speed components are separated. So, for each trajectory there is represented by an altitude and a speed profile that combines all the three main phases of the flight, see Figure 9a and 9b. Also, for comparison purposes all five different trajectories are illustrated in the same figure.

The altitude profiles present a lot of similarities. First, within the Terminal Manoeuvring Area (TMA), that is an airspace control area that surrounds the airport, the trajectories are almost identical. This is because the departures and arrivals flight instruction charts given to aircraft operators, called Standard Instrument Departure (SID) and Standard Terminal Arrival Route (STAR), respectively, have very strict bounds. Hence, there is less flexibility for any modifications and much similarity is expected at both ends of the trajectory. Sometimes, the aircraft must pass exactly from a certain waypoint at the right speed. Since each trajectory has a combination of different waypoints, ground distance travelled will not be exactly the same.

The altitude profile description follows. No stepped CLIMB was observed in any trajectory. Right after the end of TMA, the aircraft lowers the flight level, and then keeps climbing until it reaches the TOC. The lowering of flight level, as shown in Figure 10 for greater detail, is only temporary and does not violate the ATM regulations. Thereafter, it maintains the same flight level and speed throughout the CRUISE phase until TOD, where it starts to descent. The rest of the CLIMB phase, up to 42 NM of ground distance, is almost the same. However, depending on the position of TOC altitude, some aircraft fly longer on CLIMB mode. The length of CLIMB mode is almost the same for every case. Interestingly enough,

some trajectories share the same CRUISE altitude in groups. The TOC for Datum and Minimum Time trajectory is at 22965.9 ft, whereas the others' is at 28965.9 feet. Although Datum's TOC starts between other TOCs, the duration of CRUISE is the shortest and, hence, the DESCENT is the longest. Only Minimum Time trajectory has a TOC later than Datum's but the CRUISE phase is the longest and, therefore TOD is very late. The Compromise trajectory is very similar to Minimum NOx one with the only difference that it's TOC is slightly earlier. So, the whole altitude profile shifted a few NM before. Minimum Fuel trajectory initially resembles Minimum NOx until CRUISE, where it behaves like the Compromise trajectory. Certainly, Datum trajectory needs a prolonged CRUISE in order to improve overall performance. Finally, none of the trajectories follows the CRUISE-CLIMB practice trend, which is supposed to be the most optimal way according to modern aviation practices.

There is an obvious diversity in the speed profiles, as shown in Figure 9b. Only within TMA and between 25 and 40 NM, the speeds are about the same. Lower emissions for Minimum NOx are achieved by flying at slower speed during CRUISE and DESCENT. Following its definition, the Minimum Time trajectory has the highest speed in CRUISE, which exceeds the second fastest by 0.068 Mach and it's the only one that does not increase speed after the end of CRUISE. Besides Minimum Time trajectory, another common trend is at the end of each CRUISE, where there is a surge of speed. The main difference between Datum design and the other trajectories is at initial part of CLIMB and throughout DESCENT, where the speed is significantly lower. Minimum fuel seems to behave well in terms of fuel consumption by travelling slowly within TMA but in general is not the slowest. Again, Compromise and Minimum NOx, trajectories are very similar

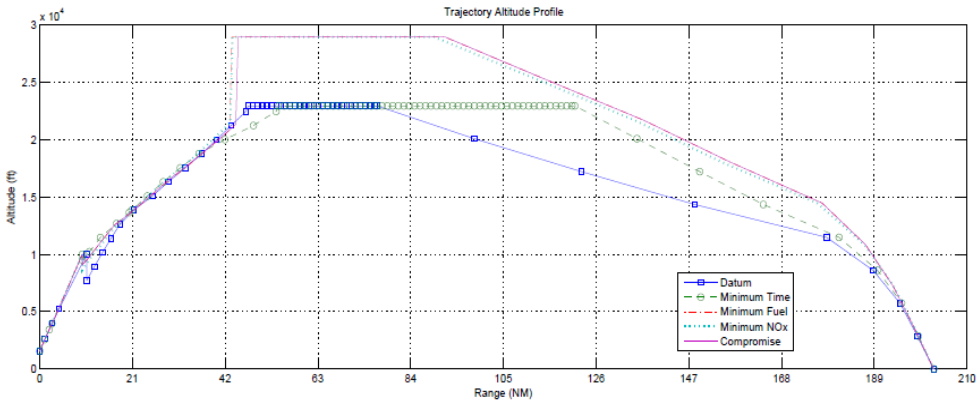

Figure 9(a): Trajectory altitude profiles

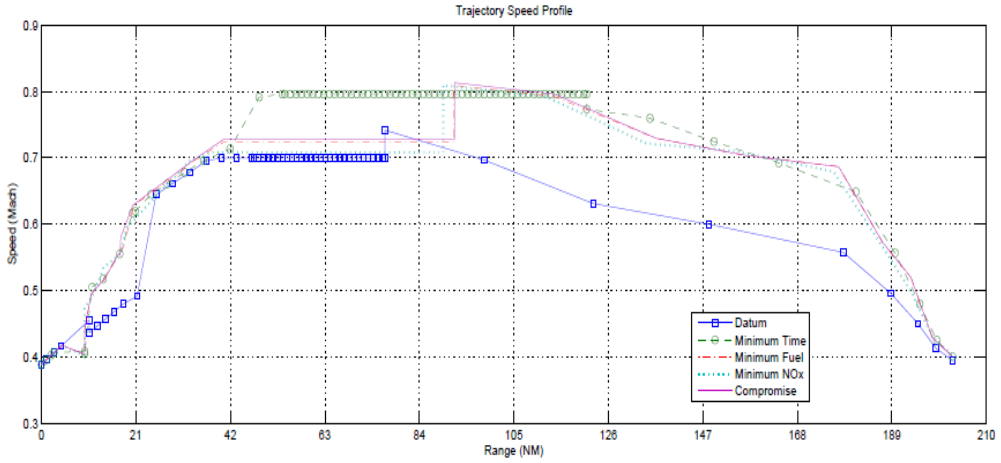

Figure 9(b): Trajectory speed profiles

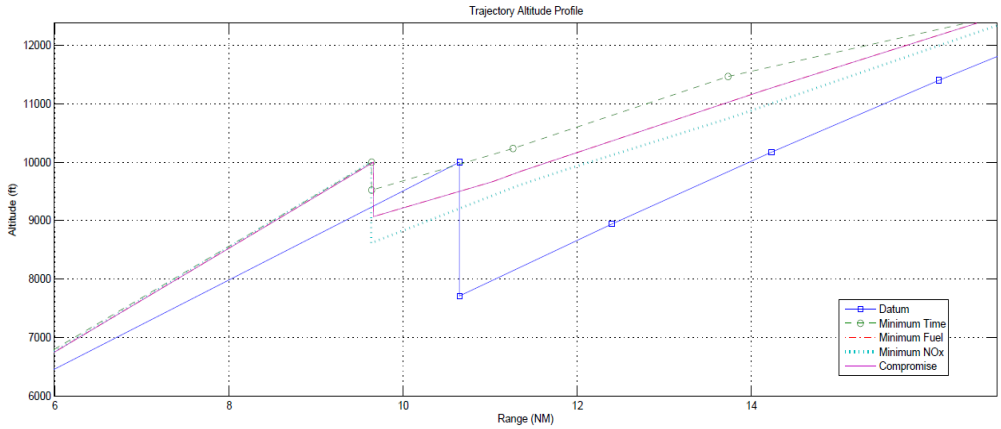

Figure 10: Zooming trajectory altitude profiles

4 Conclusions and Future Work

This report presented the methodology and results for environmentally-friendly trajectories, where significant reductions (see Figure 6) in TIME, FUEL and NOx have been achieved, while reducing environmental impact, too. The optimiser searched through a very highly constrained design space, due to the operational and ATM constraints, only 1.35% valid designs were found out of 68000 evaluations. Starting from a Datum trajectory, all the optima solutions improve TIME. Moreover, Compromise improves all the objectives by 5.7%, 7.7% and 1.9% for TIME, FUEL and NOx, respectively. Methods about speeding-up the optimisation process either by changing the configuration settings, algorithmic behaviour or problem description have been discussed. Difference between datum and newly generated trajectories were highlighted.

More specifically, the Knowledge extraction mechanisms should consider both HISTORY and optimal sets. Although, via history set, it is proven that all of the objectives generally conflict each other, just by observing the optimal trade-off this relation is not revealed. The most important parameters have been identified, too. The first altitude value of the initial segments heavily affects the performance of the trajectory, the progress of optimisation search and, hence, the shape of the optimal trade-off. This was expected since all the following segments depend on the first one. In fact, altitude values affect the overall performance of the trajectories. Trends for optimal trajectories have been identified, which can be simulated with tools of higher fidelity for increased accuracy. This will lead to multi-fidelity optimisation case studies.

Future work will focus at using a parameterisation scheme for the trajectories, which will further speed up the optimisation process. Also, the discovered trends will be integrated within the new trajectories. A more realistic scenario will involve trajectories in 3D and more objectives, by including additional emission values, engines' life expectancy, and contrails path. In order to further understand the optimised environmental friendly trajectories that can be deployed by airliners, it is important to investigate the impact of degraded engine performance on these trajectories at a multi-disciplinary level. This will bring environmentally sustainable and economically feasible solutions to the operator.